WELDING OF HIGH STRENGTH AND STAINLESS STEELS: A STUDY ON WELD METAL STRENGTH AND STRESS RELIEVING

by

JOHN EMMANUEL AGAPAKIS

Dipl., National Technical University, Athens, Greece

(1979)

SUBMITTED IN PARTIAL FULFILLMENT
OF THE REQUIREMENTS FOR THE
DEGREES OF

MASTER OF SCIENCE IN MECHANICAL ENGINEERING

and

MASTER OF SCIENCE IN OCEAN SYSTEMS MANAGEMENT

at the

MASSACHUSETTS INSTITUTE OF TECHNOLOGY

MAY, 1982

Signature of Author ______________________ Department of Ocean Engineering
April 30, 1982

Certified by ______________________ Koichi Masubuchi Thesis Supervisor

______________________ Klaus-Jurgen Bathe Thesis Reader

______________________ Harilaos Psaraftis Thesis Reader

Accepted by ______________________ A. Douglas Carmichael
Chairman, Departmental Graduate Committee

______________________ Warren M. Rohsenow
Chairman, Departmental Graduate Committee

WELDING OF HIGH STRENGTH AND STAINLESS STEELS

A STUDY ON WELD METAL STRENGTH

AND STRESS RELIEVING

by

JOHN EMMANUEL AGAPAKIS

Submitted to the Departments of Mechanical Engineering and Ocean Engineering on May 7, 1982 in partial fulfillment of the requirements for the Degrees of Master of science in Mechanical Engineering and Master of science in Ocean System Management.

ABSTRACT

The approach of weld metal strength undermatching in the fabrication of high strength steel structures is presented and justified in the Part I of the study.

Analytical techniques for the evaluation of the tensile strength of undermatched butt welded joints are presented and a numerical verification of assumptions and results is performed using the finite element program A.D.I.N.A.

The applicability and effectiveness of various stress-relieving methods is examined in Part II. An analytical model for the study of stress relaxation during post-weld heat treatments is also developed.

Welding and stress relieving experiments performed on stainless steel specimens in order to test the validity of the analysis, are described in Part III of the study. The development of a microcomputer-based data acquisition system for these experiments is also covered.

Finally in Part IV a welding cost model is developed and the economic aspects of welding production are outlined, together with the cost savings possible through the application of weld metal strength undermatching.

Thesis Supervisor : Koichi Masubuchi

Title : Professor of Ocean Engineering and Materials Science

ACKNOWLEDGEMENTS

I would like to express my gratitude to my advisor Professor Koichi Masubuchi for his guidance and support during my graduate study at M.I.T. and the preparation of this study. I am also grateful to Professor Klaus-Jurgen Bathe for his very helpful suggestions on the finite element part of this thesis and to Professor Harilaos Psaraftis for his guidance in my Ocean Systems Management Program.

Special thanks are due to my friend, Research Associate, Vassilios Papazoglou for his very constructive comments. I would also like to thank my friends and colleagues, Yianni Mavrikios, Akihiko Imakita, Kevin Carpentier and Chris Wee for their help in the experiments. Mr. Imakita's help in translating part of the Japanese references was also invaluable.

Many thanks are further due to Tony Zona for his assistance in the Welding Lab, to Ms. Muriel Morey for her excellent work in the Figures of Chapter III, and to Ms. Froso Mavrikiou for her proficient proofreading of the text.

Finally, but by no means any less, I would like to thank my wife Efie not only for her expert typing of this whole manuscript, but also for her continous support, understanding and sacrifices throughout my studies.

To Efie

TABLE OF CONTENTS

LIST OF FIGURES

LIST OF TABLES

CHAPTER I

INTRODUCTION

1.1 Background and General Considerations

Welding is extensively used today in the fabrication of many structures including ships, buildings, pressure vessels and aerospace vehicles and certainly provides many advantages over other fabrication techniques. Welded structures however are by no means free from problems. The local nonuniform heating during welding and the subsequent cooling cause complex thermal strains to develop that finally lead to residual stresses, distortion and all their adverse consequences (such as brittle fracture, fatigue fracture, stress corrosion cracking or even buckling).

The extent to which these effects appear is directly related to the design and fabrication parameters and to the material properties of both the base plate and the weld metal. So for example, when the material is brittle, residual stresses can reduce the fracture strength of the weldment significantly. On the other hand, when the material is ductile the effects of the residual stresses on fracture are negligible. Most of the above problems are also seriously aggravated in the case of higher strength materials which find an increasing number of applications today.

For the case of high strength steels in particular, which are examined in this study, their inherent characteristic of decreasing fracture toughness with increasing strength should also be considered. Furthermore the fracture toughness of the weld metal is usually less than that of the base plate. This is due to the existance of both high residual stresses and various types of defects such as cracks, porosity or slag inclusions. It should also be noted that good fracture properties in high strength steels are usually obtained through heat treatments, that are drastically different from the thermal cycles encountered in the weld metal during welding. Therefore, as the strength of the steel increases, it becomes more and more difficult to obtain weld metals that match the base plate in both strength and fracture toughness, as is traditionally required by the codes.

In addition, preheating is usually required before welding of high strength steel systems, in order to avoid hydrogen-induced delayed cracking of the weldments. It is generally believed that preheating results in slower cooling rates and therefore permits more hydrogen to diffuse and in the same time leads to lower thermal stresses. However, preheating complicates the whole welding operation and increases fabrication costs.

An alternative approach that results in lower stresses in the weld metal and requires less or no preheating is to use a filler metal having yield strength lower than the one of the base plate but ample fracture toughness. This "undermatching" philosophy is successfully applied in Japan and is under serious consideration in U.S. Justification of this approach is basically the underlying objective of Part I of this study. The cost reductions realizable through undermatching are further examined in Part IV.

It should be pointed out here, however, that despite of the precautions taken residual stresses of significant magnitude and possibly distortion will usually develop during welding of high strength steels. These can sometimes be brought under acceptable limits by some kind of stress relieving operation. Uniform or localized heat treatments are frequently specified by the fabrication codes. Such treatments, however, would again complicate the welding operations and increase the production costs. Furthermore, they might be detrimental to the microstructures and therefore to the mechanical properties of the base and / or the weld metal.

The effectiveness and applicability of stress relieving heat treatments and possible alternatives are examined in Part II and III of this study.

1.2 Objectives

The basic objectives of this study are (in the order they appear in the text):

(a) A literature survey of the past studies dealing with the applicability and justification of the undermatching philosophy in high strength steels.

(b) An analytical evaluation of the strength of undermatched butt welded joints.

(c) A numerical evaluation of the strength of undermatched joints using the Finite Element Method.

(d) An evaluation of the various stress relieving methods and their effects as well as a survey of the applicable industrial codes.

(e) The development of an analytical model for the calculation of remaining stresses after stress relieving operation.

(f) The experimental verification of the analytical model.

(g) The development of a welding cost model and the evaluation of the cost savings possible through weld metal strength undermatching.

Finally an important byproduct of the experimental part of this study that should be mentioned separately was:

(h) The development of a microcomputer-based data acquisition system for welding and / or stress relieving experiments.

1.3 Organization of the study

The next several chapters of this study deal with the objectives set forth in the previous section. Specifically in Chapter II a justification of the undermatching philosophy is attempted and to this end results of various past studies (mostly by Japanese investigators) are reviewed. In Chapter III analytical techniques for the evaluation of the strength of simple undermatched butt welded joints are presented. Further in order to verify the assumptions and to confirm the results of the analysis a numerical evaluation of the strength of the same joints is performed using the finite element program ADINA.

The various stress relieving methods and the applicable codes are reviewed in Chapter IV. Special consideration is given in the assessement of the effects of thermal stress relieving treatments and the evaluation of possible alternatives. In Chapter V an one dimensional model is developed for the analysis of stress relaxation due to heat treatments. However, since necessary creep properties were not available for high strength quenched and tempered steels further analysis was limited to 304 stainless steels.

For comparison, welding and stress relieving experiments, described in Chapter VI, were performed. Furthermore, the basic characteristics of the developed microcomputer-based data acquisition system are also presented in this chapter. Results conclusions and recommendations were summarized in Chapter VII.

In Chapter VIII a welding cost model is developed and various economic aspects of welding production are outlined. The possible cost savings through the application of weld metal strength undermatching are finally examined in Chapter IX

PART I

WELD METAL STRENGTH UNDERMATCHING

CHAPTER II

THE APPROACH OF WELD METAL STRENGTH UNDERMATCHING-A LITERATURE SURVEY

2.1 Overmatching Versus Undermatching

In the design and fabrication of welded structures efforts are usually made, in accordance with the codes, to ensure that the weld metal has both adequate strength and toughness. When welding ordinary low-carbon steel it is not difficult to obtain weld metals that match the base metals in both strength and fracture toughness,[5],whereas for higher yield strength steels,this match becomes increasingly difficult to maintain.

This problem is particularly evident in the case of quenched and tempered steels, such as the HY-series U.S. Navy steels, whose high yield strength and excellent toughness are obtained through heat treatments. There are basically two approaches in coping with the problem.

The first is to require a weld metal with tensile strength at least equal to the specified minimum tensile properties of the base metal and toughness that can be achieved reliably by good welding practices,which is often less than that of the base metal. The second approach is to accept weld metals that slightly undermatch the base metal in strength but have adequate fracture toughness.

The overmatching approach, that has been traditionally followed by U.S. Navy codes, evolved in order to ensure that the weldment was not a "weak link" in the structure [6]. The adequacy of the approach for ordinary low-carbon steels was proven by explosion bulge tests, by Masubuchi [5] and Pelini [3]. However,it is questionable whether an extrapolation of this philosophy is appropriate for high strength steel systems. That is,there exists little evidence that strength overmatching would guarantee adequate performance.

In contrary to U.S. specifications, some Japanese industrial standards have accepted the undermatching approach both for repairs and for initial welding of various layers in multipass welds, following extensive research efforts. Lower strength filler metals may permit reductions in the preheating temperatures required and would result in easier welding of highly restrained heavy sections. Additionally, with weld metals of lower yield strength, local plastic deformations can reduce stress concentrations in hard spots. It should also be noted, that the overall strength and ductility of an undermatched joint is usually not adversely influenced by the existance of the lower yield strength zone. Specifically as was observed by various investigators the joint strength can often reach that of the base metal,if the reduction in strength is not large and the weld size sufficiently small.

A number of researchers in different countries have studied the effects of the mechanical properties of the weld metal and the heat affected zone on the mechanical behavior of weldments in different materials ([7] to [10]) . Specifically in Japan,however,the S.J. (Soft Joint) Committee of the Japan Welding Engineering Society (J.W.E.S.) has undertaken extensive research efforts,during the past decade,to determine the mechanical behavior of undermatched welded joints and to find reasonable strength levels for the filler metal from the standpoint of both workmanship and joint performance,[11].

The initial fundamental studies of Satoh et al.,[12],[13],[14] and [15],were followed by detailed performance analysis of static tensile strength, fatigue strength and brittle fracture strength of undermatched butt and fillet welds. The next sections of this chapter present in summary the results of these studies. A more extensive review was performed by the author in [16].

The analytical and numerical evaluation of the strength of an undermatched butt welded joint will be presented in the next chapter.

2.2 Tensile Strength of Undermatched Butt Welds

2.2.1 Fundamental Experimental Studies

The static tensile properties of welded plates,including soft interlayers and loaded either across or parallel to the weld line,were evaluated in an extensive research program completed by Satoh and Toyoda in the late 1960's and early 1970's at Osaka University,[12],[13],[14]and [15].

Round bar specimens of a medium carbon steel including a flash welded soft interlayer of low carbon steel were initially tested,[13]. Heterogeneity in mechanical properties along the specimen was estimated by the hardness distribution over a longitudinal section. Results of the tensile tests suggested that the strength of the joint approaches that of the base metal when the ratio of the thickness of the soft interlayer to the diameter of the bar is sufficiently small. Tests of flat bar specimens loaded across the weld line followed [14]. The specimens, shown in figure 2.1 ,were prepared either by flash welding of round bars of S15C* and S35C* structural steels or by gas metal arc welding of high tensile strength, HT-80*,steel plates (minimum tensile strength of 80 Kg/mm^2), using electrodes producing weld metal with minimum tensile strength of 50 Kg/mm^2. Results of the tensile tests given in figure 2.2 and 2.3 indicate that the ultimate tensile strength and yield stress of the joint depend on both the relative thickness X_t (the ratio of the soft interlayer thickness, H, to the plate thickness, t) and the plate width to thickness ratio (w/t). Specifically the joint strength increases as the X_t decreases and reaches the strength of the base metal when X_t is sufficiently small. Additionally figure 2.3suggests that when the plate width to thickness ratio increases, the ultimate tensile strength of the joint increases also up to a certain definite value that depends on X_t. The plate width, W_∞ ,above which the tensile strength becomes equal to the one of an infinite plate depends on both H and t . This influence was also verified by Yoshinaga [17] and Hisamitsu [18]. For $X_t < 1$, in general , W_∞ can be roughly estimated by $W_\infty = 5\ t$ and is independent of H. When $X_t > 1$, however, plastic constraint in the plate thickness direction - which is the cause of the strength increase - will disappear at the mid cross-section of

* S15C , S35C and HT-80 are Japanese steel grades. Note that HT-80 has nothing to do with HY-80 (the primary U.S. Navy hull construction high strength steel)

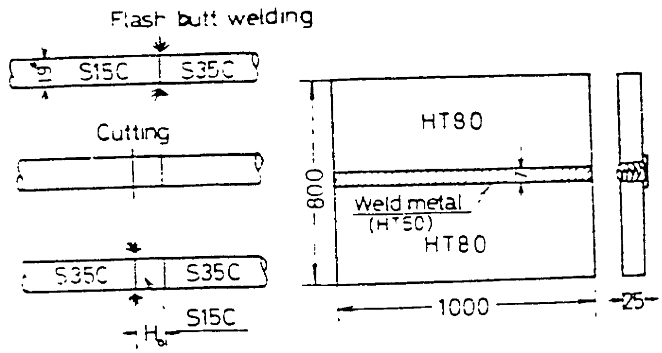

(a) Series A, B (b) Series S, T

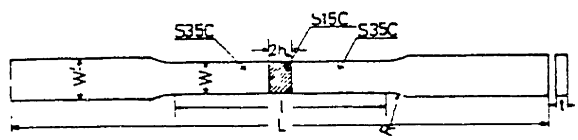

	Dimension mm					
	l	L	W	W'	R	t
Series A	90	240	10	18	20	3
Series B	90	240	15	18	25	5

Dimensions of specimens (Series A, B)

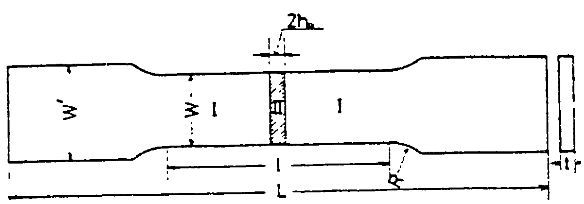

	Dimension mm						
	l	L	W	W'	R	t	$2h_b$
Series S	200	600	20-120	40-200	25-60	20	7
Series T	200	500	35-100	60-140	30-50	15	7

Dimensions of specimens (Series S, T)

Figure 2.1 : Specimen sizes and configuration

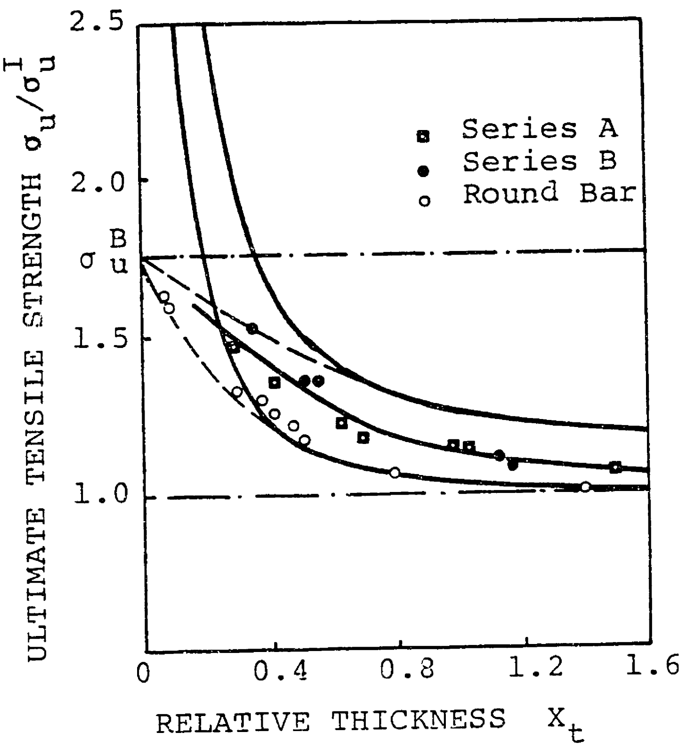

Figure 2.2 : Ultimate tensile strength vs relative thickness (Series A,B)

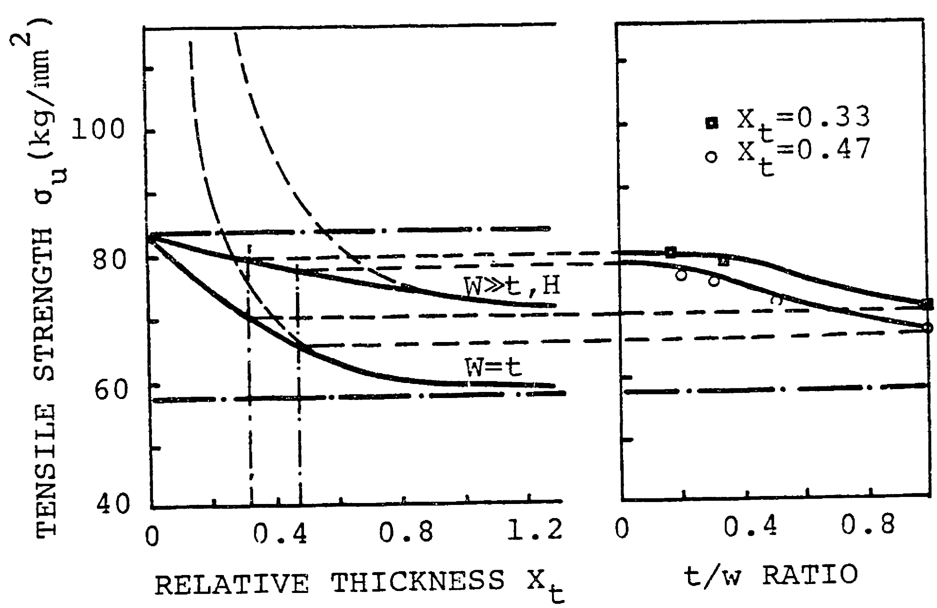

Figure 2.3 : Effect of plate width on ultimate tensile strength of welded plates(Series S,T)

the soft interlayer and the W_∞ -value will depend only on the H-value . Experimentation and analysis showed that in this case we can roughly estimate $W_\infty = 5H$.

To simulate more applications , other experiments were carried out with loading parallel to the weld line, [15]. The results of these tests suggest that the strength and the ductility of the joint depend on the value of the ratio of the width of the hard zone to that of the soft zone and become almost equal to those of the hard metal when the ratio is larger than 10.

Strain distributions in the conposite weldment are almost uniform along the mid cross-section of the specimen at each load level except when yielding and after the maximum load. Behavior of the axial strain around yielding seems to be influenced by the ratio of the width of the soft metal to the thickness of the plate . When this ratio is smaller than 2 ,the strain increases almost uniformly along a cross section until general yielding occurs. At that point, base metal strains are temporarily larger than those of the soft metal. When the ratio is larger than 2, nonuniform distribution of the strain occurs at average stress somewhat larger than the yield strength of soft material and continues until general yielding.

2.2.2 Performance Study

The initial experimental studies, indicated that, for the idealized joints examined, the ultimate tensile strength may be as high as that of the base metal if the average width of the weld metal is sufficiently small.

To assess the applicability of undermatching in actual structures, the S.J. committee of the Japan Welding Engineering Society carried out a performance study presented in [19],[20] and [21]. Wide plate specimens shown in figure 2.4 were prepared by shielded metal arc welding of 70 mm thick HT-80 plates with various under- or overmatching electrodes. Results indicated that for butt welded specimens with an average relative thickness $(X_t)_{av}$ between 0.2 and 0.3, the strength of the joint reached the strength of the base plate when the ultimate tensile strength of the weld metal, σ_u^W, was nearly 90% of the ultimate tensile strength of the base metal, σ_u^B. That is for (σ_u^W/σ_u^B) ratio larger than 0.9, the undermatched welded joint behaved in almost the same way as the base plate in terms of both strength and ductility.

2.3 Tensile Strength of Undermatched Fillet Welds

The S.J. Committee of the J.W.E.S. also investigated the applicability of undermatching in fillet welds. Experiments were performed with various specimens of high strength steel (U.T.S. of 84.1 Kg/mm^2) welded with undermatched electrodes (U.T.S. of 40 to 80 Kg/mm^2). Detailed presentation and results for tensile and shear tests appear in [11]. It should however be noted that the geometry and the size of the fillet is also important now, since they can be adjusted to compensate for the lower strength of the weld metal.

2.4 Fatigue Strength of Undermatched Welded Joints

Gelman and Kudrayartzev showed experimentally, [9], that the fatigue strength of bars with a soft interlayer increased

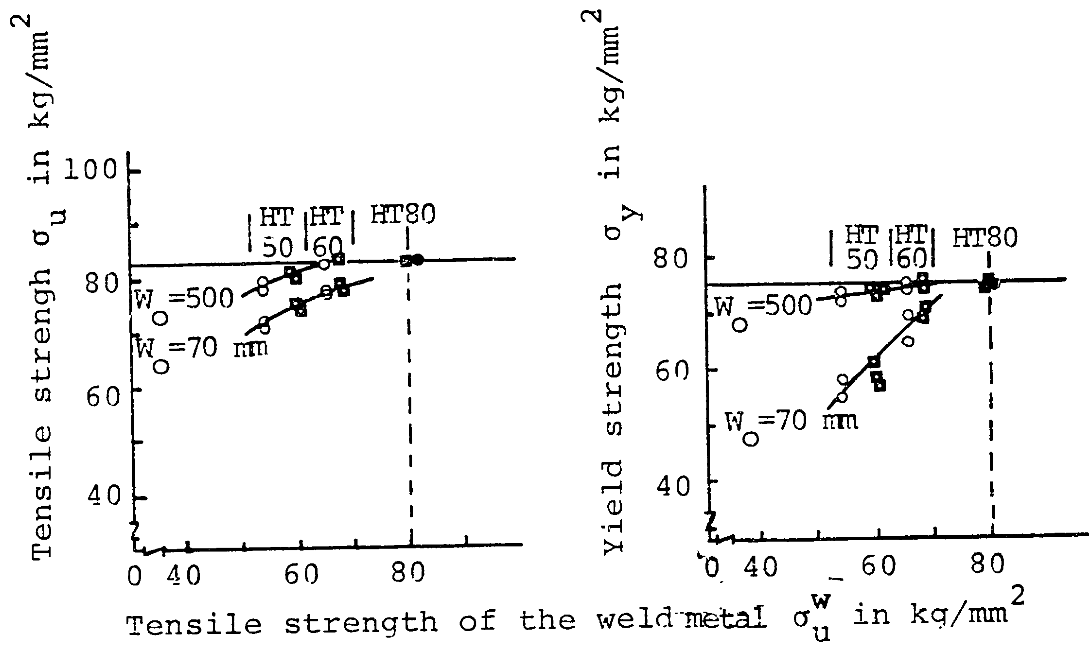

Figure 2.4(a): Results of the tensile tests

Type	W_o	L_o	t_o	W'	R
L	500	400	70	800	200
M	70	400	70	140	200

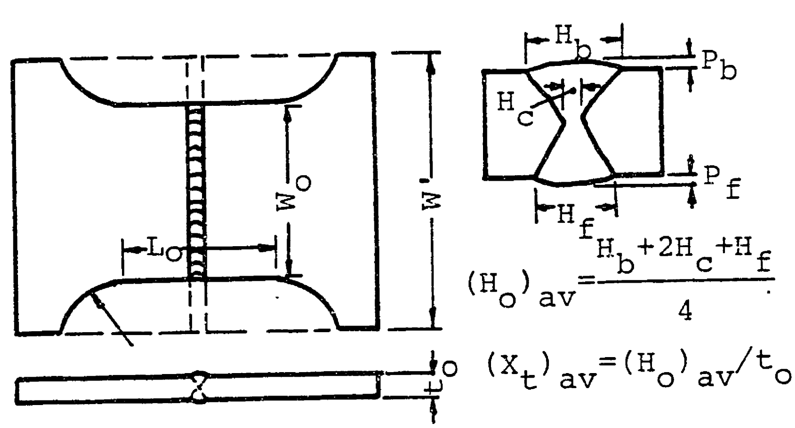

Figure 2.4(b): Specimen design and dimensions for static tensile tests

when the thickness of the interlayer decreased. In the late 1960's Ṡatoh and Nagai,[12], investigated the fatigue strength of welded or locally work hardened round bars having hard or soft interlayers. Fatigue tests were performed with a rotating bending machine and the results indicated in general that the hard interlayer had no effect on fatigue strength, whereas for the soft interlayer the fatigue strength decreases drastically as the thickness of the interlayer increases.

To evaluate the performance of actual undermatched welded joints, the S. J. Committee of the Japan Welding Engineering Society conducted a series of fatigue tests using HT-80 specimens welded with E7016 and E11016 electrodes. The first series of specinens tested (FT, FL) is shown in Figure 2.5.

The mechanical properties of the base metal and the weld metals together with fatigue test results are shown in Table 2.1. Specimens were tested under a pulsating load between zero and 35 Kg/mm^2, and between zero and 55 Kg/mm^2. In the FT specimens, where tensile stress was applied transversely to the weld, fatigue cracks occured at the toe of reinforcement and propagated in the direction of the thickness. No appreciable difference in the number of cycles to fracture appeared between the overmatched and the undermatched joints. In FL specimens, however, where tensile stresses were applied parallel to the weld, the fatigue life of the overmatched joint was somewhat longer because fatigue cracks were initiated on the surface of the weld metal. In both FL and FT specimens, the weld reinforcement had not been removed. Further tests for other

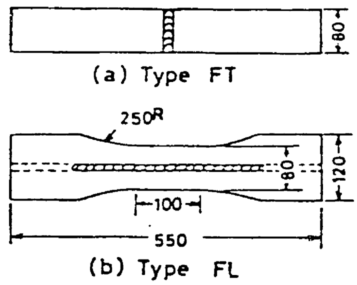

Figure 2.5 : Type FT and FL fatigue specimens [28]

Table 2.1 : Mechanical Properties of the materials used in the fatigue tests [28]

Material		Tensile Strength (Kg/mm^2)	Yield Strength (Kg/mm^2)
Base metal HT 80 (a)		84	79
Weld	E 11016	86	74
Metal	E 7016	55	-

(a): Chemical composition: C 0.10%, Mn 0.79%, Si 0.26% P 0.004%, S 0.007%, Ni 0.83%, Cr 0.52%, Mo 0.34%

Maximum Stress applied (Kg/mm^2)	Electrode used	No. of cycle at fracture Type FT (x10^4)	Type FL (x10^4)
35	E 11016-G	15.2	20.8
		13.2	23.1
	E 7016	13.8	16.2
		14.1	22.3
55	E 11016-G	3.72	2.62
		1.38	2.45
		3.17	
	E 7016	8.65	4.63
		6.63	5.34

geometries, as well, verified the above results and showed that in general removing the reinforcement led to improved fatigue behavior [11] as shown in Figure 2.6.

2.5 Brittle Fracture Behavior of Undermatched Welded Joints

Various studies were performed to investigate the brittle fracture strength of undermatched welded joints in high strength steels. ([22],[23] and [24]). It was generally indicated from test results that higher fracture toughness or lower transition temperature should be required for the undermatching weld metal than for the overmatching one.

Satoh and Toyoda, [23], have further shown that if ${}_vT_s$ is the fracture transition temperature obtained from a V-notch Charpy test and $\Delta_v T_s$ is the difference in the fracture transition temperature, between overmatching and undermatching filler metals, required to obtain the same fracture initiation temperature, T_i, for a welded and notched wide plate, then:

$$\Delta_v T_s = 80 \ln (S_r)_Y \; [1-65(1/T_i-1/273)]$$

where $(S_r)_Y$ is the ratio of the yield stress of the undermatching and overmatching filler metals and T_i is in degress K^o.

So if for example the $(S_r)_Y = 0.8$ and $T_i = -50^oC$ to -150^oC then the transition temperature required for the undermatching filler metal is 15^oC to 20^oC less than that of the overmatching one.

2.6 Residual Stresses in Undermatching Welded Joints

In low carbon steel weldments maximum tensile residual stresses in the weld metal usually reach the yield stress of

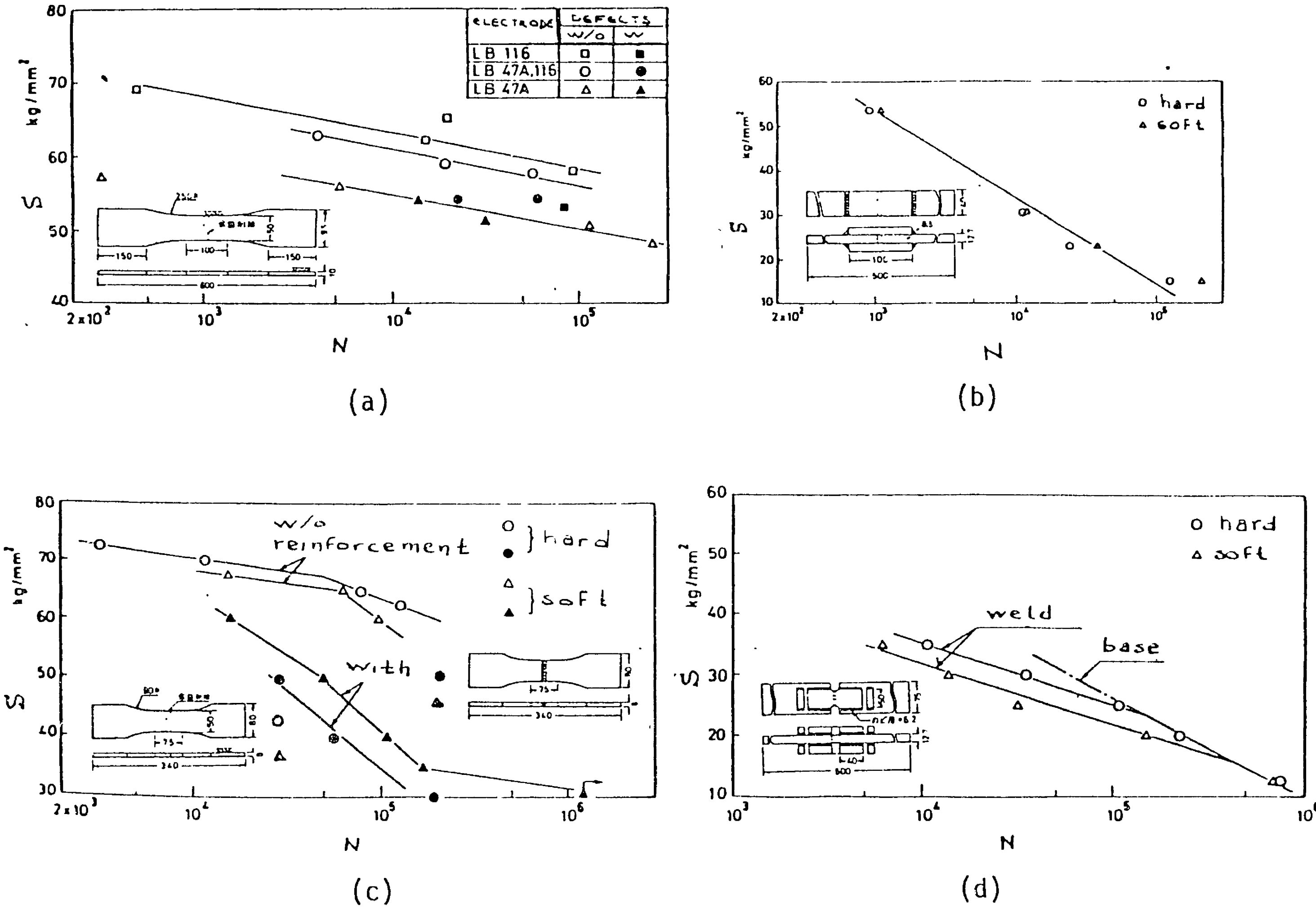

Figure 2.6 : Fatigue test results for various specimens tested by JWES [11]

the material, [1]. In high strength steel weldments, however, the experimentally obtained distribution of residual stresses has maximum peaks lower than the yield strength of the material. Additionally the width of the tensile stress zone is usually observed to be wider than what it should have been if the material behaved analogously to lower strength steels.

This behavior has been confirmed by various investigators, [25],[26],[27], and is depicted schematically in Figure 2.7 adapted from [1]. Direct analogy with lower strength steels would suggest curve (1). Analytical predictions, support (2) whereas experiments tend to indicate that (3) is correct. It is assumed in the bibliography, however, that the actual distribution lies between (2) and (3). The discrepancies are usually attributed to additional expansion during cooling, due to phase changes that occur in the higher strength steels.

Although no actual results have been reported it is believed that lower yield strength filler metals would result in lower residual stress peaks.

2.7 Structural Applications

The applicability of undermatching filler metals in structural fabrication, as established by the initial fundamental studies and joint performance tests was further verified by actual structural applications.

One of the early examples was the burst test of welded pipes 4100 mm long, 950 mm in diameter and made of 12 mm thick HT-80 steel plates. Weld metal had a measured ultimate strength of 77 Kg/mm^2. However, as reported in [28] and [11], during the

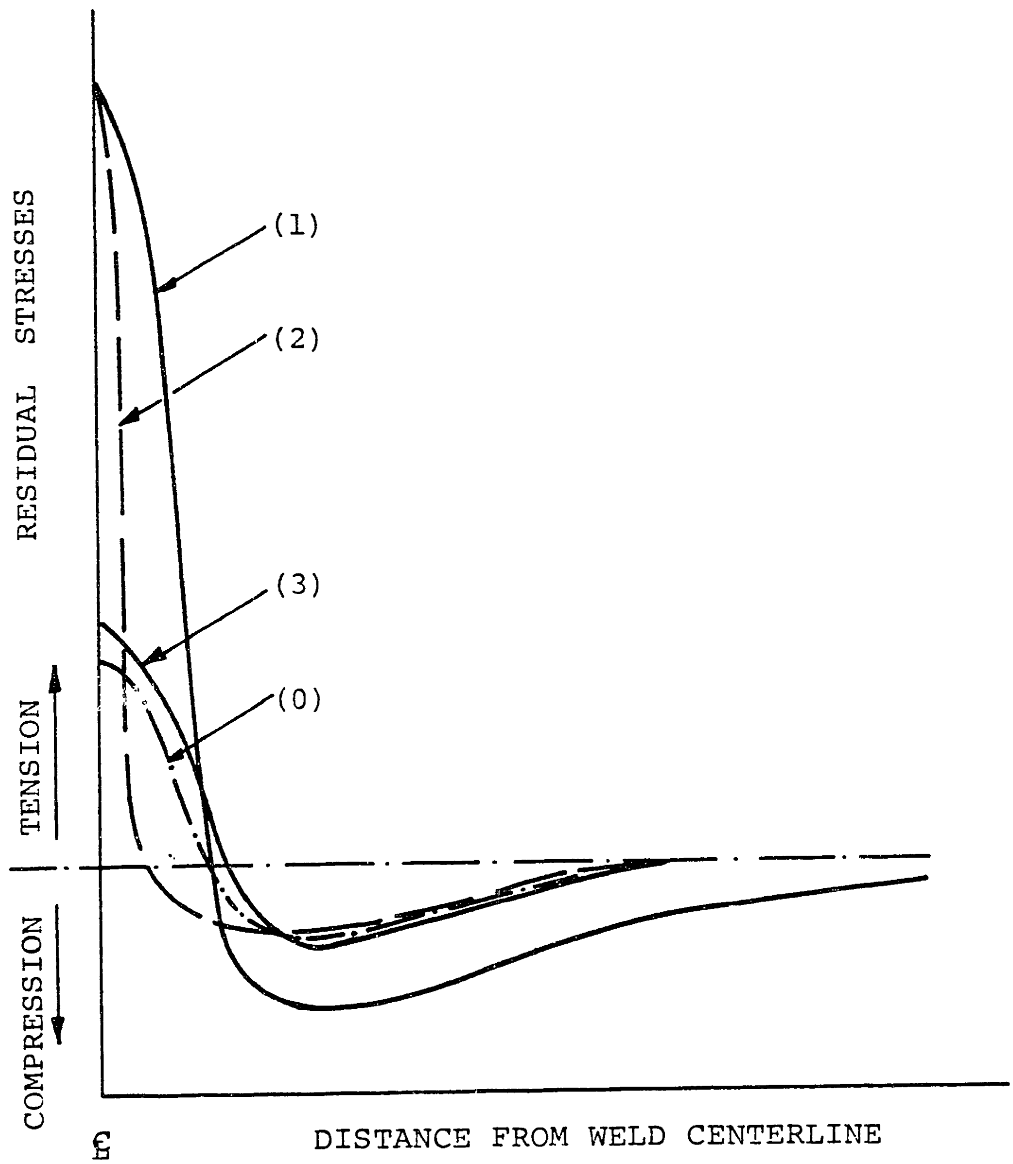

Figure 2.7 : Possible distributions of longitudinal residual stresses in butt welded plates of high strength steel.

burst test, fracture started at an internal pressure of 235 Kg/mm^2 corresponding to a circumferential stress of 90 Kg/mm^2 (just above the minimum ultimate tensile strength of the base plate, 89 Kg/mm^2).It is apparent therefore that the undermatched filler metal had no harmful influence.

Another extensive investigation of the potential applicability of undermatching in the field welding of HT-80 heavy plates was also carried out by Satoh et al, [21],[29] and [30]. Both experiments and service experience verified that the use of undermatching electrodes effectivelly lowered the preheating temperature, required to prevent root cracking caused by the first pass, and weld metal cracking, caused by the subsequent passes, in multipass welding of 50 mm thick sections.

Additionally not appreciable differences in tensile strength and uniform elongation between the overmatched and the undermatched welded joints was objerved. Tests were performed on wide plate tension specimens, with or without notch, tested at a temperature slightly lower than the minimum service temperature experienced in the field.

CHAPTER III

ANALYTICAL AND NUMERICAL EVALUATION OF THE STRENGTH OF UNDERMATCHED BUTT WELDED JOINTS

3.1 Analytical Strength Evaluation

3.1.1 General Discussion

The effect of a region of lower yield strength weld material on the mechanical behavior of a joint, depends, in general, on the type of the joint, the size of the weldment, the degree of reduction in strength, the width of the lower strength zone, the types of loading encountered and the loading directions.

Thus refering to Figure 3.1(a) we note that when tensile loading is applied to a transverse butt weld, the joint is under constant stress. When the applied stress exceeds the yield strength of the weld material, strain concentrations occur in the weld metal and result in fracture. However, the extent of the effects of the L.Y.S. zone depends on the degree of reduction in strength and the width of the zone. In the case of Figure 3.1(b), where the tensile loading is applied to a longitudinal butt weld, the joint is under constant strain and the effect of the lower yield strength material is very small as long as the zone has enough ductility and the width of the weldment is reasonably larger than that of the weld metal.

Thus, in what follows, we will only restrict ourselves in the analytical evaluation of the strength of butt welded joints, loaded in a direction perpendicular to the weld line, and later in the numerical verification of assumptions and results

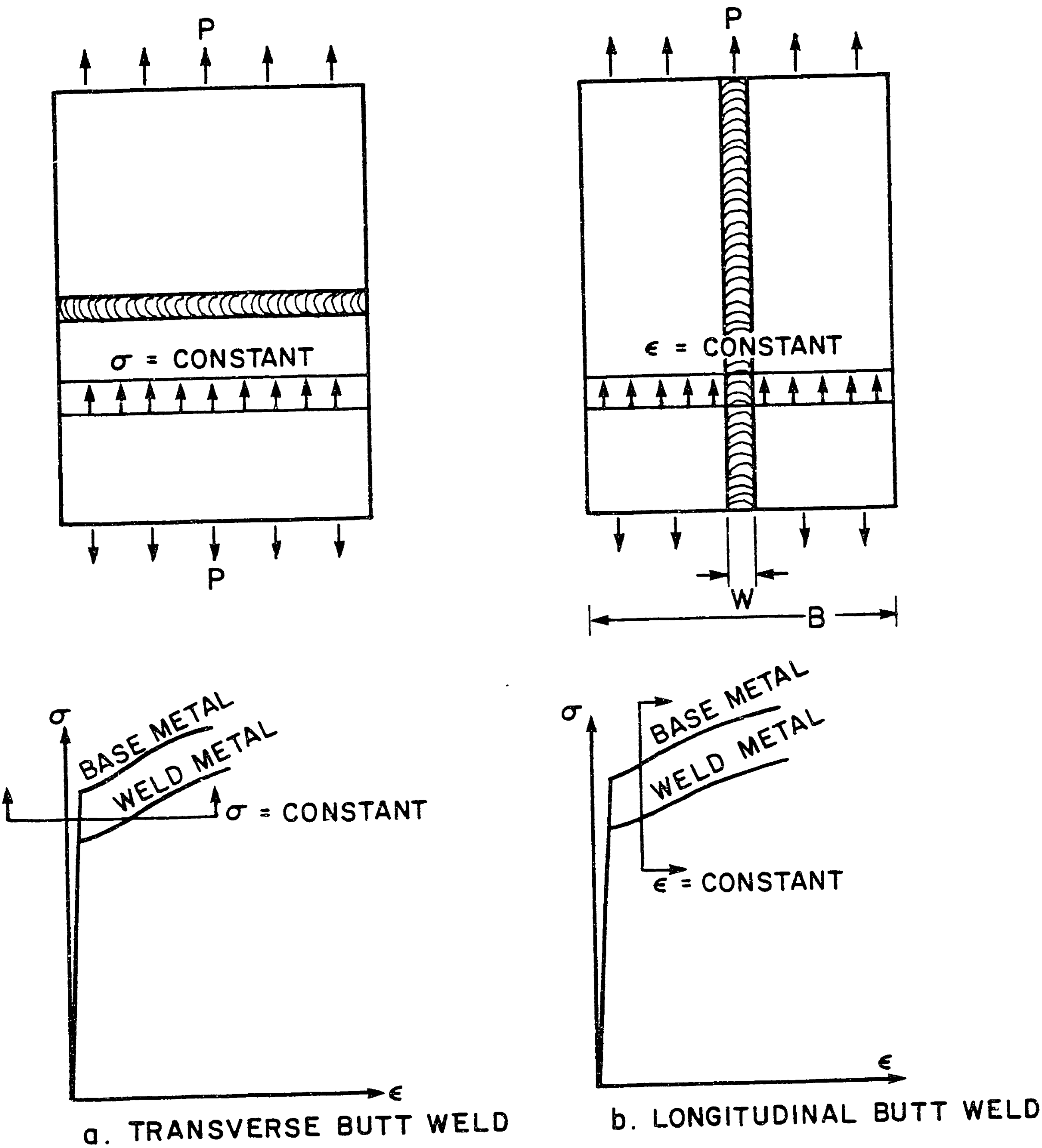

Figure 3.1 : Butt welds subjected to tensile loading,
(a) transverse to the weld line and
(b) parallel to the weld line.

(by the F.E.M. method).

3.1.2 Plane Strain Case-Infinite Width Plate

An idealized butt welded joint is shown in Figure 3.2. If the weld metal is of lower yield strength the plastic flow under tensile loading starts in the interlayer. Large transverse plastic flow near the base metal will be prevented and the triaxial stress state in the interlayer will be similar to the one of the neck of a tension specimen.

When the joint width W_o is much larger than the thickness t_o and H_o, deformations in the direction of the width will take place in planes perpendicular to the x axis except for parts close to the ends. The case is eventually one of plane strain with $\varepsilon_x = 0$.

We further assume the following:

- The joints consist only of two kinds of metals each being an isotropic and homogeneous material.
- The base metals behave like rigid bodies and do not contract in the thickness direction even when plastic flow occurs sufficiently in the soft interlayer.
- During the deformation of the neck there is no permanent volume change.
- The equivalent stress $\bar{\sigma}$ versus equivalent strain $\bar{\varepsilon}$ relation of the soft interlayer is

$$\bar{\sigma} = K\bar{\varepsilon}^n \tag{3-1}$$

  where K and n are material constants.

The analysis of the triaxial stress state in the neck was performed by Satoh and Toyoda,[13],in a way similar to the one

(I) Hard base metal
(II) Soft interlayer

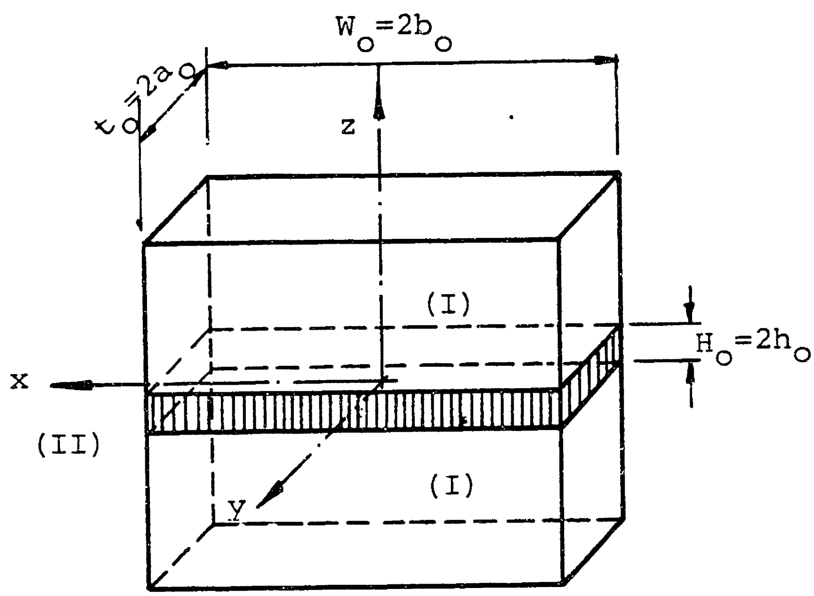

Figure 3.2 : Idealized model of two butt welded plates with a lower strength interlayer. (Plane strain case for $W_o \gg t_o$)

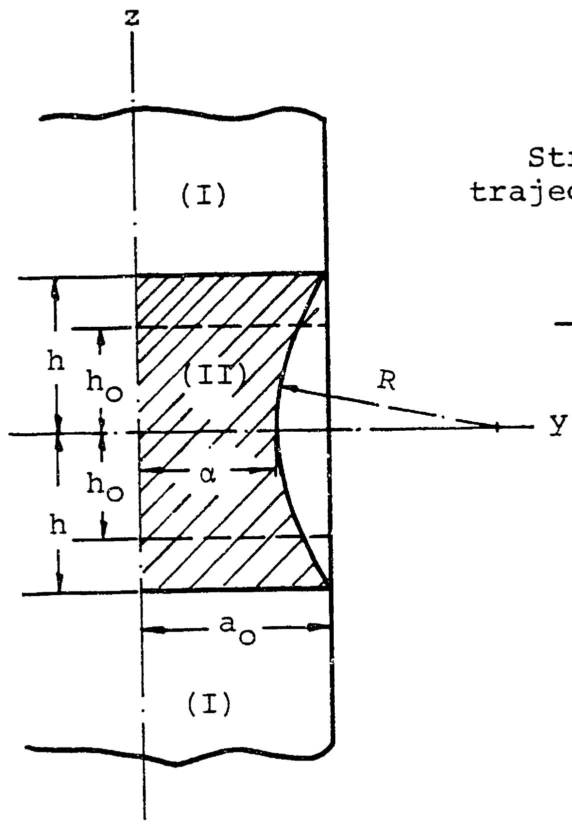

(I) Hard base metal
(II) Soft interlayer

Figure 3.3 :
Deformation of welded joints including a soft interlayer (plane strain case)

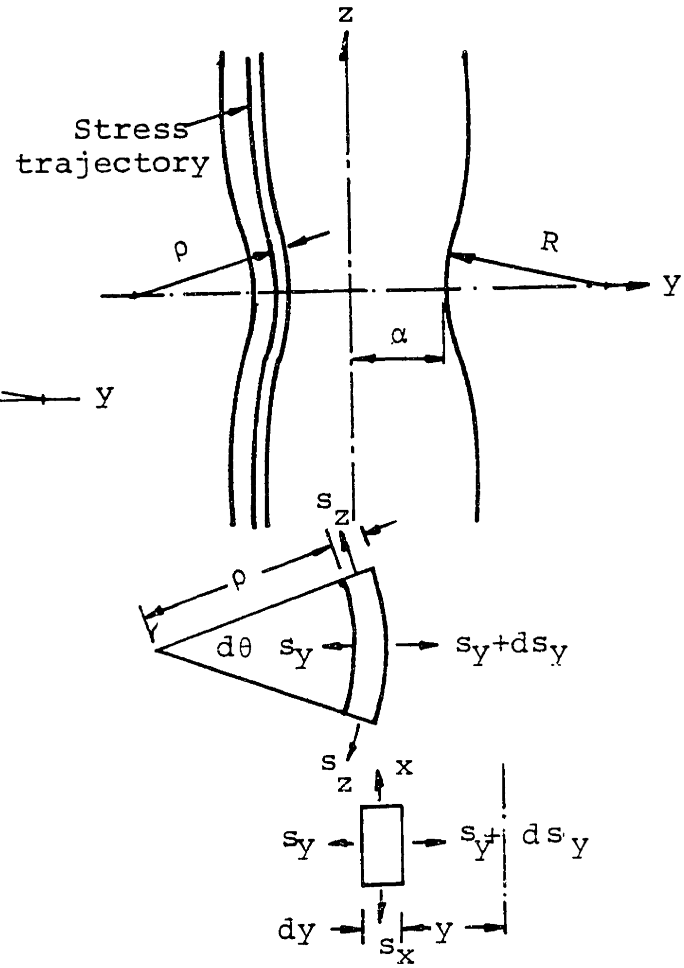

Figure 3.4 :
Deformation of the neck area. Stress trajectories and equilibrium. (plane strain case)

followed by Davidenkov and Spiridonova [31].

Let s_x, s_y, s_z be the true stress components at the neck, e_x, e_y, e_z the true strains and ε_x, ε_y, ε_z the corresponding engineering strains. Refering to Figure 3.4, we denote by ρ the radius of curvature of a certain stress trajectory in the yz plane. For an element at the neck having a unit length in the x-direction, the stress equilibrium in the y-direction will give:

$$-s_y \rho \, d\theta + (s_y + ds_y)(\rho + dy)d\theta - s_z dy d\theta = 0 \qquad (3\text{-}2)$$

but since $d_y/\rho << 1$, (2) gives:

$$ds_y = \frac{1}{\rho}(s_z - s_y)dy \qquad (3\text{-}3)$$

Supposing that the material yields according to Von Mises yield condition we have :

$$(s_x - s_y)^2 + (s_y - s_z)^2 + (s_z - s_x)^2 = 2\bar{\sigma}^2 \qquad (3\text{-}4)$$

where $\bar{\sigma}$ the equivalent stress. But for the plane strain state

$$e_x = 0$$

and

$$s_x = \frac{1}{2}(s_z + s_y) \qquad (3\text{-}5)$$

thus, from (4) and (5), the yield condition will be:

$$s_z - s_y = \frac{2}{\sqrt{3}}\bar{\sigma} \qquad (3\text{-}6)$$

(6) in (3) gives

$$s_y = \frac{2}{\sqrt{3}}\int_y^{\alpha} \bar{\sigma}\frac{dy}{\rho} \qquad (3\text{-}7)$$

and then from (6)

$$s_z = \frac{2}{\sqrt{3}} \left\{ \bar{\sigma} + \int_y^{\alpha} \bar{\sigma} \frac{dy}{\rho} \right\} \tag{3-8}$$

Now we use two experimental observations made by Davidenkov and Spiridonova (and also used by Bridgman [32] with no experimental basis).

(a) the e_y and e_z strains are independent of y (same across the section).

(b) the curvature $1/\rho$ of the stress trajectory is proportional to y that is

$$\frac{1}{\rho} = \frac{y}{\alpha R} \tag{3-9}$$

(7), (8) and (9) then give:

$$s_y = \frac{2}{\sqrt{3}} \bar{\sigma} \frac{\alpha^2 - y^2}{2\alpha R} \tag{3-10}$$

$$s_z = \frac{2}{\sqrt{3}} \bar{\sigma} \left(1 + \frac{\alpha^2 - y^2}{2\alpha R} \right) \tag{3-11}$$

Thus, the average axial stress at the neck will be:

$$\tilde{s}_z = \frac{1}{\alpha} \int_0^{\alpha} s_z dy = \frac{2}{\sqrt{3}} \bar{\sigma} \left(1 + \frac{\alpha}{R} \right) \tag{3-12}$$

But from (1)

$$\bar{\sigma} = K\bar{\varepsilon}^n$$

and

$$\bar{\varepsilon} = \frac{2}{\sqrt{3}}\sqrt{e_x^2 + e_y^2 + e_z^2} \qquad (3\text{-}13)$$

However, for plane strain $e_x = 0$ and for volume conservation $e_y = -e_z$, therefore the equivalent strain will be:

$$\bar{\varepsilon} = \frac{2}{\sqrt{3}} e_z \qquad (3\text{-}14)$$

and

$$\bar{\sigma} = \left(\frac{2}{\sqrt{3}}\right)^n K\, e_z^n \qquad (3\text{-}15)$$

which substituted back to (12) gives:

$$\tilde{s}_z = \left(\frac{2}{\sqrt{3}}\right)^{n+1} K \left(1 + \frac{\alpha}{3R}\right) e_z^n$$

or rewriting it in terms of nominal stress σ_z and strain ε_z

$$\sigma_z = \left(\frac{2}{\sqrt{3}}\right)^{n+1} \frac{K\{\ell n(1+\varepsilon_z)\}^n}{1+\varepsilon_z} \left(1 + \frac{\alpha}{3R}\right) \qquad (3\text{-}16)$$

since

$$\tilde{s}_z = \sigma_z(1+\varepsilon_z)$$

and

$$e_z = \ell n(1+\varepsilon_z)$$

From geometry in Figure 5, we have for the nominal strain ε_y

$$\varepsilon_y = \frac{\alpha - \alpha_o}{\alpha_o} = \frac{\alpha}{\alpha_o} - 1$$

But $$e_y = \ln(1+\varepsilon_y)$$

and from volume conservation

$$e_y = -e_z$$

then

$$\frac{\alpha}{\alpha_o} = e^{-e_z} = e^{-\ln(1+\varepsilon_z)} = \frac{1}{1+\varepsilon_z} \qquad (3\text{-}17)$$

Also from the geometry

$$\sqrt{R^2 - h^2} = R - (\alpha_o - \alpha)$$

or,

$$h^2 = (\alpha_o - \alpha)\ [2R - \alpha_o + \alpha] \qquad (3\text{-}18)$$

and from volume conservation:

$$\alpha_o h_o = (\alpha + R)\ h - \frac{1}{2}\left(R h \sqrt{1-\left(\frac{h}{R}\right)^2} + R^2 \sin^{-1}\frac{h}{R}\right) \qquad (3\text{-}19)$$

If we now introduce:

$$X_t = \frac{h_o}{\alpha_o}, \qquad Y_t = \frac{\alpha}{3R}, \qquad \varepsilon = \frac{1}{1+\varepsilon_z} \qquad (3\text{-}20)$$

we get from eqns. (17), (18) and (19)

$$X_t = \frac{1}{\sqrt{3}} \sqrt{(1-\varepsilon)\left\{\frac{2\varepsilon}{Y_t} - 3\ (1-\varepsilon)\right\}} \cdot \left\{\frac{2\varepsilon + 1}{3} - \frac{(1-\varepsilon)^2 Y_t}{2\varepsilon}\right\} \qquad (3\text{-}21)$$

Equation (21) relates ε to Y_t for every X_t and together with (16) gives the stress strain (σ_z vs. ε_z) relation for every $X_t = h_o/\alpha_o$.

Based on equations (16) and (21) Satoh and Toyoda

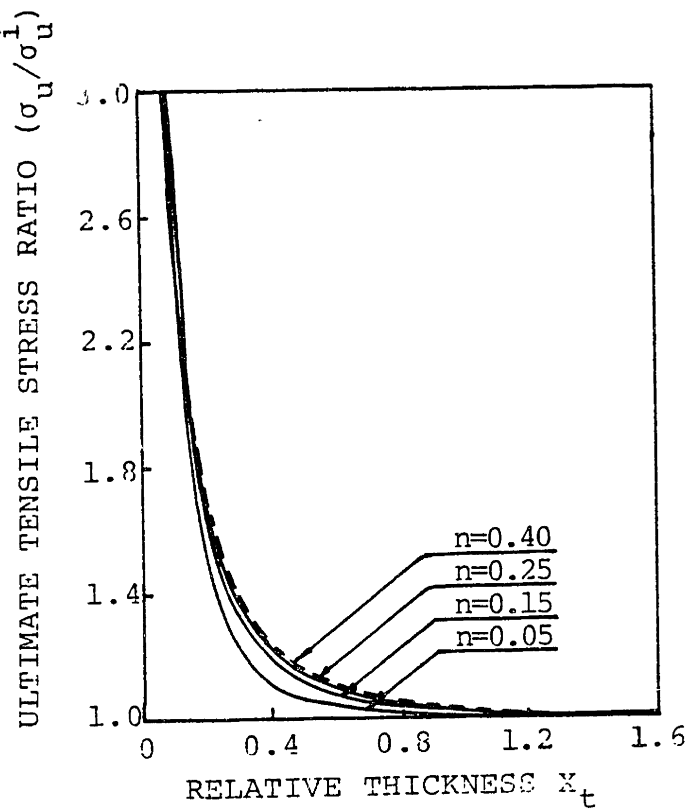

Figure 3.5 : Ultimate tensile strength in the plane state case as a function of relative thickness X_t (Assume a stress strain law : $\sigma=K.\varepsilon^n$) ,[13]

calculated different $\sigma_z - \varepsilon_z$ curves and determined the effect of relative thickness on the ultimate and yield strength (Figure 3.5).

Taking into account the effect of plastic flow in the base metals, however, the results derived earlier are modified, as shown by the dotted curves of Figure 2.2 [14]. In the same figure, are shown some experimental results also by Satoh and Toyoda.

3.1.3 Axisymmetric Case

For the case of a round tensile specimen which deforms as in Figure 3.6, we will start with similar assumptions as before.

- Both base material and the soft interlayer are uniform and isotropic materials.
- Suppose (in a first approximation) that the base material is rigid.
- Suppose that the interface between the soft and the hard layer remains perpendicular to the loading direction.
- After necking the joint configuration will be as in Figure 3.6.
- Volume remains constant.
- The true stress-true strain law will be

$$S = Ke^n \tag{3-22}$$

Again based on Davidenkov's analysis and assuming that the stress trajectories will be as in Figure 3.7, we further assume that

- the tangential and radial true strains are equal, and since volume is constant we get:

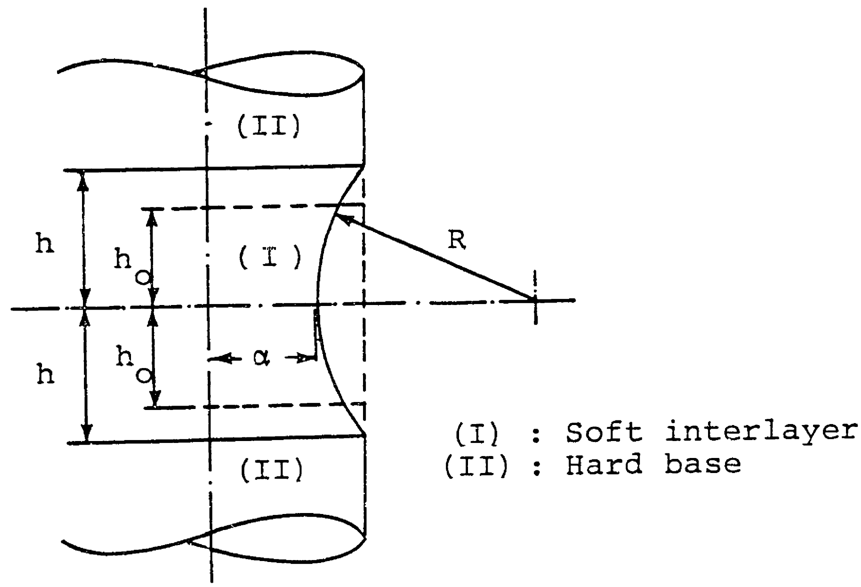

Figure 3.6 : Welded joint including soft interlayer - Axisymmetric case

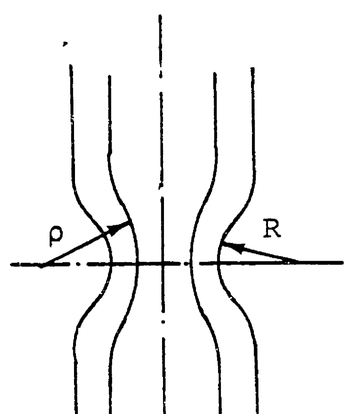

Figure 3.7 : Sketch of the stress trajectories in the neck of a round tensile specimen

$$e_r = e_\theta = -\frac{1}{2} e_z \qquad (3\text{-}23)$$

and

-the curvature is linearly related to the radius or

$$\frac{1}{\rho} = \frac{r}{\alpha R} \qquad (3\text{-}24)$$

We further assume that the strain does not change along the neck cross section and, thus, the differences in principal stresses are also the same, according to hypotheses of both maximum shearing stress and the octahedral shearing stress. So starting with the equilibrium equation in the radial direction and integrating along a section we get:

$$s_r = s_o \int_r^\alpha \frac{dr}{\rho} \qquad (3\text{-}25)$$

where s_o denotes the difference in principal stresses. Now using (24) we get

$$s_r = \frac{s_o \, (\alpha^2 - r^2)}{2R\alpha} \qquad (3\text{-}26)$$

whereas the axial stress will then be:

$$s_z = s_o + s_r = s_o \left\{ 1 + \frac{\alpha^2 - x^2}{2R\alpha} \right\} \qquad (3\text{-}27)$$

and the average axial stress will be

$$\tilde{s}_z = s_o \left\{ 1 + \frac{\alpha}{4R} \right\} \qquad (3\text{-}28)$$

If e_r, e_θ, e_z are the true strains and ε_r, ε_θ and ε_z are the engineering ones then from geometry:

$$\varepsilon_r = \frac{\alpha - \alpha_o}{\alpha_o} = \frac{\alpha}{\alpha_o} - 1$$

or

$$\frac{\alpha}{\alpha_o} = 1 - \frac{\varepsilon_z}{2} \qquad (2\text{-}29)$$

and also from geometry

$$h_o^2 = (\alpha_o - \alpha)\ (2R - \alpha_o + \alpha) \qquad (3\text{-}30)$$

whereas from volume conservation

$$(2R^2 + 2\alpha R + \alpha^2)h - \frac{h^3}{3} - (R + \alpha)\ .$$

$$\cdot \left\{ Rh\sqrt{1 - \frac{h^2}{R^2}} + R^2 \sin^{-1} \frac{h}{R} \right\} = \alpha_o^2\ h_o \qquad (3\text{-}31)$$

which after expanding in series in h/R and keeping the first terms only gives:

$$\alpha h^3 + 3\alpha^2 Rh - 3\alpha_o^2 R\, h_o = 0 \qquad (3\text{-}32)$$

introducing now

$$x \equiv \frac{h}{R} \quad \text{and} \quad y \equiv \frac{\alpha_o}{R}\ ,\ X = \frac{h_o}{\alpha_o}$$

we rewrite eqns. (30) and (32) as

$$x^2 = y\varepsilon_z \left(1 - \frac{y\varepsilon_z}{4}\right) \qquad (3\text{-}33)$$

and

$$yx\left(1-\frac{\varepsilon_z}{2}\right)^2 + \frac{1}{3}\,yx^3\left(1-\frac{\varepsilon_z}{2}\right) = y^3x \qquad (3\text{-}34)$$

and also

$$X = \left(1-\frac{\varepsilon_z}{2}\right)^2 \sqrt{\frac{\varepsilon_z}{y} - \frac{\varepsilon_z^2}{4}} + \qquad (3\text{-}35)$$

$$+ \frac{1}{3}\left(1-\frac{\varepsilon_z}{2}\right)\cdot y \cdot \left(\sqrt{\frac{\varepsilon_z}{y} - \frac{\varepsilon_z^2}{4}}\right)^3$$

Introducing

$$Y \equiv \frac{\alpha}{4R} = \frac{y}{4}\left(1-\frac{\varepsilon_z}{2}\right)$$

(35) gives

$$X = \frac{1}{2}\left(1-\frac{\varepsilon_z}{2}\right)^2 \sqrt{\frac{\varepsilon_z\left(1-\frac{\varepsilon_z}{2}\right)}{Y} - \varepsilon_z^2} + \qquad (3\text{-}36)$$

$$+ \frac{1}{6}\,Y\left\{\sqrt{\frac{\varepsilon_z\left(1-\frac{\varepsilon_z}{2}\right)}{Y} - \varepsilon_z^2}\right\}^3$$

Now rewriting (28) using (22)

$$\tilde{s}_z = Ke^n\left(1+\frac{\alpha}{4R}\right) \qquad (3\text{-}37)$$

where pluging the nominal stress and engineering strain we finally get:

$$\sigma_z = K\{\ell n\ (1 + \varepsilon_z)\}^n \left(1 + \frac{\alpha}{4R}\right)\left(1 - \frac{\varepsilon_z}{2}\right)^2$$

or

$$\sigma_z = K\{\ell n\ (1 + \varepsilon_z)\}^n\ (1 + Y) \left(1 - \frac{\varepsilon_z}{2}\right)^2 \qquad (3\text{-}38)$$

(38) together with (36) relate σ_z and ε_z for every value of $X = (h_o/\alpha_o)$

Satoh and Toyoda used the above relations in predicting the stress-strain curves of Figure 3.8 and the relation of ultimate tensile strength and relative thickness of Figure 3.9 [14]. More results can be found in other papers reviewed in [16] and [11].

Although the assumption of rigid base plate is justifiable in the plane strain case, it is not realistic in the axisymmetric case. Analysis taking into account the yielding of the base material was also performed by Satoh and Doi and results appear in [11].

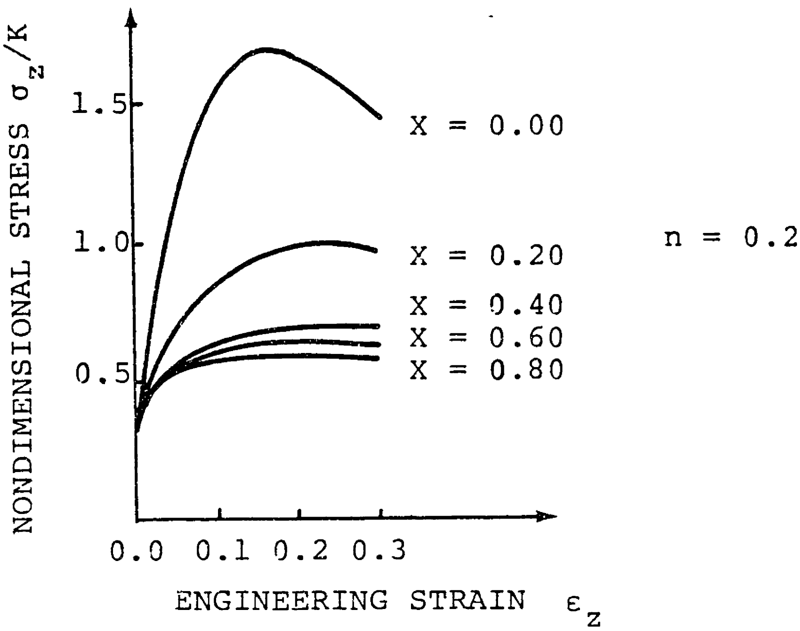

Figure 3.8 : Families of axial nominal stress vs engineering strain curves.
(K and n are the stress - strain law constants)

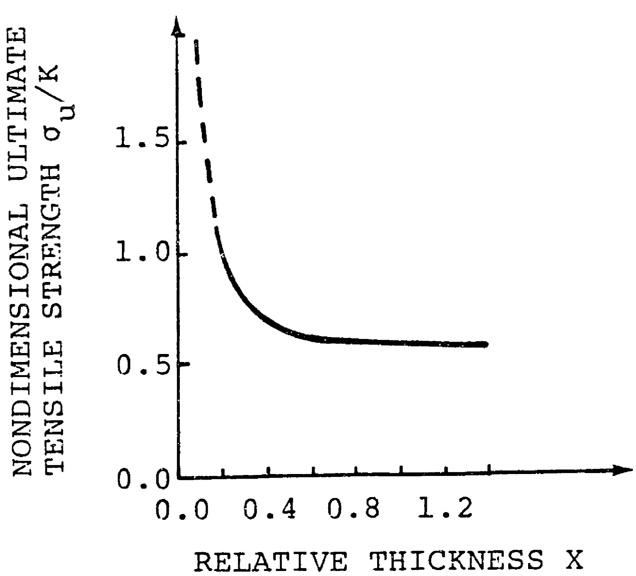

Figure 3.9 : Ultimate tensile strength as a function of relative thickness X

3.2 Numerical Strength Evaluation by the Finite Element Method

3.2.1 General Approach

Although experimental results seem to verify the analytical predictions an attempt was made in this study to confirm the assumptions and results of theoretical analysis using the finite element program ADINA , [4].

Both two dimensional plane strain and axisymmetric analysis was performed corresponding to the wide plate and round bar idealized geometries treated by other researchers.

To investigate the stress strain state at large deformations a nonlinear incremental analysis, using the Updated Lagrangian formulation, [33], was employed.

An elastic-plastic material model was used, assuming linear strain hardening and Von-Mises yield condition. The bilinear stress strain law for the model is shown in Figure 8.10, and the mechanical properties of base metal and interlayer are given in Table 8.1 .

With ADINA the material model #8 was mainly employed. However, to test the improvement of convergence, material model #10 (thermo-elastic-plastic and creep) was occasionaly used at reference temperature. The latter model incorporates an option of optimizing the time step subdivision, taking into account the convergence characteristics of the iterative calculations [4].

The ultimate strength value was not incorporated into the model but was implied in a way discussed later.

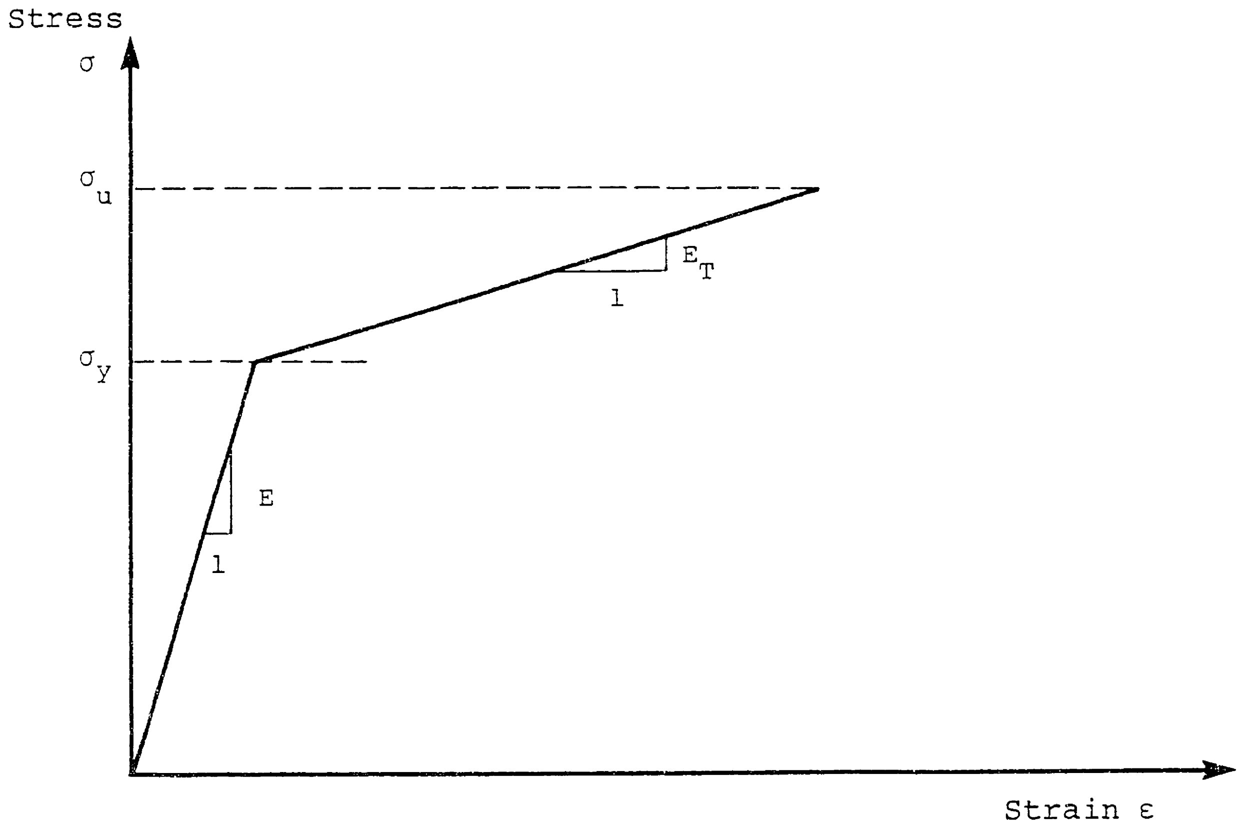

Figure 3.10 : Bilinear stress-strain law used in the model

Table 3.1 : Mechanical properties of the base and filler metal

	E Kg/mm^2	E_T Kg/mm^2	ν	σ_y Kg/mm^2	σ_u Kg/mm^2
HT-80 (base metal)	2.1 10^4	1/12 10^3	0.3	78.0	84.1
HT-50 (soft interlayer)	"	"	"	48.8	58.3

3.2.2 Simulation of the Tensile Tests

For the simulation of the tensile tests, a prescribed loading formulation was preferred, because it was found better than a prescribed displacement one in equilibrium iterating in the plane strain model.

The time dependence of the loading had to be such as to ensure that for each time increment the respective strain increments were small enough. Thus an initial estimate of the loading that causes yielding was required in order to adjust the time increments.

So it was initially assumed that:

$$\sigma_2 = 0 \qquad \text{in the plane strain state}$$

and

$$\sigma_r = \sigma_\theta = 0 \quad \text{in the axisymmetric case}$$

Thus for the plane strain case where

$$\varepsilon_3 = \frac{1}{E}\left(\sigma_3 - \nu\left(\sigma_2 + \sigma_1\right)\right) = 0$$

we get:

$$\sigma_3 = \nu(\sigma_2 + \sigma_1)$$

And assumming

$$\sigma_2 = 0$$

we get

$$\sigma_3 = \nu\sigma_1$$

Substituting in the Von Mises yield condition

$$(\sigma_1 - \sigma_2)^2 + (\sigma_2 - \sigma_3)^2 + (\sigma_3 - \sigma_1)^2 = 2\sigma_{yp}^2$$

we get

$$\sigma_1^2[1 + \nu^2 - \nu] = \sigma_{yp}^2$$

Hence the loading at yield must now be

$$\sigma_1^2 = \sigma_{yp}^2 \ / \ [1 + \nu^2 - \nu]$$

which for steel ($\nu = 0.3$) becomes

$$\sigma_2^1 = \sigma_{yp}^2 \ / \ 0.79$$

or

$$\sigma_1 = 1.125 \ \sigma_{yp}$$

where σ_{yp} the yield stress in simple tension.

For the axisymmetric case the estimate of the load at yield simply is equal to the yield stress in simple tension.

This for the base metal and soft interlayer materials in Table 3.1, the estimates of load at yield were :

$$\begin{cases} P_{(I)} \approx 87.75 \ Kg/mm^2 & \text{and} \\ P_{(II)} \approx 54.9 \ Kg/mm^2 & \text{in plane strain and} \end{cases}$$

$$\begin{cases} P_{(I)} \approx 78 \ Kg/mm^2 & \text{and} \\ P_{(II)} \approx 48.8 \ Kg/mm^2 & \text{in the axisymmetric case.} \end{cases}$$

The respective loading histories are given in Figure 3.11 and 3.12

To investigate the effect of the different parameters [Length (L), plate thickness (t_o), layer thickness (H_o)] various configurations, shown in Table 3.2, were examined. Several element meshes were used and some of them are shown in Figure 3.13, 3.14, and 3.15.

To minimize the bandwidth of the resulting stiffness matrices, the numbering scheme shown in the above figures was used.

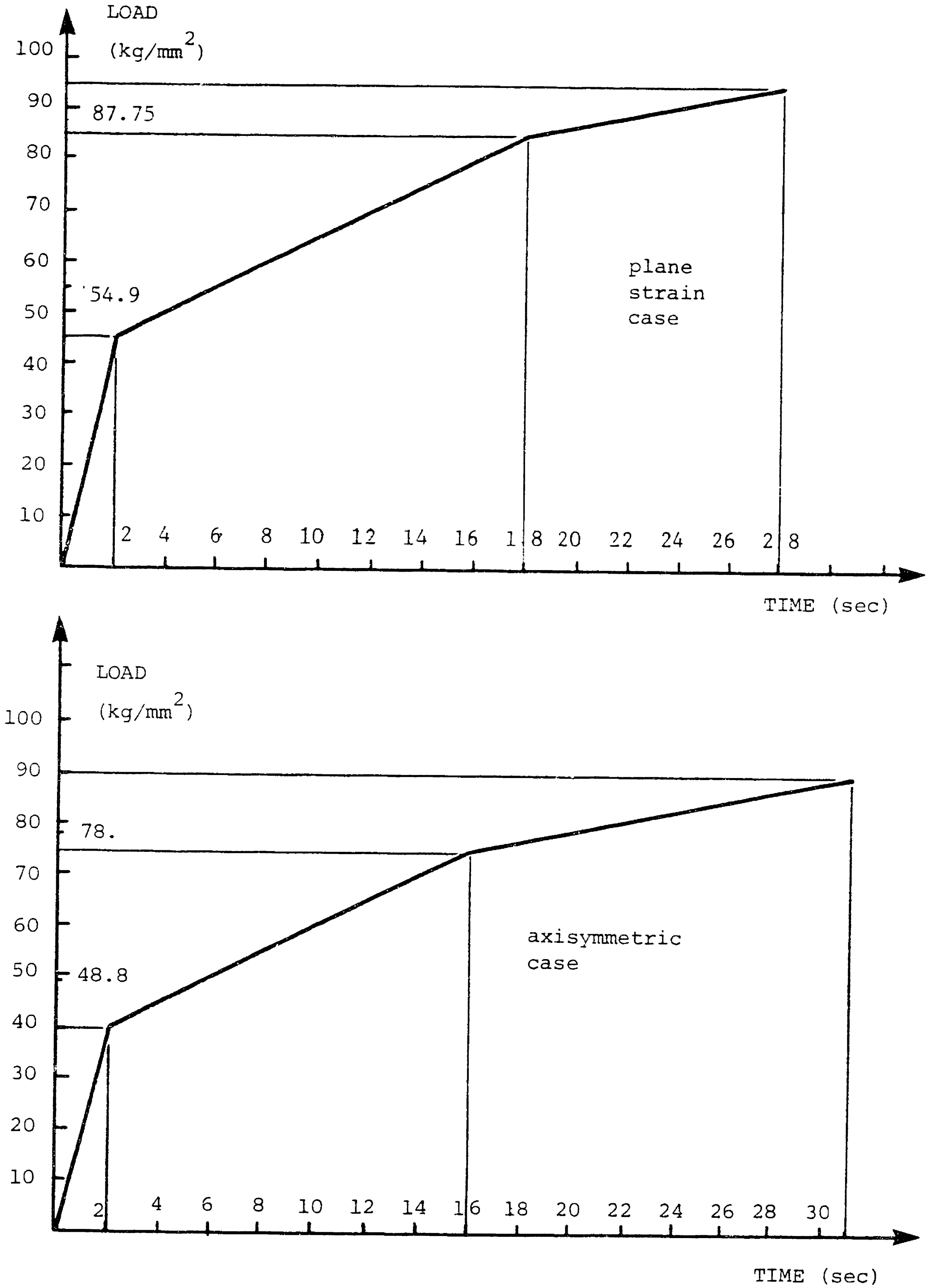

Figure 3.11 and 3.12 : Applied load history for the plane strain and axisymmetric case.

Table 3.2 : Dimensions of specimens modeled.

	Half length $L/2$ (mm)	Half plate Thickness $a_o = t_o/2$	Half interlayer Thickness $h_o=H_o/2$	Relative Thickness $X_t=h_o/a_o$
A1	200.	12.0	0.0	0.000
A2	200.	12.0	1.0	0.083
A3	200.	12.0	2.0	0.167
A4	200.	12.0	3.0	0.250
A5	200.	12.0	4.0	0.333
B1	200.	6.0	0.0	0.000
B2	200.	6.0	2.0	0.333
B3	200.	6.0	3.0	0.500
C1	200.	3.0	1.0	0.333
C2	200.	3.0	3.0	1.000
D1	100.	5.0	0.75	0.150
D2	100.	5.0	1.0	0.200
D3	100.	5.0	2.0	0.400
D4	100.	5.0	4.0	0.800

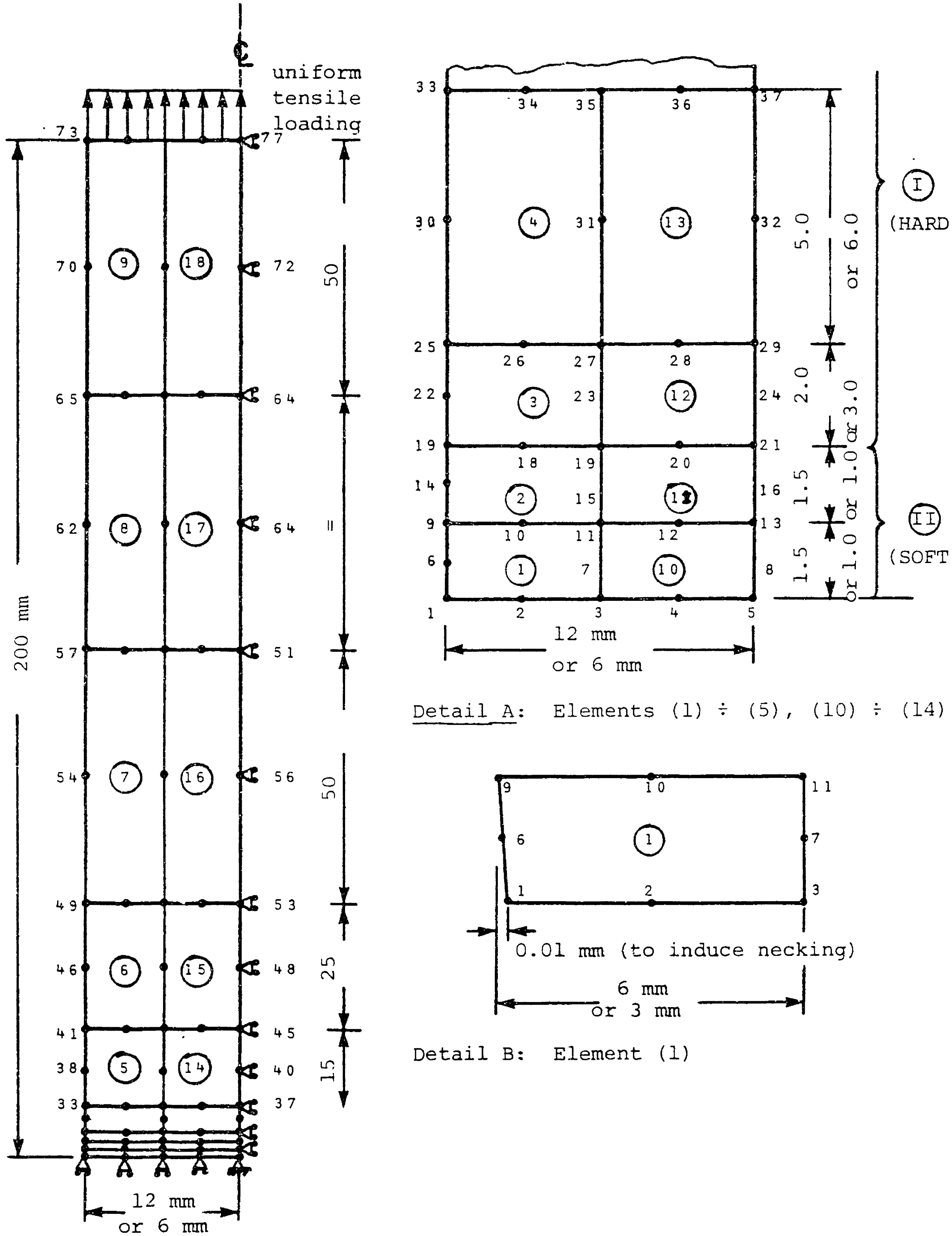

Figure 3.13 : Element mesh for undermatching joint.
Long specimen, plane strain case.
(Only a quarter of the specimen was modeled)

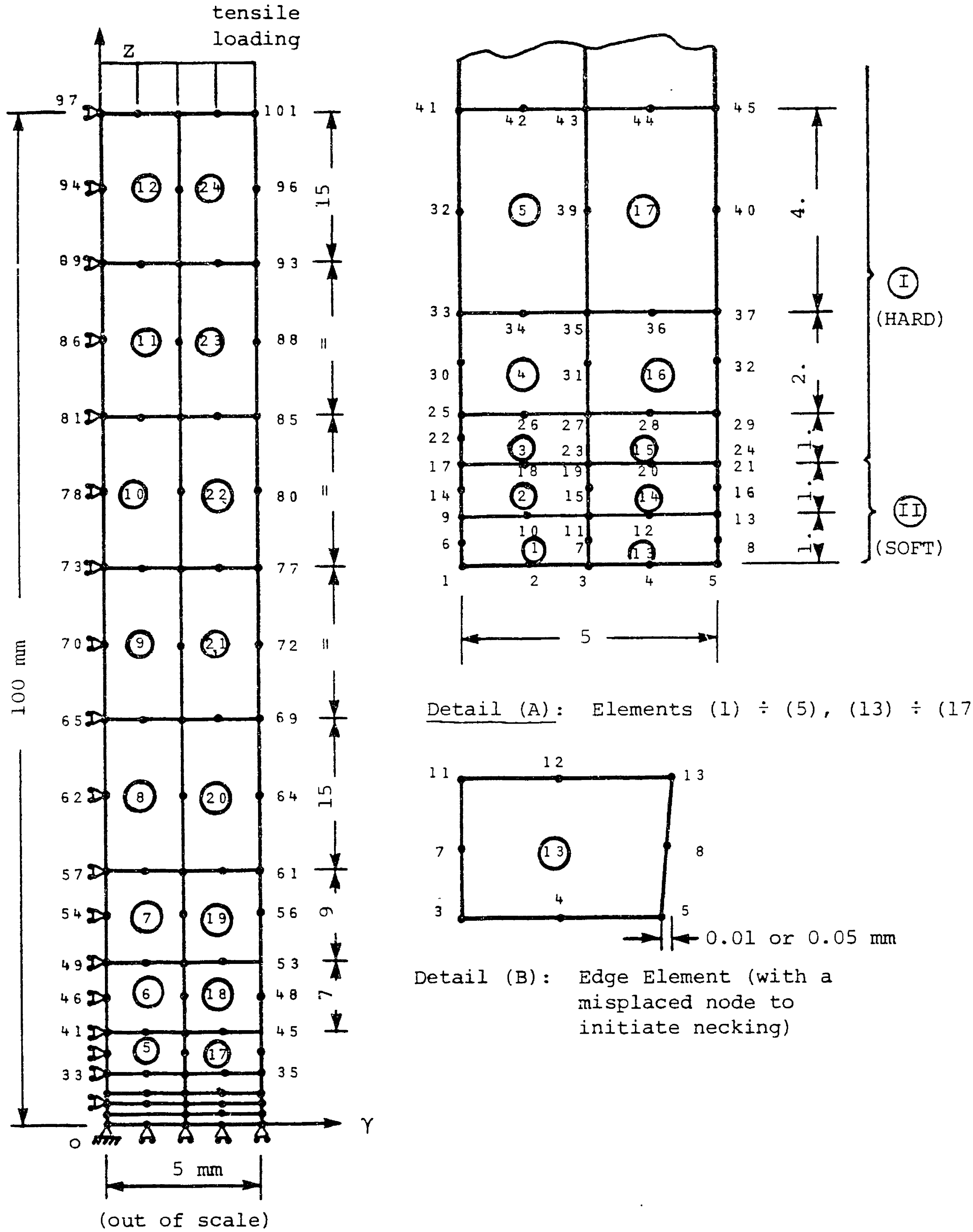

Figure 3.14 : Dense element mesh for undermatching joint. Short specimen . (Only a quarter of a specimen was modeled)

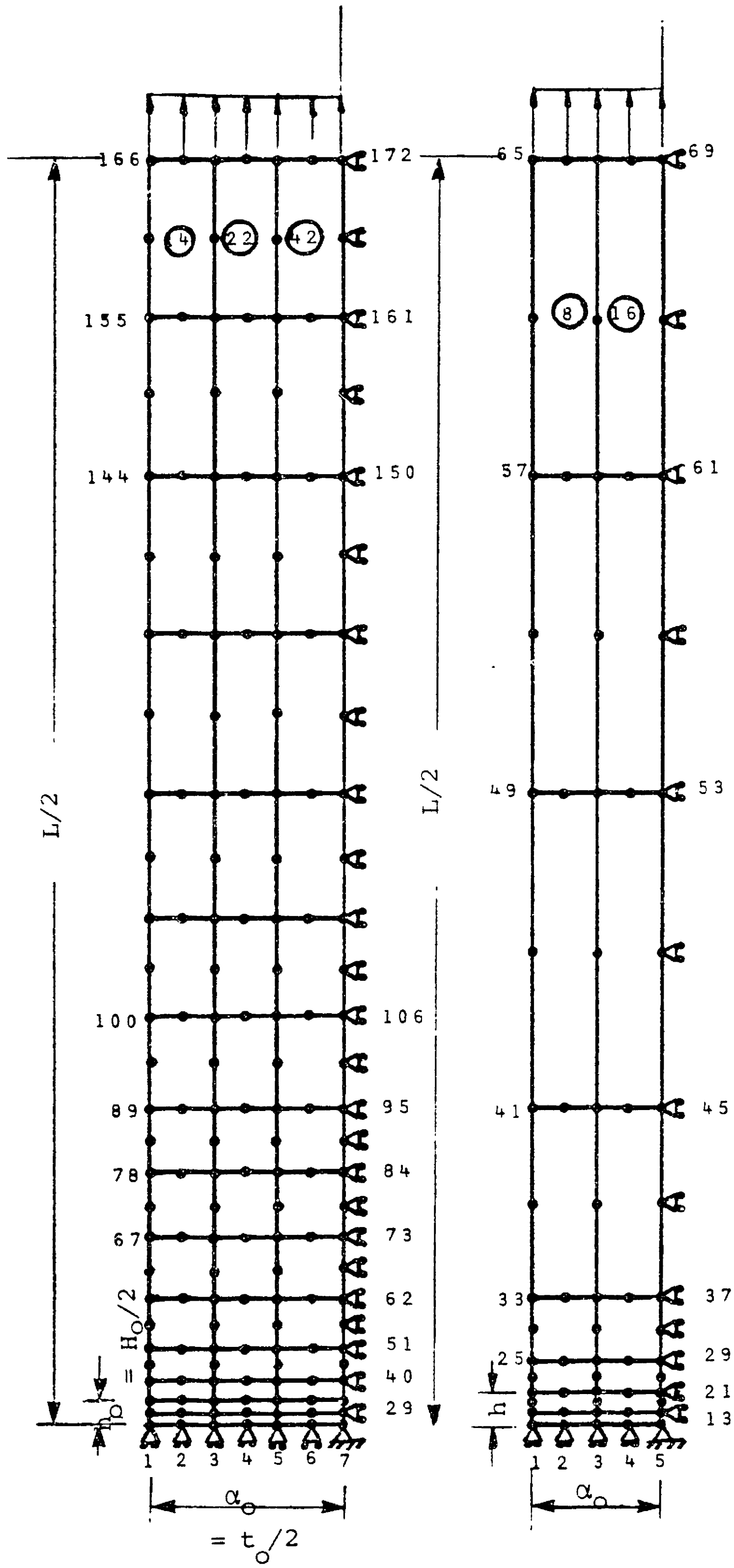

Figure 3.15 : Other element meshes used .

In all cases, 8 node quadratic isoparametric elements were employed. Using symmetry only a quarter of the plate's cross section had to be considered. Rigid body motion was prevented by fixing the center node.

Another important characteristic of the analysis was that, in order to induce necking, we had to incorporate a geometric imperfection. This was actually realized by slightly misplacing (e.g. 0.01 mm for a specimen half thickness of 12 mm) the end node of the middle cross section, as shown in Figures 3.13 and 3.14.

The material model used does not incorporate an ultimate tensile strength value. Therefore, during loading the finite element solution will give stress states not actually possible. Therefore, the load at fracture can be approximated as the one where the maximum observed equivalent stress, in either the base plate or the interlayer, is larger or equal to the ultimate tensile strength of the material in hand.

3.2.3 Results and Conclusions

The previously outlined procedure for the calculation of ultimate tensile strength of the joint is highlighted in Figure 3.16, where the maximum observed equivalent stress is plotted versus the applied tensile load for two different values of relative thickness. From the plot, we can easily estimate that the values of the applied load are

at yield of the interlayer:	55 Kg/mm^2	always
at yield of the base metal:	68 Kg/mm^2	for $X_t = 0.2$
	74 Kg/mm^2	for $X_t = 0.4$

at fracture (of interlayer): 78 Kg/mm^2 for $X_t = 0.2$

85 Kg/mm^2 for $X_t = 0.4$

Obviously fracture occurs first (and thus only) in the interlayer. The base metal yields at substantially higher load than the interlayer and thus confirms the assumption of the theoretical analysis that the base plate is rigid. Similar results were obtained also for the other investigated cases and some are given in Figure 3.17.

The applied load at fracture for different relative thickness $X_t = h_o/\alpha_o$ is shown in Figure 3.18. Similarly the load at yield of both the base plate and the interlayer is shown in Figure 3.19. The results of Figure 3.18, show a very good correlation with the theoretical ones for an infinite plate obtained by Satoh and Toyoda and confirm the fact that for decreasing X_t ($X_t<0.5$) the ultimate tensile strength of the joint is substantially higher than the U.T.S. of the interlayer (close to the U.T.S. of the base metal).

To estimate the yield strength of the overall joint, the applied load versus the elongation of a gauge length was plotted. The load at yield of the joint can then be approximated as the one that causes a sudden increase in the elongation. However, due to the arbitrariness of this gauge length (this is <u>not</u> an ordinary tensile specimen) no quantitative results are shown. The general trend, for all gauge lengths, was again increasing yield strength for decreasing $X_t (X_t<1)$. The relation between the applied load and the observed <u>end</u> displacements (gauge length equal to the specimen length) is shown in Figures 3.20 and 3.21

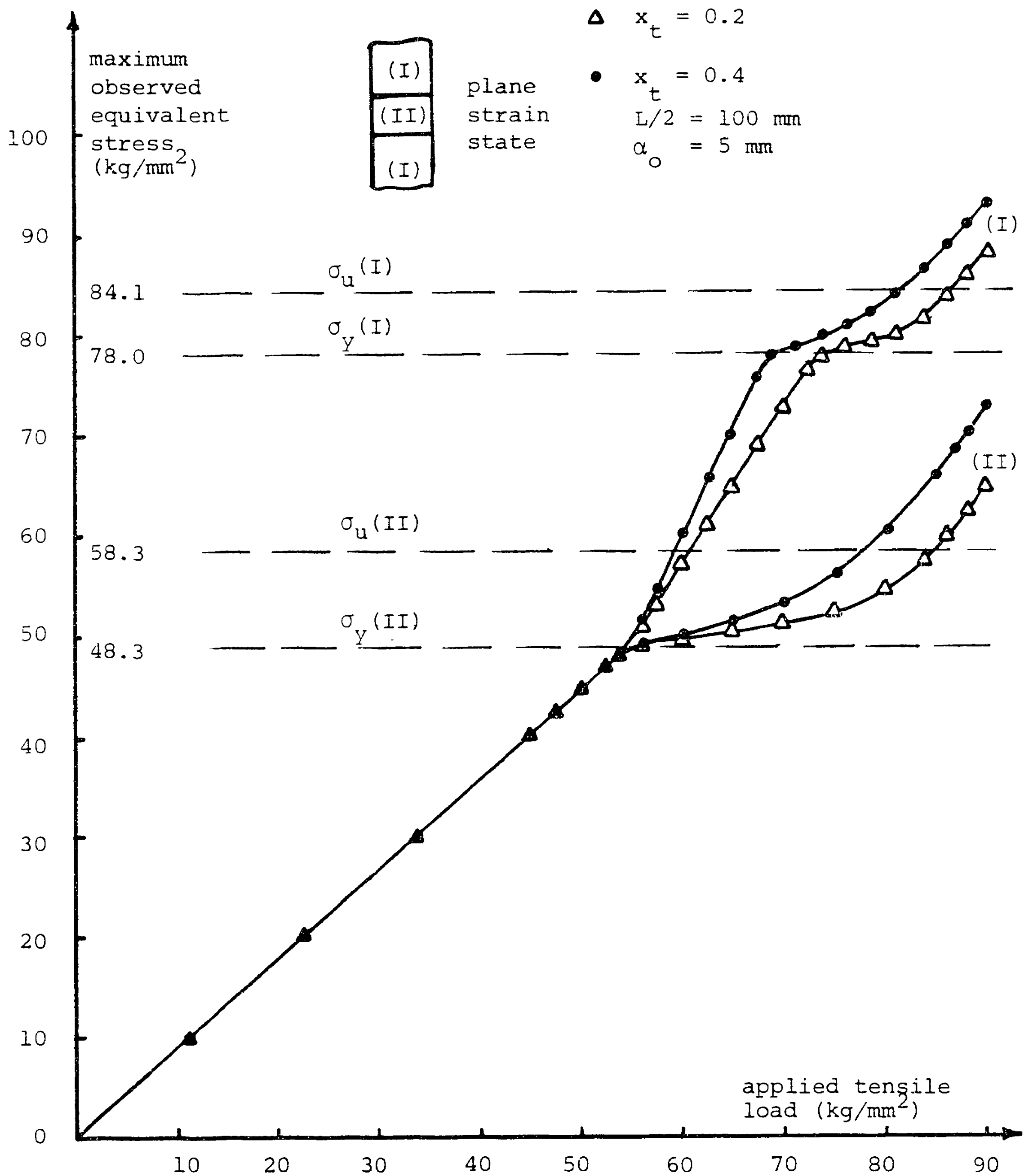

Figure 3.16 : Maximum observed equivalent stress versus applied tensile load. Short specimen ,plane strain case.

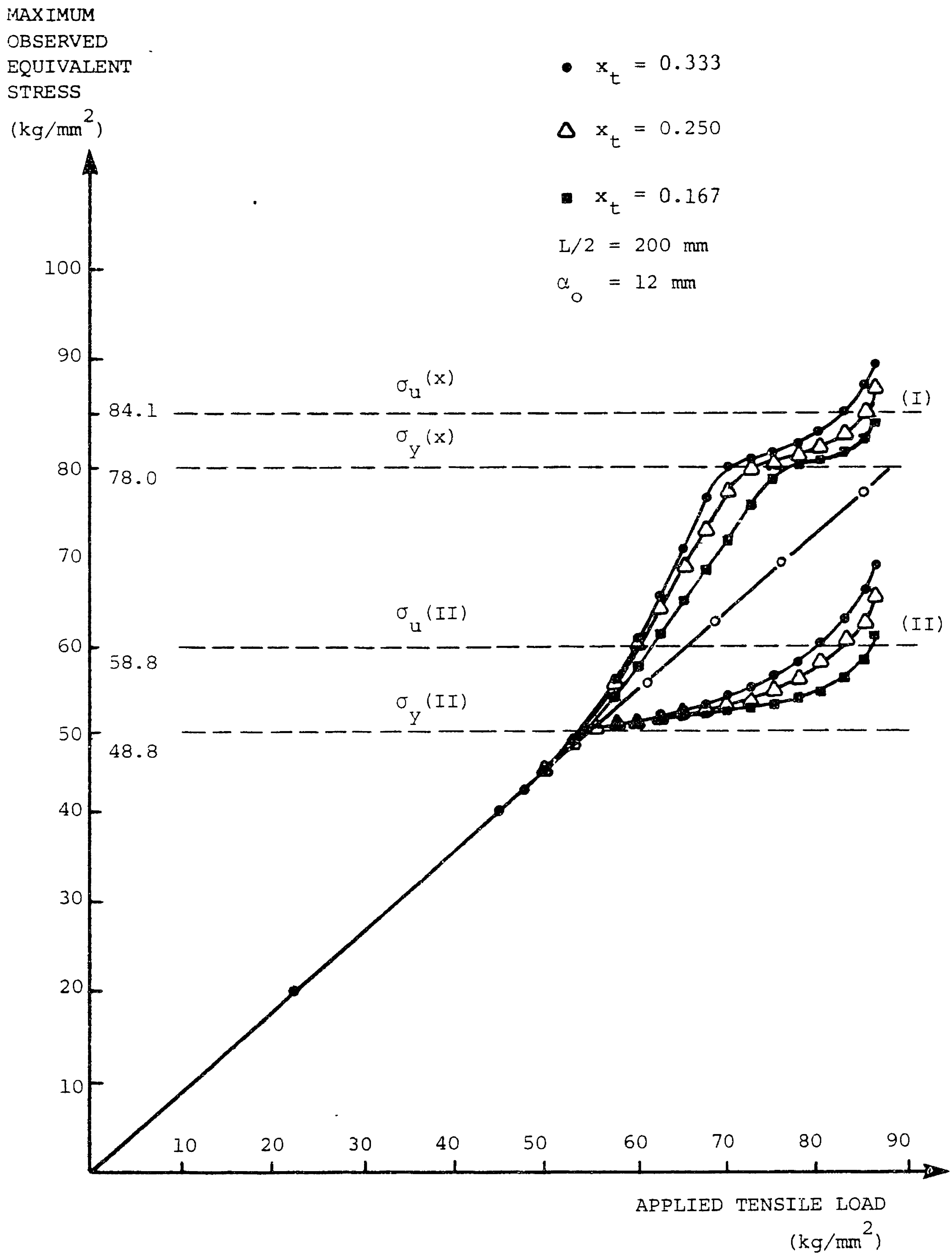

Figure 3.17 : Maximum observed equivalent stress vs applied load. Long specimen ,plane strain.

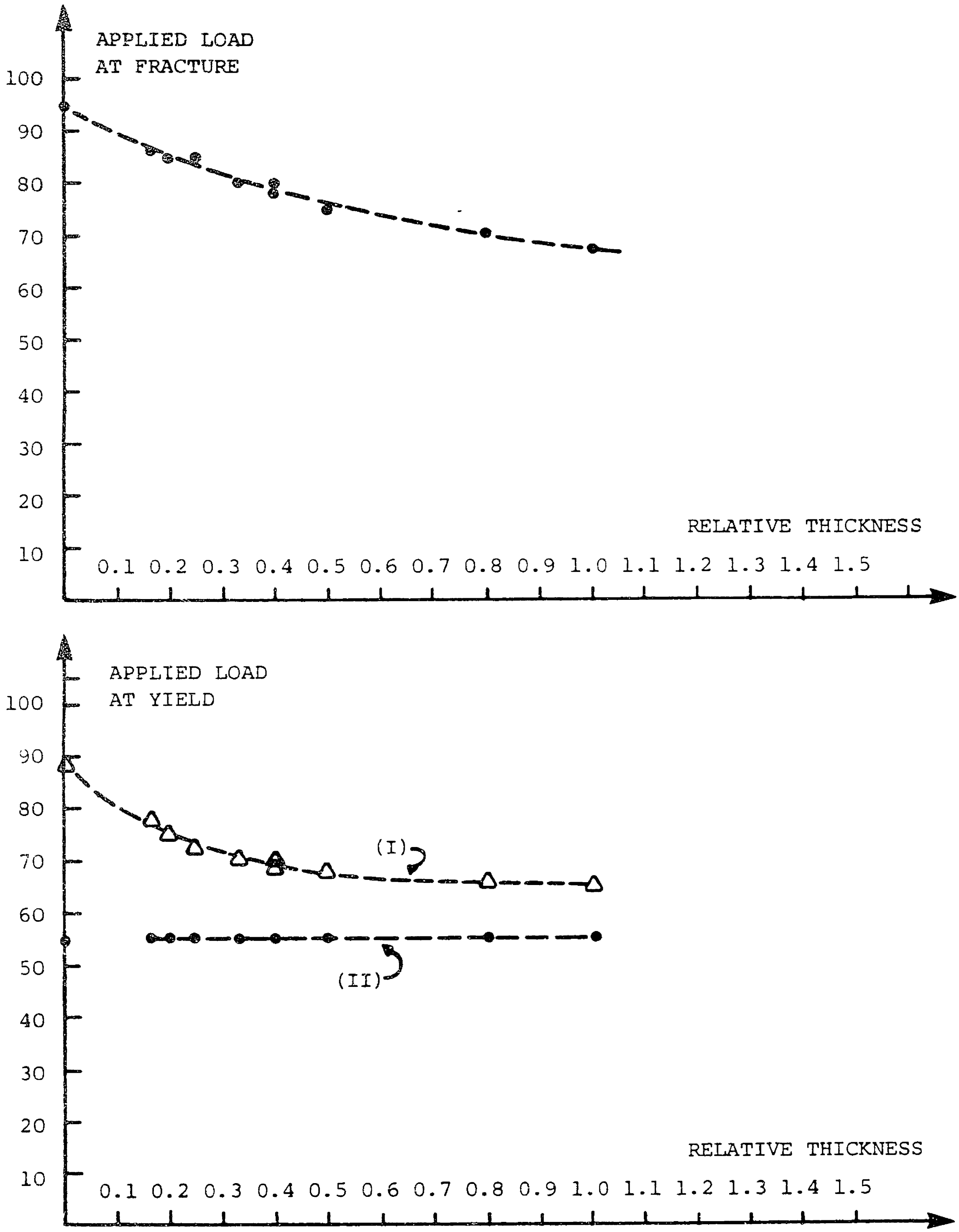

Figures 3.18 and 3.19 : Applied tensile load at fracture and yield.

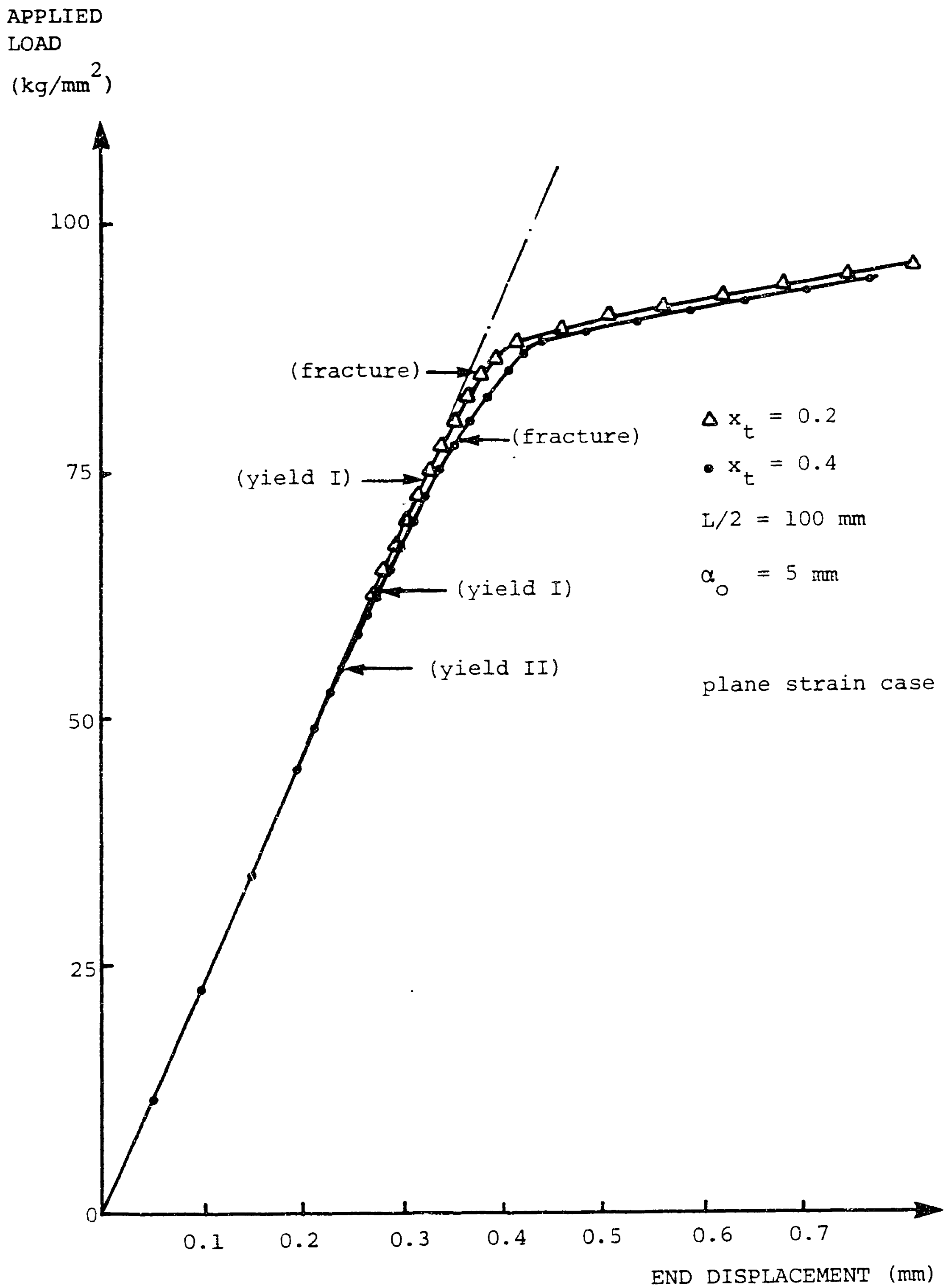

Figure 3.20 : Applied tensile load versus end displacement of the joint. Short specimen plane strain case.

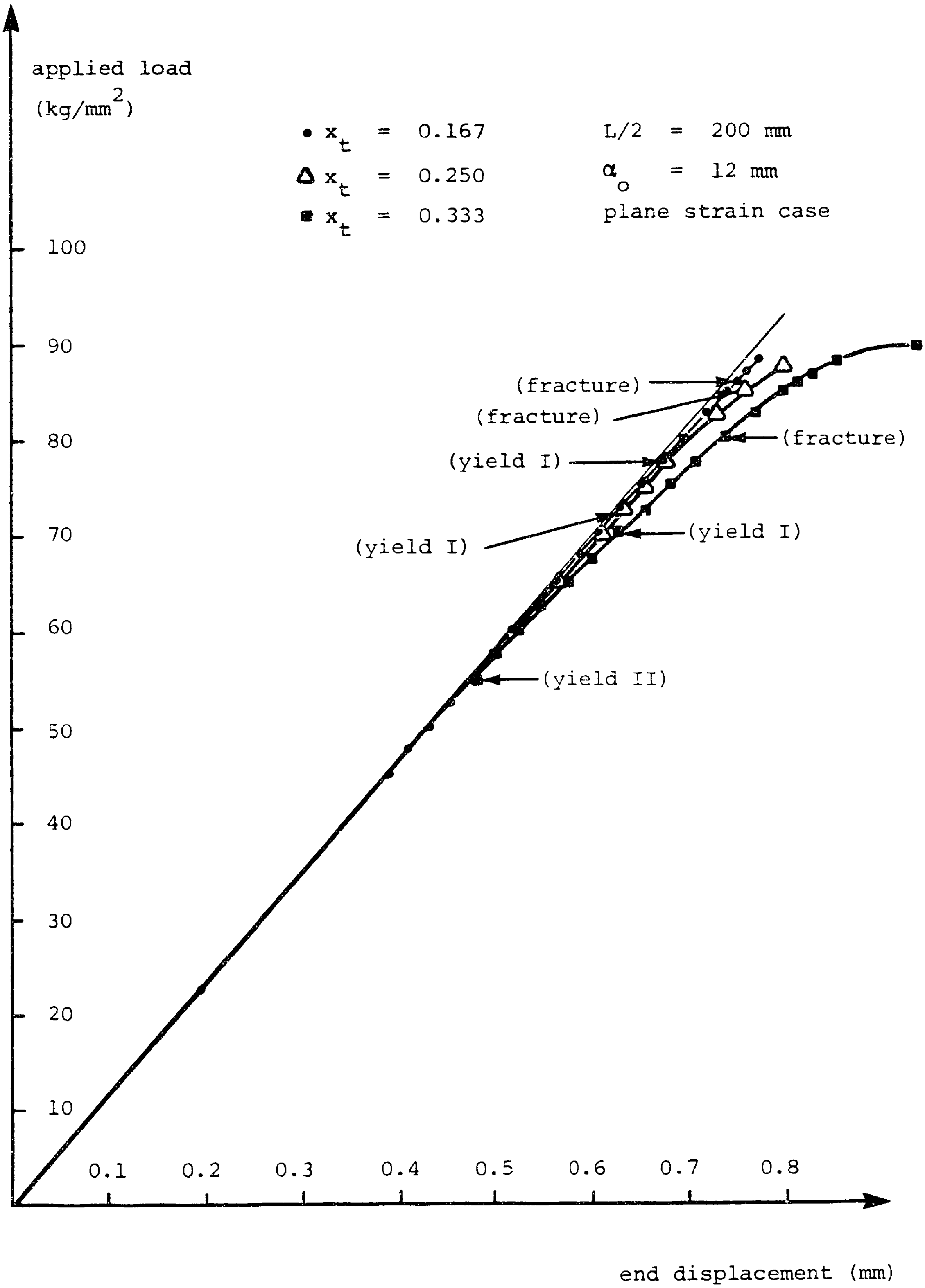

Figure 3.21 : Applied load versus end displacement.
Long specimen.

for some of the analyzed cases. It should be noted here, however, that those curves correspond to the idealized model used and thus have no physical meaning for loads over the load at fracture.

Further analysis of the obtained results showed that indeed the assumptions or rigid base metal are more or less justifiable. This is because, for most of the specimens the transverse deformation of the skin nodes of the base metal was two orders of magnitude less than the respective of the interlayer, before the yield of the base metal, and one order of magnitude less, well after yield (close to fracture).

Also, with good approximation, the interface between the layers remained perpendicular to the center line (loading direction) (at least before the yielding of base metal). The linear dependence between the curvature and the thickness was not checked since the element mesh was not very fine.

Since most of the assumptions and results of the theoretical analysis of the idealized joints were verified by the finite element modeling it appears that the simulation of more realistic joint geometries would be easily accomplished. However,due to the lack of sufficient funds such a study was not undertaken here.

PART II

STRESS RELIEVING

CHAPTER IV

STRESS RELIEVING TREATMENTS

4.1 Residual Stresses due to Welding

The local non uniform heating and subsequent cooling, which takes place during any welding process, causes complex thermal strains and stresses to develop that finally lead to residual stresses, distortion and all their adverse consequences.

Residual stresses and distortion must be a major cause of concern to the designer since they usually are detrimental --directly or indirectly-- to the integrity and the service behavior of a welded structure. High tensile residual stresses in the region near the weld might promote brittle fracture, change the fatigue strength or aid, under suitable environmental conditions, stress corrosion cracking. Compressive residual stresses, combined with initial distortion may reduce the buckling strength of the structure whereas excessive distortion might directly prevent the structure from performing its intended task.

Three sources of welding residual stresses are usually identified in the literature, [1], [34]. One is the difference in shrinkage of differently heated and cooled areas of a welded joint. The weld metal, originally subjected to the highest temperatures, tends upon cooling to contract more than all other areas. This is hindered by the other parts of the joint, thus resulting in the formation of high longitudinal stresses in the weld metal, and equilibrating compressive stresses in the rest of the base material. The residual stress peaks often are as high as the weld metal yield stress.

A schematic representation of the temperature and longitudinal stress changes during welding is given in Figure 4.1 adapted from [1]. Similarly residual stresses develop in the weld in the transverse direction, but are quite smaller in magnitude (Figure 4.2).

A second source of residual stresses is the uneven cooling in the thickness direction of the weld. The surface layers cool more rapidly than the interior ones, especially in thick plates. This gives rise to thermal stresses which can lead to nonuniform plastic deformations and thus to residual stresses , compressive at the surface and tensile ones in the interior.

Finally, residual stresses can arise from the phase transformations that might occur during cooling. Such transformations are accompanied by an increase in specific volume of the material being transformed. This expansion is hindered by the cooler material and thus causes residual stresses.

In analysing residual stresses various investigators have followed a number of different approaches. A brief presentation of these methodologies is given by Masubuchi and the author in [35], together with results of recent studies at M.I.T. A more extensive discussion on the subject can be found in [1], a recent book by Masubuchi. Specifically for high strength HY steels, results of analytical and experimental studies at M.I.T. are presented in [36] and [37] by Papazoglou.

The adverse effects of residual stresses and distortion can,

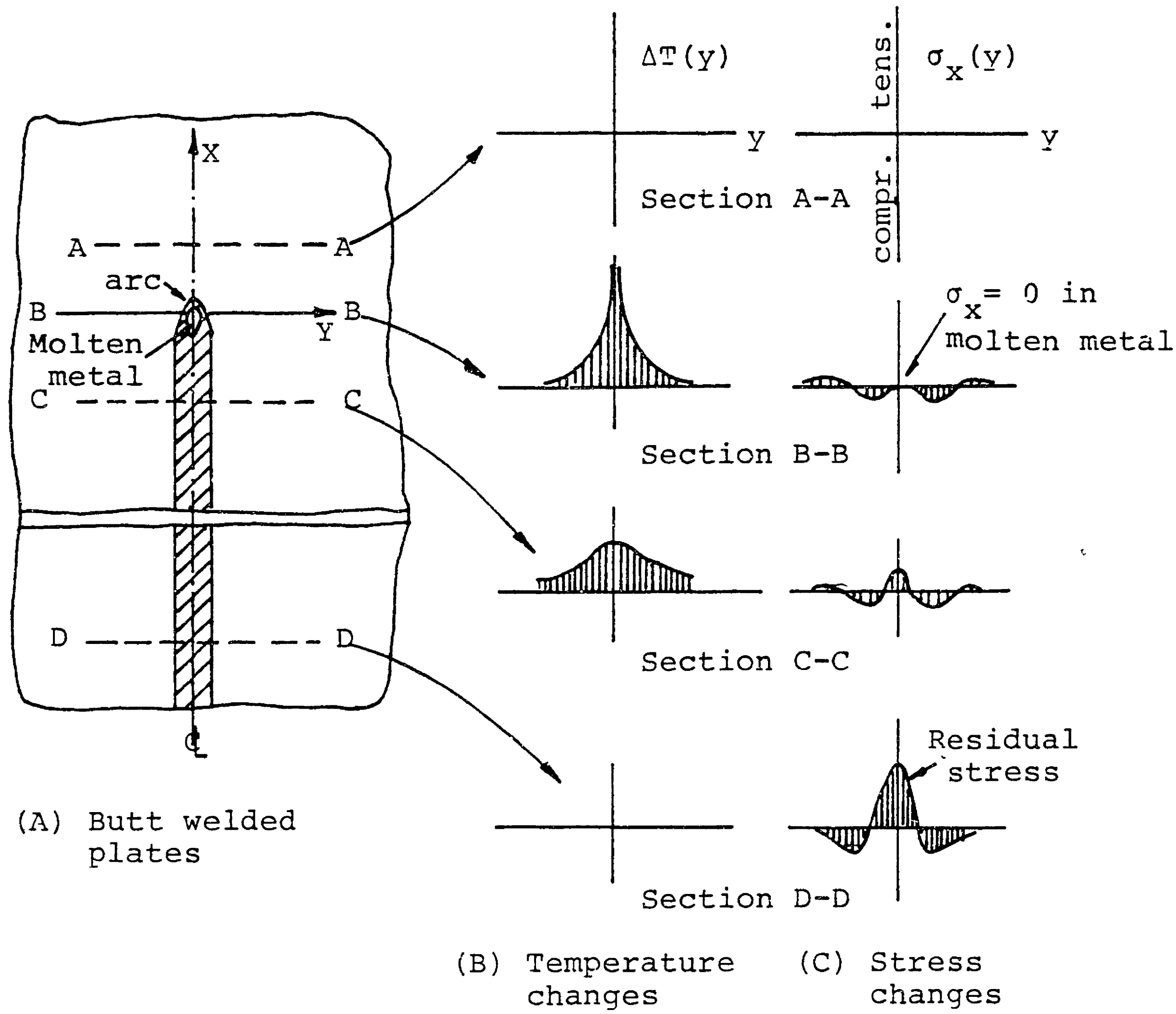

Figure 4.1 : Schematic representation of changes of temperature and logitudinal stresses during welding.

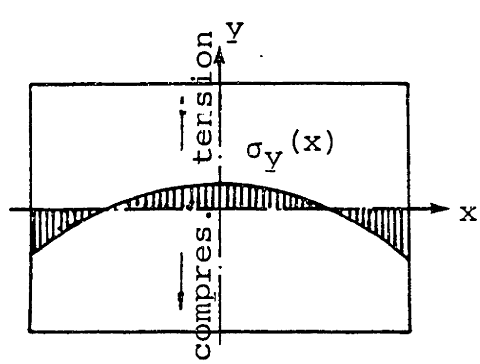

Figure 4.2 : Typical distribution of transverse residual stresses in butt welded plates.

sometimes, be kept under acceptable limits by selecting proper design and fabrication parameters and suitable material properties. Such design parameters include the geometry of the structure, the plate thickness and the joint types that are used. Fabrication parameters include the type of the welding processes employed, the actual procedure parameters, welding sequence, etc. As for the effect of the material properties, the designer must be concerned with both the base and the filler metal selection, as was already pointed out in the previous chapters.

Nevertheless, despite the precautions taken, residual stresses and distortion do usually develop during the fabrication of a welded structure. These can often be brought under acceptable limits by some kind of stress relieving process. Post weld heat treatment is frequently specified by the codes since it can reduce the level of residual stresses and also change the microstructure. However, the latter effect is sometimes a disadvantage and this is why mechanical and vibrational stress relieving methods are often also used.

The various stress relieving treatments will be presented in the next few sections of this chapter. The underlining mechanisms will be examined and the problems associated with their application will be highlighted.

4.2 Thermal Methods for Stress Relieving

4.2.1 Post-Weld heat treatments in general

Heat treatment can be defined as any process wherby metals are better adapted to desired conditions or properties in predictably varying degrees by means of controlled heating and cooling in their solid state without alteration of their chemical composition, [38]. A vast variety of such treatments exists each applicable to specific materials and for specific purposes. An in depth presentation of these processes is given by A.S.M. in [39]. Some necessary definitions, however, follow.

Lower critical Temperature (for steels): the temperature at which perlite begins to transform into austenite. Shown in the iron equilibrium diagram by the line A_1 (A_{C1} for heating, A_{r1} for cooling)

Upper critical Temperature: the temperature at which the steel becomes composed entirely of austenite. Shown as A_3 in the equilibrium diagram. (A_{C3} for heating and A_{r3} for cooling) it defines together with A_1 temperature the critical range or the transformation range for the particular alloy.

Annealing is the process of applying alternate heating and cooling cycles to induce softening of the metal, to alter physical or mechanical properties and / or to produce a specific microstructure. For ferrous alloys full annealing involves heating to just above the upper critical temperature for hypoeutectoid steels and just above the lower critical temperature for hypereutectoid ones, followed by slow furnace cooling to under $1000^{o}F$ ($537^{o}C$). This results in the softest pearlitic structure and thus to a steel with reduced hardness and tensile properties but improved ductility.

During recrystalization annealing the sites of high residual stress concetrations begin to rearrange themselves into new stress-free grains, at a temperature which is determined by the purity of the metal, the grain size and the amount of cold work. During recovery annealing, which is performed at a temperature between ambient and recrystalization temperature, the residual stresses are partially relieved but the tensile strength dces not decrease, as with recrystalization.

Solution annealing is the heating of a multi-phase alloy into a temperature range where only one homogeneous phase exists at equilibrium, holding at this temperature until the desired degree of homogeneity is achieved and then rapidly cooling to retain the elements in solution until they can be precipitated in the required manner.

Age or Precipitation Hardening refers to the processing of an alloy wherein precipitation of the hardening phase occurs over a period of time, at room or higher temperature, after solution annealing.

Normalizing involves heating of the steel well above the upper critical temperature A_{C3} followed by still-air cooling to room temperature to obtain the "normal" pearlitic structure in that steel. This treatment refines the grain size and leads to increased yield strength and better fracture resistance.

Quenching involves heating the material to a certain temperature and then subjecting it to a controlled cooling rate by immersing it in a fluid or by air blast. It is rarely applied after welding. In steels, quenching from above the upper critical temperature gives rise to microstructures of higher strength than those obtained by normalizing. However, to improve fracture toughness it is always followed by tempering.

<u>Tempering</u> is a treatment that involves heating of the material to a temperature below that of transformation but high enough to cause some metallurgical changes. The higher the tempering temperature, or the longer the time at that temperature, the softer and more ductile the steel gets.

4.2.2 Stress Relieving Heat Treatments

Stress relieving basically involves heating of the part to a subcritical temperature, below A_{c_1}, holding it at that temperature to ensure uniformity, and slow cooling to room temperature, usually in air, to prevent the reintroduction of stresses. The stress relieving temperatures usually are of the order of 1100°F to 1300°F (590°C to 700°C), where the yield strength has drastically decreased and creep occurs. The welding residual stresses can no longer be supported. Thus the stress distribution will be uniform and at a very low level.Up to A_{c_1}, the higher the stress-relieving temperature, the more completely the stress is removed, as shown in Figure 4.3 (adapted from [40]).

Full relief of the residual stresses can only be ensured through an annealing treatment. This, however, would be more costly and time consuming and would cause more problems due to the higher temperatures.

Stress relieving is always followed by some dimensional changes. Even warpage and distortion can result when the residual stresses are high enough. It may therefore be necessary to straighten the part and some times to stress relieve again to reduce the straigthening stresses.

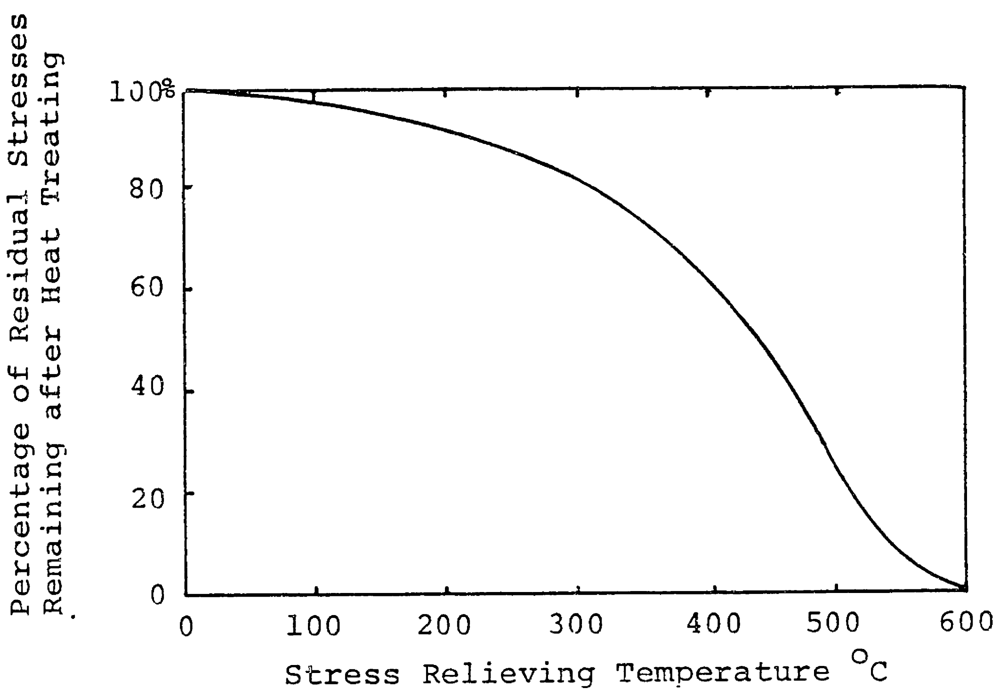

Figure 4.3 : Effect of stress relieving temperature in mild steel weldments.

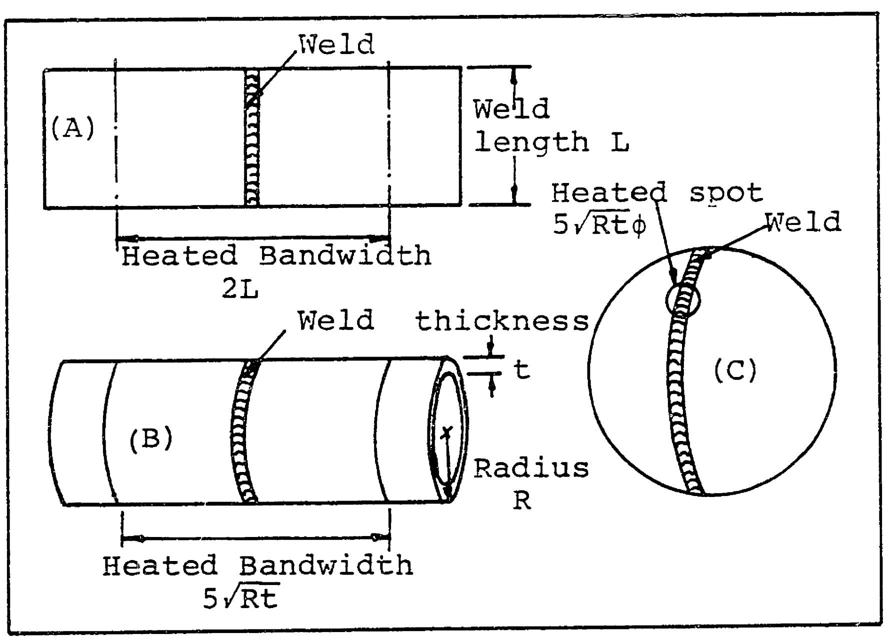

Figure 4.4 : Bandwidth of heated zone necessary for stress relief in: (A) Flat plate, (B) Cylinder , and (C) Sphere

4.2.3 Heat Treating Ovens and Localized Heating Equipment and Procedures

The size and shape of the fabrication and the type of the material determine, in most cases, the best method for applying a stress relieving heat treatment. However, there are three main requirements that must be in general fulfilled by the heat treating method:

(a) It should be able to produce the required temperature.

(b) The temperature should be controllable within specified limits (e.g. $\pm$ 20° to 40° F for steels),(10° to 20° C).

(c) It should be possible to achieve a uniform and even heating and cooling rate throughout the thicker section to be treated. This requirement is especially important for the case of joints of complex geometry and variable thickness.

Post weld heat treatments at high temperatures can be ideally performed by placing the structure in a fixed furnace where temperature uniformity and controllability are excelent in most cases. Furnaces for stress relieving are usually of the batch type and can be heated by various methods utilizing either gas or oil flames, or electrical energy. The most recent types are of low thermal mass with insulation of ceramic fiber and mineral wool, instead of brick, which was conventionally used. Such construction reduces the erection and operation costs. High velocity gas burners give excellent temperature distribution and improved heat transfer. However, the final selection of heating mode, largerly depends on fuel costs and availability.

More details on furnaces can be found in [38],[39] and [43].

However, in many instances postweld heat treatment of a complete fabrication is not possible due to the size of the structure or because heat treatment has to be applied in the field. Such cases arise when stress relieving closing welds in pressure vessels, or joints between prefibricated (and stress relieved) sections of pipework. Also repair maintenance welding might necessitate localized stress relieving.

Such a treatment can be performed in a temporary furnace erected around the structure, or by localized heating of an area around the weld zone. Appropriate insulation should always be applied. An extensive presentation of the localized heat treating methods is given in [39] by A.S.M. and in [41] by A.W.S. Some discussion on their applicability and relative advantages follows.

Electric resistance heaters, (Figure 4.5), direct the Joule heat, which is produced in the resistance elements, to the part by proper placement and insulation. The four commonly used heater types are: finger element heaters, braided heaters, flexible ceramic pads, and wrap-around heaters. The achieved temperature can be adjusted quickly and easily and can be maintained even through a welding operation. Uneven heat input can be obtained if required. However, the elements have a relatively short life and may short circuit with the part.

In induction heating, (Figure 4.5), alternating current is applied to coils wrapped around the parts to be heated and thus induces magnetic fields and currents inside the part. The low mains frequency (50 or 60 Hz) is used for heaters of power

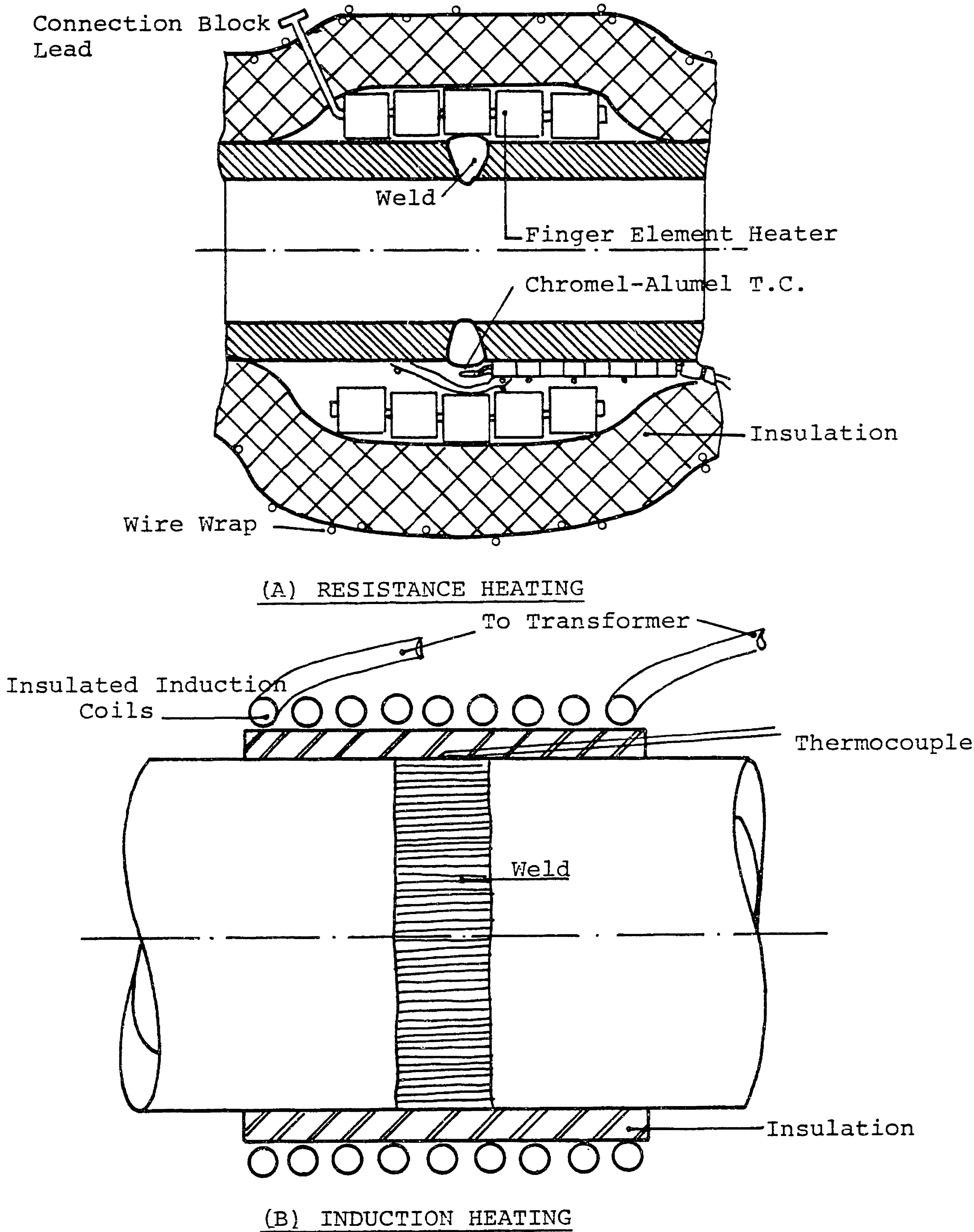

Figure 4.5 : Localized heat treating equipment.

up to about 25 KVA whereas medium frequency (1000 to 10,000 Hz) is used for powers between 20 and 400 KVA. The coils have a long life and the achieved temperature is very uniform and can be controlled within a very accurate range. However, the initial cost is high, the portability of equipment low and uneven heat input is difficult to achieve. Furthermore the heater has to be turned off during welding. More details about the process are given in [42] by Müller.

Manual flame heating by gas torches is convenient low cost method particularly suited for field work. However, minimal precision and repeatability can be achieved and if not performed by a very experienced operator it is likely to damage the weldment.

Exothermic heating employs a consumable heat source. Such a process is the thermite reaction between Fe_2O_3 and Al. Exothermic packages that can produce the required holding temperatures are marketed. No capital investment cost or operator during heating is required and the equipment is very portable. However, there is no possibility for adjustments after ignition and limited flexibility in meeting code requirements regarding heating and cooling rates and holding time.

Finally gas flame generated infrared heating and radiant heating by quartz lamps utilize radiation as the principle mechanism for heat transfer. The former method uses relatively economical fuel and can be readily controlled. The latter has an extremely fast response time (4000° F in one second) and fast cool down due to minimal thermal mass and large efficiency.

No combustion takes place and no heat is wasted. However, the cost is high and a separate "furnace" has to be fabricated for each different part configuration.

4.2.4 Requirements and Specifications for Localized Heat Treatments

For local stress relieving heat treatments it is absolutely necessary to ensure that the temperature distribution during the heat treatment does not induce new thermal stresses which exceed the material yield stress and can lead to the development of new residual stresses on cooling. This imposes strict requirements on the level and uniformity of temperature, on the heating and cooling rates, and width of the heating zone. The latter largely determines the existing temperature gradient through the thickness (between the heated and unheated surfaces). Most of these requirements are usually specified by the applicable codes (e.g. ASME Pressure Vessel Codes, Section VIII).

For butt welded plates it was experimentally proven by Cotterell in [44], that satisfactory relief of residual stresses can be expected if uniform heat input is applied over a band-width of twice the length of the weld, as shown in Figure 4.4(A).

For circumferential welds in cylinders and pipes of diameter R and thickness t, it was shown by Burdekin in [45], that relief of residual stresses can be achieved if uniform heat input is applied over a circumferential band width of $5\sqrt{Rt}$ (Figure 4.4(B)). This is also what BS 1515 and 5500 (British Standards) suggest. However Shifrin and Rich, in [46], had clearly shown that satisfactory through thickness gradients can be achieved with a minimum heated band with of five times the wall thickness, (5t), irrespective of the technique used for heating (resistance or induction). ASME codes on the other hand require that "the width of the heated band on each side of the greatest width of the finished weld shall be not less than two times the weld metal thickness". This again results in a bandwith of approximately 5t which is generally much smaller than what specified by the British standards. Further both standards require that temperature gradients beyond the heated zone should be not harmful, although no clear definition of "harmful" is given. British codes also suggest that the full heat treatment temperature range be achieved for a distance of 3t on each side of the weld seam and a minimum of half the soak temperature be achieved at the edges of heated zone.

For welded spherical vessels it has been shown theoretically by Cotterel, [47], that local stress relief heat treatment is possible by slowly moving a heated spot (cap) of diameter $5\sqrt{Rt}$ or by heating a circumferential band of the same width.(Figure 4.4(C)).

For complex junctions of branches in pipes or pressure vessels it is necessary to ensure that the heating of a weld will not induce substantial thermal gradients around the junction. Therefore exact thermal stress analysis might be needed and additional background heating of the vessel as a whole might be required.

4.3 Effects of Stress Relieving Heat Treatments

4.3.1 Effect of Treatment on the Mechanical Properties

Stress relieving heat treatments are usually very effective in reducing the high residual stresses present in a weldment. However, they also have an effect on the microstructure and the properties of both the base plate and the weld metal since they are carried out at relatively high temperatures. These effects vary with the material under consideration.

During the last decade, the desirability of post weld heat treatments and their effects were extensively investigated by the Working Group on Thermal Stress Relief of the Commission X of the Intermational Institute of Welding. Information from the series of documents that were produced, (References [48] to [51]) is presented in this section.

Specifically for non work-hardened base metal of C-Mn and microalloyed steels, it was generally concluded that tensile properties are impaired to a significant extent, especially at higher temperatures. Resistance to brittle fracture is affected but not drastically. Temperature is a more important factor than soaking time. For low alloy and creep resistant steels, which are used in a normalized and tempered or quenched and tempered condition, the effect of stress relieving treatments on the properties will depend on the temperature. The effect will be minimal if the treatment is carried out at a temperature lower than that of initial tempering. Additional tempering will result however, if higher temperature treatment is performed. This is usually benefical for the resistance to brittle fracture but detrimental for other properties, such as creep resistance, and usually is not recomended by the codes.

For the case of work hardened base material, on the other hand, the heat treatments usually restore the base properties and prevent strain aging and are therefore beneficial.

The effect of stress relieving heat treatments on the properties of the heat affected zone (H.A.Z.) will not only depend on the type of steel but also on the microstractural state of the H.A.Z. Therefore welding procedure and conditions, heat input, plate thickness and distance to the fusion line are important parameters. For C-Mn steels the heat treatment will in general soften the H.A.Z. structures, except if carbide precipitation occurs. The yield strength of the H.A.Z. will usually be higher than that of the base material after the same treatment. Heat treatments are in most cases also beneficial to the resistance to brittle fracture for these steels. For low alloy steels the main problem is to retain satisfactory toughness in the H.A.Z. The effect of treatment is usually strongly dependent on the type of steel and the exact metallurgical changes associated with the welding and heat treating tempering. The problem of stress relief cracking that is known to occur in the H.A.Z. of some steels will be examined in detail in the next section.

Although not much work has been done on the effect of heat treatments on the properties of weld metal, it appears that tensile properties diminish considerably on tempering. Again temperature seems to be more important than the soaking time .

As in the base metal, embrittlement can occur and some instances of stress relief cracking have been reported.

4.3.2 Stress-Relief Cracking

Stress-relief cracking is defined as "intergranular cracking in the heat affected zone or weld metal that occurs during the exposure of welded assemblies to elevated temperatures produced by post weld heat treatments or high-temperature service", [52]. It has also been refered to in the literature as "post-weld-heat cracking" or "reheat cracking" and in general is caused when some relief of stresses by creep occurs. This form of cracking became a problem with the austenitic stainless steels in the 1950's and with the low-alloy constructional steels in the 1960's. It also occurs to ferritic creep-resisting steels and nickel base alloys and is generally related to precipitation hardening. Non-precipitation hardening materials such as plain carbon steels and certain nickel alloys are not susceptible to reheat cracking.

The cracks can be possitively identified by metallographic examination due to their characteristic branching intergranular morphology, along the coarse-grain region of the heat-affected zone, [53]. Cracking usually occurs at high temperature when creep ductility is insufficient to accomodate the strains required for the relief of applied or residual stresses. When residual stresses are high, as in thicker and restrained sections reheat cracking is most likely to occur.

Stress relief treatments are required for almost all pressure vessels and piping systems fabricated today, and this is why stress-relief cracking caused considerable concern. Extensive investigations of the cracking mechanism and of possible remedies have been undertaken all over the world, and are in detail reviewed by Meitzner in [53] and Dhooge, et al., in [54]. In 1970 I.I.W. established, in Commission X, a Working Group on "Reheat Cracking" to collect and assimilate information on the subject, (References [55] to [60]).

In an effort to develop a simple, reliable specimen that includes all the pertinent variables related to cracking, such as high stresses, triaxiality, thermal history and microstructure, a large number of tests are used today. These tests are extensively reviewed by Dhooge,et al. in [54] and are either:

(a) Tests on complete weldments.

(b) Tests on specimens containing a weld.

(c) Tests on specimens containing a thermally simulated H.A.Z.

In (a) and (b) weld/H.A.Z. thermal cycles and microstructures are produced by an actual welding operation, whereas in (c) the H.A.Z. microstructure is created by subjecting base metal coupons to a simulated H.A.Z. thermal history, as in a Gleeble. In both cases the specimens are then reheated and tested at temperatures typical of stress relief treatments.

Tests have shown that there is definite influence of chemical composition on stress relief cracking susceptibility. Japanese researchers have used regression analysis to derive two predictive formulae [61],[62].

(a) $\Delta G = Cr\,\% + 3.3\,Mo\,\% + 8.1\,V\,\% - 2.0$ (by Nakamura, et al.)

and

(b) P_{SR} = Cr % + Cu % + 2.Mo % + 10 V % + 7 Nb % + 5Ti % - 2

(by Ito and Nakanishi)

Positive values of the ΔG or P_{SR} parameters would indicate susceptibility to stress relief cracking. However, other investigators have shown that such formulae were not general enough to be used conclusively, [63].

It has also been established by these studies that martensitic or lower bainitic microstructures are more prone to S.R. cracking than the upper bainitic or ferritic-perlitic ones. Thus risk of cracking can be reduced by the choice of welding heat inputs or preheat levels ensuring lower cooling rates in the H.A.Z. The same holds for proper choice of consumables and the use of a temper bead in the last welding pass.

4.3.3 Stress Relieving of HY-130 Steels

The very high residual stresses that develop during welding of HY-130* steels make stress relief treatments very attractive. Substantial reduction of stresses was shown to occur, in both the base and weld metal at temperatures between 950° F (510° C) and 1050° F (566° C). This is evidenced in Figure 4.6 and 4.7 , adapted from [64]. However, a severe degradation of notch toughness may also occur at these temperatures. This embrittlement, which phenomenologically is similar to temper embrittlement, is believed to be influenced by the soaking

---

*Also refered to as 5 Ni-Cr-Mo-V, HY-130(T),HY-130/150 in different stages of its developement. (Appendix A).

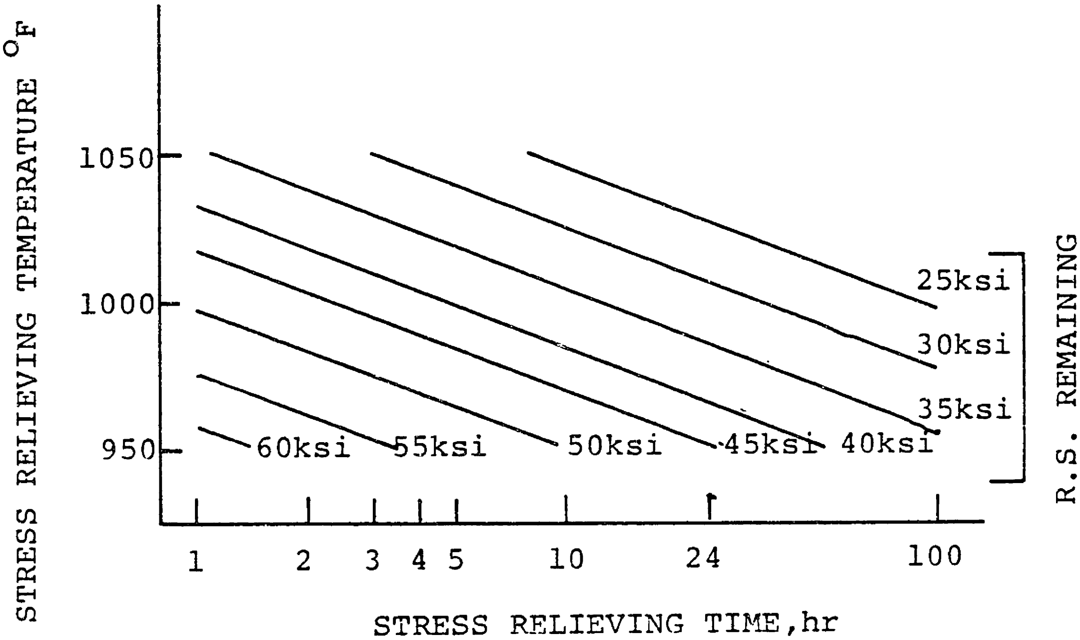

Figure 4.6 : Estimated residual stress after stress relief.

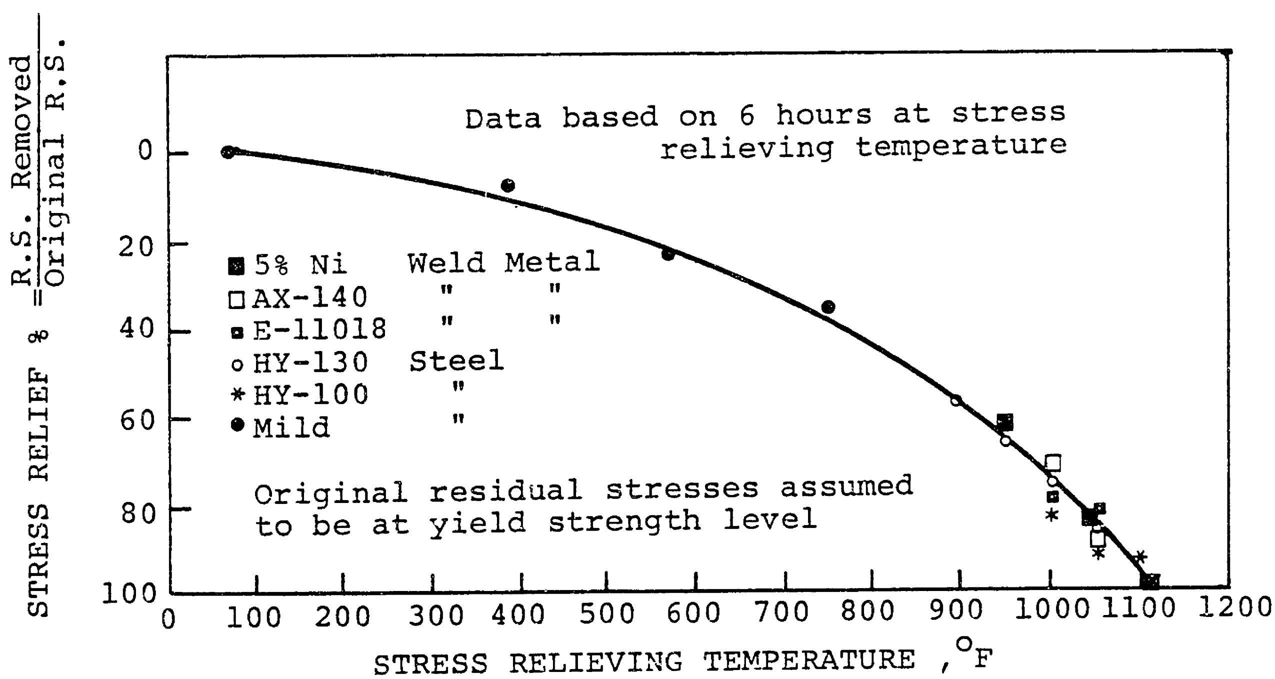

Figure 4.7 : Comparison of relaxation properties.

temperature, the time at temperature, the cooling rates, the plastic strain, the exact alloy composition and prior heat treatment.

Extensive investigation on the subject was performed by the U.S. steel Corporation and the U.S.Navy (N.S.R.D.C. Materials Laboratory). Results by Rosenstein, [65], indicated that stress relief cycles are cumulative in nature, by comparing the tensile and Charpy properties resulting from consequent heat treatments of short duration and one single treatment of long duration, both having the same soaking times.

Furthermore it was observed that the degradation of notch toughness was maximum when stress relieving at 950° F (510° C) and minimum when at 1050° F (566° C), as evidenced in Figure 4.8. However, investigations of the effects of stress relieving on the weld metal,[64],[65], have shown that the higher temperatures may substantially reduce the yield and tensile strength of the weld metal and thus may cause undermatching. Therefore the most practical temperature range for effective stress relieving of HY-130 weldments is between 1000° F (538°C) and 1025° F (552° C).

Additionally, it was established that the degradation of toughness at 950° F (510° C) occurs during both soaking and cooling. The isothermal degradation was shown to be directly dependent upon time at temperature. The degradation during cooling, on the other hand, is inversely related to the cooling rate and does not depend on the soaking time. Therefore, cooling embrittlement constitutes the major portion of

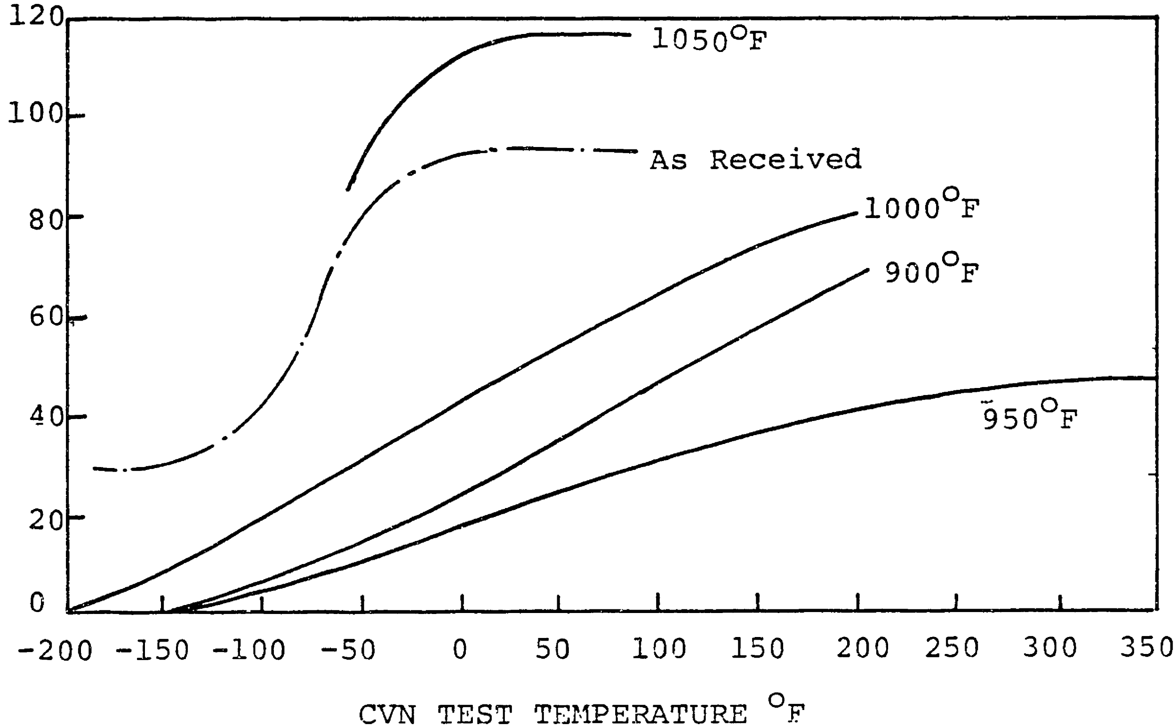

(Specimens stress-relieved for 100 hours at indicated temperature and air cooled to roomtemperature)

Figure 4.8 : Effect of stress-relief temperature on toughness of HY-130 steels.

degradation after short times at temperature and only a minor one after long soaking periods.

It was also shown that stress relief at the tempering temperature of 1050° F (566° C) results in softening at temperature (accompanied by increased toughness) and embrittlement on cooling. Therefore, the resulting properties will depend both on the cooling rate and the soaking time.

The toughness degradation due to stress-relief can in general be recovered by retempering to a lower strength level. It should also be finally noted that the fundamental difference between stress relief embrittlement and temper embrittlement is the presence of strain due to creep at high temperature or due to previous plastic deformation, [66].

4.3.4 Stress Relieving of Austenitic Stainless Steels

Austenitic stainless steels have to be heated to about 1650° F (900° C) to attain adequate stress relief because of their good creep resistance. Only partial stress relief can be attained at temperatures lower than 1600° F (870° C). Best stress-relieving results can be achieved by slow cooling. Quenching or rapid cooling in general reintroduce high residual stresses.

Additionally, an optimal stress relieving temperature is usually difficult to select, since the heat treatments that would provide adequate stress relief can be detrimental for the corrosion resistance and the ones that are not harmful to corrosion resistance may not provide adequate stress relief.

The major metallurgical effects of a stress relieving treatment are:

(a) When heating between 900 and 1500° F (480 to 815° C), chromium carbides might precipitate in the grain boundaries of wholly austenitic unstabilized grades and can promote intergranular corrosion.

(b) When heating between 1000 and 1700° F (540 to 925° C), hard sigma phase may result decreasing both corrosion resistance and ductility.

(c) When slow cooling the above nondesirable effects have more time to take place.

(d) When heating between 1500° F and 1700° F (815 to 925° C), improvements in the corrosion resistance and mechanical properties can result due to coalescence of chromium carbide precipitates or sigma phase.

(e) Heating above the annealing temperature at 1750 to 2050° F (955 to 1120° C) fully softens the steel and causes all the grain-boundary precipitates to redisolve.

In the final selection of a proper stress relieving treatment due consideration must be given not only to the material itself, however, but also to the fabrication parameters and to the operating environment. Table 4.1, by A.S.M., adapted from [39], summarises the suggested stress-relieving treatments for various applications and environments.

Table 4.1 Stress-relieving treatments for austenitic stainless steels

Application or desired characteristics	Suggested thermal treatment(a) Extra-low-carbon grades, such as 304L and 316L	Stabilized grades, such as 318, 321 and 347	Unstabilized grades, such as 304 and 316
Severe stress corrosion	A,B	B,A	(b)
Moderate stress corrosion	A,B,C	B,A,C	C(b)
Mild stress corrosion	A,B,C,E,F	B,A,C,E,F	C,F
Remove peak stresses only	F	F	F
No stress corrosion	None required	None required	None required
Intergranular corrosion	A,C(c)	A,C,B(c)	C
Stress relief after severe forming	A,C	A,C	C
Relief between forming operations	A,B,C	B,A,C	C(d)
Structural soundness(e)	A,C,B	A,C,B	C
Dimensional stability	G	G	G

(a) Thermal treatments are listed in order of decreasing preference.
A : anneal at 1950 to2050^{o} F (1065 to 1120^{o} C), slow cool.
B : stress relieve at 1650^{o} F (900^{o} C), slow cool.
C : anneal at 1950 to 2050^{o} F (1065 to 1120^{o} C), quench(f) or cool rapidly.
D : stress relieve at 1650^{o} F(900^{o} C), quench or cool rapidly.
E : stress relieve at 900 to 1200^{o} F (480 to 650^{o} C), slow cool.
F : stress relieve at below 900^{o} F (480^{o} C), slow cool.
G : stress relieve at 400 to 900^{o} F (205 to 480^{o} C), slow cool (usual time, 4h per inch of section).

(b) To allow the optimum stress-relieving treatment, the use of stabilized or extra-low-carbon grades is recommended.

(c) In most instances, no heat treatment is required, but where fabrication procedures may have sensitized the stainless steel the heat treatments noted may be employed.

(d) Treatment A,B or D also may be used, if followed by treatment C when forming is completed.

(e) Where severe fabricating stresses coupled with high service loading may cause cracking. Also, after welding heavy sections.

4.4 Alternative Methods of Stress Relieving

4.4.1 Mechanical Overstressing

When any of the undesirable metallurgical effects of thermal treatments cannot be tolerated, it is possible to stress relieve by mechanical means. Specifically, refering to Figure 4.9, adapted from [1], if tensile loading is applied parallel to the weld line, yielding will be caused in the highly stressed weld metal. The adjucent plate material, however, will be stressed further into tension, as depicted by curve(1). Further increase in loading will even out the stress distribution across the plate, as in curve (2). If the applied load increases further, yielding will take place across the entire cross-section, as in curve (3). If the plate is then unloaded the remaining stress will be very low and more or less uniform (curve 3´). So overloading of the structure can greatly reduce the level of residual stress peaks.

In addition, if any cracks or defects exist, the first application of loading will cause localized yielding at their tips. Subsequent unloading will produce a patern of compressive residual stresses around these defects and other points of stress concentration.

Therefore after the first succesful overstressing of a structure appreciable assurance is usually provided against both brittle fracture and fatigue fracture, [1],[40]. Obviously, however, no improvement of the basic fracture toughness of the HAZ microstructures is to be expected through mechanical treatments. This should be contrasted with the metallurgical

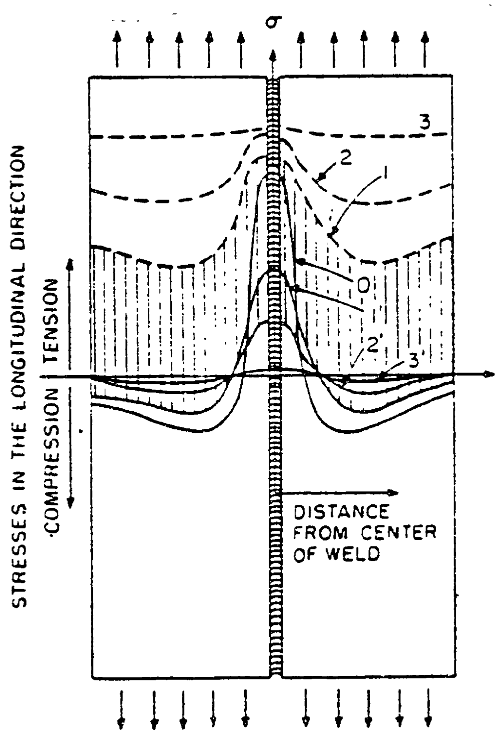

Curve 0: Residual stresses in the as welded condition
Curve 1: Stress distribution at $\sigma = \sigma_1$
Curve 2: " " " $\sigma = \sigma_2, (\sigma_2 > \sigma_1)$
Curve 3: " " " $\sigma = \sigma_3, (\sigma_3 > \sigma_2)$
Curve 4: Residual stresses after $\sigma=\sigma_1$ is applied and then released
Curve 5: " " " $\sigma=\sigma_2$ " " " " "
Curve 6: " " " $\sigma=\sigma_3$ " " " " "

Figure 4.9 : Schematic distributions of stresses in a butt weld when uniform tensile loads are applied and of residual stresses after the loads are released.

benefits often resulting from thermal stress relieving treatments.

4.4.2 Vibratory Stress Relief (V.S.R.)

It has been reported by various investigators that reductions of residual stresses occured and dimensional stability during subsequent machining was ensured when a welded structure was vibrated. The technique, employing eccentric weight type vibrators attached to various positions on the structure, is currently in industrial use with some degree of success. However, evidence on the capability of the method to effectively and repeatedly relieve residual stresses is rather contradictory at this point. It still remains much to be understood as to how and even whether the method actually works. Numerous studies have been undertaken in this direction during the past forty years. A survey of most of the published results appears in [68] by Dawson and Moffat and in [69] by Brogden.

Early work by Mc Goldrick and Saunders, [70], postulated that occurrence of plasticity at some time during the treatment was required for successful stress relief,and that in order to achieve the necessary amplitudes, the structure should be vibrated at a frequency very close to resonance. Relief of residual stresses at this time was inferred from the reduction of warpage. Buhler and Pfalzgraf, in the early 1960's, were among the first to attempt to directly measure residual stresses after vibratory treatment, [71]. Their results were not encouraging however, because they restricted the applied cyclic stresses below the fatigue limit of the materials used. The same concern for fatigue damage was shared by other investigators as well. Nevertheless, more recent studies concluded that for any stress relief to occur during vibration, the fatigue limit of the material has to be exceeded and fatigue damage must therefore occur, although this is likely to be small, [68].

Substantial relief of residual stresses by vibration was reported in latter investigations. Specifically Sagalevich and Meister claimed 50% reduction in welding deformations of wagon bodies [68] and Zubchencho and Gruzd reported 67% decrease in residual stress peaks in welded truck frames [72]. In 1968 Wozney and Crawmer reported in [73] a 33% reduction of residual stresses by cyclic bending of residually stressed Almen strips. Furthermore they used a derived cyclic stress strain curve of the material (similar to the one in Figure 4.10) to predict successfully the residual stress reduction. In 1972 Weiss, et al. reported in [74] a substancial reduction of residual stresses in plain carbon steel weldments vibrated on a laboratory shaker.

In an effort to analyze the mechanism of the reduction of residual stresses, Kazimirov et al. presented in [75] a rigorous derivation of the stresses and strains caused in a flat plate by a pulsating load and their interaction with existing residual stresses. Makhnenko and Pivtorak used a finite difference approach to show that the presence of residual stresses did not affect the condition of resonance in a beam. Additionally they proved that the vibration amplitude would be decreased when high residual stresses exist in the structure and concluded that in order to appreciably redistribute residual stresses, it would

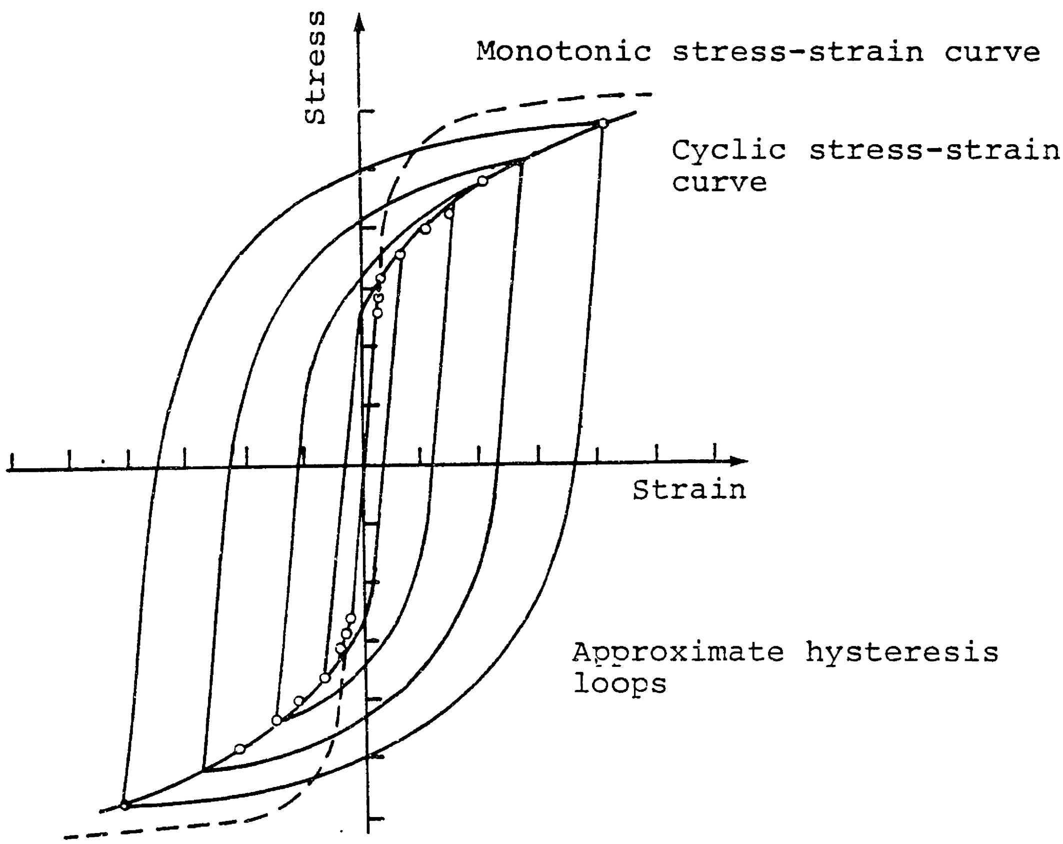

Figure 4.10 : Monotonic and cyclic stress strain curves for SAE 4340 steel. Data points represent tips of stable hysteresis loops .

be necessary to apply cyclic additional strains at least of the same order of magnitude as the residual strains themselves. Experimental investigations by Mryka led to similar conclusions, [77]. In 1979, Sagalevich, et al., showed by energy methods that it is possible to completely eliminate the residual stresses in welded beams by a rational combination of static and vibrational loading. Satisfactory agreement between calculated data and experimental results was observed,[78].

Despite these encouraging studies, however, other extensive investigations, such as one completed at Battelle Memorial Institute by Cheever gave rather incoclusive final results [79]. Additionally there is no clear consensus in the literature regarding the exact mechanism of the stress reduction. Further examination of vibratory stress relief treatments was considered to be outside the scope of this study. The next chapters will only deal with thermal stress relief treatments.

4.4.3 Explosive Stress Relieving

The impact from explosive contact charges was shown to be capable to redistribute (rather than to relieve) welding residual stresses. Important parameters in such a treatment are the intensity and distribution of the explosive load. Some results on the optimal selection of these parameters are given in [80]. However,since the method is rarely used it will not be examined any further in this study.

4.5 Fabrication Techniques to Reduce Residual Stresses and to Eliminate Postweld Treatments

There are cases in welding fabrication, where even a modification of the residual stress patterns is beneficial. For example, it is the tensile residual stresses usually developed in the inner surface of welded stainless steel pipes that promote intergranular stress corrosion cracking in boiling water reactor instalations. The various fabrication methods that were developed to solve this problem are effective exactly because they limit and change these tensile stresses to compressive, [81].

Specifically in the <u>heat sink welding</u> technique the first two welding passes are made conventionally with an inert gas back purge. Then the inside of the pipe is cooled with flowing or stagnant water or water spray while the remaining weld passes are completed. Since the inside surface is kept relatively cool during most of the welding passes the circumferential shrinkage is less than with a conventional weld. In addition, when the outer weld layers shrink axially while cooling, they tend to induce compressive axial stresses on the already cool inside surface. Results of investigations in G.E. by Chrenko appear in Figure 4.11. The axial residual stress patterns on the inside deameter of 304 stainless steel pipes were measured by X-ray diffraction for conventional and heat sink welding, [82].

Beneficial compressive stresses can also be induced in the inner surface of pipes that have been already welded. One method developed by I.H.I. in Japan the <u>induction heating stress improvement</u> (I.H.S.I.). In this case the interior of the pipe is cooled with water, while heat is applied to the outside near the weld. The resulting temperature gradient (between 400° C and 500° C) causes yield in compression at the outside surface and in tension at the inside. When the outside heating is removed compressive stresses are induced on the interior. Some experimental results appear in Figure 4.12 again adapted from [82].

Another technique that is usually employed in order to avoid postweld heat treatment is buttering. The joint preparations are first buttered, inspected, heat treated and remachined before final butt welding. Detailed description of the technique is given by Lochhead in [83].

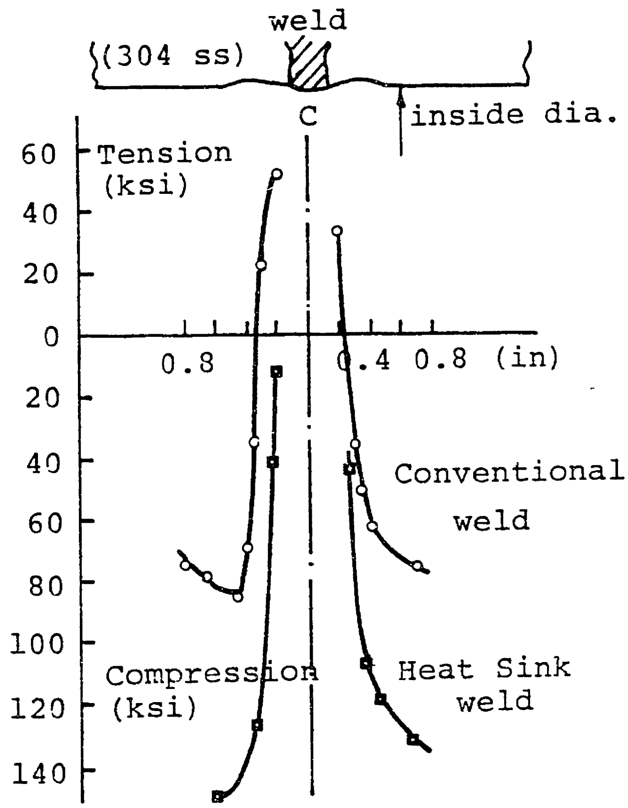

Figure 4.11 :
Axial residual stresses at the inner surface of a 10 in. dia. schedule 80 type 304 stainless steel pipe for both conventional and heat sink welding.
(adapted from [82])

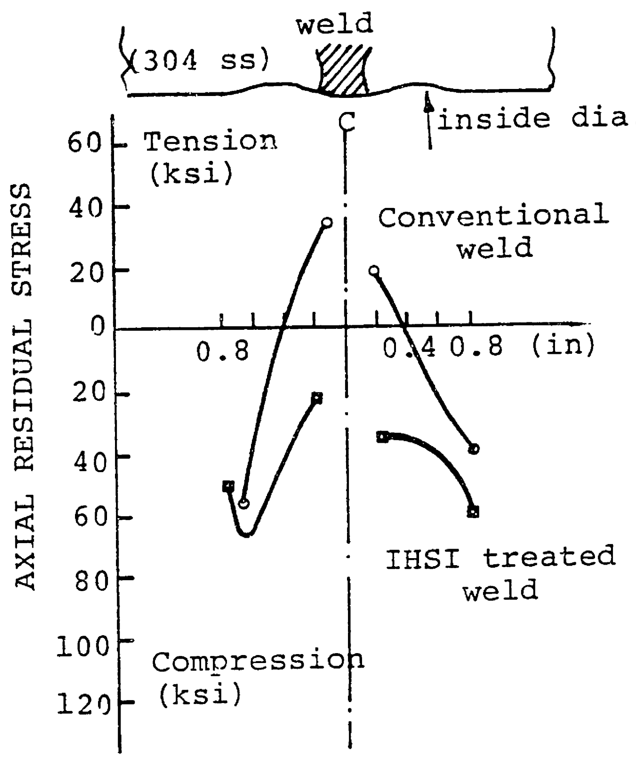

Figure 4.12 :
Axial residual stresses at the inner surface of a 16 in. dia. schedule 80 type 304 stainless steel pipe for conventional welding and subsequent induction heating stress improvement, (IHSI).
(adapted from [82])

Note : Residual stresses were measured by X-ray diffraction.

CHAPTER V

ANALYSIS OF RESIDUAL STRESS RELAXATION DUE TO HEAT TREATMENTS

5.1 General Considerations

Stress relieving heat treatments are usually applied in order to reduce residual stresses and to induce metallurgical benefits. The metallurgical changes, positive or negative, have been briefly dealt with in the previous chapter, and are not the main concern of this study. The reduction of residual stresses, however, will be further examined now.

Residual stress changes can arise during all three stages of a heat treatment. Specifically, refering to Figure 5.1, during the heating part of the process residual stresses decrease due to the temperature dependance of the mechanical properties, mainly through a reduction of the yield strength with temperature. During the holding (or soaking) period the temperature is kept constant and residual stresses are reduced due to creep. Experimental evidence suggests that the major portion of this stress reduction occurs in the first part of this stage. This is clearly shown in Figure 5.2 depicting load versus time for constant-strain relaxation tests performed on HY-130 steel, and matching weld metals, by N.S.R.D.C., [64]. Finally, during the cool-down period, residual stresses increase due to the temperature dependence of the mechanical properties, but hopefully (when the treatment is successful) not to their initial levels.

To judge the effectiveness of a stress relief treatment, with regards to the accomplished reduction of residual stresses,

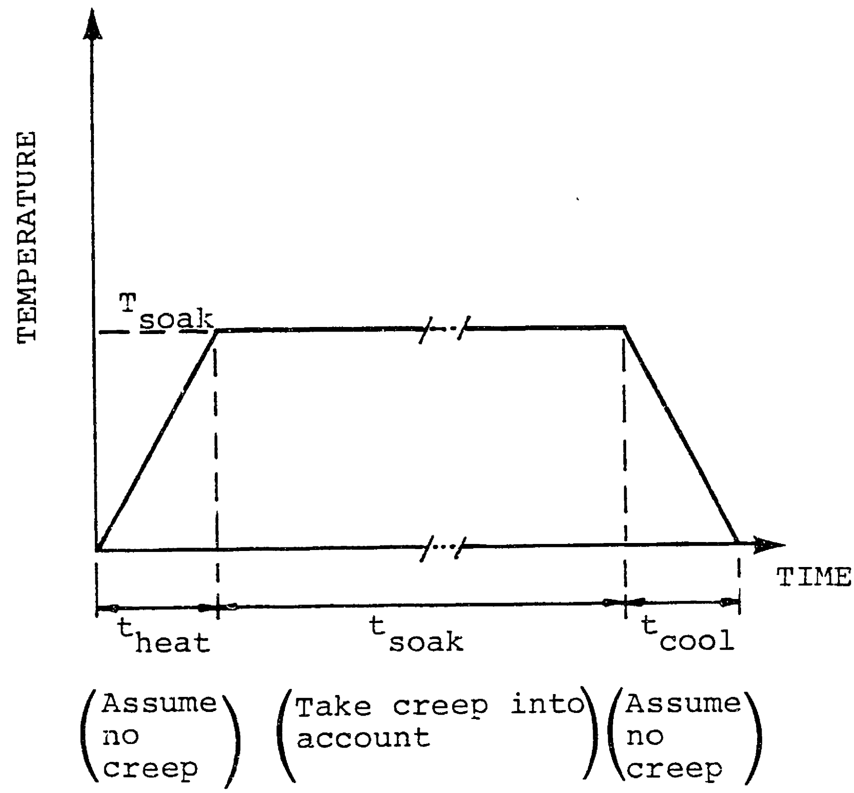

Figure 5.1 : Stress relieving temperature history

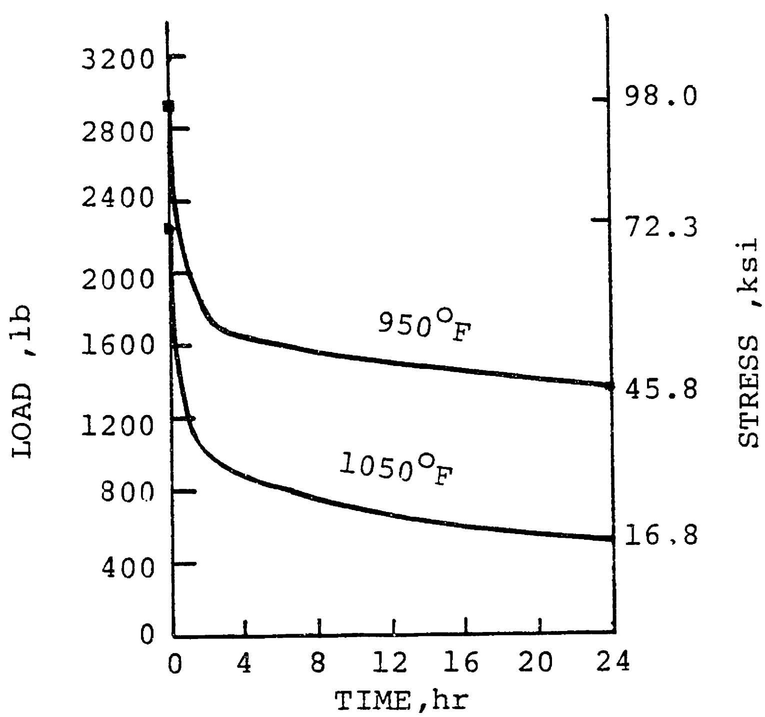

Figure 5.2 : Load vs. time from constant-strain relaxation tests on HY-130 steels and matching weld metals

it should be necessary to measure the maximum residual stresses before and after the treatment. The difference would be a realistic maasure of performance. An acceptable alternative, however, to the time-consuming, costly and usually destructive residual stress measurements, would be a proper analytical model. Furthermore , such a model would be very helpful in determining an optimal lower temperature heat treatment, where a properly selected heating pattern would most effectively reduce stresses, while keeping the metallurgical changes minimal.

In that direction, various approaches have been followed in the literature by several investigators. Very simple uniform residual stress destributions are usually assumed for the weld metal, so that the unidimensional stress-strain curves can be directly employed. Such analytical results are obtained and experimentally verified by Tanaka in [84] and [85]. For more complex cases and two-or three-dimensional stress states numerical models have been proposed to handle the thermal-elastic-plastic and creep analysis required.Ueda and Fukuda present in [86],[87] a finite element model capable of calculating welding residual stresses and stress relief due to creep. Fujita, et al., develop in [88] a thermo-visco-elastic-plastic model to study the mechanism of stress relief annealing. In [89] finally, Cameron and Pembreton present a numerical model of the thermal stress relief in thin shells of revolution.

For the purposes of this study, it was decided that the analysis of the thermal stress relieving operation be accomplished using an one-dimensional model, similar to that successfully employed in the past at M.I.T. for the prediction of residual stresses in long, thin, butt or edge welded plates, [90],[1]. The program was modified so as to calculate residual stresses, not only after welding, but also after any specified heat treatment. These modifications will be presented in the next few sections of this chapter.

5.2 The One-Dimensional Model

5.2.1 Assumptions

The fundamental assumptions incorporated in this model are:

(a) The plate is infinite and very thin (Refering to Figure 5.3, $L \to \infty$, $h \to 0$)

(b) The welding arc is modeled as a line heat source and there is no temperature gradient through the thickness of the plate. (Two-dimensional temperature distribution).

(c) Furthermore the temperature distribution is stationary if viewed from a system moving with the heat source. (Quasi stationary state [1]).

(d) Stress is non-zero only in the direction parallel to the weld centerline. (One-dimensional stress distribution).

(e) These stresses are a function of the transverse distance from the weld centerline only.

Additional assumptions for the analysis of thermal stress relief treatment were made as follows:

(f) Any arbitrary temperature distribution and history would be input to the modified program. However, for the purposes of this study uniform temperature distribution was assumed over the entire plate, changing with time as in Figure 5.1.

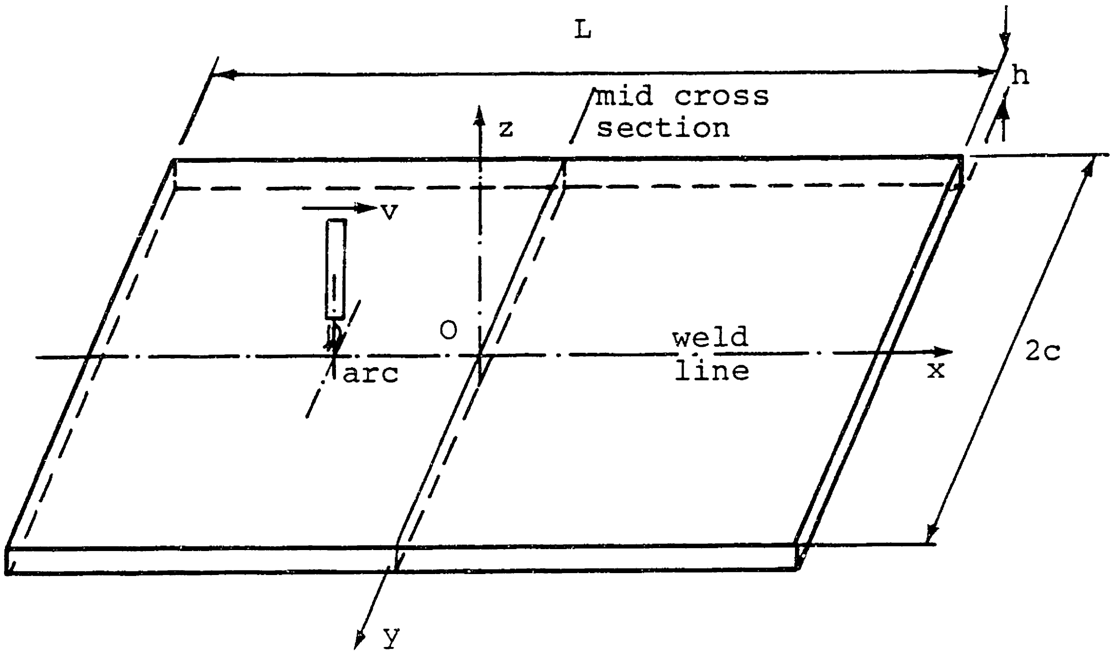

Figure 5.3 : Weldment configuration (Butt welding of plates)

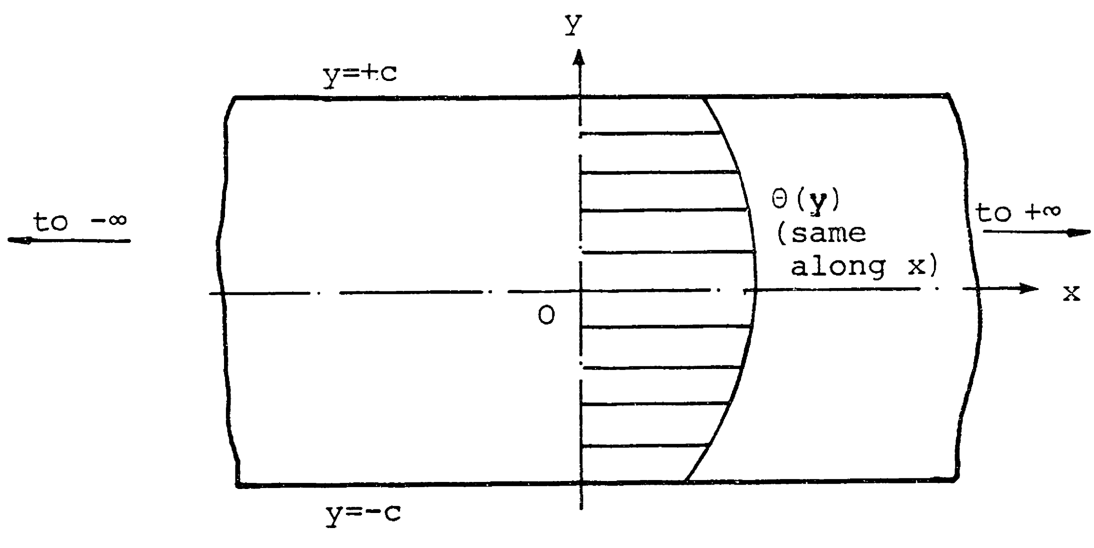

Figure 5.4 :Thin infinite strip with temperature distribution across the width

(g) Due to the relatively fast heating and cooling rates it was assumed that no creep occurs during these periods.

(h) During the holding or soaking period at the stress relieving temperature, residual stresses can only decrease due to creep. In other words, if creep is not included in the model, no change in stresses will take place during this period.

5.2.2 Temperature Distribution

During welding the non uniform and changing with time temperature distribution is estimated in the one dimensional program by the well-known Rosenthal solution. Specifically, as proved in [91], the exact solution for a line heat source moving along an infinite plate is:

$$\Theta - \Theta_o = \frac{Q}{2\pi\lambda\ h} \cdot e^{-\frac{v}{2\kappa}\xi} \cdot K_o\left(\frac{vr}{2\kappa}\right) \qquad (5\text{-}1)$$

where : Θ = Temperature at point (x,y) at time t

Θ_o = Initial temperature

h = Plate thickness

λ = Thermal conductivity

κ = Thermal diffusivity ($\kappa = \frac{\lambda}{\rho c_p}$)

ρ = Density

c_p = Specific heat

Q = Total heat input

v = Welding speed

$K_o(x)$ = Modified Bessel function of second kind and zero order

The moving coordinates ξ and r are:

$$\xi = x - vt \tag{5-2}$$

and

$$r = (\xi^2+y^2)^{1/2} \tag{5-3}$$

The total heat input, Q, is

$$Q = V.I.n_a \tag{5-4}$$

where : V = Arc voltage

I = Arc current

n_a = Arc efficiency

During heat treatment in a furnace the temperature distribution can be assumed to be uniform along the entire plate. For the case of a localized treatment, however, by flame heating for example the temperature distribution can be calculated modifying the solution for a point heat source moving on an semi-infinite body. Specifically the point heat source (three-dimensional) solution is : ([91],[1]).

$$\Theta - \Theta_o = \frac{Q}{2\pi\lambda} \cdot e^{-\frac{v}{2\kappa}\xi} \cdot \frac{e^{-\frac{v}{2\kappa}R}}{R} \tag{5-5}$$

where : $R = (\xi^2 + y^2 + z^2)^{1/2}$ (5-6)

and all the other variables same as in (5-1).

The boundary conditions that have to be satisfied on the surfaces of a finite plate are

$$\frac{\partial \Theta}{\partial n} = 0$$

where : n the normal to the surface.

Therefore the solution has to be modified including infinite series of images of the heat source with respect to the boundaries as depicted in Figure 5.5, adapted from [128].

The Rosenthal solutions, two- or three-dimensional, assume that the material is isotropic ($\lambda_x = \lambda_y$) and that properties are independent of temperature. The latter assumption is by no means realistic for the welding or heat treating temperatures and an iterative scheme, described in section 5.4, has to be incorporated in the model to account for that.

Finally, it should be noted that equation 5.1 was also modified to account for heat losses due to radiation and convection from the surfaces of the plate, becoming:

$$\Theta - \Theta_o = \frac{Q}{2\pi\lambda h} \cdot e^{-\frac{v}{2\kappa}\xi} \cdot K_o\left(r\sqrt{\left(\frac{v}{2\kappa}\right)^2 + \frac{H}{\lambda T}}\right) \qquad (5\text{-}7a)$$

where : H = Average surface heat loss coefficient .

Furthermore, for a plate of finite breadth c, equation (5-1) has to be modified using an infinite number of images of the heat source. Thus it becomes in general :

$$\Theta - \Theta_o = \frac{Q}{2\pi\lambda h} \cdot e^{-\frac{v}{2\kappa}\xi} \cdot \sum_{-\infty}^{+\infty} K_o\left(r_m \cdot \sqrt{\left(\frac{v}{2\kappa}\right)^2 + \frac{H}{\lambda T}}\right) \qquad (5\text{-}7b)$$

where : $r_m = (\xi^2 + (y \pm 2mc)^2)^{1/2}$ for the mth image source.

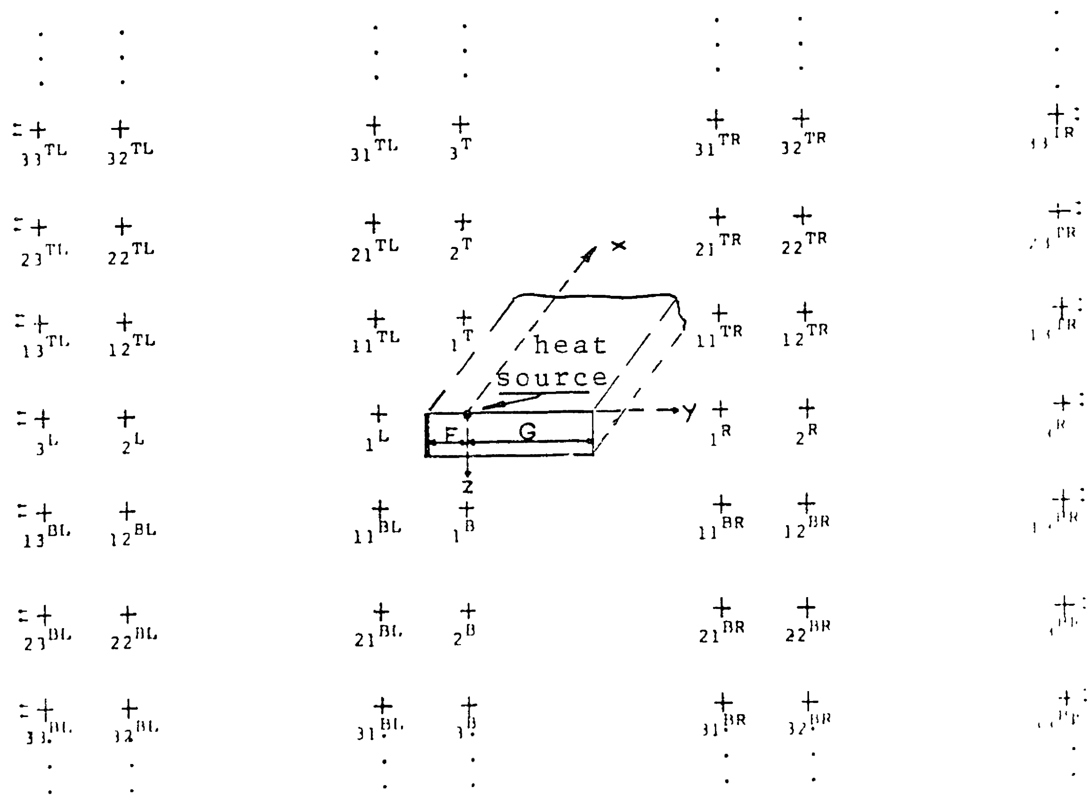

Figure 5.5 : Arrangement of heat source images for a finite width and thickness plate.

5.2.3 Stress Analysis

To calculate the transient and residual stresses during and after welding and subsequent heat treatments the method of successive elastic solutions is employed. The procedure, outlined by Mentelson in [92], was first used in the solution of welding problems by Tall, [93],[94], and later by Masubuchi, [95].

To analyse the stress state at the center cross section of the plate (Figure 5.3) due to an arbitrary, and changing with time, temperature distribution, $\Theta(y,t)$, it is assumed that at time t the section is a part of an infinitely long plate subject to the same temperature distribution over its entire length, as in Figure 5.4. This temperature profile will remain the same during the current time increment, Δt.

The only non-zero stress and strain are assumed to be $\sigma_x = \sigma_x(y)$ and $\varepsilon_x = \varepsilon_x(y)$.

Compatibility equations for one dimension reduce to,

$$\frac{d^2 \varepsilon_x}{dy^2} = 0 \qquad (5\text{-}8)$$

or

$$\varepsilon_x = c_1 + c_2 \, y \qquad (5\text{-}9)$$

where : c_1 and c_2 are constants to be determined. The above equation essentially states that plane sections will always remain plane.

Considering an incremental approach, at the end of a time interval Δt the following will hold along the cross section.

$$\varepsilon_x = \frac{\sigma_x}{E} + \alpha \, . \, \Delta\theta + \varepsilon_x^{in} + \Delta\varepsilon_x^{in} \qquad (5\text{-}10)$$

or

$$\sigma_x = E(\varepsilon_x - \alpha . \Delta\theta - \varepsilon_x^{in} - \Delta\varepsilon_x^{in}) \tag{5-11}$$

where : σ_x/E = Elastic part of strain, ε_x^{el}

$\alpha \cdot \Delta\theta$ = Thermal strain, ε_x^{th}

$\Delta\Theta$ = $\Theta - \Theta_o$

ε_x^{in} = Accumulated(during the previous time increments)inelastic strain = $\varepsilon_x^{pl} + \varepsilon_x^{c}$

ε_x^{pl} = Plastic strain

ε_x^{c} = Creep strain

$\Delta\varepsilon_x^{in}$ = Change in inelastic strain during the time increment Δt

From global equilibrium (no external forces and moments acting on the plate).

$$\int_{-c}^{+c} \sigma_x \, dy = 0 \tag{5-12a}$$

$$\int_{-c}^{+c} \sigma_x \, y \, dy = 0 \tag{5-12b}$$

Substituting Eqns. (5.9) and (5.11) into (5.12), a set of linear equations is obtained for the determination of the unknown coefficients c_1 and c_2. Solving this system and substituting back into Eqn. (5.9) the following expression is obtained for the total strain:

$$\varepsilon_x(y) = (A_1 - yA_2)\int_{-c}^{+c} E(\alpha \cdot \Delta\theta + \varepsilon_x^{in} + \Delta\varepsilon_x^{in}) \, dy$$

$$- (A_2 - yA_3)\int_{-c}^{+c} E(\alpha \cdot \Delta\theta + \varepsilon_x^{in} + \Delta\varepsilon_x^{in}) y \, dy \tag{5-13}$$

where :

$$A_1 = \left[\int_{-c}^{+c} Ey^2 \, dy \right] / B$$

$$A_2 = \left[\int_{-c}^{+c} E \, y \, dy \right] / B$$

$$A_3 = \left[\int_{-c}^{+c} E \, dy \right] / B \qquad (5\text{-}14)$$

and

$$B = \left[\int_{-c}^{+c} E \, dy \right] \cdot \left[\int_{-c}^{+c} Ey^2 \, dy \right] - \left[\int_{-c}^{+c} Ey \, dy \right]^2$$

Equations (5.13) and (5.14) are not enough to solve the problem. What is still needed is a stress-strain law and a relation between stress and creep strain increments.

To proceed further the assumption was made that creep will only take place during the soaking stage of the temperature history. Thus during this period the accumulated plastic strain, ε_x^{pl} , will remain constant. The heating and cooling stages where no creep occurs, are treated in exactly the same way as the welding problem.

5.2.4 The Method of Successive Elastic Solutions

(A) During welding, when creep does not occur :

$$\varepsilon^{in}(y) = \varepsilon^{pl}(y) \qquad (5\text{-}15)$$

At each time step the total strain is first calculated along the cross section from (5-13) assuming that no plastic strain exists.

$$\varepsilon^{pl}(y) = 0 \qquad (5\text{-}16)$$

The mechanical strain , ε^{m}, then is:

$$\varepsilon^{m}(y) = \varepsilon_x(y) - \varepsilon^{th}(y) = \varepsilon_x(y) - \alpha\cdot\Delta\theta(y) \qquad (5\text{-}17)$$

Now assuming a bilinear stress-strain law, a first approximation of the plastic strain along the cross section can be obtained, as in Figure 5.6. This value can be used again in (5.13) to obtain a second approximation of the total strain and the process can be repeated until convergence is reached.

Further details of this iterative procedure, which can also be applied during the heating and cooling stages of a heat treatment, can be found in [90] and [92]. It should be noted, however, that during the calculation of the total strains, at each time step, the accumulated plastic strains from previous time steps should be included to account for possible elastic unloading or reverse yielding.

(B) During the holding period, when creep is taken into account, this procedure has to be slightly modified:

At the start of the first time increment the inelastic strain is:

$$\varepsilon_x^{in}(y) = \varepsilon_x^{pl}(y) \qquad (5\text{-}18)$$

where : ε_x^{pl} is the total accumulated plastic strain up to that instant (due to welding and heating).

As mentioned before ε_x^{pl} will remain constant during the whole soaking period.

To get a first approximation of the total strain, ε_x,

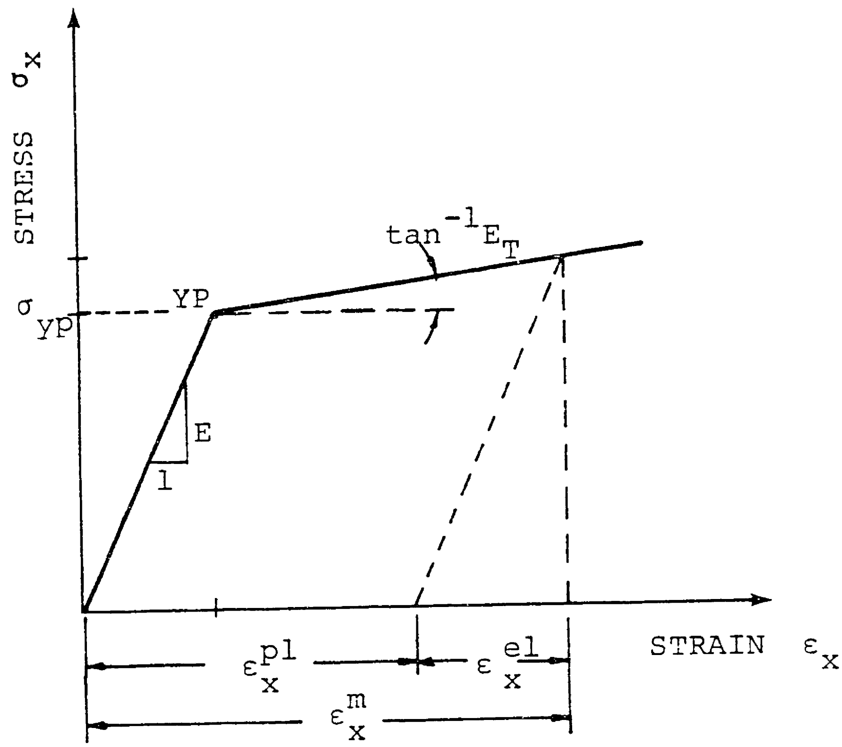

Figure 5.6 : Bilinear stress strain law used in 1-D model

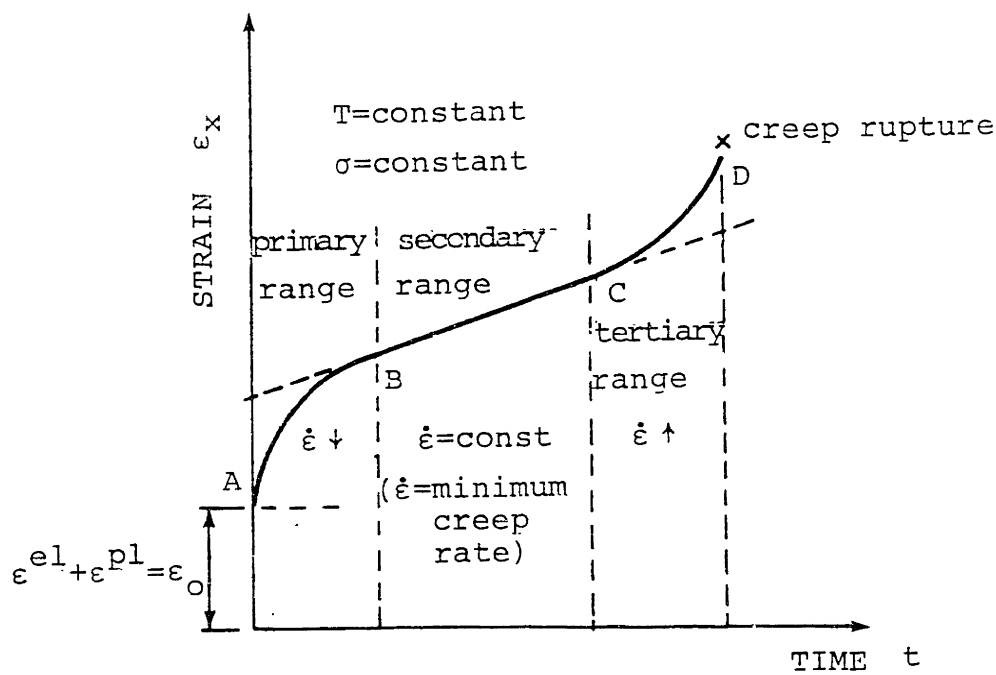

Figure 5.7 : Uniaxial creep curve

after Δt, from equation (5.13) it is now assumed that:

$$\Delta\varepsilon_x^{in} = \Delta\varepsilon_x^{c} = 0 \qquad (5\text{-}19)$$

This first approximation of the total strain, ε_x, is then substituted in equation (5-11) to obtain a first approximation of stress σ_x. Using this stress approximation and the appropriate creep law (section 5.2.5) a second approximation for the creep strain increment, $\Delta\varepsilon_x^{c} = \Delta\varepsilon_x^{in}$, is obtained. This value is now again substituted in equation (5-13) for a new approximation of the total strain ε_x; and the process is repeated until convergence is reached.

At the start of the second and any subsequent time increment the total strains will be equal to the initial plastic strain plus the accumulated creep strain during the previous time increments:

$$\varepsilon_x^{in}(y) = \varepsilon_x^{pl}(y) + \sum_{i=1}^{n-1} \Delta\varepsilon_x^{c}(y) \qquad (5\text{-}20)$$

Assuming again that $\Delta\varepsilon_x^{c}$ is zero during this time step the process outlined above can be repeated.

5.3 Creep Laws

5.3.1 Introduction

Creep, the time dependent deformation and fracture of materials, is probably the most general type of material behavior. A typical experimental uniaxial creep curve is shown in Figure 5.7 showing increasing with time strain for constant stress and temperature. At t=0 the instantaneous response ε_0 is either elastic or elasto-plastic depending on the magnitude of stress. The strain rate $\dot{\varepsilon} = d\varepsilon/dt$ is decreasing, in the primary range, reaching a minimum constant value, in the secondary range, and steeply increasing in the final tertiary range, where creep rupture occurs.

The current state of the art requires that plasticity and creep constitutive equations be formulated largerly on independent bases. However, elevated-temperature deformation is, essentially, the result of time-dependent processes where both plastic and creep behaviors are present simultaneously. Prior creep deformations influence subsequent plastic behavior and vice versa. Only limited information is available on these mutual interactions as outlined by Pugh, et al., in [96] and by Corum, et al., in [97]. Some recent studies, as [104] by Newman, et al., attempt to treat plasticity and creep with a single model. However, for the purposes of this study the two behaviors were modeled separately as already noted in the previous section.

5.3.2 Uniaxial Creep Laws for the Materials Used in this Study

Very limited information is available in the literature on the creep behavior of high-strength, quenched and tempered steels, as HY-80 and HY-130. Only some data on the minimum creep rate and creep rupture time are reported by Domis [100], and are presented in Appendix A, as adapted from [101].

For stainless steels, on the other hand, numerous studies have been performed to investigate their elevated-temperature inelastic behavior. Creep data for 304 austenitic stainless steel appear in Appendix A. Furthermore, it is reported by Clinard, et al., in [102], and Corum, et al., in [97], that the uniaxial creep behavior of stainless steels during the primary and secondary stage can be very well modeled by an equation of the form:

$$\varepsilon^{c}(\sigma,t,T) = f(\sigma,T)\left[1-e^{-r(\sigma,T)t}\right] + g(\sigma,T).t \qquad (5\text{-}21)$$

initially proposed by Garofalo, et al., in [103],

where : ε^{c} = Uniaxial creep strain

σ = Applied uniaxial stress

T = Test temperature

t = Time

The functions $f(\sigma,T)$, $r(\sigma,T)$ and $g(\sigma,T)$ can be deduced from creep test data by curve fitting. Clinard et al., [102], report for 304 stainless steels, the following representation at $T = 1100^{o}$ F (594^{o} C).

$$\begin{aligned} f(\sigma) &= 5.436\text{x}10^{-5}\sigma^{1.843} \\ r(\sigma) &= 5.929\text{x}10^{-5}\exp(0.2029\sigma) \\ g(\sigma) &= 6.73\text{x}10^{-9}\left[\sinh(0.1479\sigma)\right]^{3.0} \end{aligned} \qquad (5\text{-}22)$$

where : σ is expressed in Ksi, t in hours and the creep strain

ε^c in in./in.

Existing data are not enough to support a creep law for compressive stresses that is different from the creep law in tension. Therefore creep response to constant uniaxial compression is usually assumed identical to that in tension (actually a reflection of it with respect to the time axis)

The creep strains predicted from equation 5-21 at various stress levels are plotted versus time in Figures 5.8a and 5.8b.

5.3.3 Multiaxial Creep Models

A "flow rule" for the case of multiaxial stress can be developed based on the experimentally verified assumptions that (a) the material is isotropic and incompressible (b) the creep strains are indifferent to hydrostatic states of stress and (c) the principal directions of stress and creep strain should coincide. (As detailed in references [96] to [99]).

Such a flow rule that would also reduce to the uniaxial creep law is of the form:

$$\dot{\varepsilon}^c_{ij} = \frac{3}{2}\,\frac{\dot{\bar{\varepsilon}}\,(\bar{\sigma},t,T)}{\bar{\sigma}}\;\sigma'_{ij} \qquad (5\text{-}23)$$

where : $\dot{\varepsilon}^c_{ij}$, σ'_{ij} = The components of creep strain and deviatoric stress tensors respectively.

$\bar{\varepsilon},\bar{\sigma}$ = The effective strain and stress

$\bar{\varepsilon}^2$ = $\frac{2}{3}\,\varepsilon^c_{ij}\cdot\varepsilon^c_{ij}$

$\bar{\sigma}^2$ = $\frac{3}{2}\,\sigma'_{ij}\cdot\sigma'_{ij}$

and $\dot{\bar{\varepsilon}}(\bar{\sigma},t,T)$ = The uniaxial creep law with axial stress and strain variables replaced by their

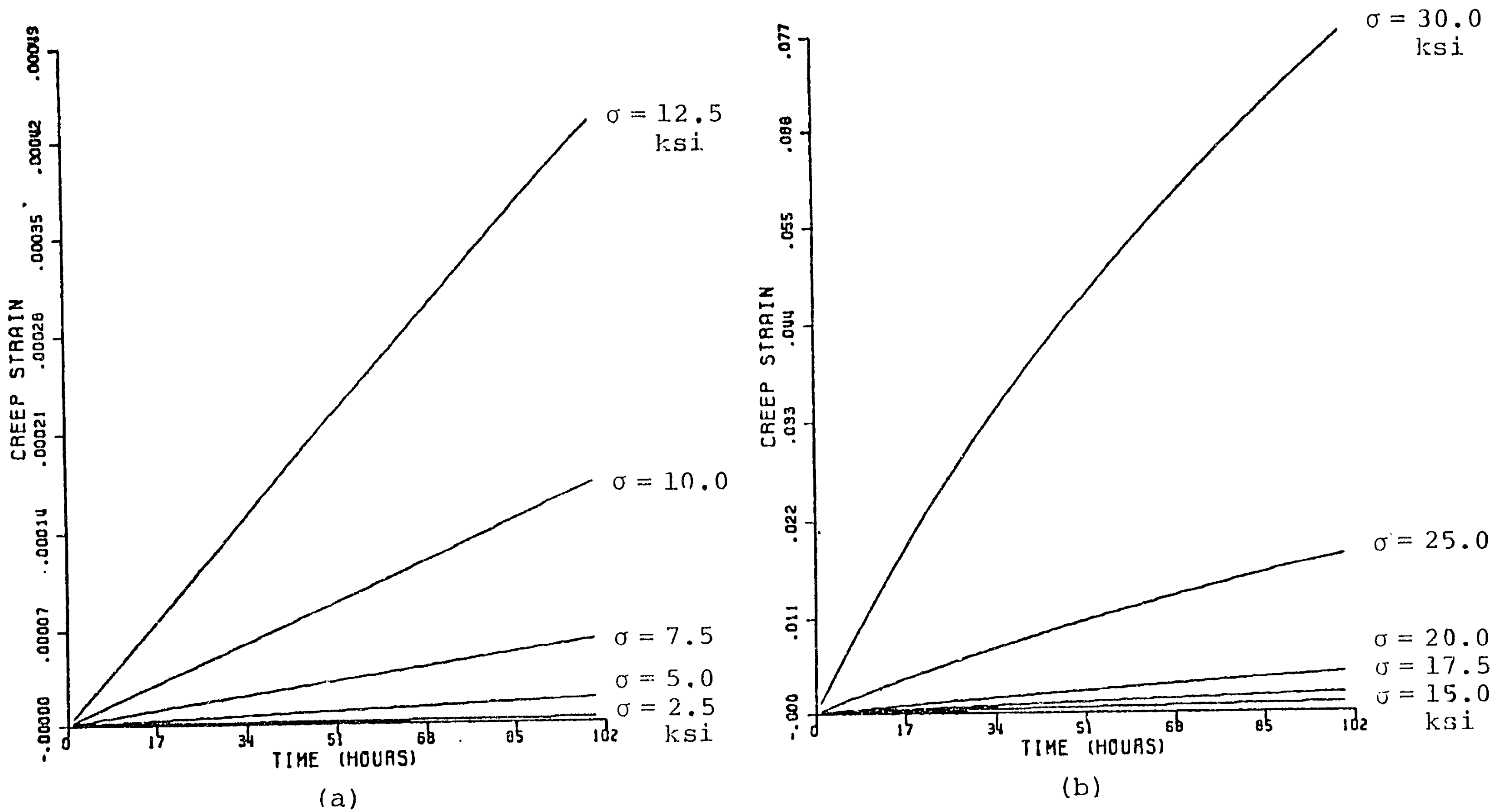

Figure 5.8 : Uniaxial creep law for type 304 stainless steel at 1100^{O}F

effective counterparts.

However, in the simplified one-dimensional model such a flow rule is not needed since a uniaxial stress state is assumed.

5.3.4 Creep Under Variable Loading

For the complete description of the time dependent behavior of the material, a "hardening rule" is needed in order to predict the creep response when the stress levels are changing. The two most commonly used rules, time hardening and strain hardening, are schematically shown in Figure 5.9. When the applied uniaxial stress is $\sigma = \sigma_1$ the creep response follows the constant-stress creep curve (σ_1). At time t_1, when the applied stress increases to $\sigma = \sigma_2$ the time hardening rule would predict that the creep response follows the (σ_2) curve beginning at point T. The strain hardening formulation, on the other hand, would indicate that the response also follows the curve (σ_2), but begining at point S.

The two different hardening rules also result in different formulations for the creep strain rate in a variable stress situation. Specifically, if time hardening is assumed, the creep strain rate is a function of stress time and temperature; if strain hardening is postulated, however, the creep strain rate becomes a function of stress, strain and temperature [99].

Experimental evidence tend to support a strain hardening formulation for the case of 304 and 316 stainless steels. Additionally, if stress reversals occur, auxiliary strain hardening rules have to be introduced in order to avoid unrealistic predictions. These auxiliary rules in detail presented by Corum, in [97], would for example indicate that

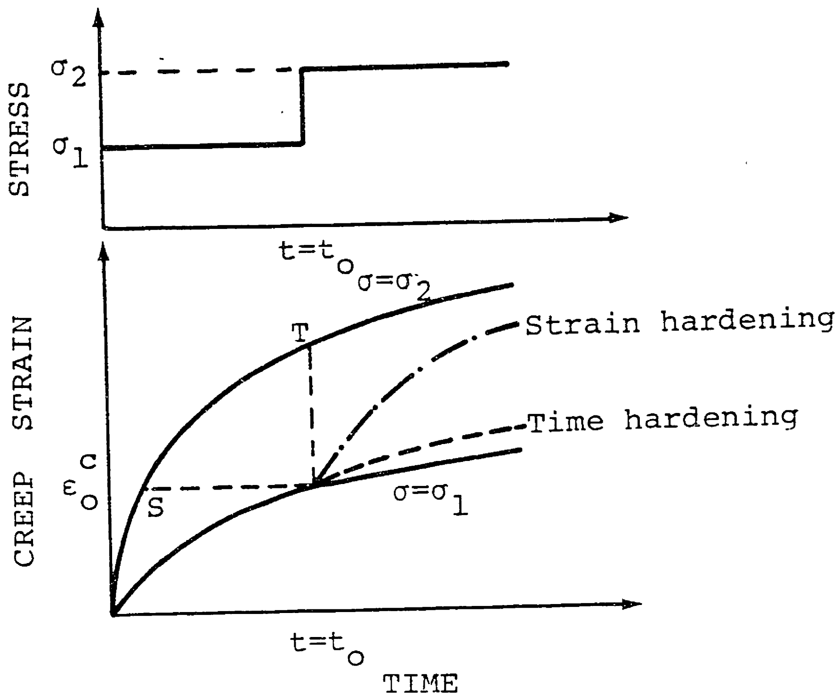

Figure 5.9 : Strain-hardening and time-hardening models of creep response under a stepwise varying load

the creep response produced by the first application of compressive stress starts at zero strain hardening as in the case of a virgin specimen. It should be pointed out, however, that these rules are strictly correct only in step changes of stress that are of long duration. In our problem where small changes of stress take place at each infinitesimal time step, it was decided, for computational efficiency, to adopt time-hardening. The reason for that will become evident in section 5.4.3.

5.4 Notes on the Computer Implementation

5.4.1 Temperature Distribution

A special iterative scheme has to be used in order to account for the temperature dependence of the material properties. The procedure starts by assuming a temperature Θ_A and using it for a first estimate of ρ and λ. Substituting these values back to equation (5-1) would give a first approximation of the temperatures $\Theta(y)$ along the cross section. These can now be used for a better estimation of the properties (ρ and λ) which again can be substituted in (5-1) for a new approximation of $\Theta(y)$. This process, shown in Figure 5.10, can then be continued until convergence is attained.

5.4.2 Stress Analysis

A non-dimensional form of the equations is used in the program. Specifically we define the non-dimensional stress and strains:

$$S = \frac{\sigma_x}{\sigma_o}, \quad e_x = \frac{\varepsilon_x}{\varepsilon_o}, \quad \tau = \frac{\alpha\ \Delta\Theta}{\varepsilon_o}$$

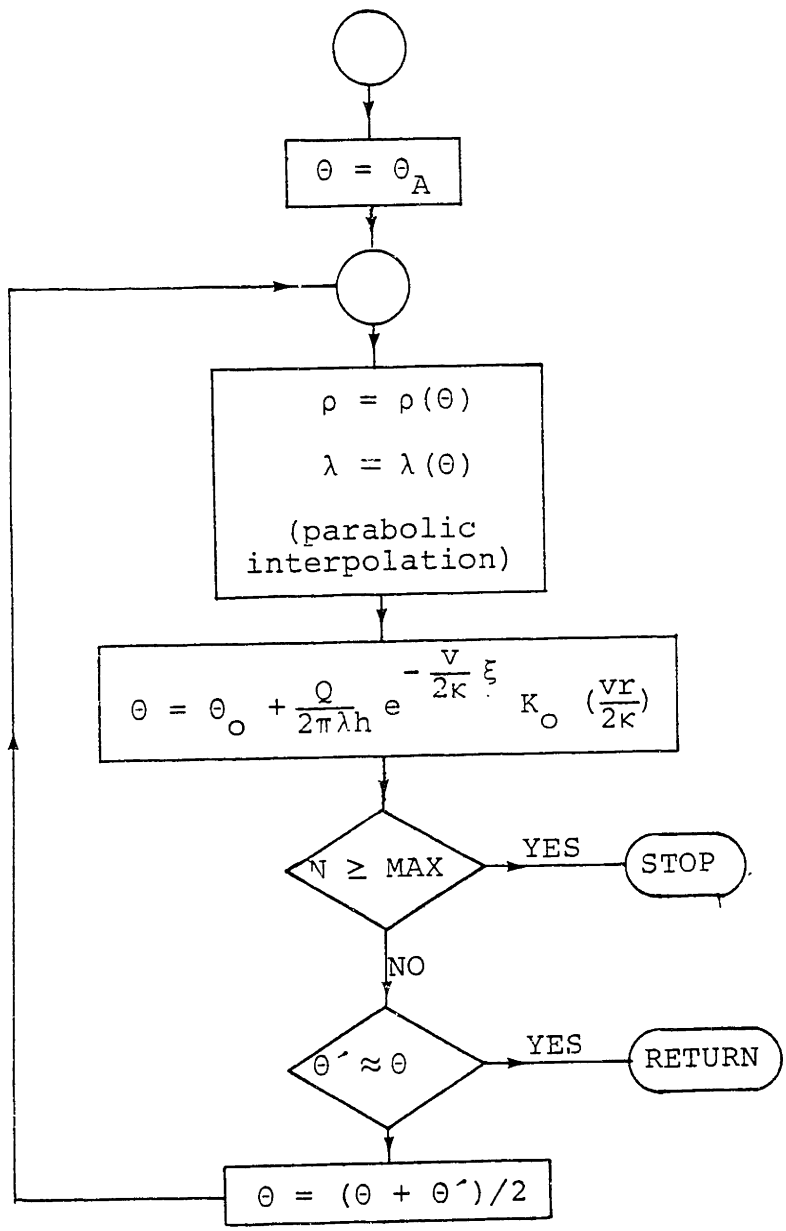

Figure 5.10: Iterative scheme to take into account the variation of properties with temperature.

$$e_x^{el} = \frac{\varepsilon_x^{el}}{\varepsilon_o} , \quad e_x^{pl} = \frac{e_x^{pl}}{\varepsilon_o} , \quad e^c = \frac{e_x^c}{\varepsilon_o} \qquad (5\text{-}24)$$

and the non-dimensional transverse distance and Youngs modulus:

$$\eta = \frac{Y}{c} \quad \text{and} \quad H = \frac{E}{E_o} \qquad (5\text{-}25)$$

where : σ_o = Yield stress at reference temperature

ε_o = Yield strain at reference temperature

E_o = Young's modulus at reference temperature

Now equations (5-8) to (5-12) can be expressed in non-dimensional form and the total strain will be given by :

$$e_x(\eta) = (A_1 - \eta A_2) \int_{-1}^{+1} H(\tau + e_x^{in} + \Delta e_x^{in})\, d\eta - $$
$$- (A_2 - \eta A_3) \int_{-1}^{+1} H(\tau + e_x^{in} + \Delta e_x^{in})\, \eta \, d\eta \qquad (5\text{-}26)$$

where:

$$e_x^{in} = e_x^{el} + e_x^{pl} + e_x^c \qquad (5\text{-}27)$$

$$A_1 = \left[\int_{-1}^{+1} H \, \eta^2 \, d\eta \right] / B$$

$$A_2 = \left[\int_{-1}^{+1} H \, \eta \, d\eta \right] / B \qquad (5\text{-}28)$$

$$A_3 = \left[\int_{-1}^{+1} H \, d\eta \right] / B$$

$$B = \left[\int_{-1}^{+1} H \, d\eta \right] \left[\int_{-1}^{+1} H \, \eta^2 \, d\eta \right] - \left[\int_{-1}^{+1} H \, \eta \, d\eta \right]^2$$

The integrals are evaluated numerically and the equations can be simplified even further in specific cases.

For bead on plate welding where the temperature distribution and the resulting strains and stresses are symmetric around the weld line, equation (5-26) yields :

$$e_x(\eta) = \frac{\int_0^1 H(\tau+e_x^{in}+\Delta e_x^{in})\,d\eta}{\int_0^1 H\,d\eta} \qquad (5\text{-}29)$$

For <u>edge welding</u> along the side of a plate of breadth c equation (5-26) still holds, but with the integration limits from 0 to +1.

During <u>heat treating</u> at a <u>constant temperature</u> equation (5-26) can be further simplified. If we assume a symmetric previous distribution of strains and stresses ,we readily get from (5-29):

$$e_x = \tau + \int_0^1 (e_x^{in} + \Delta e_x^{in})\,d\eta \qquad (5\text{-}30)$$

Whereas for any nonsymmetric distribution of stresses we can get after some algebra from (5-26) that:

$$e_x = \tau+(12\eta-6)\int_0^1 (e_x^{in}+ \Delta e_x^{in})\,\eta\,d\eta +(4-6\eta)\int_0^1 (e_x^{in}+ \Delta e_x^{in})\,d\eta \qquad (5\text{-}31)$$

For butt welding of plates the solution for edge welding is used ahead of the arc and the solution for bead on plate welding behind the arc (where the weld pudle is solidified).

All the above integrations are performed numerically in the program and more details on the integration scheme that was used are given in Appendix B. A listing of the FORTRAN code can be found in Appendix C.

5.4.3 Creep Analysis

Equation (5-21) is the form of creep law employed in the numerical model developed in this study for the analysis of stress relieving of 304 stainless steel. Specifically the creep strain increment $\Delta e_x^c(y)$ accumulated between time t and t+ Δt (at each point along the cross section) is :

$$\Delta\varepsilon_x^c(y) = \varepsilon_x^c\left[\sigma_x(y),(t+\Delta t),T(y)\right] - \varepsilon_x^c\left[\sigma_x(y),t,T(y)\right] \qquad (5\text{-}32)$$

where : $T(y)$ = The temperature distribution and

$\sigma_x(y)$ = The current approximation of the stress distribution

In equation (5-32) the creep strain rate $\Delta\varepsilon_x^c(y)/\Delta t$ is a function of stress, time and temperature. That is, time hardening was assumed in order to avoid the added computations of solving (5-21) for time, as a strain hardening formulation would require. Nevertheless, however, the latter would not necessarily guarantee better results due to the small size of the time steps. It should be again noted here that both temperature and stress at each point change stepwise. That is, they are assumed to remain constant at each point for the duration of each time increment, (as in the "time increment-initial strain" method described in [96]).

5.4.4 A Sample Case

In what follows a sample case is presented. Specifically butt welding of two plates and subsequent stress relieving heat treatment at 1100°F (594°C) are analysed. The welding conditions were assumed the same as in the edge welding case of the next Chapter (Table 6.6).

Predicted temperatures strains and stresses during welding are plotted in Figures 5.11, 5.12 and 5.13 respectively. The assumed temperature history during stress relieving (uniform heating) is shown in Figure 5.14. The variation of stresses throughout the treatment is followed in Figure 5.15 and a comparison of the residual stresses before and after stress relieving can be found in Figure 5.16.

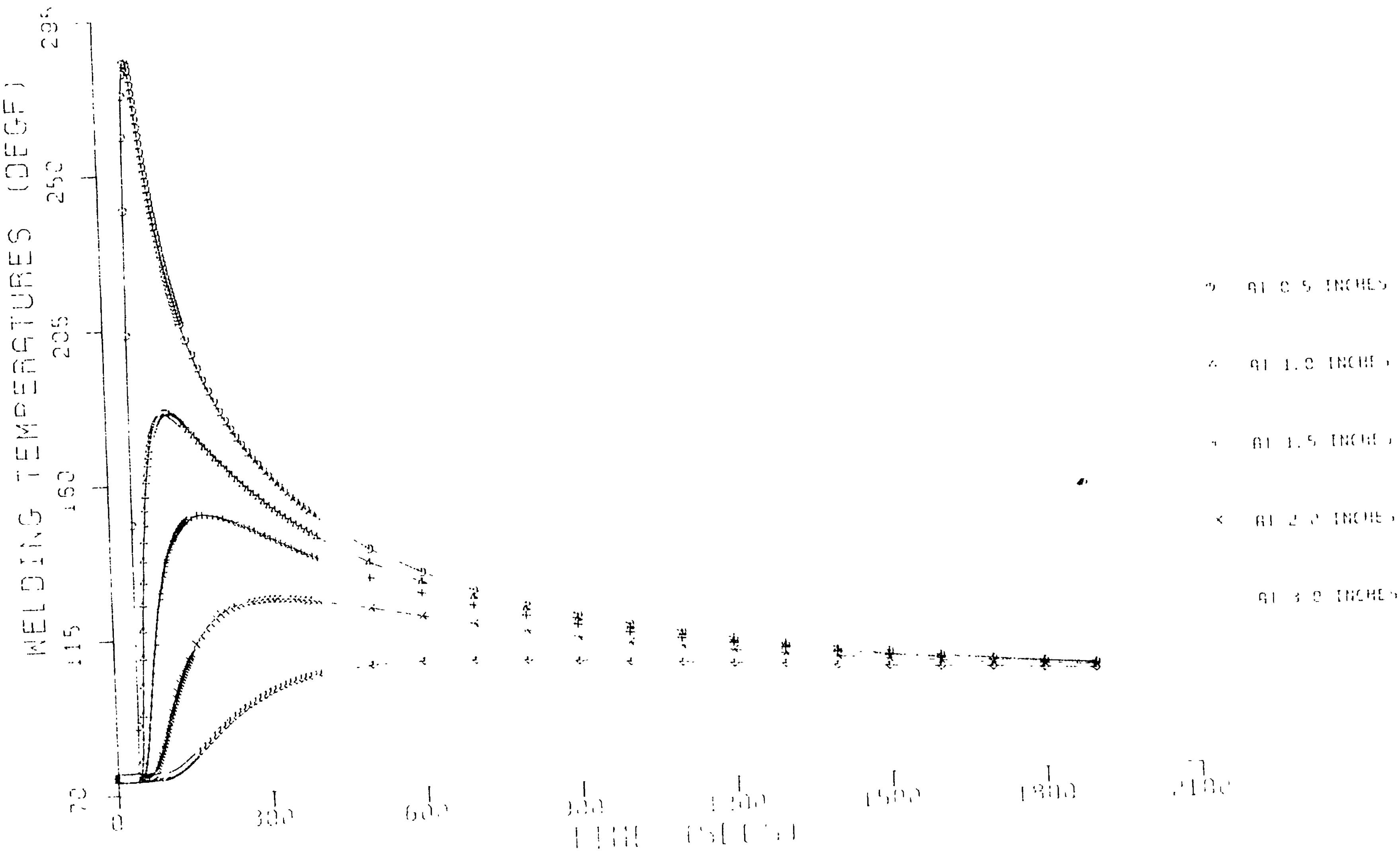

Figure 5.11 : Temperature history during butt welding, as predicted by the one dimensional program (304 stainless steel).

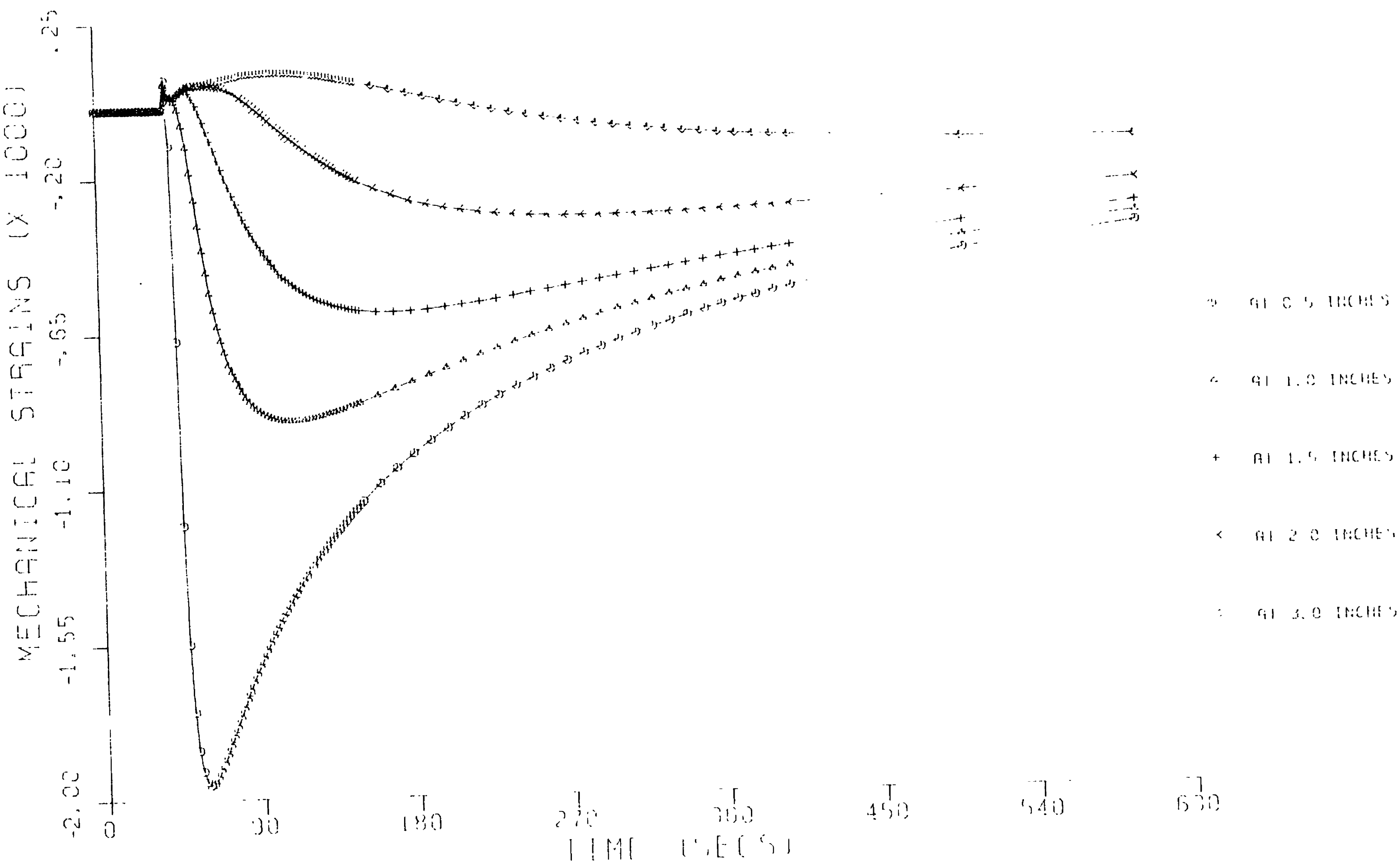

Figure 5.12 : Mechanical strains during butt welding as predicted by the one-dimensional program (304 stainless steel).

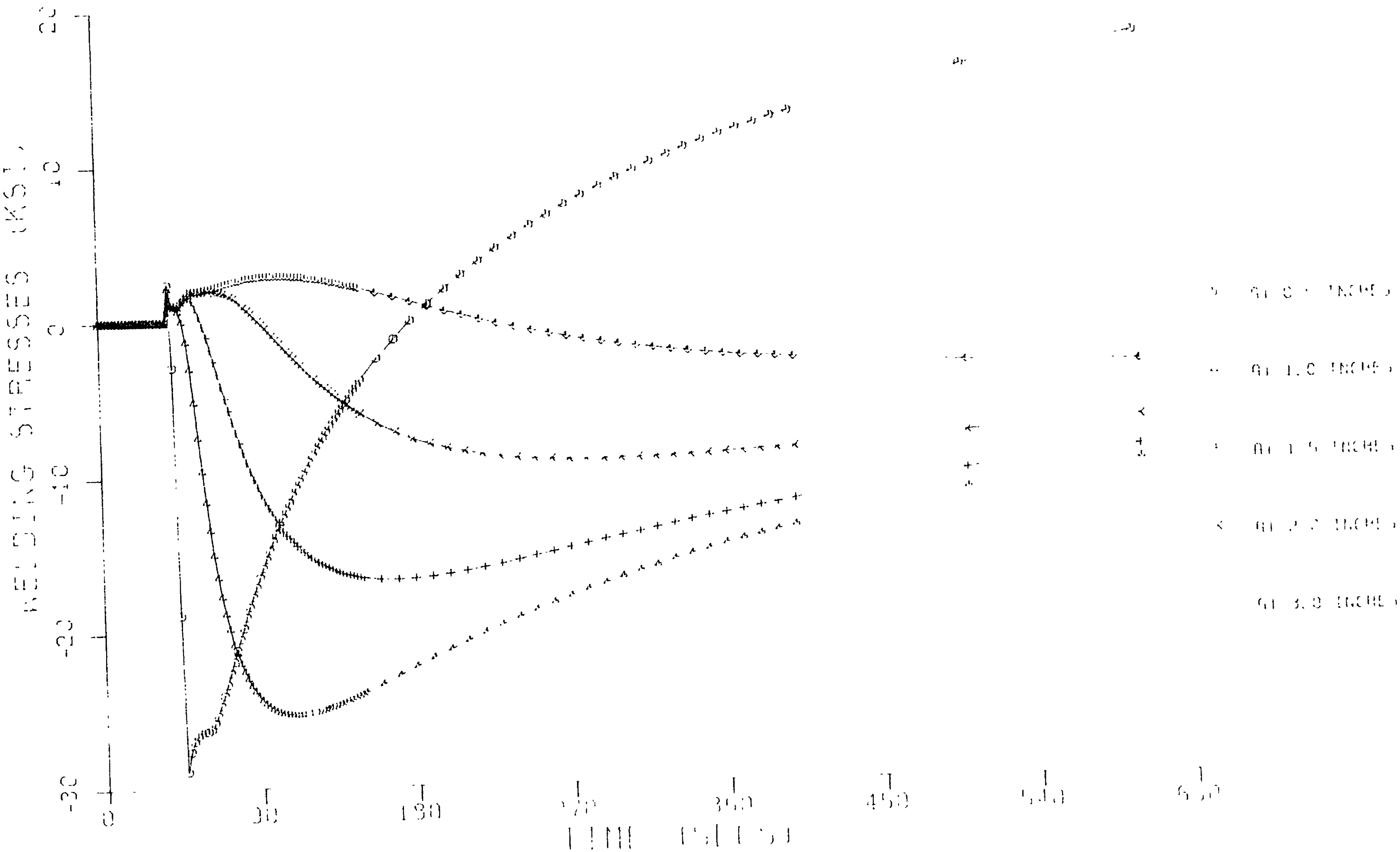

Figure 5.13 : Stresses during butt welding, as predicted by the one-dimensional program (304 stainless steel).

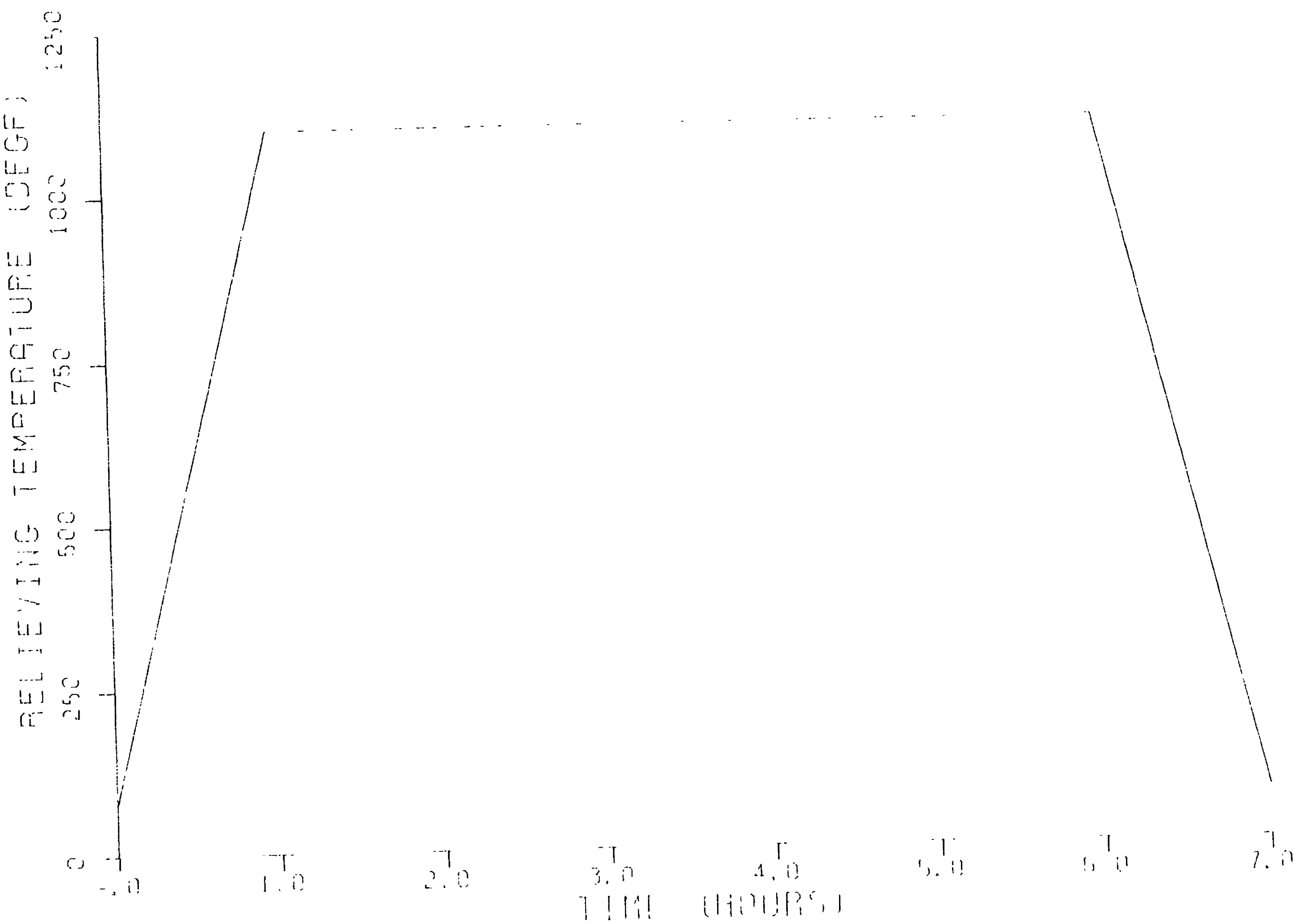

Figure 5.14 : Stress relieving temperature history, uniform along the entire plate at each time step.

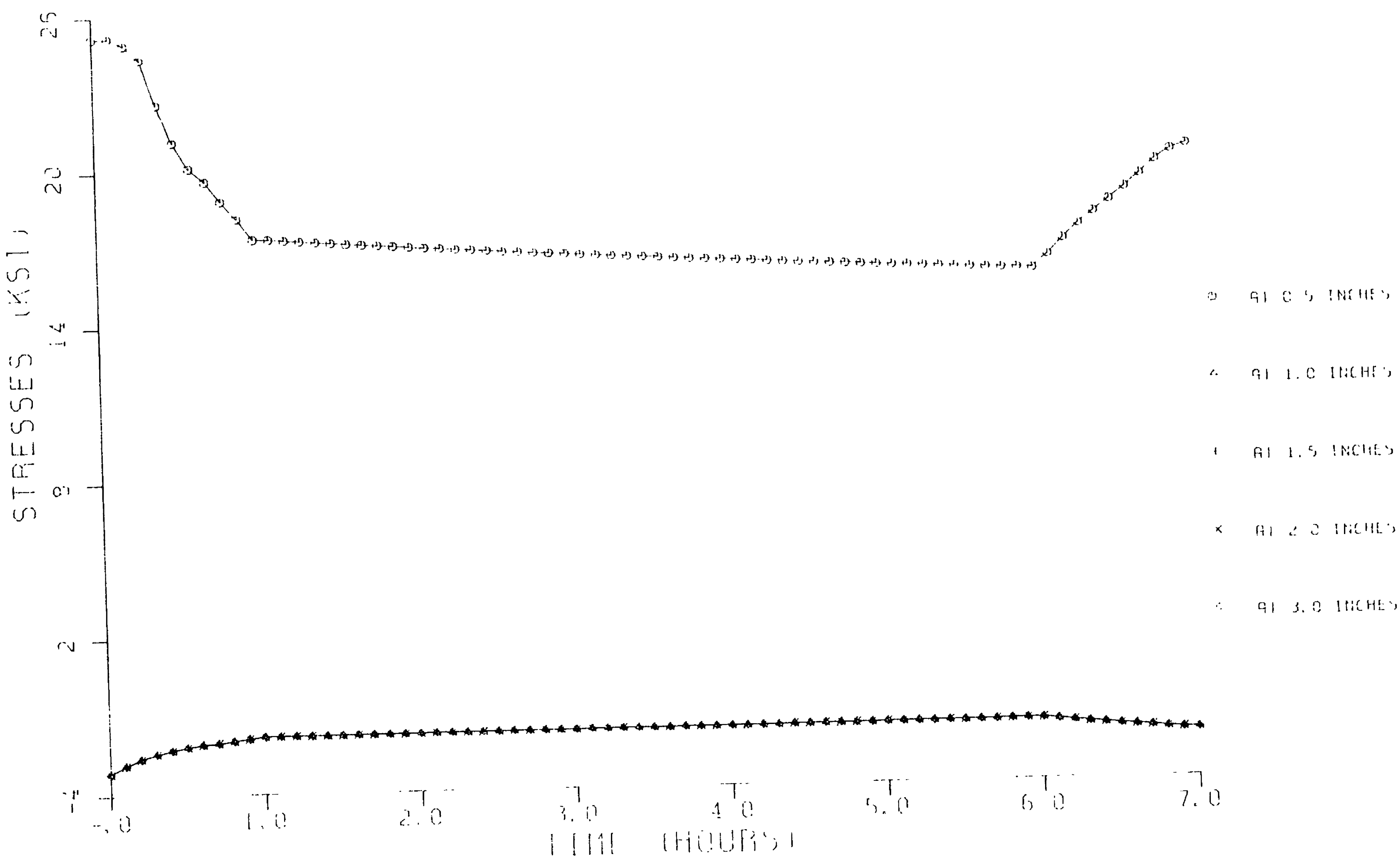

Figure 5.15 : Variation of stresses during heating, soaking and cooling (304 stainless steel)

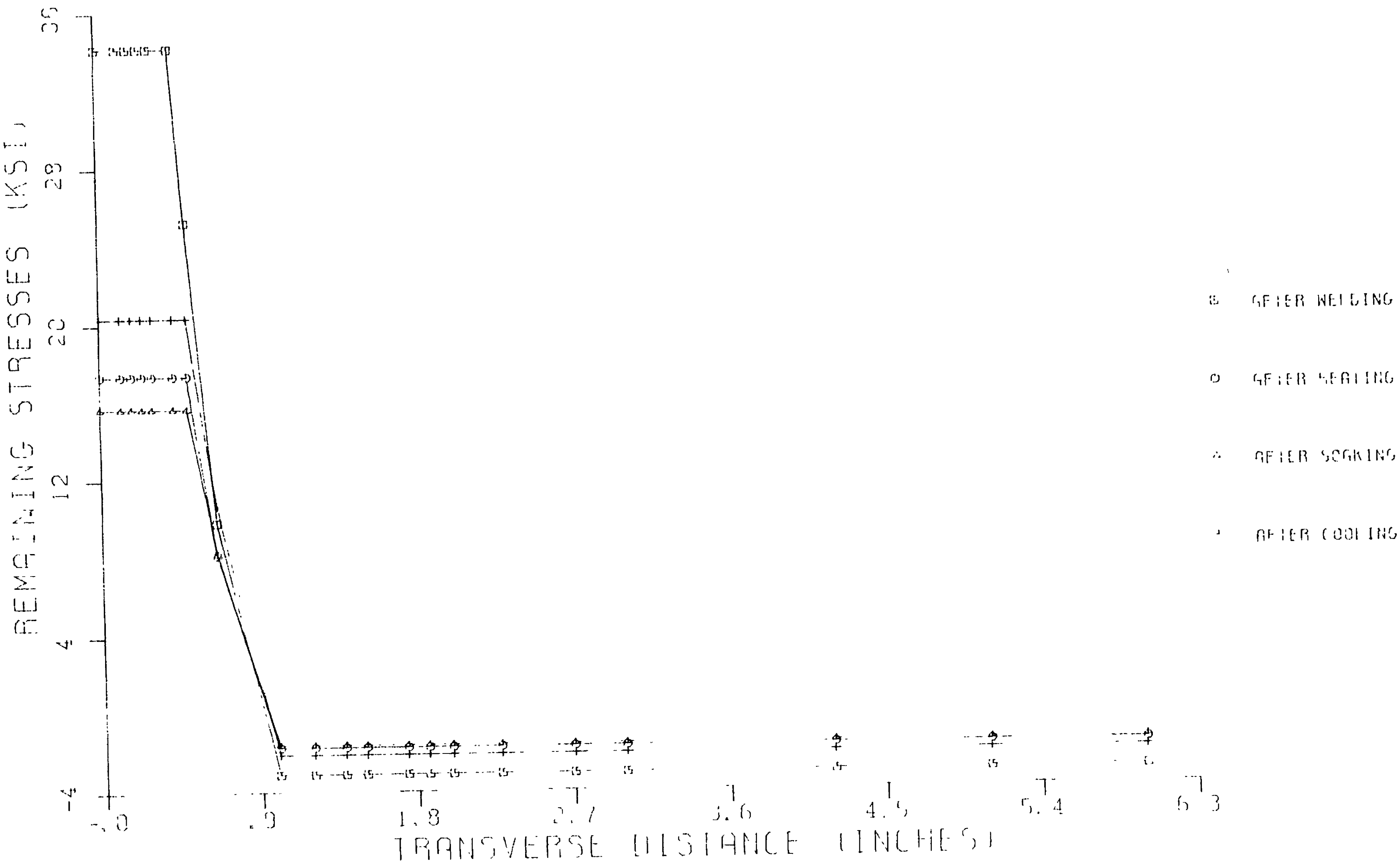

Figure 5.16 : Remaining stresses distribution along the plate after welding, heating, soaking and cooling (304 stainless steel)

PART III

EXPERIMENTS AND COMPUTER AIDED DATA ACQUISITION

CHAPTER VI

EXPERIMENTS AND COMPUTER-AIDED DATA ACQUISITION

6.1 General Description of Experiments

To verify the analytical results, experiments were performed with 304 stainless steel plates. All plates were edge welded and all but one were subsequently stress relieved in a furnace at different holding temperatures. The plates were finally sectioned and residual stresses were measured by stress relaxation.

Temperatures and strains at various locations on the plates were monitored throughout welding and stress-relieving operations. For this purpose a microprocessor-based data aquisition system was interfaced with the minicomputer (MINC-23) that performed the data reduction, processing and plotting.

The geometry and the dimensions of the specimens are given in Table 6.1 together with a brief description of the experiments performed on each of them. Exact welding conditions and stress relieving parameters are given in the next sections of this chapter.

6.2 Specimen Instrumentation (Strain Gages and Thermocouples)

The temperature and strain changes during welding and subsequent heat treatment were measured by thermocouples and electrical-resistance strain gages attached on the plates. The thermocouple and strain gage locations are depicted in Figure 6.1. The total number of strain gages and their configuration is given in Table 6.2 for all specimens.

Thermocouples were of Chromel-Alumel type (ANSI symbol K)

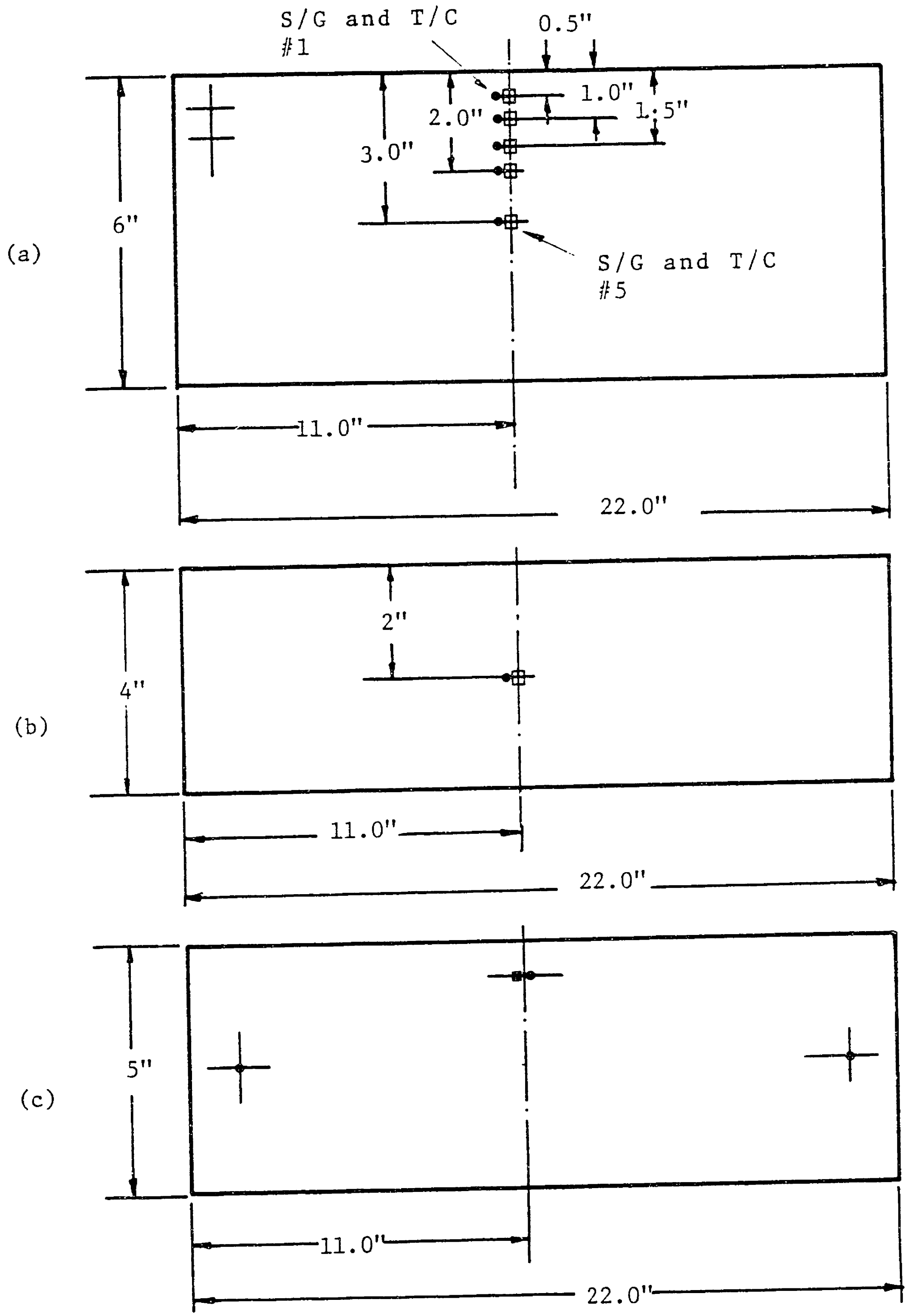

Figure 6.1 : Specimen geometry and instrumentation

Note : □ Strain gage locations
■ ● Thermocouple locations

Table 6.1: Specimen Dimensions and Experiments Description

Specimen Number	Dimensions inches (mm)	Experiments Performed
1	22 x 6 x 3/8 (555.8x152.4x9.5)	Instrumented, edge welded (one pass), stress relieved (oven), cut.
2	as above	Instrumented, edge welded (one pass), strain gages added, cut.
3	as above	Instrumented, edge welded (one pass), stress relieved, cut.
4	as above	Instrumented, edge welded (one pass), stress relieved, reinstrumented, cut.
5	22 x 4 x 3/8 (555.8x101.6x9.5)	Instrumented, bead on plate welded (multiple passes). Test of data aquisition system.
6	22 x 5 x 3/8 (555.8x127.0x9.5)	Instrumented (T/C only), stress relieved to test oven heating uniformity.
7 to 9	as above	Welded -edge and bead on plate- to determine welding conditions (multiple passes).

Table 6.2: Arrangement of Strain Gages and Thermocouples

Specimen	Strain Gages		Thermocouples		Arrangement
No	Number	Configuration	Number	Configuration	as in
1	5	A	5	C	Fig 6.1 (a)
2	5 (1)	A	5	C	Fig 6.1 (a)
3	10	B	5	C	Fig 6.1 (a)
4	10 (2)	B	5	C	Fig 6.1 (a)
5	1	A	1	C	Fig 6.1 (b)
6	0	-	3+1	C+D	Fig 6.1 (c)

Key: (A): Single gages in the longitudinal direction on the one side of the plate only.

(B): Single gages in the longitudinal direction on both sides of the plate.

(C): Thermocouples located at the surface of the specimen on one side only.

(D): Thermocouples burried at the mid-thickness of the plate.

Notes: (1): 5 more gages were added before cutting in the transverse direction.

(2): 10 new gages were installed before cutting in both longitudinal and transverse direction.

Table 6.3: Strain Gage Characteristics

Type	:	WK-09-062AP-350
Temperature Range	:	
Continous use: $-452^{\circ}F$ ($-269^{\circ}C$) to $550^{\circ}F$ ($+290^{\circ}C$)		
Short term exposure: up to $700^{\circ}F$ ($+370^{\circ}C$)		
Strain limits	:	
Room temperature		±1.5%
$-320^{\circ}F$ ($-195^{\circ}C$)		±1.0%
$+400^{\circ}F$ ($+205^{\circ}C$)		±3.0%
Fatigue life	:	10^5 cycles at ± 2000 μin./in. (μm/m)
		10^7 cycles at ± 2200 μin./in. (μm/m)
Resistance	:	350.0 ± 0.3%
Gage factor	:	2.01 ± 1.0% (at $75^{\circ}F$)

recommended for use up to 2300°F (1260°C).

Strain gages used were all of the same type, WK-09-062AP-350, made by Micro-Measurements. They are fully encapsulated single-element, K-alloy gages with general characteristics summarized in Table 6.3. The temperature - induced apparent strain, ε_{app}, for these gages and the variation of the gage factor, S_g, is plotted versus temperature in Figure 6.2. Gage resistances at the time of instalation were measured and summarized in Table 6.4.

During stress relieving at 1100°F (593°C) the strain gages of specimen #4 were destroyed and were replaced before cutting with gages of the same type, at the same positions, but oriented both in the longitudinal and transverse direction. In that way both the longitudinal and transverse strain relaxation during cutting could be measured. For the same reason five strain gages were added on the specimen #2 before cutting.

6.3 Welding and Stress Relieving Operations

6.3.1 Welding Equipment

Welding of the specimens was performed in the Ocean Engineering Welding Laboratory at M.I.T. with equipment shown in photo 6.1 and basically consisting of:

(a) Welding Power Supply: Deltaweld 650 made by the Miller Electric Manufacturing Company. This is a solid-state, direct current, constant potential welding power source suited for 100% duty cycle up to 650 Amperes.

(b) Gas Metal Arc Welding Torch: An Air-cooled, concentric Barrel model AM50-C by Airco, was mounted on a Machine Head

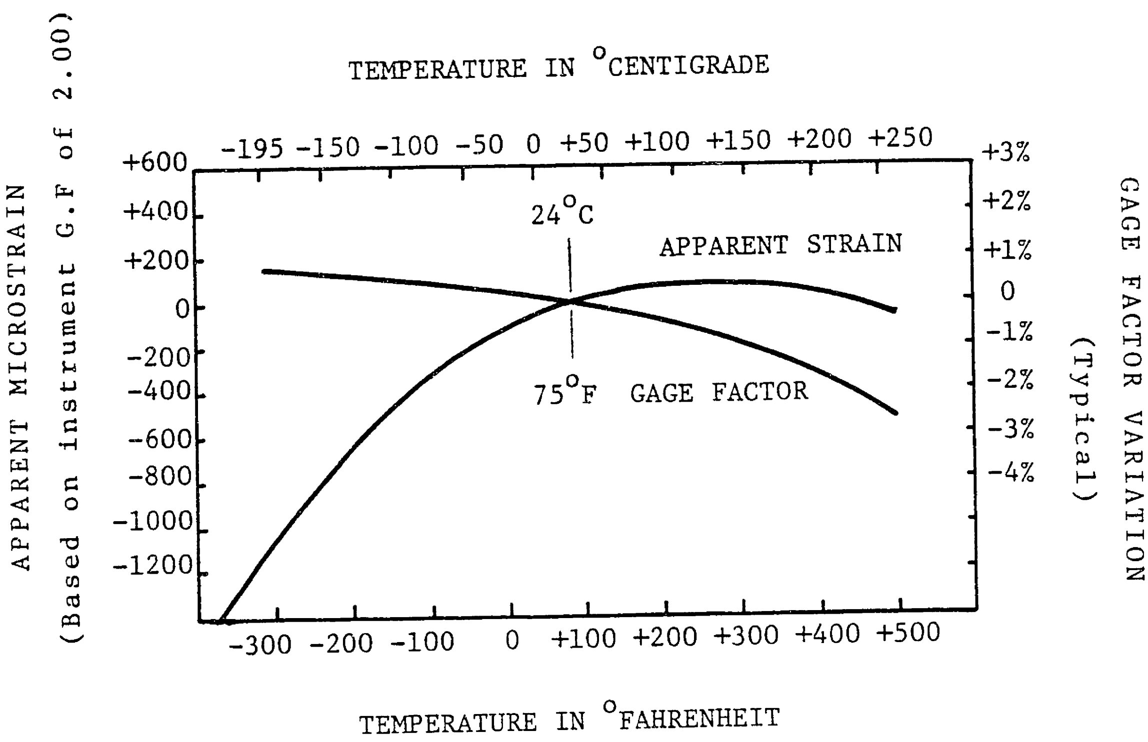

Figure 6.2 : Temperature induced apparrent strain for strain gages type WK-09-062AP-350, Lot #K14FE01 (Tested on 304 stainless steel by Micro-Measurements).

Table 6.4 : Measured gage resistance (in ohms)

Plate \ Gage	1	2	3	4	5	6	7	8	9	10
#1	349.6	349.9	349.7	349.7	349.5					
#2	349.5	349.7	349.5	349.2	349.8					
#3	349.2	349.4	349.7	349.8	349.6	349.7	349.4	349.1	349.7	350.1
#4	349.9	350.1	349.6	349.6	350.3	349.5	349.1	349.2	349.4	349.5
#5	349.5									

Resistance to ground for all gages > 20k

Table 6.5 : Stainless steel welding wire typical welding parameters

Process	Wire Diameter	Operating Current Range (amps)	Operating Voltage Range	Shielding Gas
Pulsed power	.035	40-200	16-27	$A+2\%O_2$
	.045	50-300	18-32	
	1/16	70-300	19-33	
Spray transfer	.035	125-300	18-32	$A+2\%O_2$
	.045	155-450	20-34	
	1/16	210-500	26-36	
Dip transfer	.035	55-200	15-23	$90\%He+7\text{-}1/2\%A+2\text{-}1/2\%CO_2$
	.045	75-200	16-24	

NOTE : Ranges subject to change due to variances in welding conditions.

Positioner also by Airco (Stock No 2354-01-91). The positioner and torch assembly was bolted on a Jetline Travel Carriage moving on a Jetline horizontal side beam, at a controllable speed.

(c) Wire feeder: Wire was fed to the torch at controllable speed by a Miller Model S-54D, digitally controlled feeder. The wire feed wheels and guides were suited for use with 0.035 inches diameter wire.

(d) Voltage Controller: Weld arc voltage was controlled by a Miller Digital Voltage Controller Model DVC DW-1.

(e) Spot-Continuous Control Panel: A Miller Model CS-4 panel allowed selection of either spot or continuous welding and control of pre- and post- flow time and burnback time.

Exact specifications for all the equipment used can be found in the respective owners' manuals. However there was no calibration chart for the multi-turn weld-travel-speed dial on the Jetline carriage and thus time-distance checks had to be performed.

6.3.2 Welding Process and Consumables

Straight polarity (electrode negative), dip transfer, Gas Metal Arc (G.M.A.), welding was performed on all the specimens.

The wire used was type 308 stainless steel wire, 0.035 inches (0.89 mm) in diameter (AWS specifications A 5.9 and ASME SFA 5.9).

To make dip transfer possible a 90% He - $7\frac{1}{2}$ % A - $2\frac{1}{2}$ % CO_2 shielding gas mixture was used.

6.3.3 Welding Conditions

Some typical welding parameters for stainless steels are given by Airco in Table 6.5 [116]. Specifically for 304 stainless steels, however, experiments were performed utilizing dip transfer by Koreisha for bead on plate welding, [117], and by the author for edge welding. Figure 6.3 gives the maximum possible wire feed speed (for satisfactory welds) versus arc voltage at various tested weld travel speeds.

The finally chosen welding conditions, summarized in Table 6.6, were tested to ensure that the strain gages closest to the weld line will not encounter temperatures above 550^{o}F during welding.

The exact variations of arc voltage and arc current are shown in Figures 6.4 (a) and (b). Current was measured across a shunt resistance (50 mV / 500 A) inserted in the circuit next to the torch. Arc voltage was measured between the torch and the specimen. The short circuiting is evidenced by the voltage drops and the immediately following current peaks.

6.3.4 Stress Relieving Equipment and Conditions

A "Lucifer" furnace, model # HDL-7021H, was used for the stress relieving of specimens #1, #3, #4, and #6. The furnace was electrically heated up to 2300^{o}F consuming 13KW at 440 Volts (3 phases). The temperature in the furnace was controlled by a "Guardsman" type on-off controller.

The stress relieving conditions are shown in Table 6.7. Exact records of the temperature during stress relieving will be given in the next chapter.

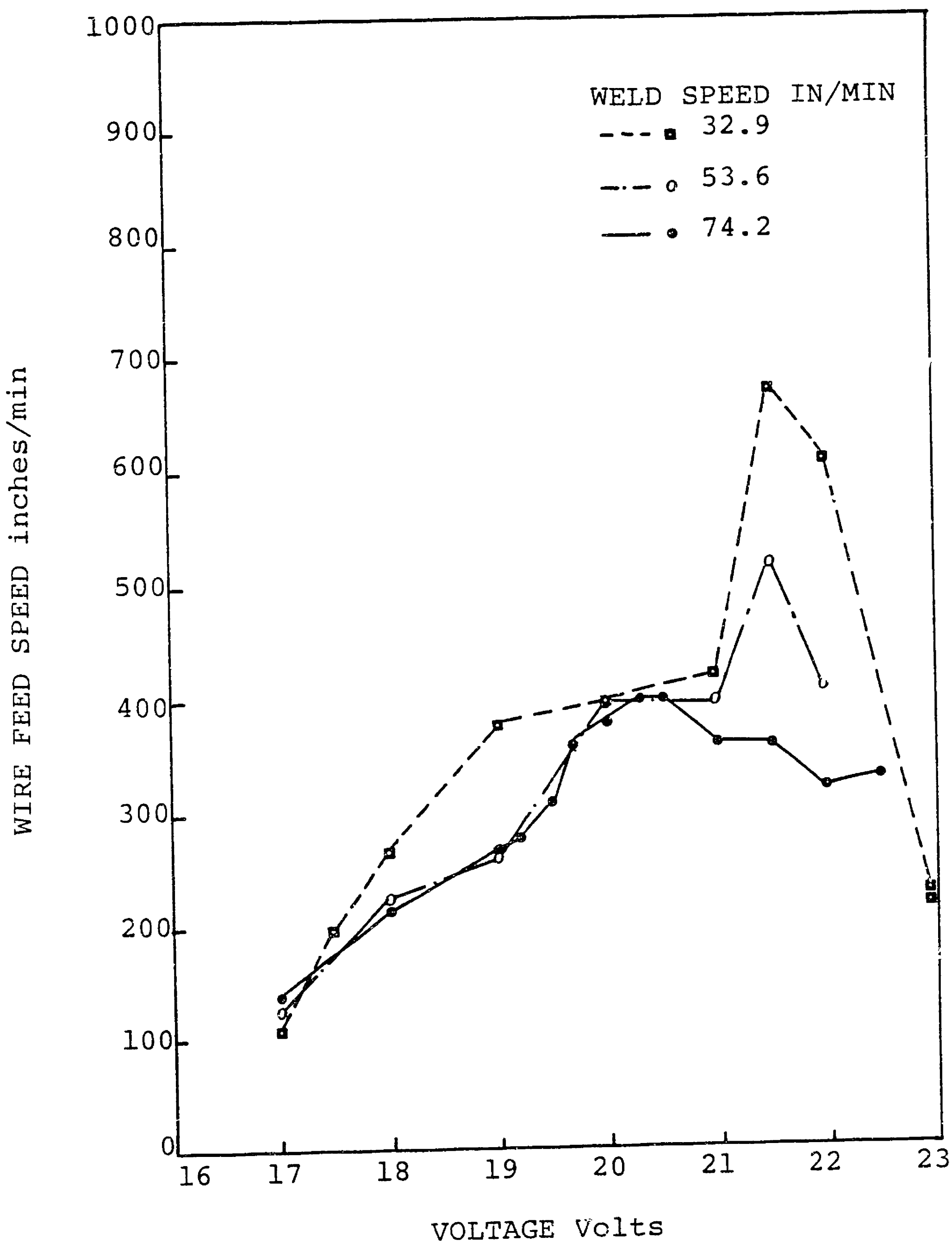

Figure 6.3 : Maximum wire feed speed vs. arc voltage for satisfactory welds at different weld travel speeds.

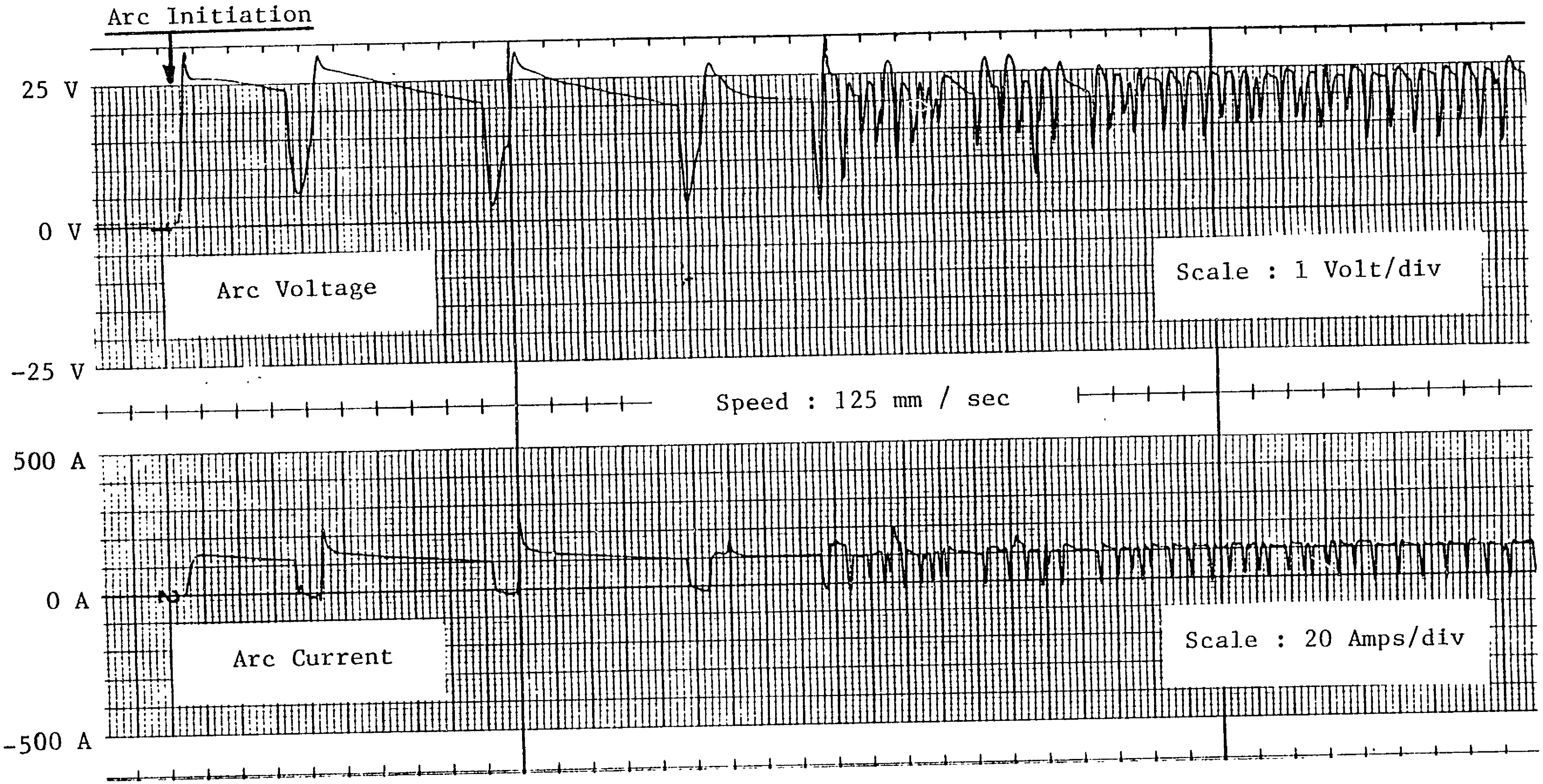

Figure 6.4 : Arc voltage and current variations during short circuiting welding of 304 stainless steels (Measured during welding of specimen #1)

Table 6.6 : Selected Welding Conditions (Same for speciments #1 through #6)

Arc Voltage	
set at	23 Volts
Arc Current	
measured off the Amp-meter	90 Amperes (approx)
Wire feed Speed	
set at	175 in/min
Weld travel Speed	
set dial at	700
	(equivalent to 15.96 in/min)

Table 6.7 : Stress Relieving Conditions

Specimen Number	Holding Temperature °F (°C)	Time in Furnace hr
1	500°F (260°C)	6
2	not stress relieved	-
3	approx. 370°F (188°C)	4
4	1100°F (593°C)	7
6	500°F (260°C)	2
	370°F (188°C)	

6.4 Computer Aided Data Acquisition System

6.4.1 General System Configuration

In the past, light-writting oscillographs -"visicorders"- were almost exclusively used as data recording devices during welding experiments at M.I.T. However, the relative simplicity of operation and low cost of such systems should be contrasted with the significant manual data reduction effort required in order to decipher the various traces from endless rolls of photo-sensitive paper. These considerations coupled with the availability of compact and powerfull microcomputers led to the decision to develop a computer-aided data aquisition system. Such a system would not only be used for recording strains, temperatures or welding conditions during experiments but could possibly be the first necessary element in real-time welding process control applications.

The finally configured system, that will be in more detail described in the next few sections of this chapter, basically consisted of:

(a) A MINC-23 Laboratory Data Processing System by Digital Equipment Corporation including a 16-channel analog to digital converter module and a programmable clock module.

(b) A 9000 Data Acquisition System by Daytronic Corporation, including thermocouple and strain gage conditioners, scanner slave modules and a microprocessor based computer interface module.

The system is versatile enough permitting operation under three different configurations:

(a) Sampling of the Daytronic signal conditioners directly from the MINC A/D converter module.

(b) Sampling of the signal conditioners from the Daytronic computer interface module and serial data transfer to the computer (or an independent terminal) via an RS-232-C (or 20-mA current loop), serial ASCII, full duplex, communications link.

(c) Sampling as in (b) but parallel data transfer via a IEEE-488 instrument interface bus.

Furthermore the modular nature of the system makes expansion or modification a straight forward procedure.

In what follows a description of the system is given and the specifics pertaining to our application are covered. An in depth treatment of all the related issues is considered outside the scope of this study and will be given by the author in [118]. Further details and background information can be found in the literature (for example in Osborne [119] or Tocci [120] for an introduction to microprocessors/microcomputers and in Artwick [121] or Lipovski [122] for a relatively more detailed treatment of interfacing issues).

6.4.2 System Elements Description

(A) MINC-23 Hardware

The microcomputer used, built by D.E.C., basically consisted of:

(a) An MNC-chasis, housing the following modules:

-KDF11-AB Central Processing Unit based on the 16-bit

LSI 11/23 microprocessor

-MSV11-DD 32K word Memory Single Road (Up to four MSV11-DD can operate with LSI 11/23 microprocessor)

-BDV11-A Bootstrap/Diagnostic ROM module

-IBV11-A IEEE-488 Instrument Bus Interface

-DLV11-J 4-Line Asynchronous Serial Interface

-RXV21 Disk Controller Interface

-MNCAD 16 channel Analog/Digital Converter module

-MNCKW Real Time programmable clock module

(b) An RX02 1.0 M byte dual, double density, Floppy Disc Subsystem

(c) A VT-105 Alphanumeric and Graphic Display Terminal

(d) An LA-36 DECWriter II terminal and

(e) A 4662 Tektronix Interactive Digital Plotter.

The actual system configuration as described above is outlined in figure 6.5.

(B) <u>MINC-23 Software</u>

The system software included

(a) The RT-11 Operating System (Version 4.0)

(b) FORTRAN IV programming language and

(c) FORTRAN Enhancement Package FEP-11 containing the following groups of FORTRAN callable subroutines

-REAL-11/MNC providing real-time control of all MNC-series modules

-IBS, the IEEE Instrument Bus Subroutines Package

-SSP, the Scientific Subroutine Package

-LSP, the Laboratory Subroutine Package and

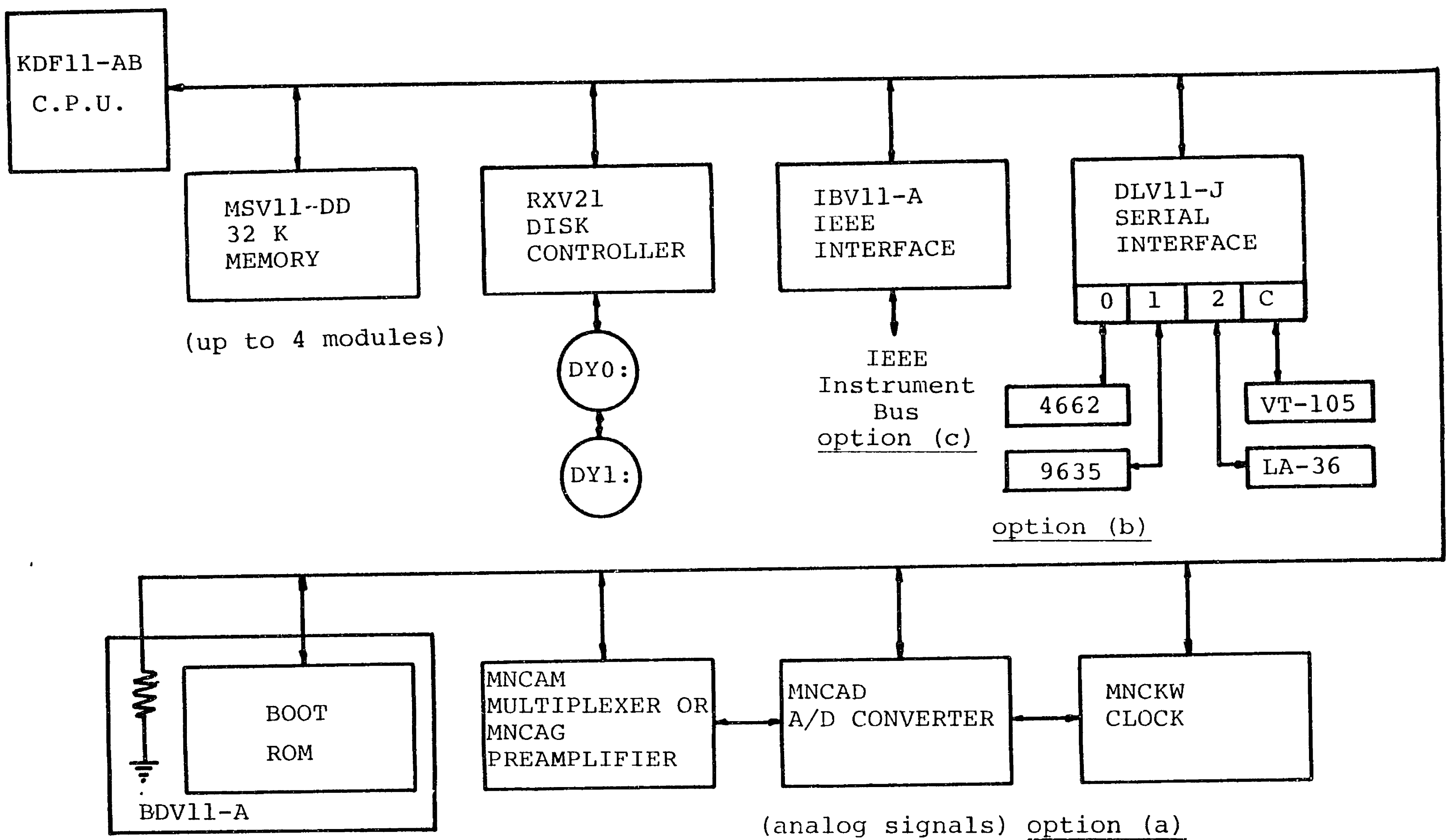

Figure 6.5 : MINC-23 System Configuration and possible communication options

-FDT, the FORTRAN Debugging Technique Package

(C) Daytronic 9000 data aquisition system

The basic system components housed in a 9020 Daytronic Mainframe are:

(a) One 9110AK, Type k (Chromel-Alumel) Single Thermocouple Conditioner

(b) One 9610TC, Thermocouple Scanner Slave, capable of multiplexing ten thermocouple inputs into a single 9110AK conditioner

(c) Five 9170 Strain Gage Conditioners for full or half bridge transducer inputs and 5 or 10V D.C. bridge excitation

(d) Ten 9178A X-12 Strain Gage Conditioners with 6V A.C. (3.28 KHz) bridge excitation, modified to accept quarter bridge transducer inputs (single gages)

(e) Two 9610 scanner slaves each capable to "call" up to ten signal sources

(f) One 9635 Computer Interface Module, based on the Intel 8086 16 bit microprocessor and capable of:

-Setting-up and calibrating up to 398 data channels, with calibration data stored in a battery protected memory

-Scanning of analog, digital and logic data channels at a rate of 1500 ÷ 1800 channels per second depending on the microprocessor workload.

-Automatic digital zeroing and scaling of the analog channels

-Operator-to-computer communications via a front-panel keyboard

-Random access servicing of the external computer's requests for input data, via an RS-232-C, or 20mA current loop, communications link (or optionally via an IEEE instruments bus)

The system configuration is outlined in Figure 6.6 . Detailed specifications, circuit schematics and operating instructions are given in the system manuals, [124].

6.5 Data Acquisition System Set-up and Operation

6.5.1 Sampling and Interfacing Considerations

As was outlined in section 6.4.1, system operation under three different configurations is possible. However, for the experiments of this study only the second configuration was used, since it would require minimal modification of both systems. Discussion for the rest of this chapter will only refer to this configuration and details on the other two will be given by the author in [118].

Specifically, refering to Figure 6.6, during operation the 9635 Computer Interface module scans continuously at high speed (1500 ÷ 1800 channels per second) a number of operator selected channels (T/C or S/G signal conditioners in our case), and writes the measurements, properly scaled, into the DATA RAM, an internal buffer memory. Via an RS-232-C full duplex port, the external computer (MINC-23) can "read" the contents of the DATA RAM by simply prompting commands in ASCII. These writing and reading operations are completely transparent to each other.

From the computer's point of view the 9635 emulates a standard RS-232-C/ASCII data terminal (D.T.E.) responding

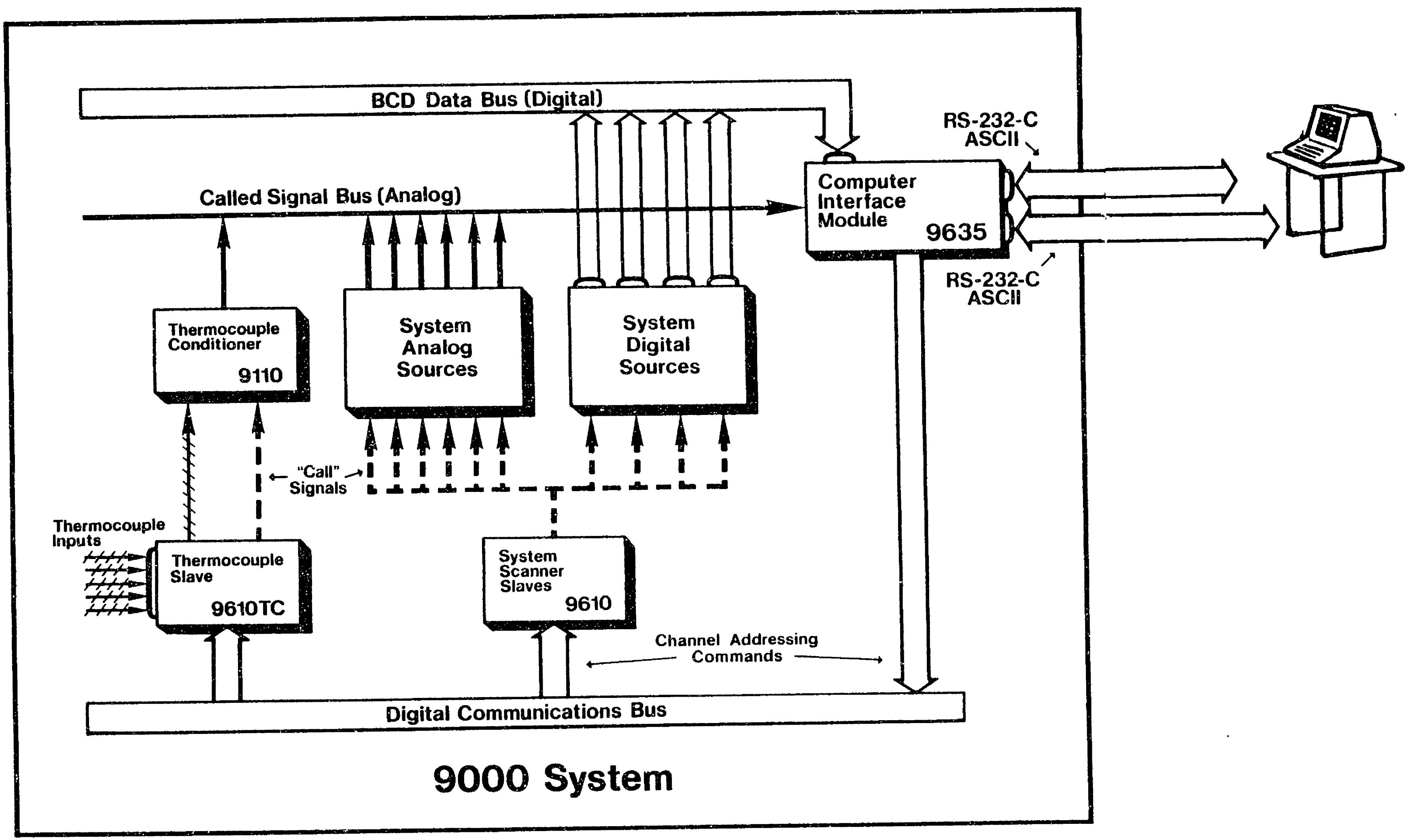

Figure 6.6 : Daytronic 9000 system configuration and possible communication options

"instantly" to simple interrogation and control commands. The response time, by default set to 384 milliseconds, is controllable to prevent problems when I/O buffer is not provided. In the MINC-23 computer the four SLU ports, connected to the DLV11-J interface channels, are used for serial I/O (Figure 6.5).

Both systems are flexible enough permitting communication at various baud rates (bits per second) and different parity and stop bit schemes. The maximum (for DLV11-J) receive/transmit speed of 9600 baud was selected and the character format was set to:

-1 start bit

-8 data bits

-1 stop bit

-No parity

It should be noted here that serial data transmission and subsequent data processing take certain amount of time, orders of magnitude greater than the sampling period in the A/D of 9635. This would cause severe cross-channel time-skew problems in the measurements. Therefore in order to take full advantage of the actually very high scanning rates, the "LOC" command available in the 9635 software was used. This option permits the computer to instantly freeze the contents of the DATA RAM - that is, in effect to "take a snapshot", of the monitored channels - and then take whatever time it needs to serially transfer or process the "effectively simultaneous" measurements.

The actual required pin-to-pin connections between the 9635, SLU port #1, and DLV11-J are shown in Figure 6.7 together

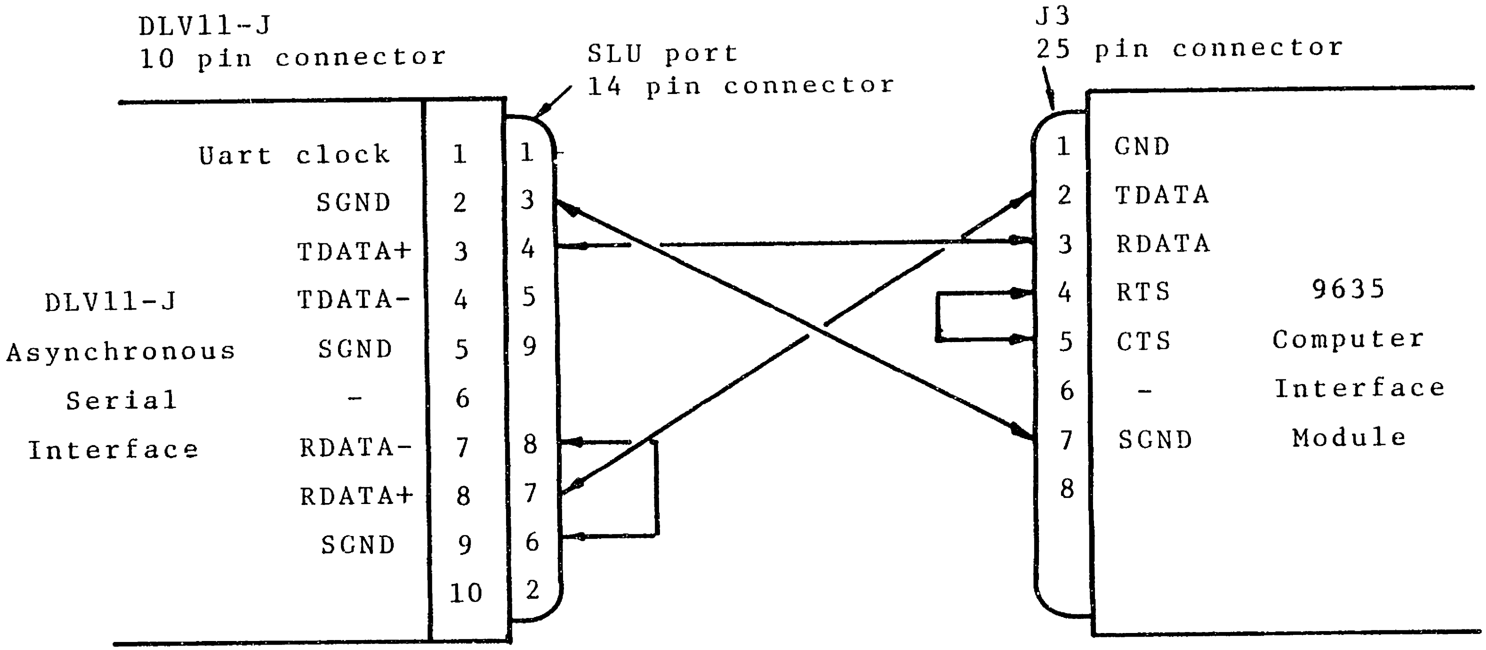

Figure 6.7 : Interconnections between the two systems

Note: GND : Protective ground

SGND : Signal ground (common reference)

TDATA: Transmit data

RDATA: Receive data

RTS : Request to send

CTS : Clear to send

with a brief description of the various signals. Although an RTS/CTS (Request To Send/ Clear To Send) "handshake" protocol can be implemented with the 9635, this was not necessary for the MINC-23 and therefore pins 4 and 5 of 9635 output connector were simply tied to each other, [124].

6.5.2 Data Acquisition Programs

Listings of the data aquisition programs used in this study are given in Appendix D. For serial character input and output through the DLV11-J interface the D.E.C. provided subroutines CIN and COUT (written in MACRO-11) had to be slightly modified for our application. Necessary details on the LSI-11/23 instruction set and addressing modes can be found in [125].

6.5.3 Calibration Procedures

(a) 9110AK Thermocouple Conditioners:

The modules are self-zeroed requiring only span adjustment (in ^{o}C or ^{o}F) and give a linear analog output for temperatures in the range -148 to +2300^{o}F (-100 to +1260^{o}C).

(b) 9178 Strain Gage Conditioners:

Shunt calibration was performed on all the strain gage conditioners. However, in order to verify the accuracy of the measurements an actual "deadweight" calibration was performed with one of the specimens.

During shunt calibration one fixed resistor is shunted across one arm of the strain gage bridge as in Figure 6.8 and produces an electrical unbalance equivalent to that caused by a particular value of strain on the active arm of the bridge. It is proven in experimental stress analysis texts, (Dally and

Riley [126]), that this value of equivalent strain input, for the one-active-arm bridge of Figure 6.8 is:

$$\varepsilon_{cal} = \frac{R_2}{S_g \ (R_2+R_c)} \qquad (6\text{-}1)$$

where R_2 = The arm's initial resistance

R_c = The shunted calibration resistance

S_g = The gage factor

For the 350 Ohm strain gages used in this study and for the originally installed 59 K Ohm calibration resistor the equivalent strain value is:

$$\varepsilon_{cal} = 2948.6 \ \mu \text{ strain}$$

In the 9635 module this value would be used as the upper limit of the linear range (0-5000 millivolts) of the strain gage conditioner output [124].

The computer simulation, however, using the one dimensional program, showed that the expected maximum strains during welding and subsequent stress relieving might be higher than this value. Therefore it was decided to replace the calibration resistor, R_c. Precision metal film resistors of 34 K Ohm value were installed on all 9178A x 12 strain gage conditioners resulting in an equivalent strain value of :

$$\varepsilon_{cal} = 5094.6 \ \mu \text{ strain}$$

A value of 2.0 was used for the gage factor S_g in the above calculations. The slightly different actual value and its variation with temperature would be taken into account during

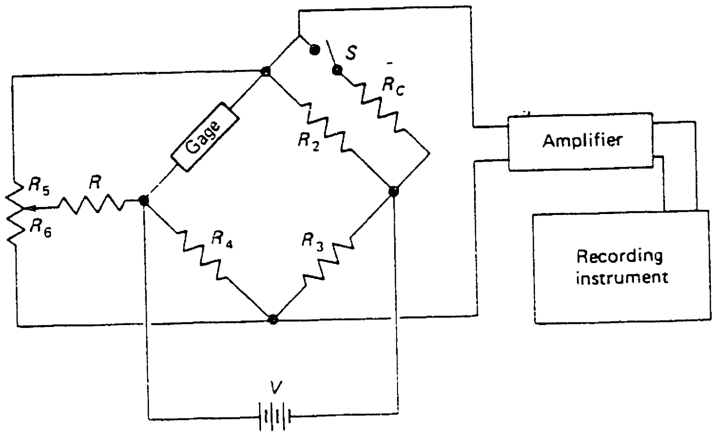

Figure 6.8 : Strain gage bridge configuration

Rg	: gage resistance
R_2, R_3, R_4	: bridge completion resistors
R , R_5, R_6	: balancing resistors
R_c	: calibration resistor
V	: excitation voltage

data reduction (Section 6.7.1) (Calibration and previous zero balancing was performed with all the gages at room temperature).

To verify the accuracy of shunt calibration a test was performed with specimen #1. The plate was simply supported on two "knife" edges along the two 6 inch sides and loaded with various loads. Strains measured in all 5 strain gages were off by 2% to 3% from the values calculated by simple beam theory.

6.5.4 Necessary System Modifications

A number of modifications were necessary in order to set-up and interface the two systems for our application. Specifically:

(a) In the DLV11-J card wire-wrapped jumpers were used to configure all channels for 8 data bits, no parity and one stop bit. Baud rates were set at 1200, 9600, 300 and 9600 for channels #0, #1, #2 and #3 respectively. (DLV11-J operation is covered in [123]).

(b) Extra software was prepared and stored on two 2k x 8 EPROM chips (type 2516JL) for use with the 9635 computer interface module. This would cause the line feed (LF) and carriage return (CR) characters to be transmitted only once, in the end of a DATA-RAM DUMP operation (DMP), [124].

(c) External bridge completion circuits for the 9170 strain gage conditioners were built and crammed in the housing of the 14 pin input connectors. 350 Ohm precision metal film resistors by Micro-Measurements (type S-350-01) were used.

(d) The initially installed 59 K Ohm calibration resistors in the 9178A modules were replaced with 34 K Ohm precision metal film resistors.

(e) Through the 9020 mainframe patch wiring card, pins 12 of all 9178A strain gage conditioners were interconnected to ensure synchronization of the 3.28 KHz excitation oscillators.

6.6 System Performance Evaluation

6.6.1 System Limitations

The installation, software development and testing of a data acquisition system from scratch could very well be viewed as a challenge to Marphy's Laws. However, apart from the trivial-but nevertheless time consuming - troubleshooting problems, some limitations in the system performance - at least in its current configuration - should be noted here:

(a) Scanning speed, probably the most important characteristic of such a system, was limited due to the relatively slow transmission and processing of serial data.

(b) The reliability of the 9635 computer interface was rather low. The module, which was introduced in the market less than a year ago, undoubtedly needs further development both in hardware and software.

(c) The 9110A/9610TC thermocouple conditioner and slave combination could not give any meaningfull temperature readings during dip transfer welding. This was most probably due to the "noisy" and unstable (short-circuiting) nature of the arc during dip transfer since it also happened during the unstable arc-initiation phase of spray-transfer welding tests performed with the same set-up on HY-130 specimens [128].

6.6.2 Suggestions for Further Improvement and Expansion

Various possibilities exist for improvement and/or expansion of the data aquisition system. Specifically:

(a) Subroutines CIN and COUT could possibly be modified or "fine tuned" to reduce further the serial data processing time in the MINC-23 computer.

(b) The new version of the RT-11 software could be installed. This version now directly supports the serial input/output ports and the new thermocouple conditioner MNC module.

(c) Slow serial data transfer could be avoided by sampling the the Daytronic (or other) signal conditioning modules directly from the A/D module of MINC-23 (MNCAD). This would bypass the 9635 computer interface module, but would necessitate installation of more thermocouple conditioners or of a dual multiplexer (MNCAM) module in the MINC.

(d) The IEEE instrument bus interface could be used for parallel data transfer but the 9635 would have to be factory modified.

(e) More modules could be added in both parts of the system. For example L.V.D.T. conditioners (type 9130) could be added on the 9020 Daytronic mainframe for welding distortion measurements. Or on the other end preamplifier (MNCAG), and/or multiplexer (MNCAM) modules could be plugged in the MINC-23 to make possible sampling of other analog inputs from the MNCAD A/D module.

(f) Finally in order to close a control loop, for a welding process control application, analog or digital output modules could be installed in both parts of the system. (MNCAA D/A converter and MNCDO digital output modules on the MINC,or 9316 control logic input, 9317 control logic output and 9410 analog control modules in the 9000 Daytronic system)

6.7 Data Reduction

6.7.1 Compensation for Temperature - Induced Apparent Strain and Gage Factor Variation

Higher than room temperatures are encountered on all specimens during welding or stress relieving. Therefore compensation for temperature-induced apparent strain and gage factor variation is necessary.

Apparent strain is caused by two concurrent and algebraically additive effects: (a) Change in the gage resistance due to the temperature dependence of the electrical resistivity of the gage material and (b) Differential thermal expansion between the grid material and the test piece or the substrate material to which the gage is bonded. The metallurgical properties of certain strain gage alloys are such that these alloys can be processed to minimize the apparent strain over a wide temperature range when bonded to specific materials.

Such "self-temperature-compensated" strain gages are the ones used in this study (M-M type WK-09-062AP-350) with apparent strain versus temperature variation presented in Figure 6.2. A regression-fitted (least-squares) polynomial expression was also provided by M-M for the apparent strain:

$$\varepsilon_{app}(T) = -81.4+1.39T-4.63x10^{-3}T^2+8.57x10^{-6}T^3-9.33x10^{-9}T^4 \quad (6\text{-}2)$$

where : T = Temperature in degrees F and

ε_{app} In microstrain (microinches/inch or micrometres/metre)

The strain gage factor, S_g, defined as

$$S_g = \frac{\Delta R}{R} \cdot \frac{1}{\varepsilon_a} \tag{6-3}$$

where : ε_a = Applied strain

ΔR = Change in gage resistance due to ε_a

R = Initial resistance

also changes slightly with temperature. For the gages used the percent variation is also presented in Figure 6.2. For use in the data reduction programs the curve was approximated by three linear segments as follows:

$$\Delta S_g(T) = \begin{cases} 0.17 - 0.69 \quad T/200 & \text{for } 0 < T < 200^{\circ}F \\ -0.52 - 1.18 \quad (T-200)/200 & \text{for } 200^{\circ}F < T < 400^{\circ}F \\ -1.70 - 1.03 \quad (T-400)/100 & \text{for } 400^{\circ}F < T < 500^{\circ}F \end{cases} \tag{6-4}$$

The actual gage factor at temperature T would then be:

$$S_g(T) = S_g(To)\left(1 + \frac{\Delta S_g(T)}{100}\right) \tag{6-5}$$

where $S_g(To)$ = The room temperature gage factor

In order to correct simultaneously for apparent strain and gage factor errors the following procedure is proposed by Micro-Measurements in [127]:

(a) Perform balance and calibration with the gage at room temperature employing the gage factor used by Micro-

Measurements in determining the apparent strain data ($S_g^*=2.0$)

(b) Get the strain gage reading, $\hat{\hat{\varepsilon}}(T)$, at temperature T ($T \neq T_{room}$)

(c) Correct for apparent strain :

$$\hat{\varepsilon}(T) = \hat{\hat{\varepsilon}}(T) - \varepsilon_{app}(T) \tag{6-5}$$

where : $\hat{\hat{\varepsilon}}(T)$ = The strain gage reading at temperature T

$\hat{\varepsilon}(T)$ = Semicorrected strain

$\varepsilon_{app}(T)$ = Apparent strain at temperature T

(d) Correct for gage factor variation

$$\varepsilon(T) = \hat{\varepsilon}(T) \frac{S_g^*}{S_g(T)} \tag{6-6}$$

Listings of the data reduction programs where the above presented compensation procedure is implemented are given in Appendix D.

6.7.2 Residual Stress Measurements

The residual stresses after welding (specimen #2) and after stress relieving (specimens #1 and #4) were measured by sectioning the plates and removing a narrow center strip carrying the strain gages. This stress relaxation technique for residual stress measurements is based upon the principle that "strains created during unloading are elastic even if the material has previously undergone plastic deformation", [1]. This fact is illustrated, for one dimension, in Figure 5.6. If the removed center strip of the plate is small enough then it can be safely assumed that residual stresses no longer exist and the measured strain changes $\bar{\varepsilon}_x$, $\bar{\varepsilon}_y$ and $\bar{\gamma}_{xy}$ are

$$\bar{\varepsilon}_x = -\varepsilon_x^{el}$$
$$\bar{\varepsilon}_y = -\varepsilon_y^{el} \qquad (6\text{-}7)$$
$$\bar{\gamma}_{xy} = -\gamma_{xy}^{el}$$

The residual stresses therefore are

$$\sigma_x = -\frac{E}{1-\nu^2}\,(\bar{\varepsilon}_x + \nu\bar{\varepsilon}_y)$$

$$\sigma_y = -\frac{E}{1-\nu^2}\,(\bar{\varepsilon}_y + \nu\bar{\varepsilon}_x) \qquad (6\text{-}8)$$

$$\tau_{xy} = -G\,\bar{\gamma}_{xy}$$

where : E = The Young's modulus

ν = The Poisson's ratio and

G = The coefficient of rigidity

The actually calculated residual stresses at various distances from the weld line in all three sectioned specimens are presented in the next chapter.

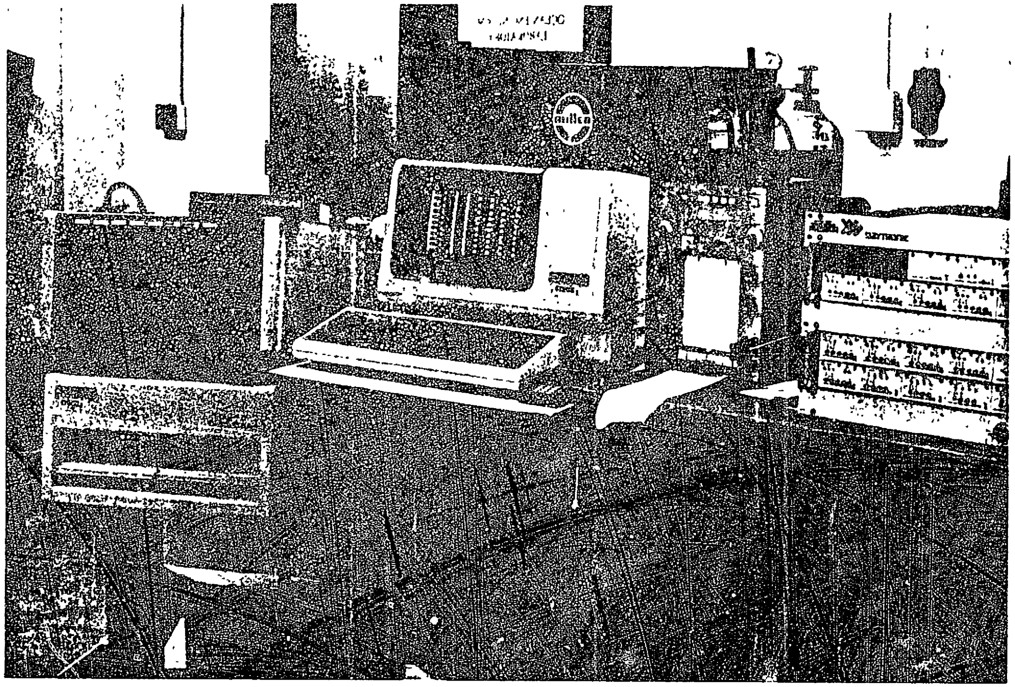

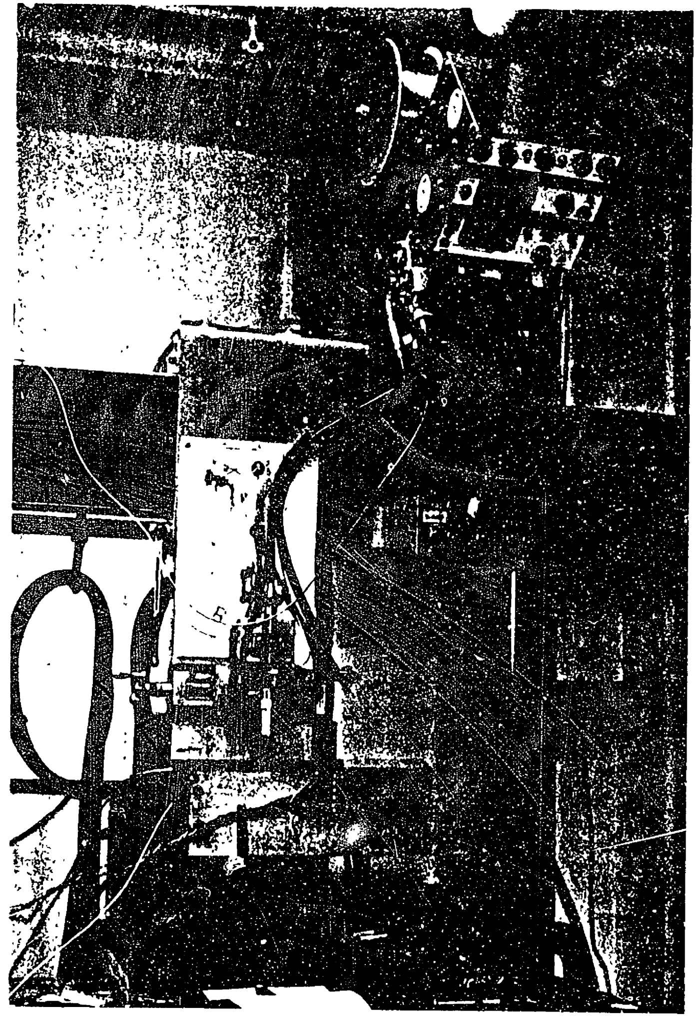

Photo 6.1 (above): The Data Acquisition System

Photo 6.2 (right): Welding Equipment

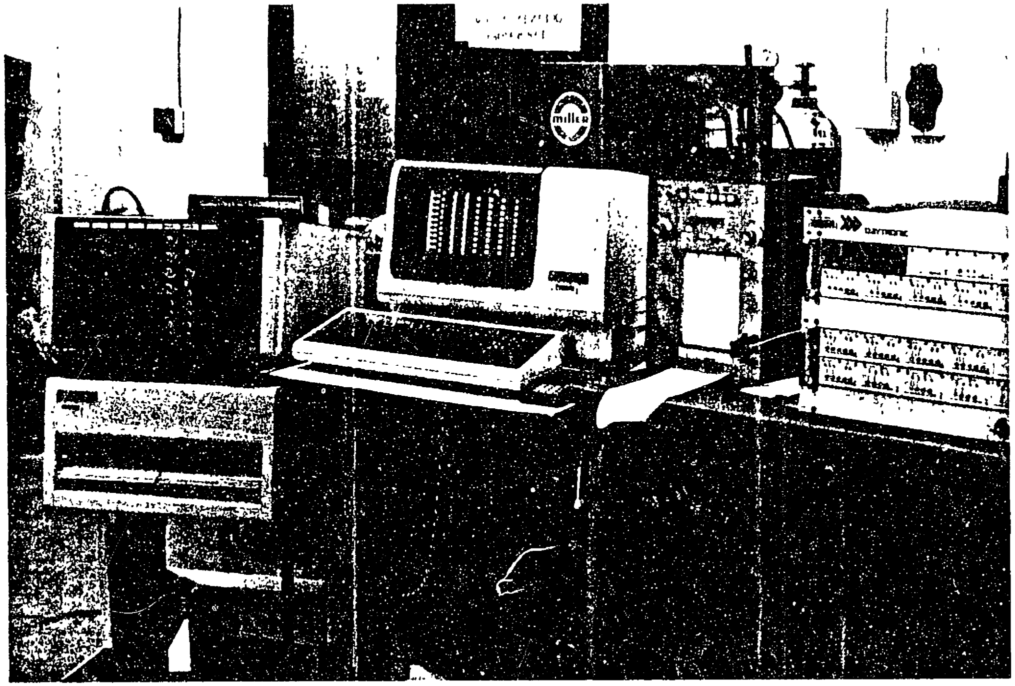

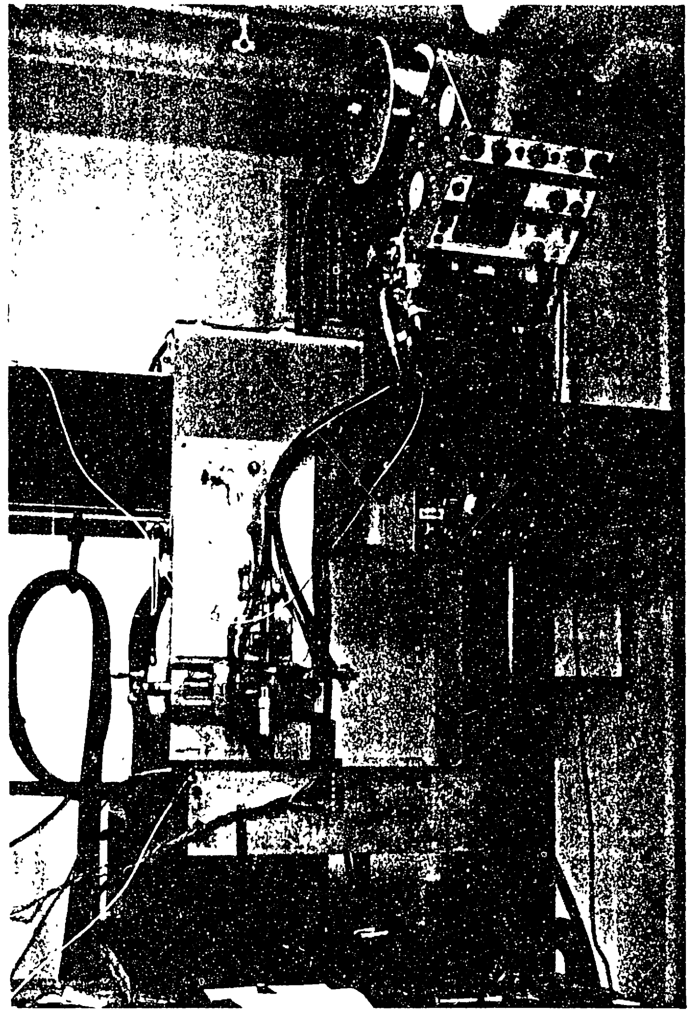

Photo 6.1 (above): The Data Acquisition System

Photo 6.2 (right): Welding Equipment

CHAPTER VII

RESULTS AND CONCLUSIONS

7.1 Experimental Results

Results of all the experiments will be presented and discussed in this section. Edge welding was performed on all the instrumented specimens using the same welding conditions (described in Table 6.6). The resulting temperature distributions are plotted in Figures 7.1, 7.4, 7.7 and 7.12 and are - not surprisingly - very similar for all four specimens. As was already discussed in the previous chapter, the short-circuiting nature of dip transfer welding introduced a significant amount of noise in the thermocouple readings during welding. Thus, for clarity, it was decided not to plot the very first part of the temperature history.

The strain gage readings taken during the welding experiments are plotted in Figures 7.2, 7.5, 7.8, 7.9, 7.13 and 7.14 for all four specimens. Noise problems with the strain gage conditioners were not encountered. It should be noted here that the observed slightly different strain readings on the two sides of specimens #3 and #4 are due to bending caused by the initial deviation of the plate from the straight-line path of the welding arc. On the back side of specimens #3 and #4 only the four strain gages closest to the weld line were monitored due to problems with one strain gage conditioner.

The strain gage readings were further corrected for temperature-induced apparent strain and gage factor variations in the way presented in section 6.7.1. Compensated strains for all specimens are plotted in Figures 7.3, 7.6, 7.10, 7.11, 7.15 and 7.16

Stress relieving heat treatments were performed on specimens #1, #3 and #4 in an electric furnace at various holding temperatures. Thermocouple and strain gage readings were continuously taken in all cases. The thermocouple readings are plotted versus time in Figures 7.17, 7.20 and 7.25. The noisy readings above 1000^{o}F are due to the fact that the glass insulation of the thermocouple wires was almost destroyed since it was subject to very high temperatures caused by radiant heating from the "red-hot" furnace elements.

Uncompensated strain gage readings for specimens #1 and #3 are plotted in Figures 7.18, 7.21 and 7.22 whereas corrected strains are given in Figures 7.19, 7.23 and 7.24. Strain gage readings for specimen #1, however, should be viewed with some reservation, since the gages were not covered and thus were subject to radiant heating from the furnace elements. In specimen #3 gages were covered with "fiberfrax" insulation and always encountered temperatures inside their permissible range. Strain gages in specimen #4 were destroyed when the plate reached temperatures between 550^{o}F and 600^{o}F. New gages had to be installed before cutting.

Specimens #1, #2 and #4 were cut in order to calculate the distribution of residual stresses after welding and stress relieving. The strain gage readings before and after cutting are summarized in Table 7.1. The residual stresses, calculated in the way presented in section 6.7.2, are also given in the same Table and are plotted in Figure 7.26(a) and (b) (Longitudinal and transverse respectively).

Finally it should be mensioned that specimen #5 was heated at various temperatures in order to investigate the uniformity of the heating attainable in the furnace. It was noticed that a gradient of 5 to 45^{O}F existed across the length of the specimen, depending on the level and the rate of increase of temperatures. More "fiberfrax" insulation around the door reduced slightly these gradients. Further more it was noticed that there existed almost no temperature gradient through the thickness of the specimen. This was evidenced by the identical measured temperatures on the surface and halfway through the thickness (where thermocouple #3 was embeded).

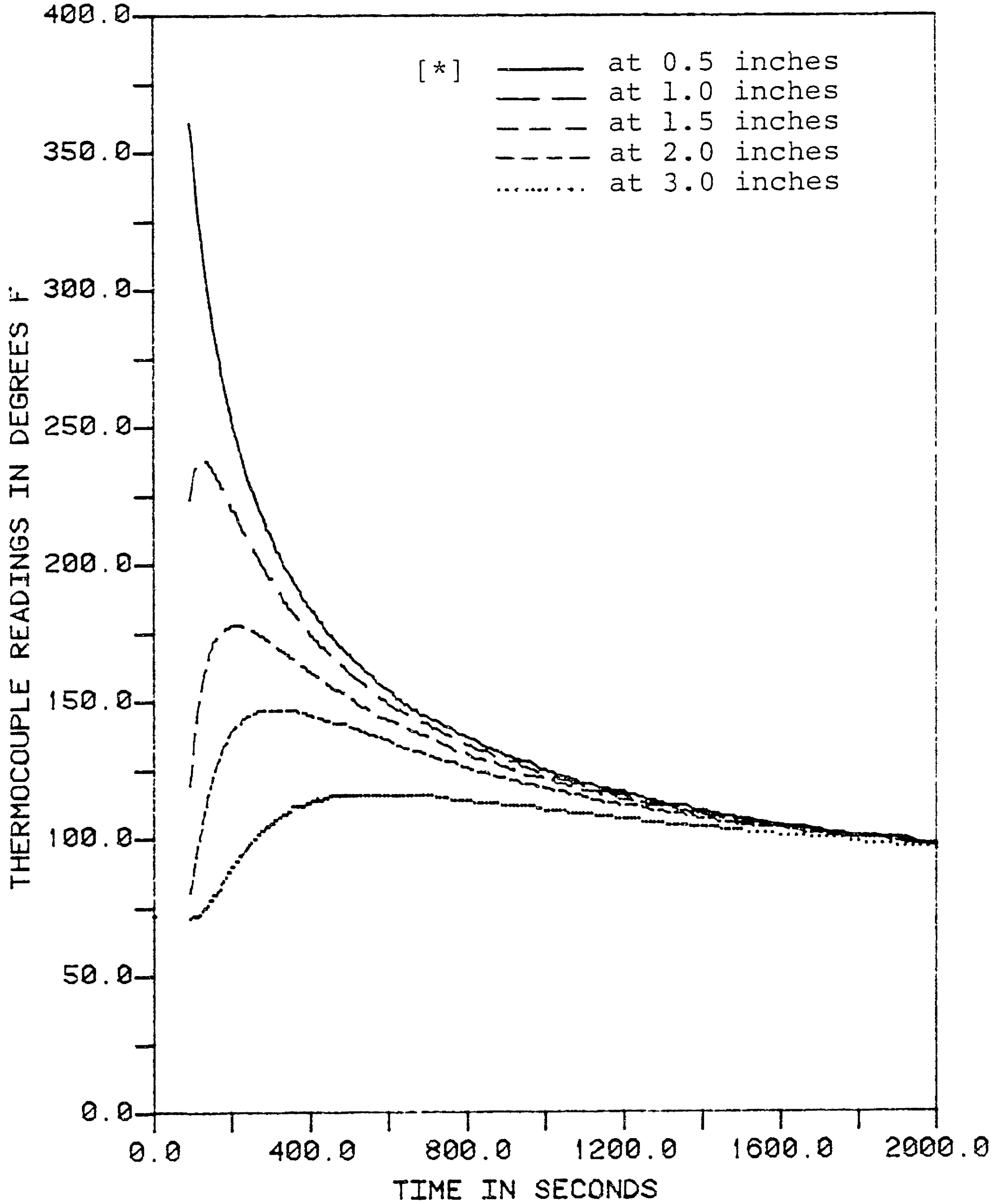

WELDING OF SPECIMEN #1

Figure 7.1 : Thermocouple readings during welding of specimen #1.

---

[*]. Note : The key to the curves of Figure 7.1 also holds for Figures 7.2 to 7.25

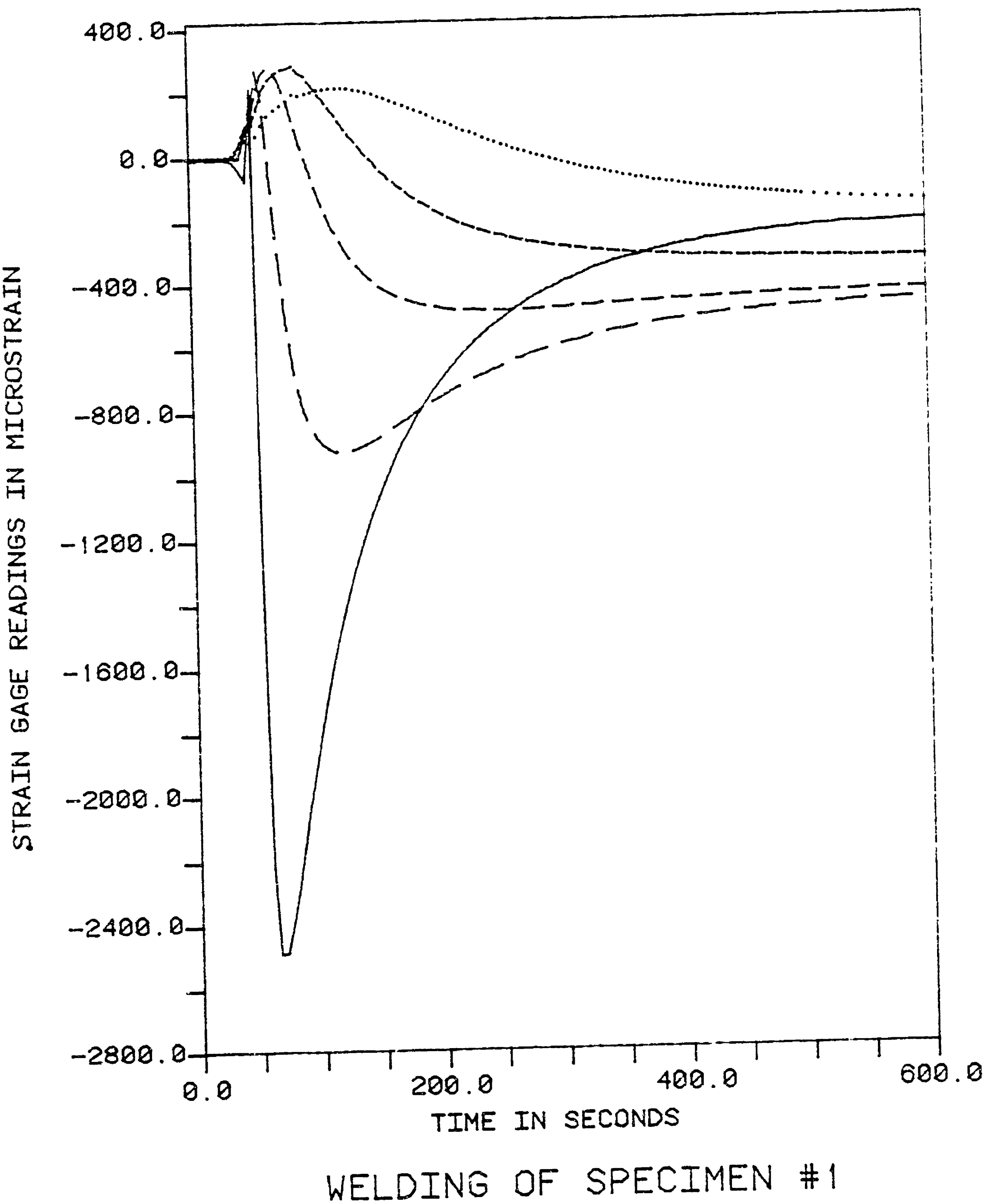

Figure 7.2 : Uncompensated strain gage readings during welding of specimen #1.

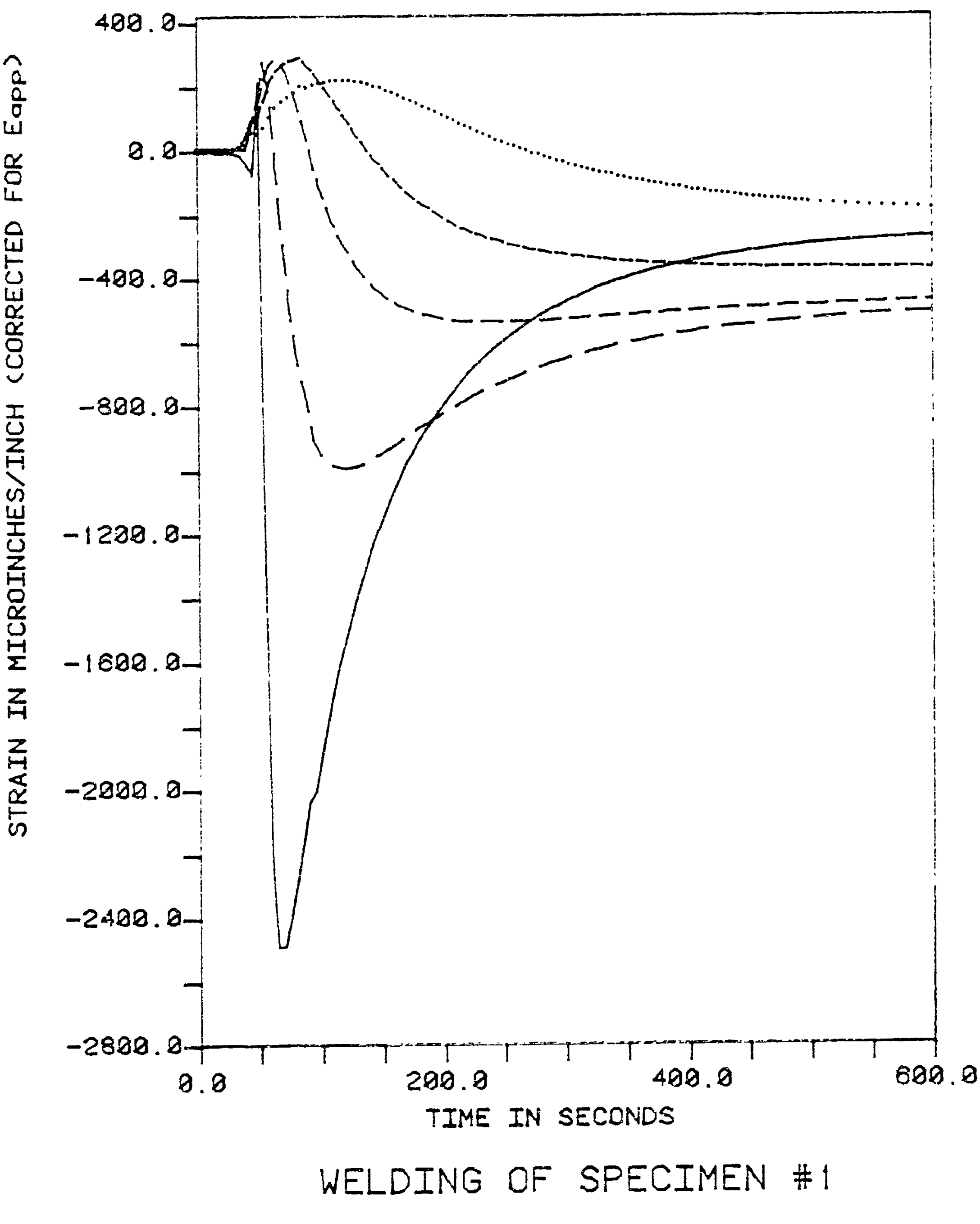

Figure 7.3 : Strains during welding of specimen #1 (corrected for temperature induced apparent strain and gage factor variations)

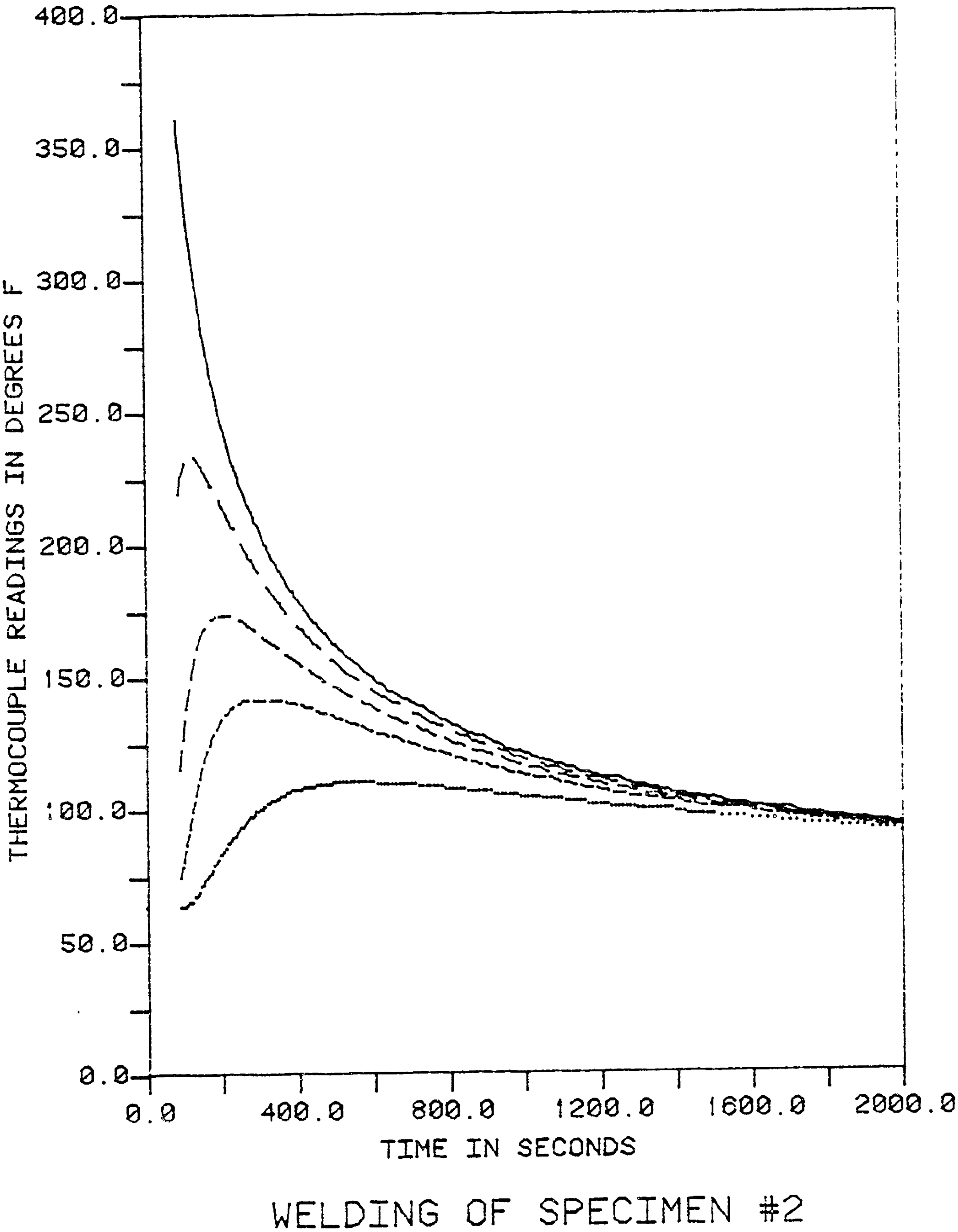

Figure 7.4 : Thermocouple readings during welding of specimen #2.

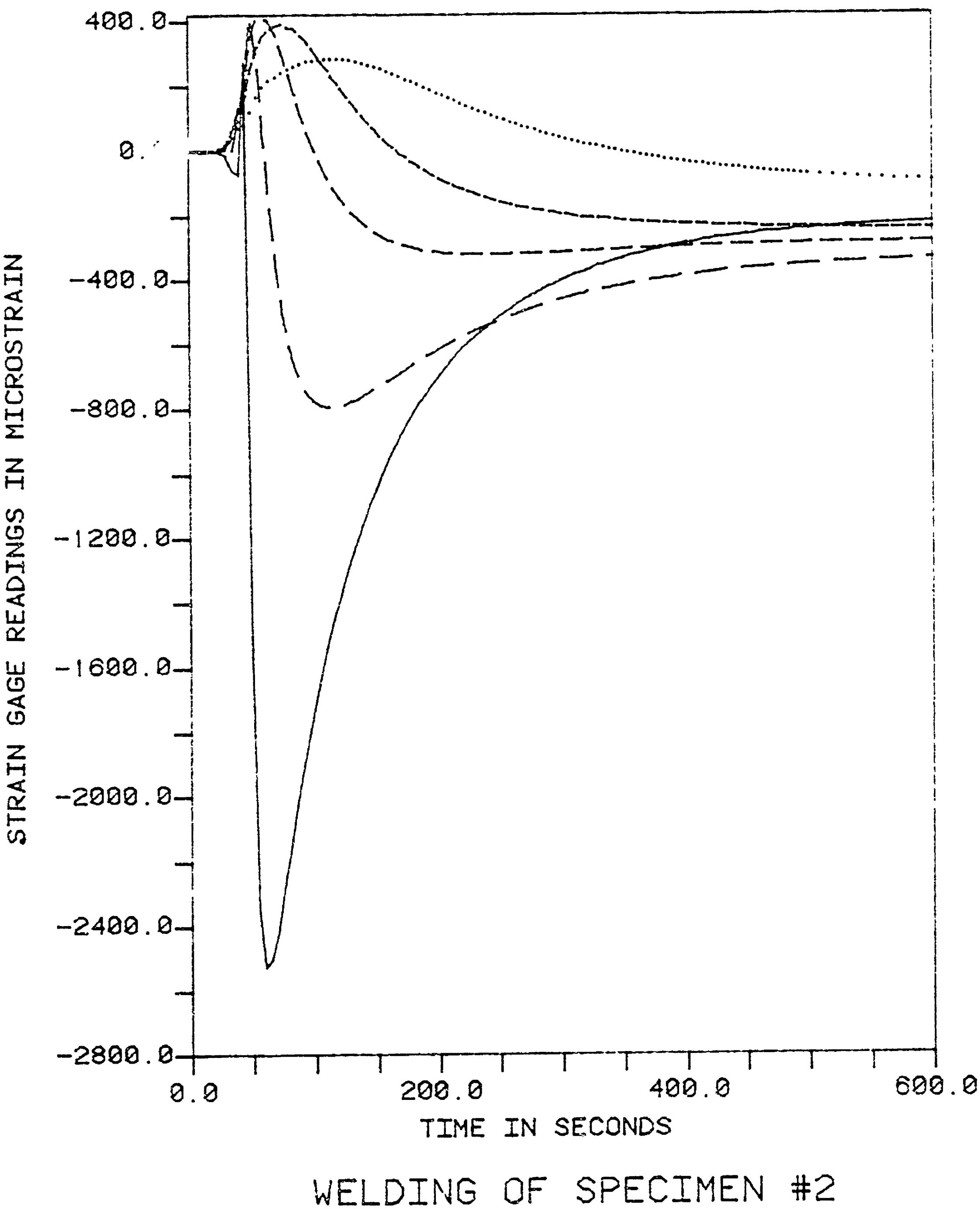

Figure 7.5 : Uncompensated strain gage readings during welding of specimen #2

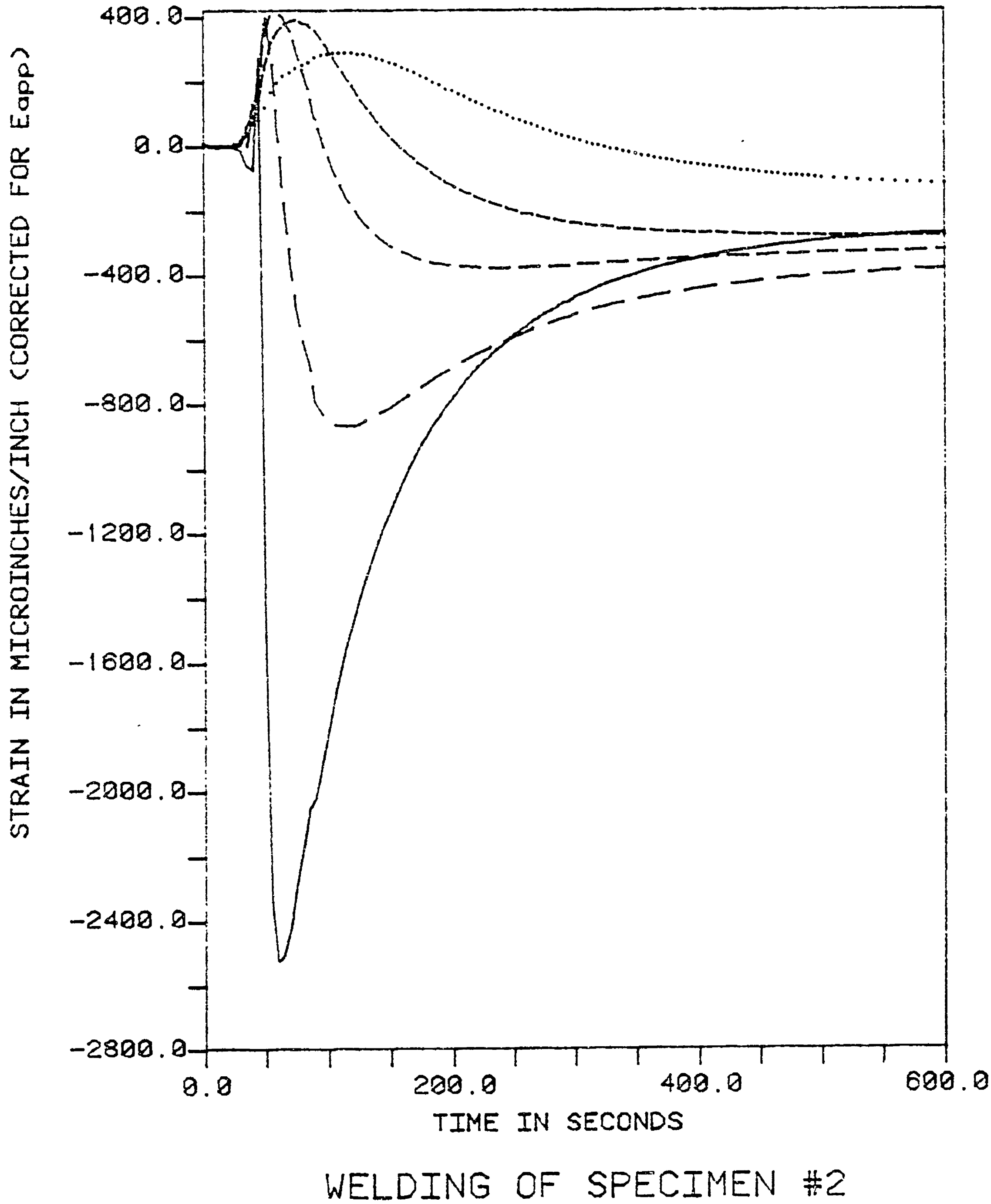

Figure 7.6 : Strains during welding of specimen #2 (corrected for temperature-induced apparent strain and gage factor variations)

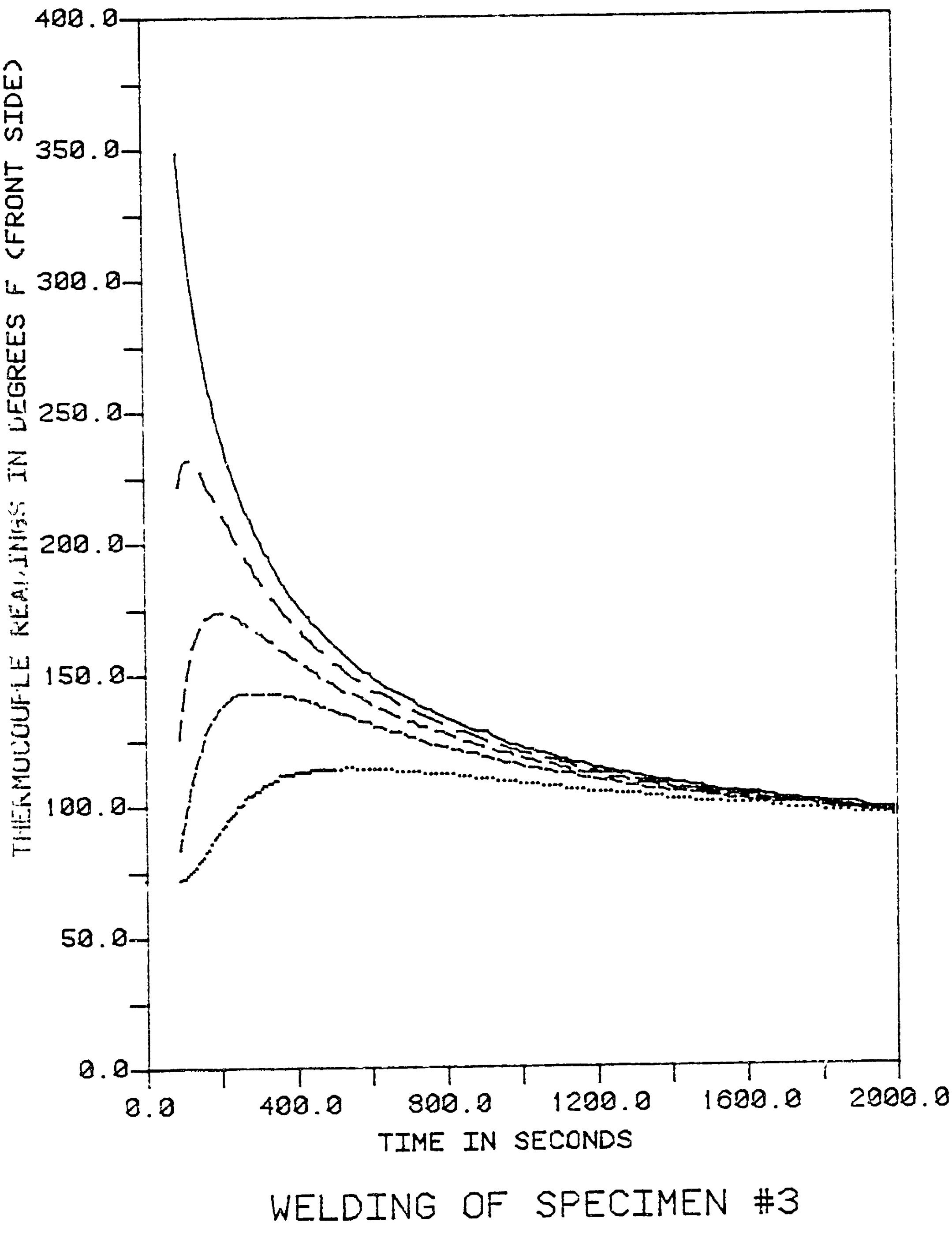

Figure 7.7 : Thermocouple readings during welding of specimen #3

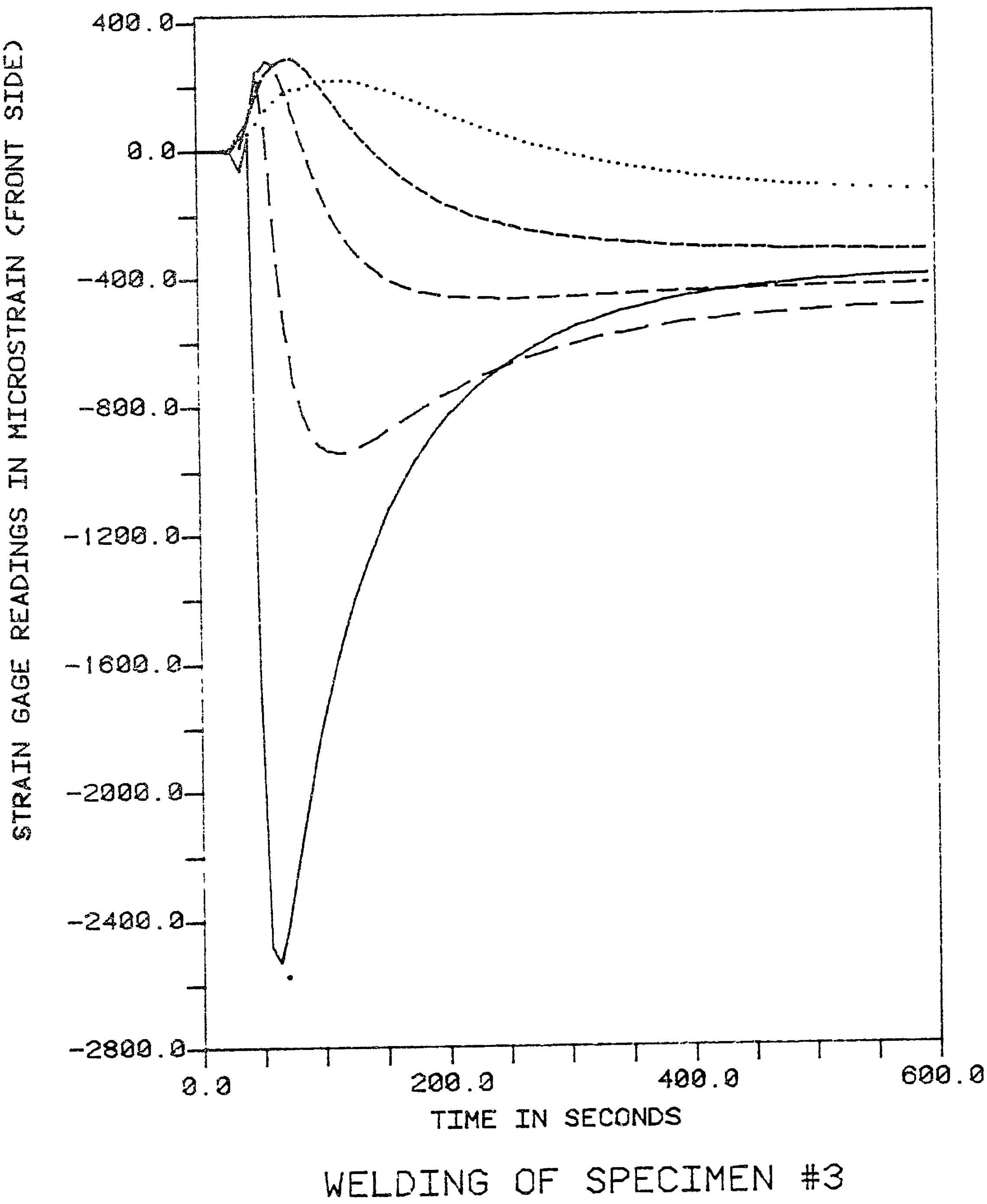

Figure 7.8 : Uncompensated strain gage readings during welding of specimen #3, front side

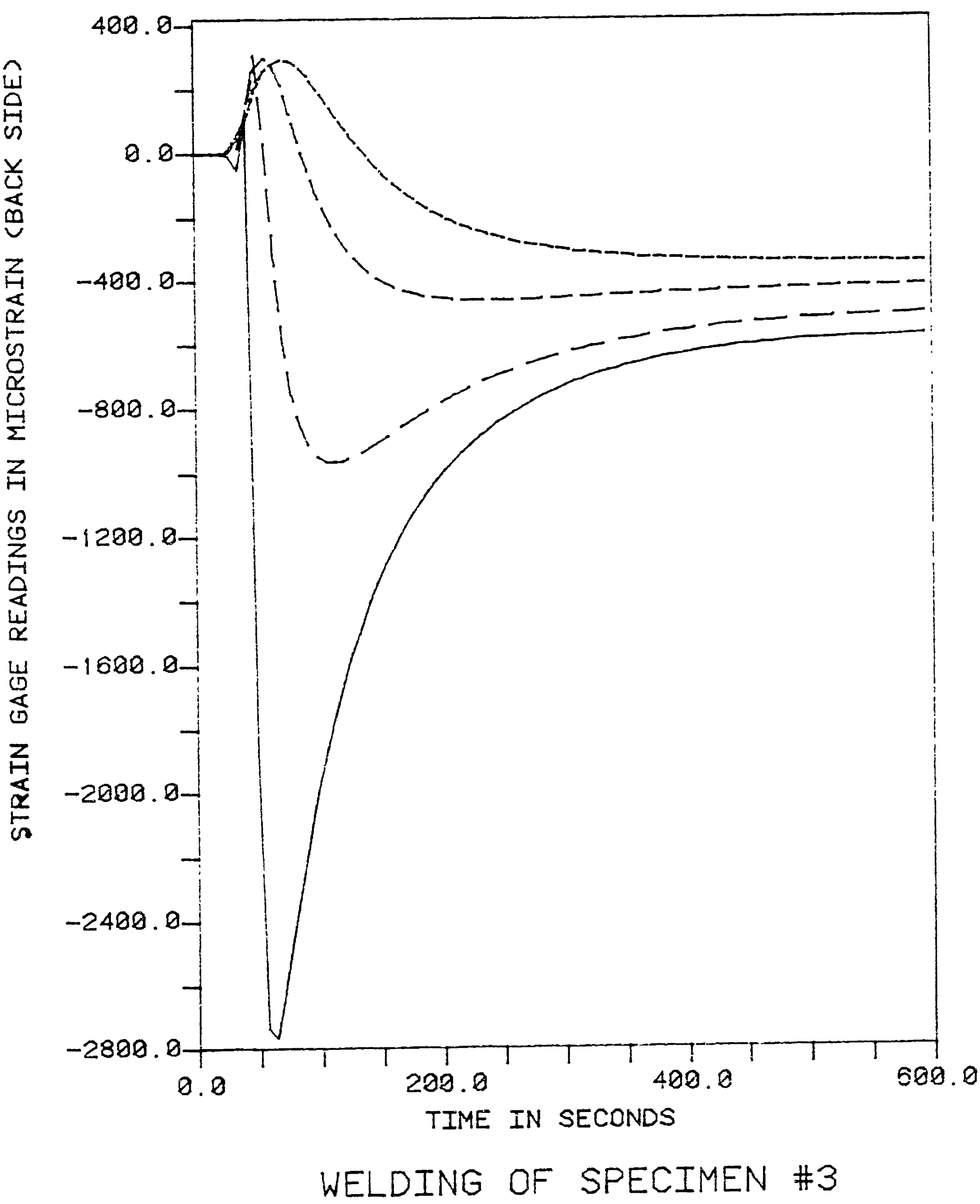

Figure 7.9 : Uncompensated strain gage readings during welding of specimen #3, back side

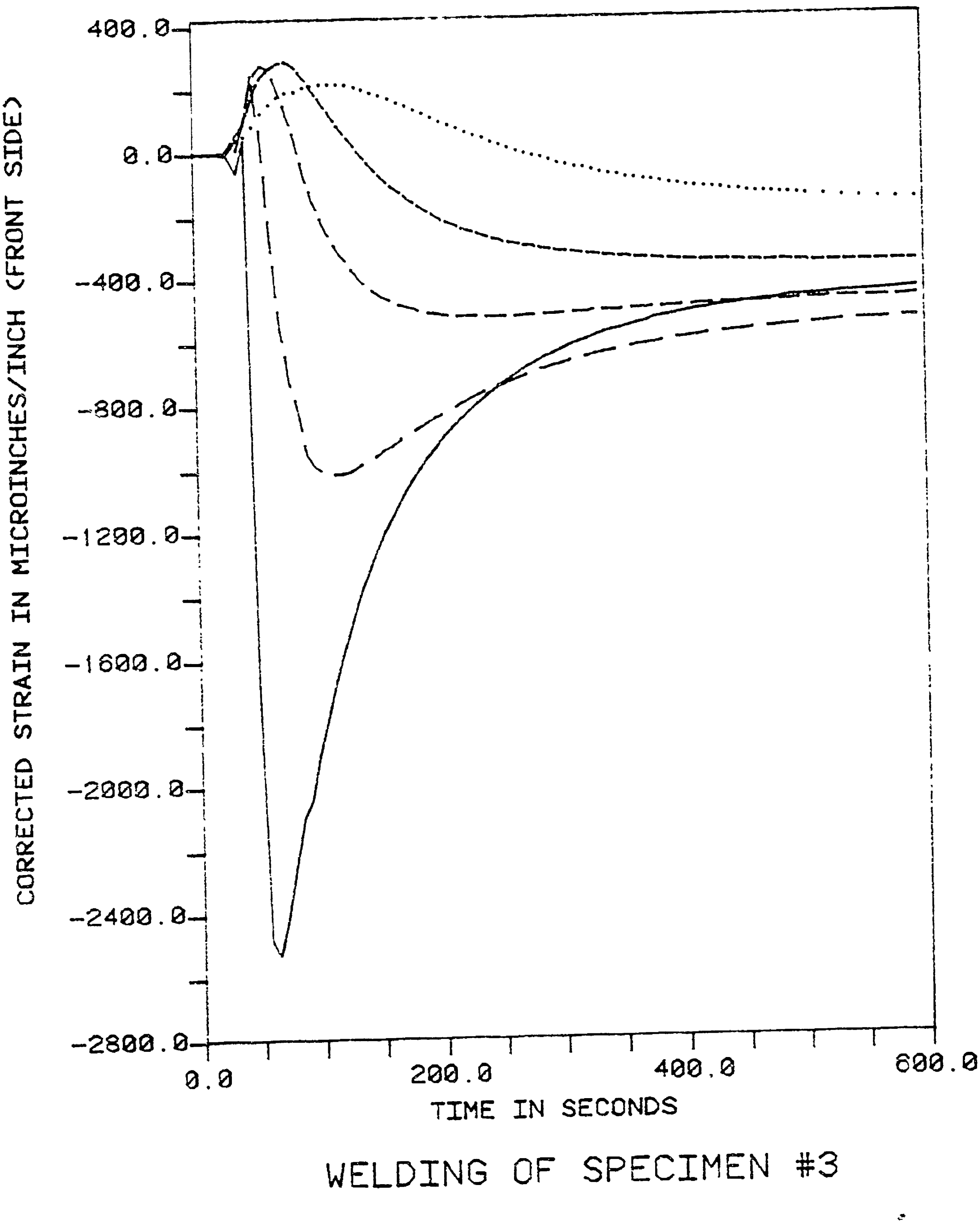

Figure 7.10 : Strains during welding of specimen #3, front side (corrected for temperature induced apparent strain and gage factor variations)

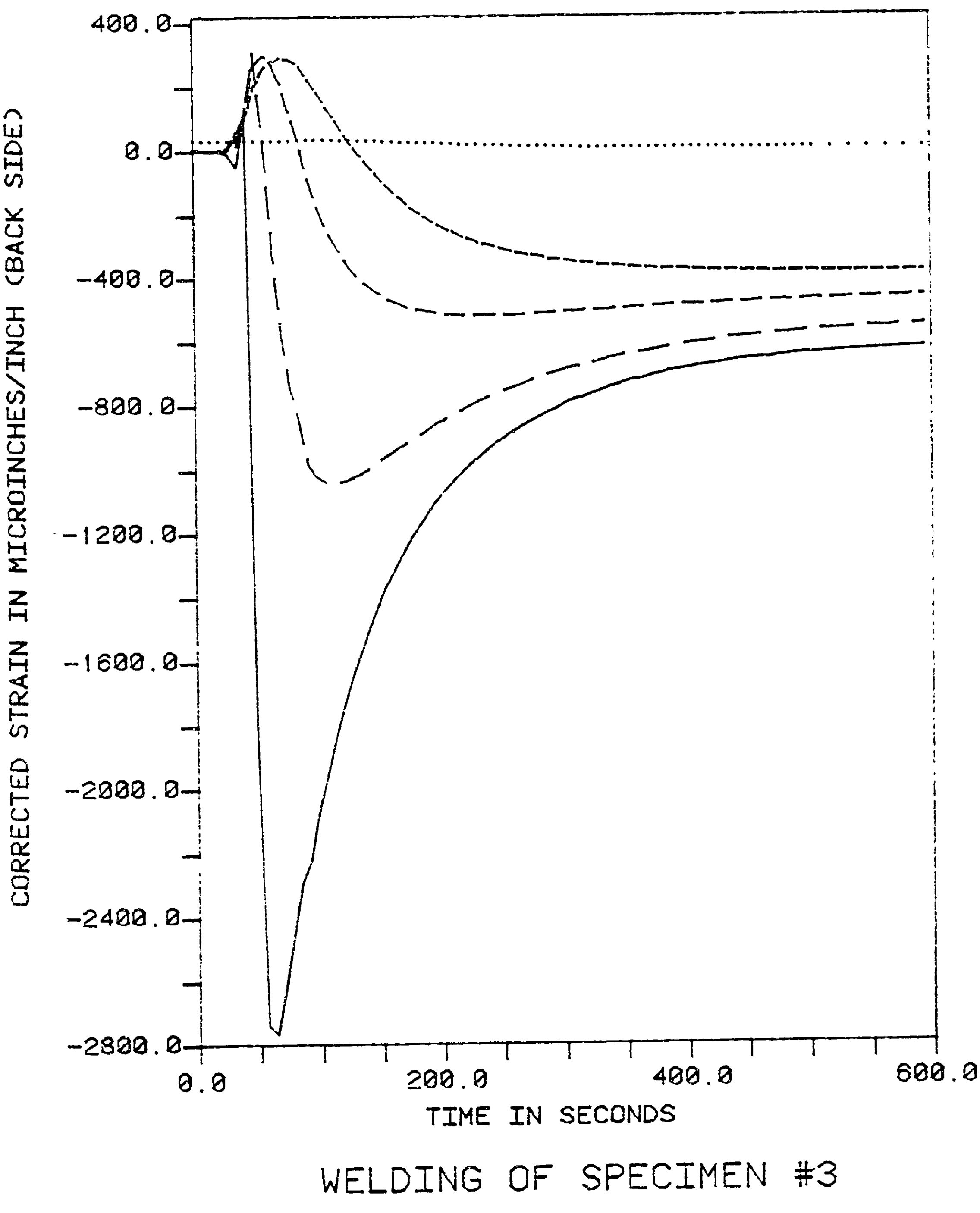

Figure 7.11 : Strains during welding of specimen #3, back side (corrected for temperature induced apparent strain and gage factor variations)

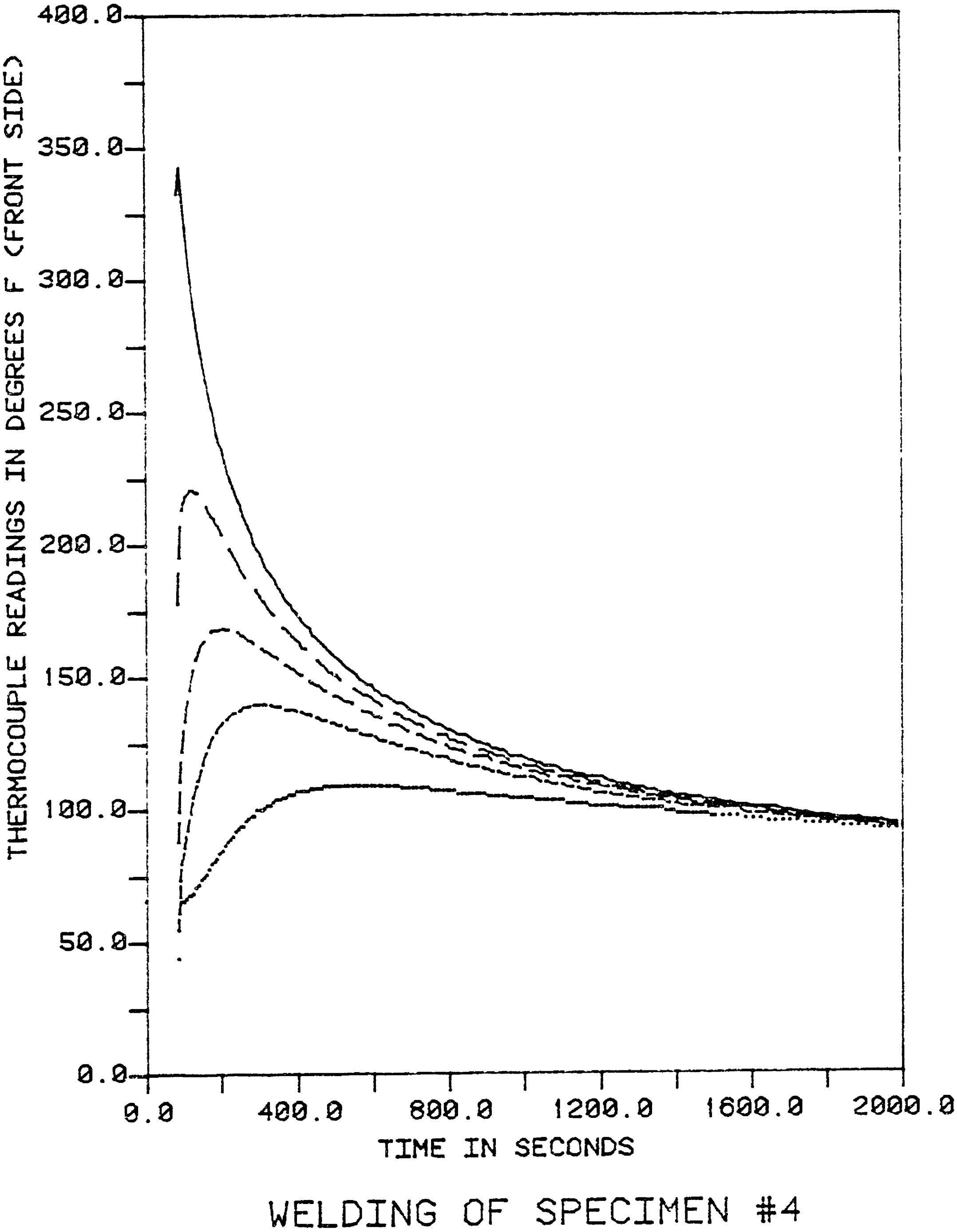

Figure 7.12 : Thermocouple readings during welding of specimen #4

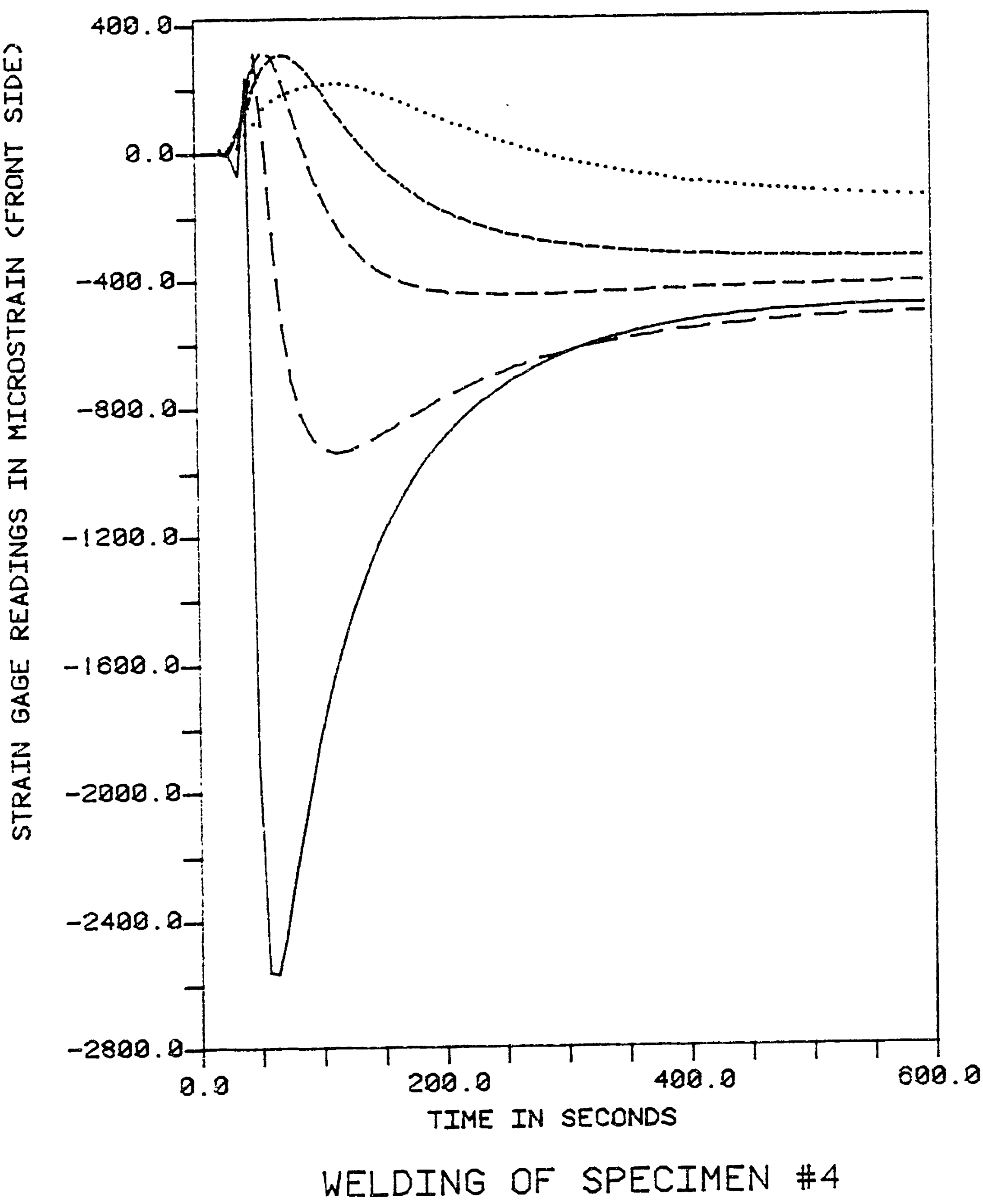

Figure 7.13 : Uncompensated strain gage readings during welding of specimen #4, front side

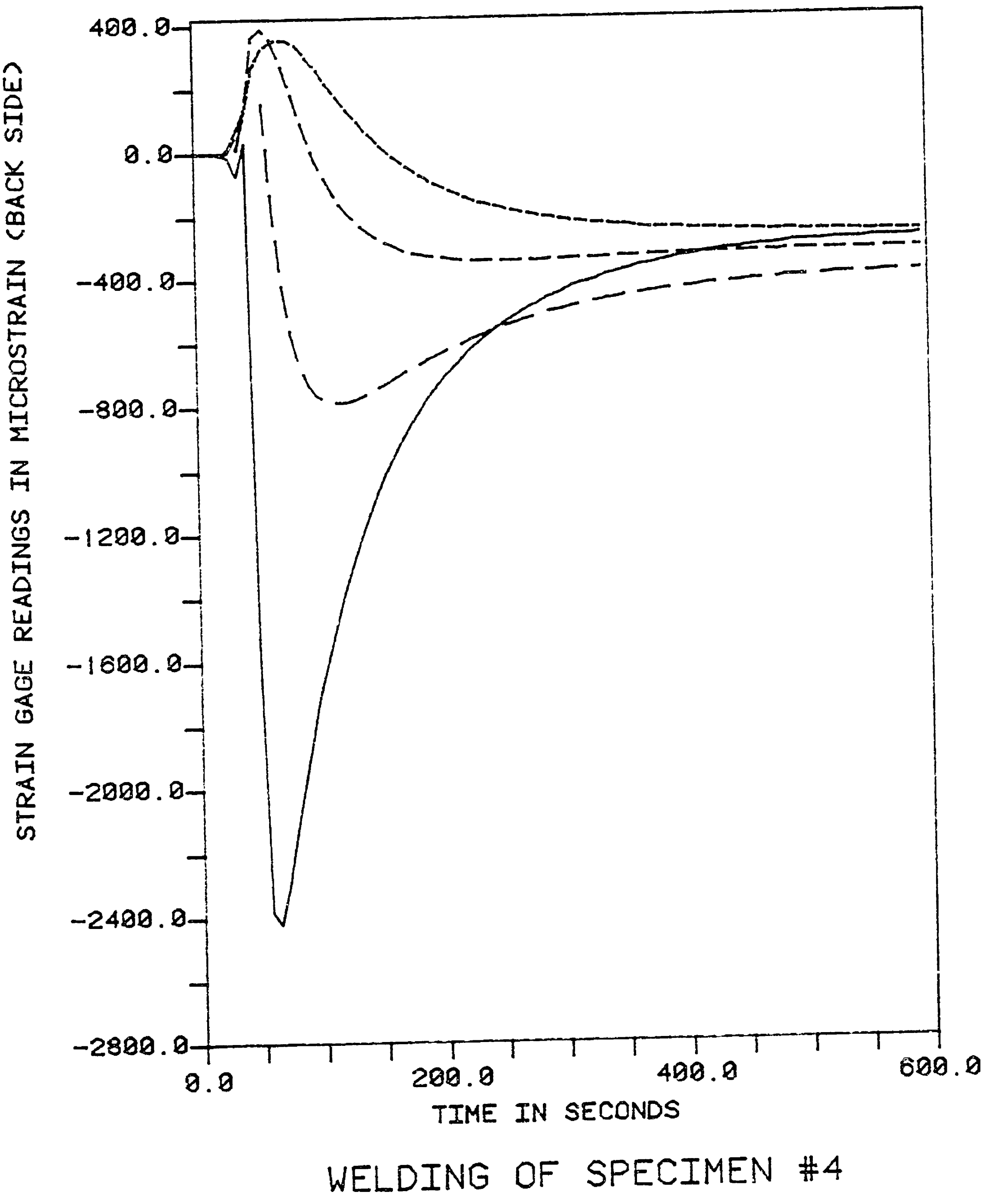

Figure 7.14 : Uncompensated strain gage readings during welding of specimen #4, back side

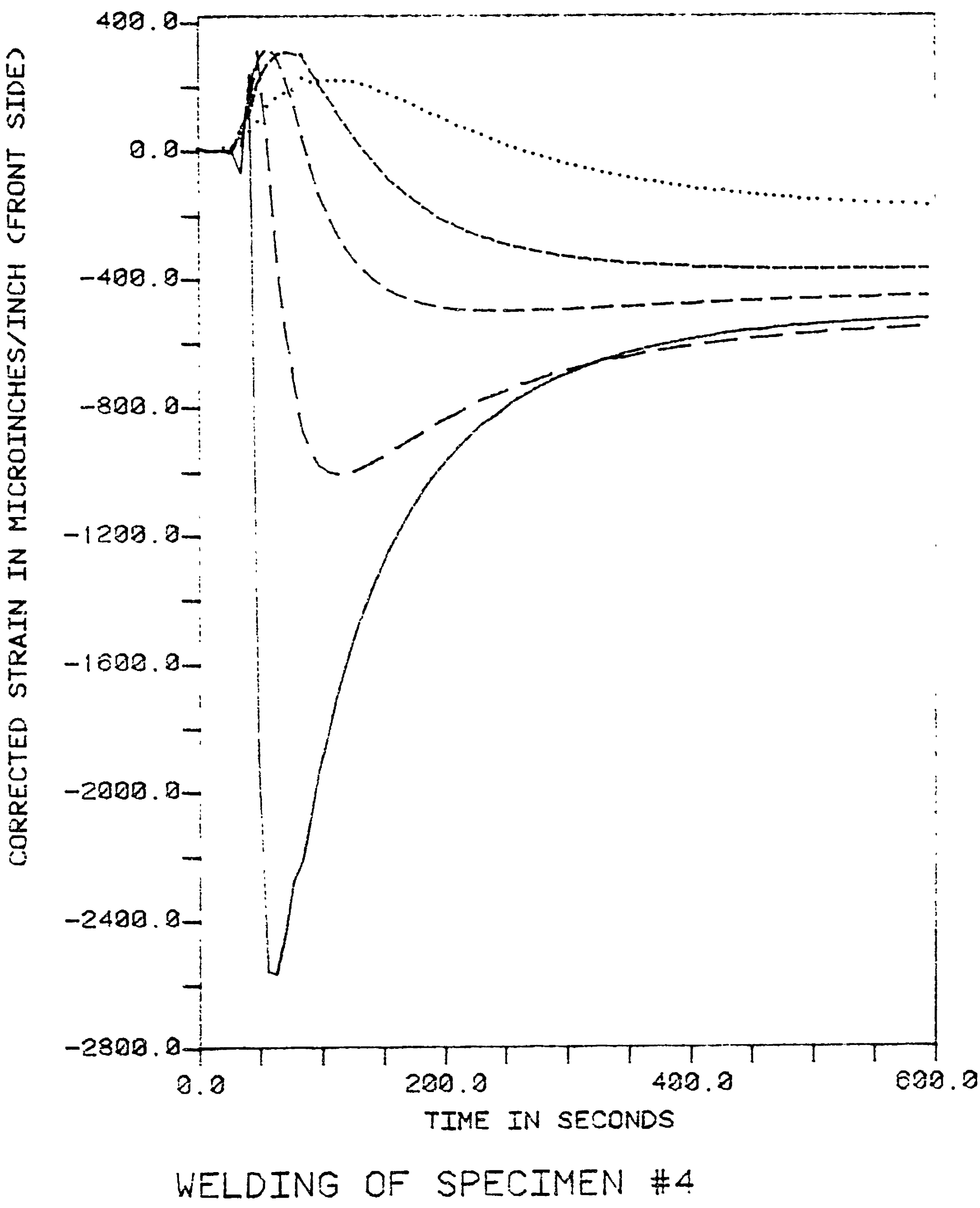

Figure 7.15 : Strains during welding of specimen #4, front side (corrected for temperature induced apparent strain and gage factor variations)

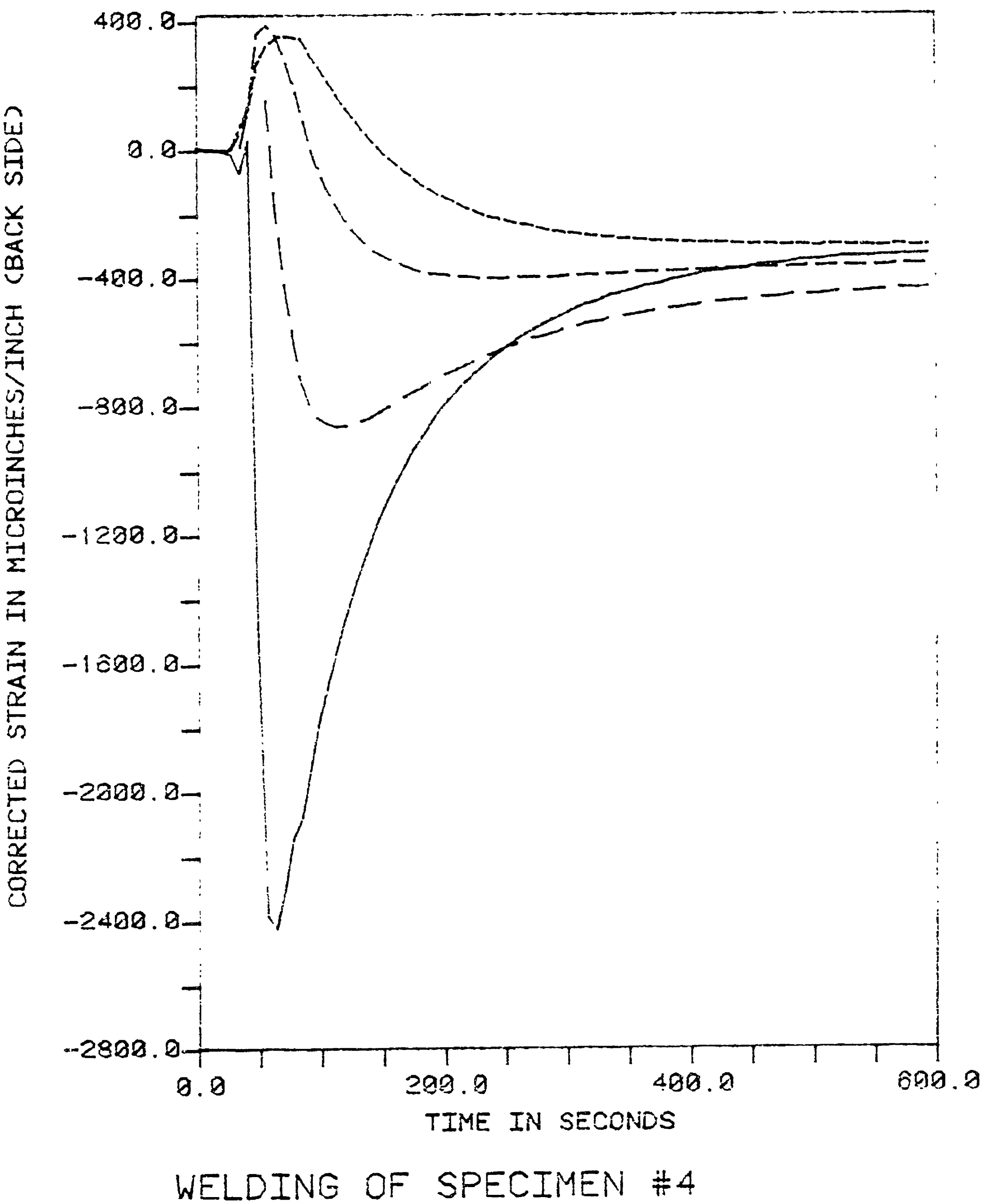

Figure 7.16 : Strains during welding of specimen #4, back side (corrected for temperature induced apparent strain and gage factor variations)

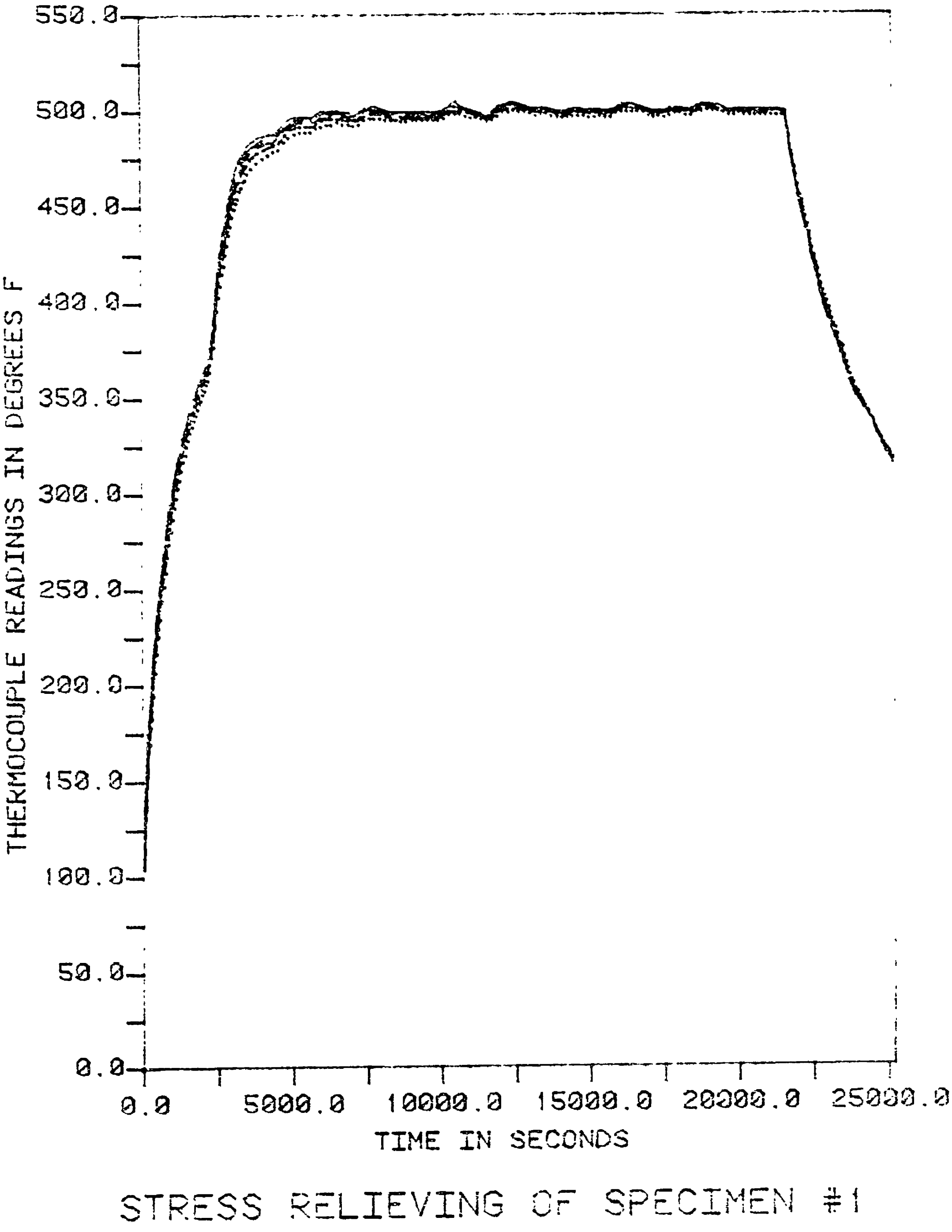

Figure 7.17 : Thermocouple readings during stress-relieving of specimen #1

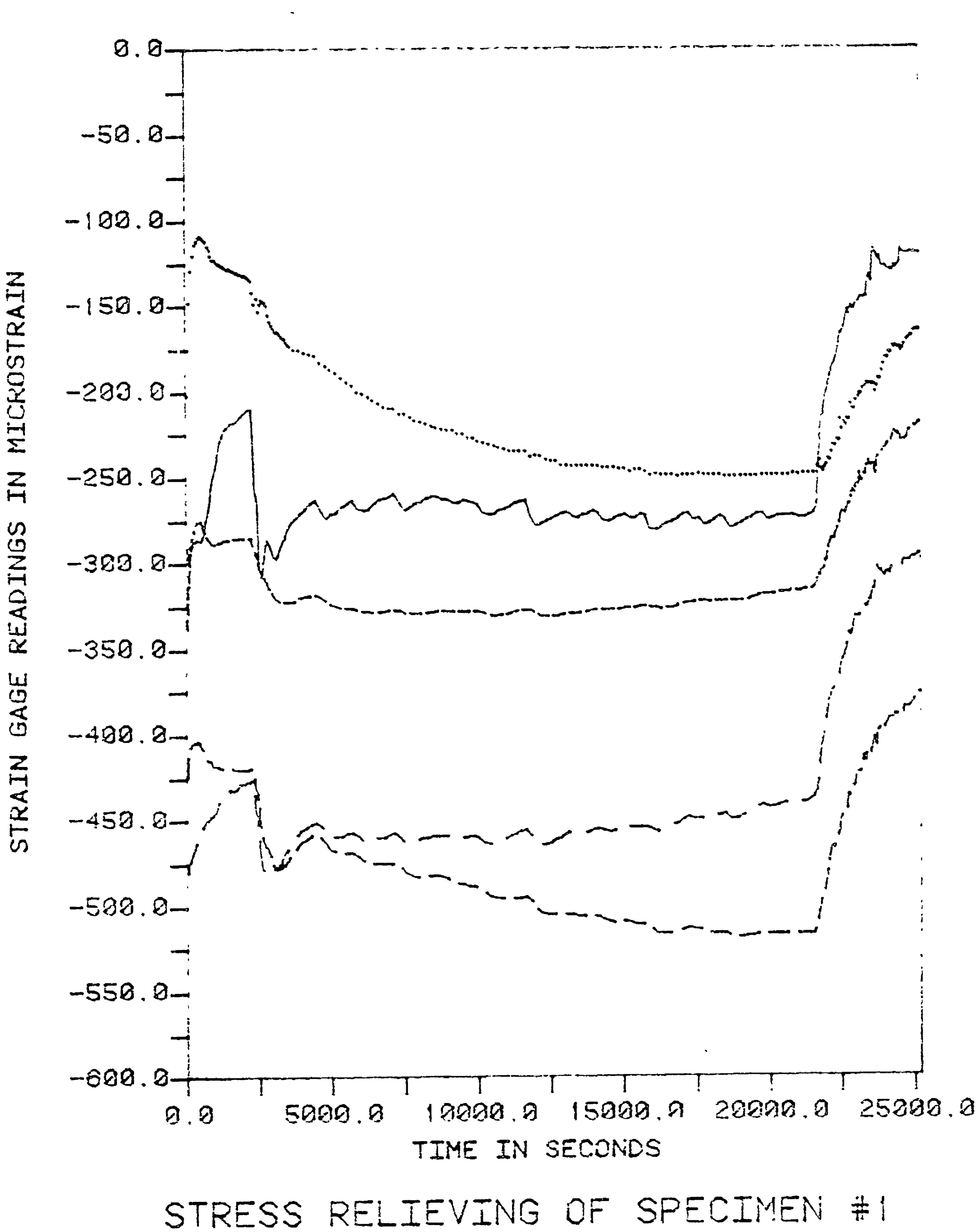

Figure 7.18 : Uncompensated strain gage readings during stress-relieving of specimen #1

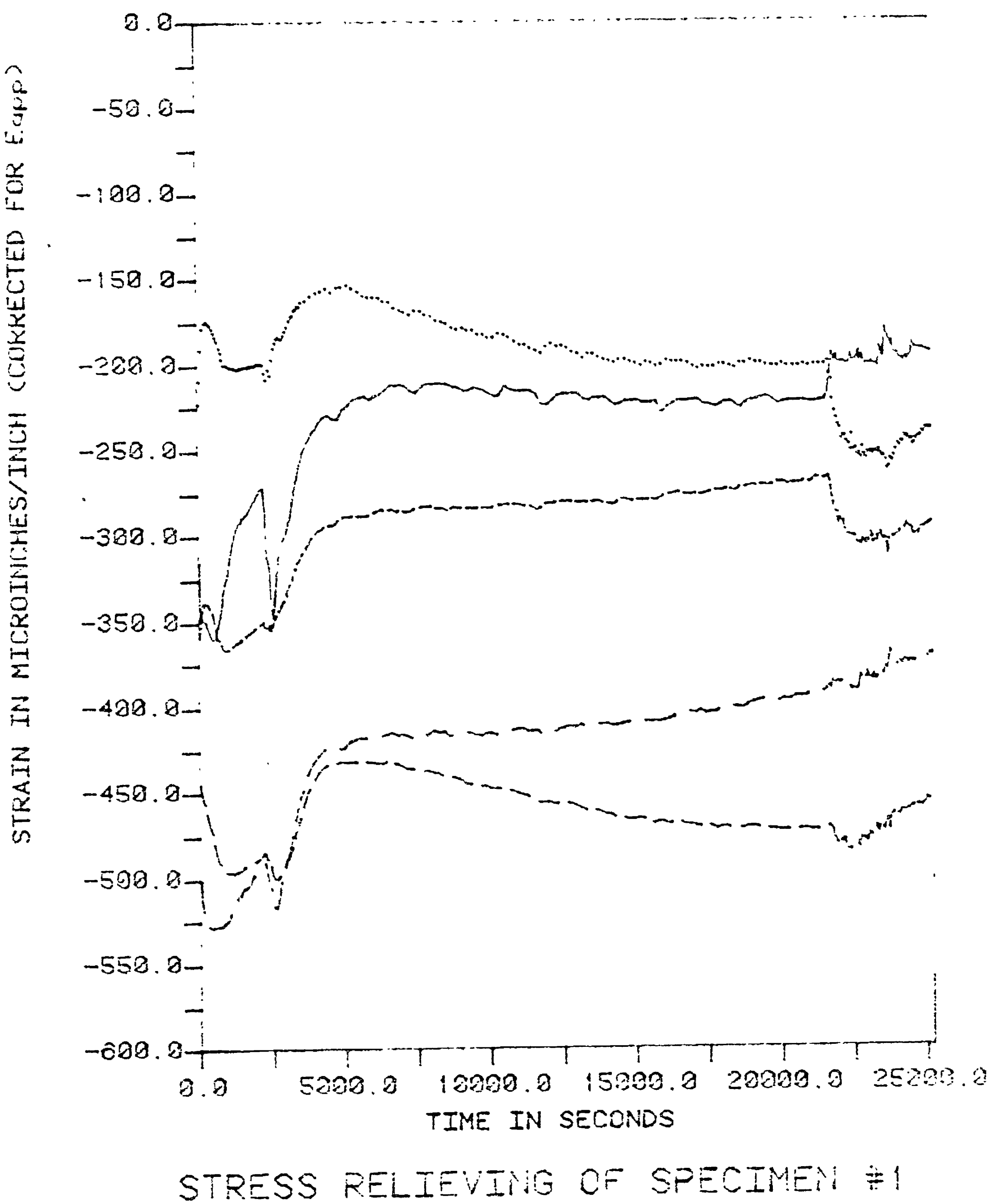

Figure 7.19 : Strains during stress-relieving of specimen #1 (corrected for temperature-induced apparent strain and gage factor variations)

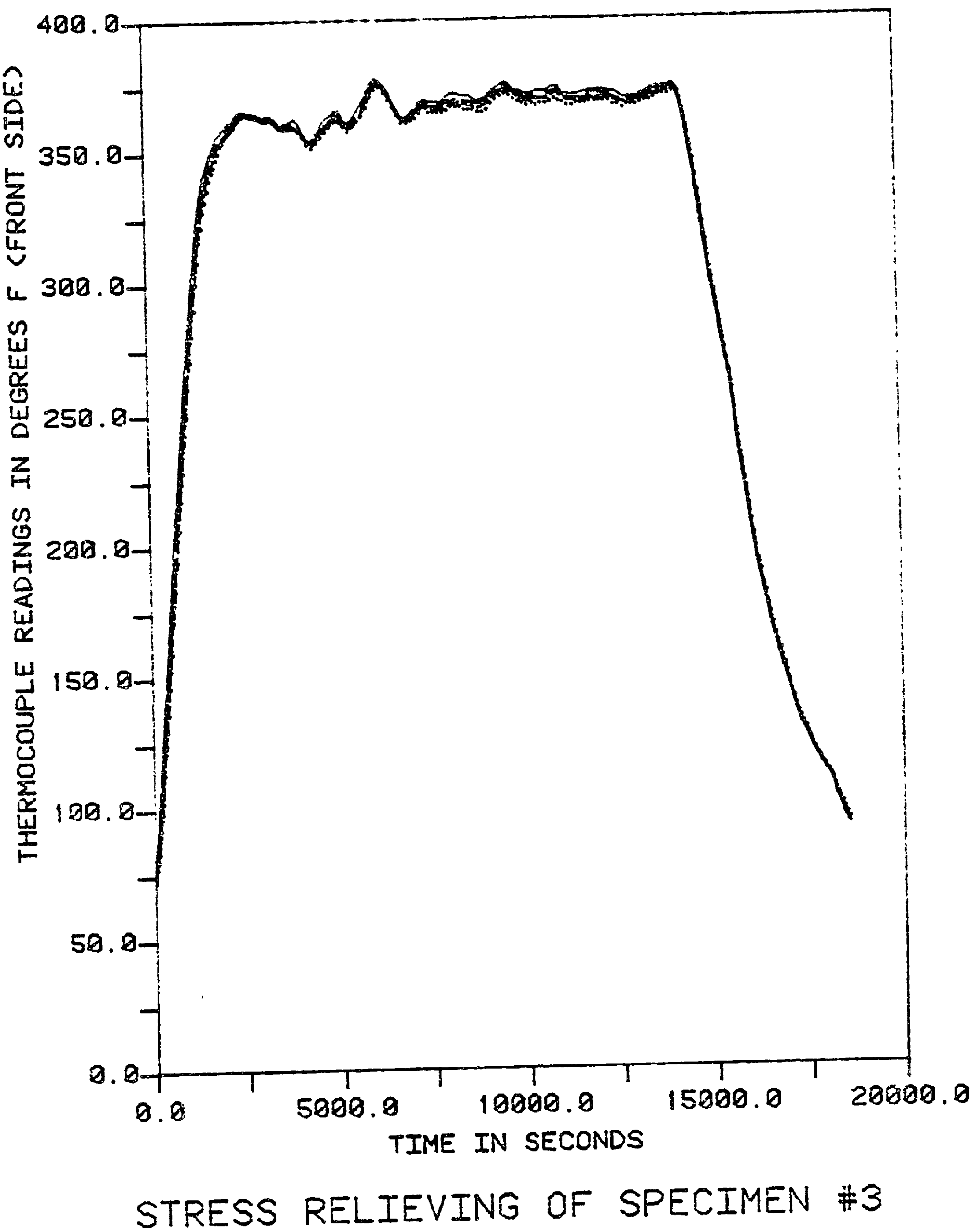

Figure 7.20 : Thermocouple readings during stress-relieving of specimen #3

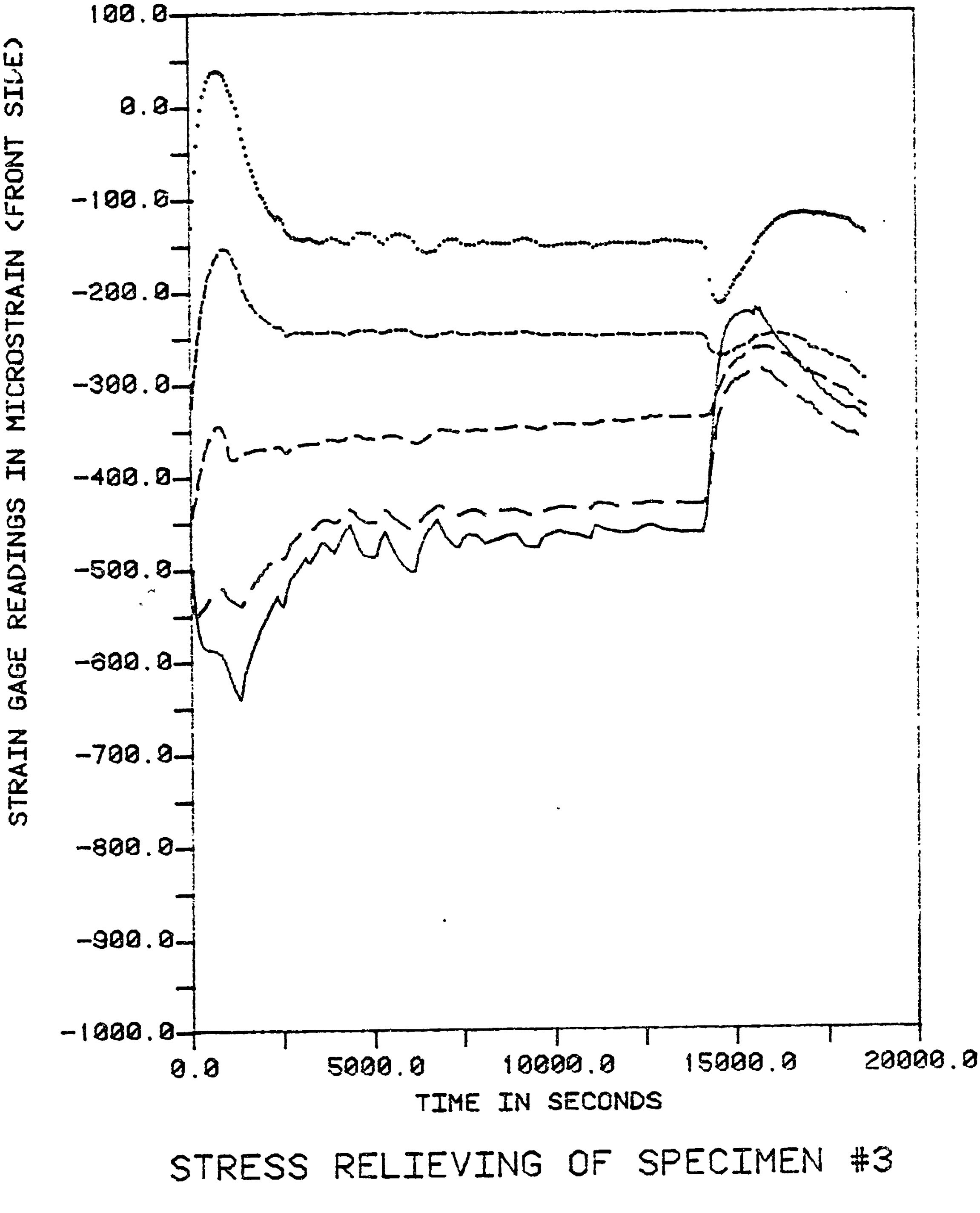

Figure 7.21 : Uncompensated strain gage readings during stress-relieving of specimen #3, front side

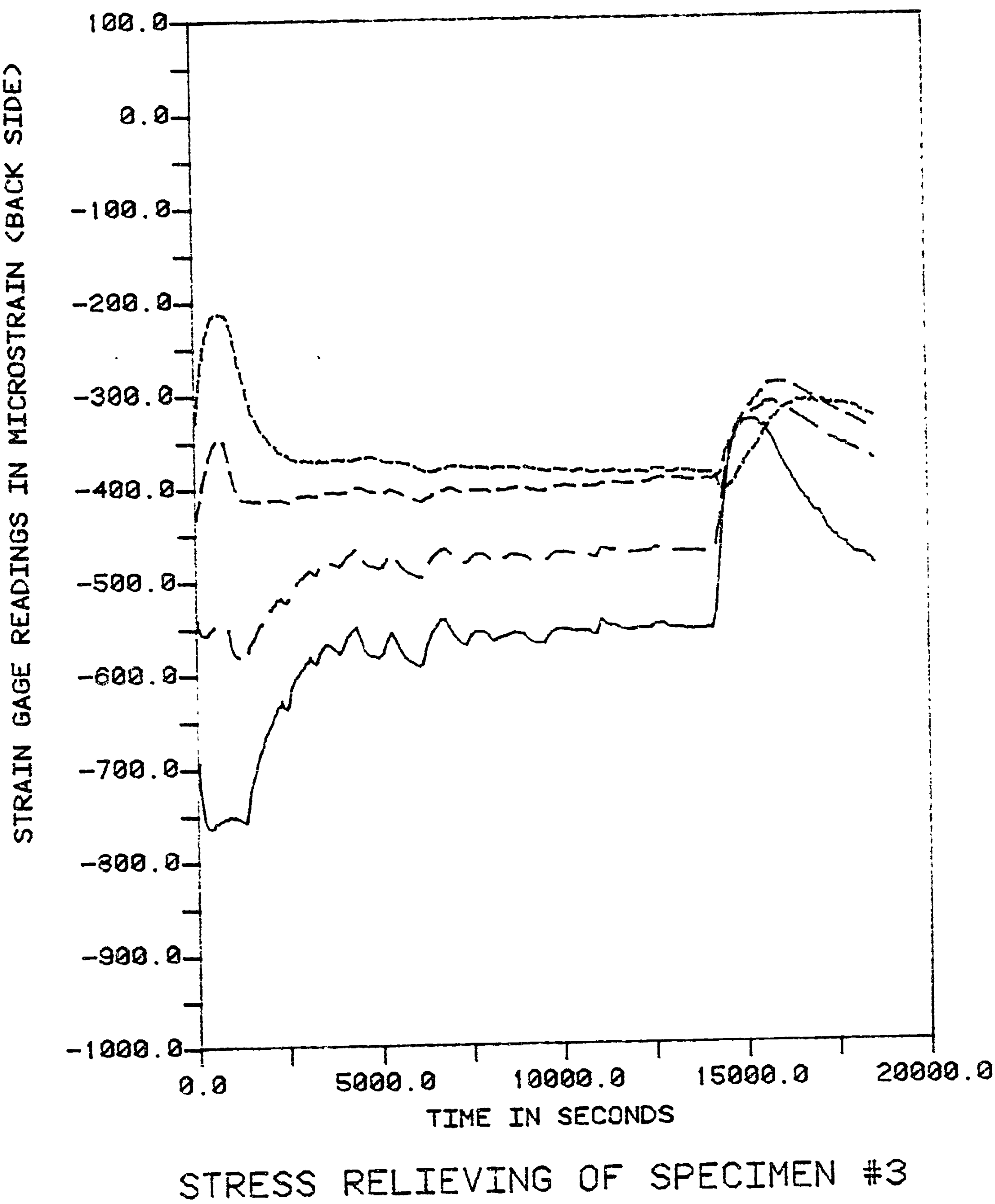

Figure 7.22 : Uncompensated strain gage readings during stress-relieving of specimen #3, back side

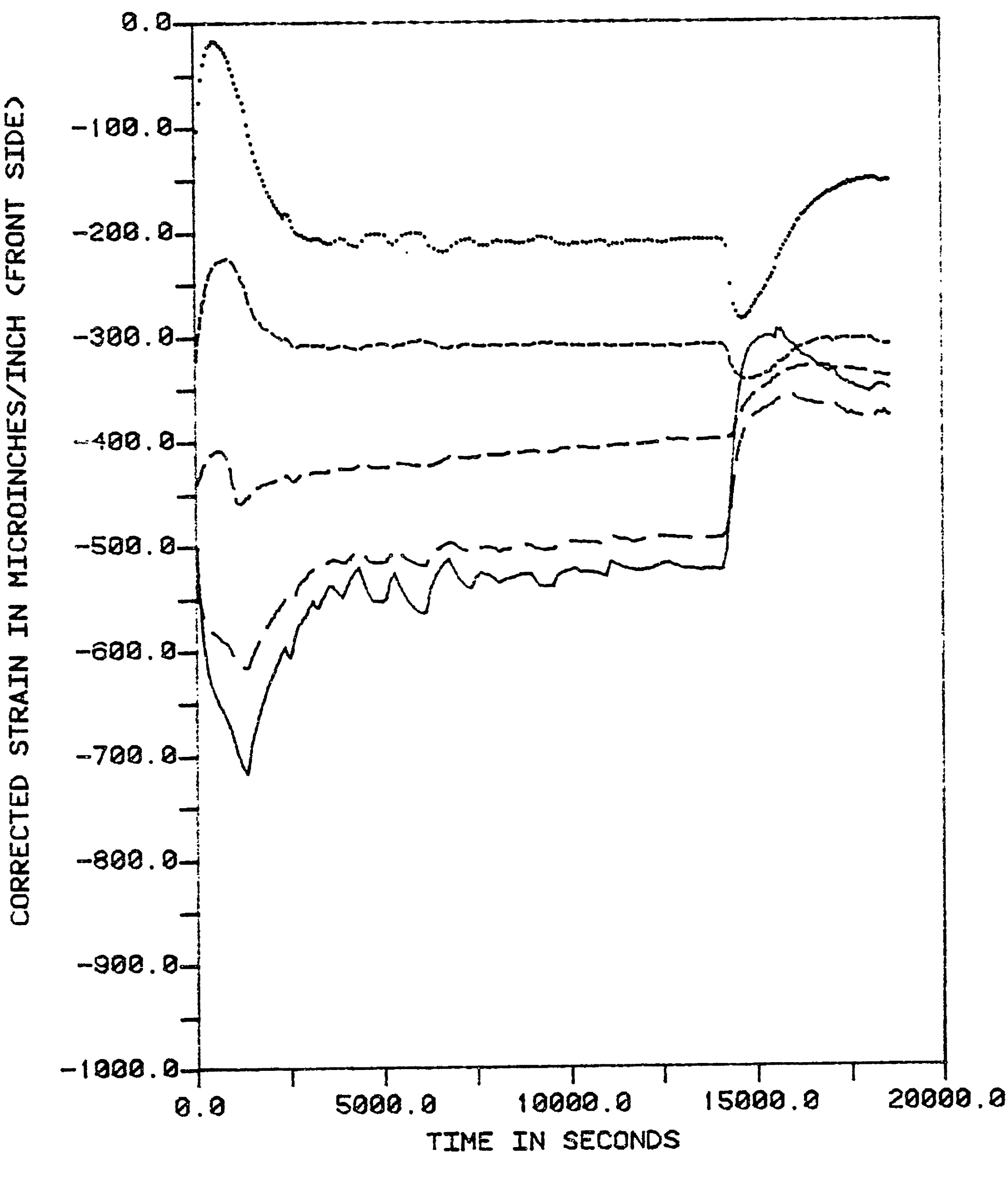

Figure 7.23 : Strains during stress-relieving of specimen #3, front side (corrected for temperature induced apparent strain and gage factor variations)

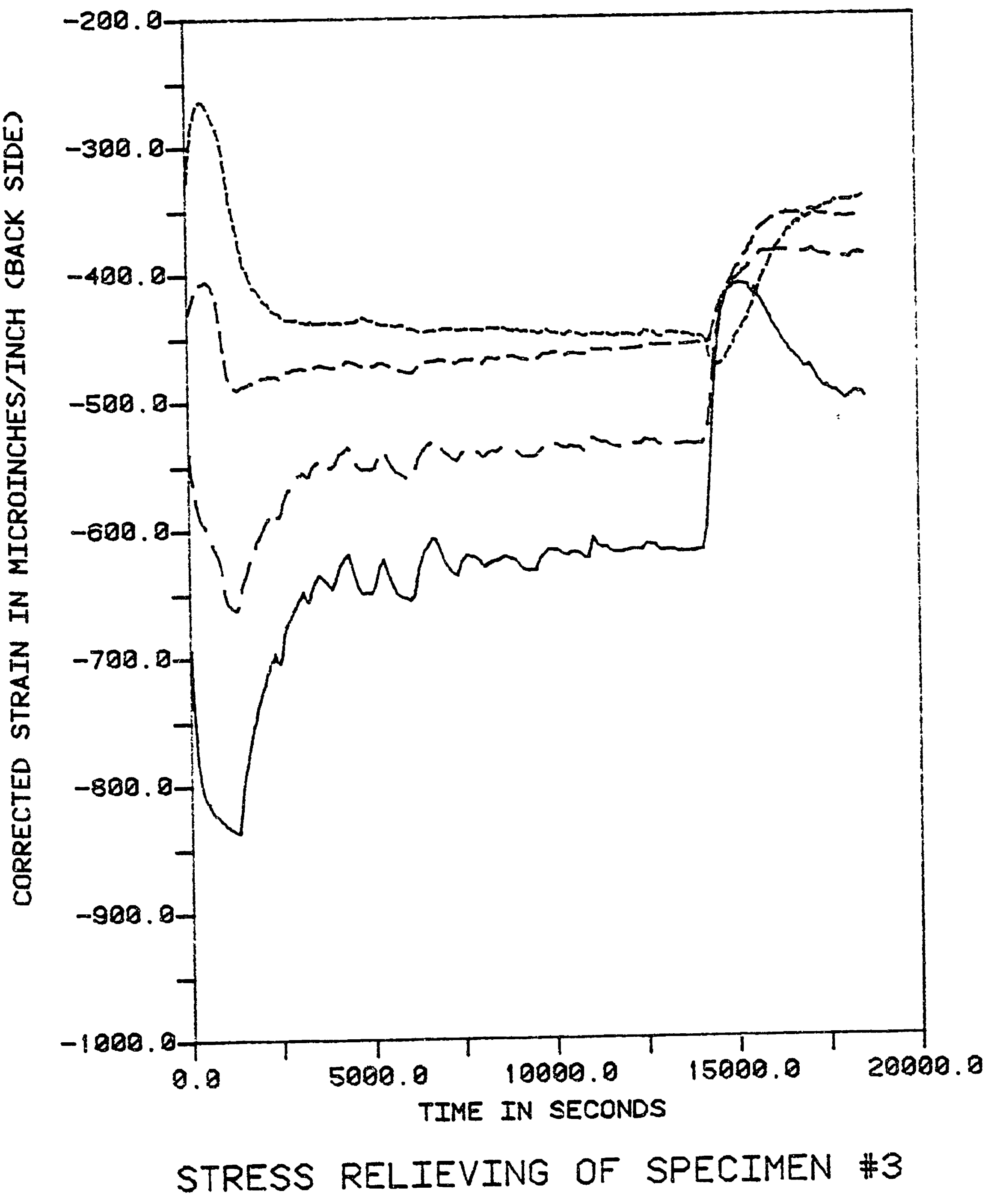

Figure 7.24 : Strains during stress relieving of specimen #3, back side (corrected for temperature induced apparent strain and gage factor variations)

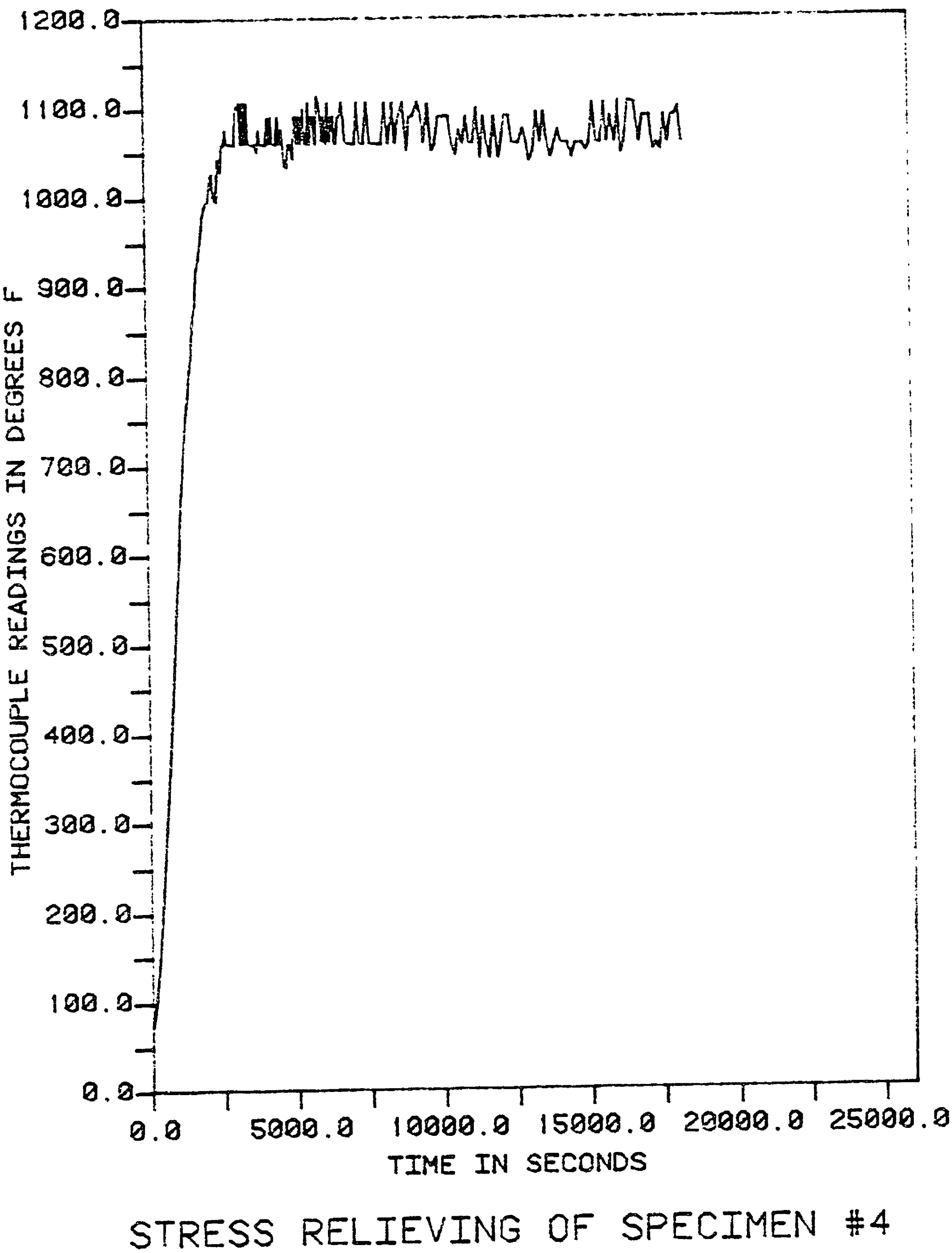

Figure 7.25 : Thermocouple readings during stress-relieving of specimen #4

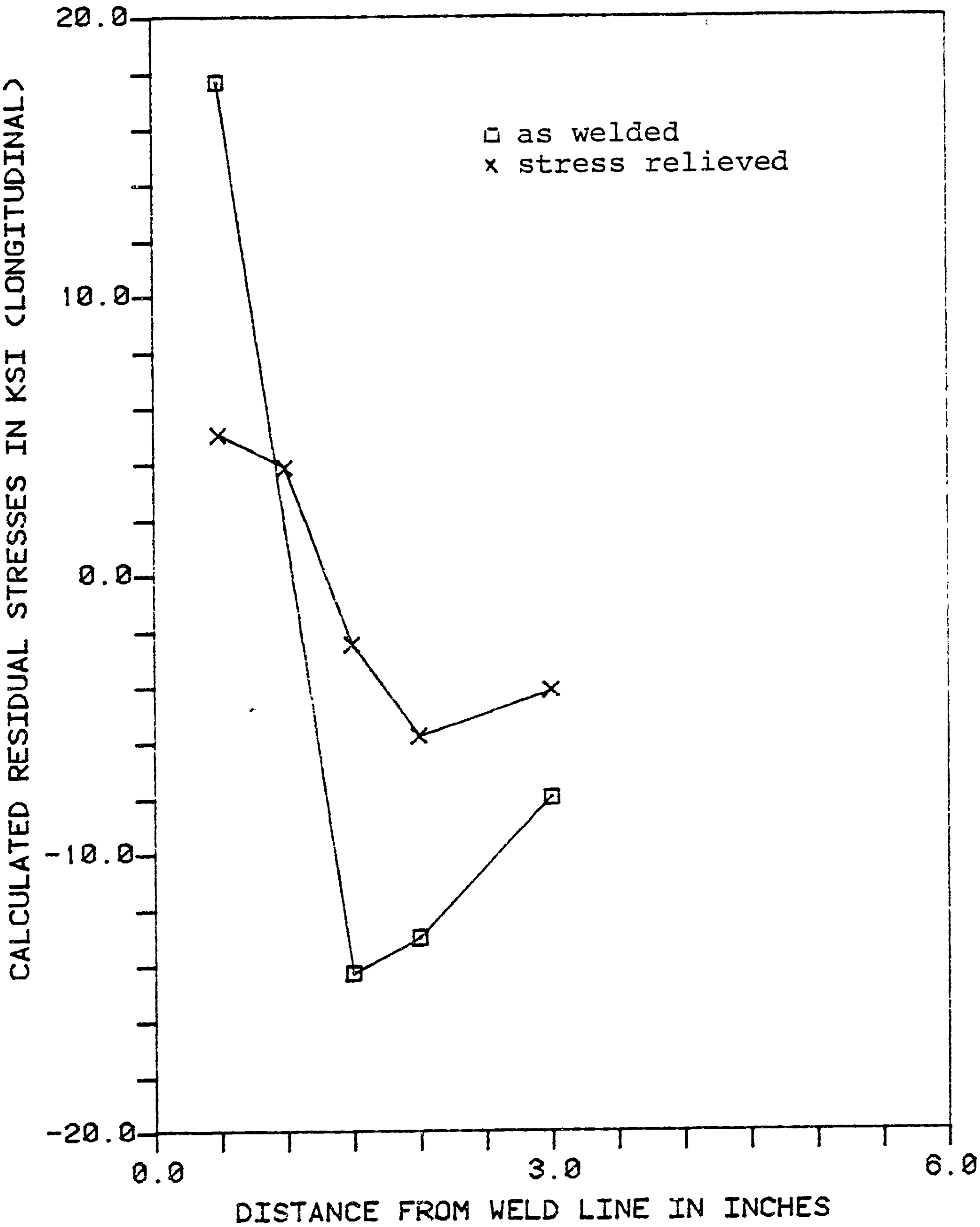

Figure 7.26 (a): Comparison of longitudinal residual stresses after welding and stress relieving (1100° F)

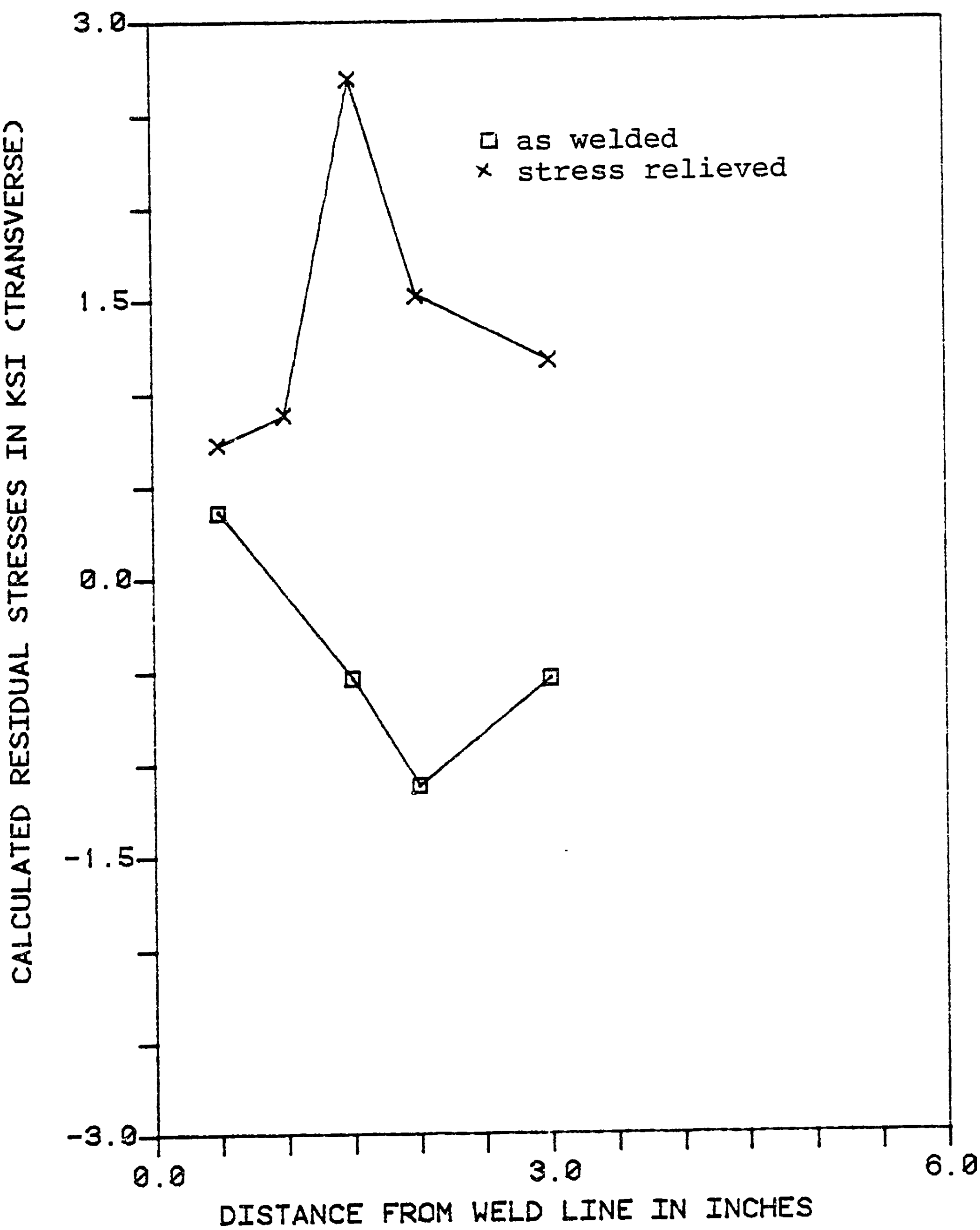

Figure 7.26 (b): Comparison of transverse residual stresses after welding and stress relieving (1100° F)

Table 7.1 : Strain gage readings before and after cutting

Location	$\bar{\varepsilon}_{xBEF}$ µin/in	$\bar{\varepsilon}_{xAFT}$ µin/in	$\Delta\bar{\varepsilon}_x$ µin/in	$\bar{\varepsilon}_{yBEF}$ µin/in	$\bar{\varepsilon}_{yAFT}$ µin/in	$\Delta\bar{\varepsilon}_y$ µin/in	σ_x ksi	σ_y ksi
SPECIMEN #1								
1	-209	-722	-513	/	/			
2	-358	-121	237	/	/			
3	-400	32	432	/	/			
4	-280	106	386	/	/			
5	-195	101	296	/	/			
SPECIMEN #2								
1	0	-622	-622	0	175	175	17.71	0.36
2	1	+221	220	2	*	-	-	-
3	1	+499	498	-1	-133	-132	-14.26	-0.54
4	1	+448	447	2	-96	-98	-12.99	-1.12
5	1	+276	275	-159	-224	-65	- 7.95	-0.54
SPECIMEN #4								
1	1	-170	-171	-1	27	28	5.06	0.72
2	0	-128	-128	0	10	10	3.89	0.88
3	0	115	115	0	-121	-121	-2.45	2.69
4	-1	219	220	0	-115	-115	-5.77	1.52
5	-1	157	158	437	352	-85	-4.12	1.17

Key: / : Gage not installed

* : Gage destroyed during cutting

7.2 Comparisons with Predictions of the One-Dimensional Program

The predictions of the one-dimensional program for the case of edge welding and subsequent stress relieving are presented in this section. Welding conditions were assumed exactly the same as in the experiments and temperatures, strains and stresses were calculated across a center strip of the specimen throughout welding and stress relieving operations.

The actually used input data can be found in the end of Appendix C. A range of values was found in the literature for the arc efficiency, n_a, and surface heat loss coefficient, H, ([1],[37],[135]). Since, no experimental measurements of these parameters were made in this study, the actually selected values - more or less within that range - were such as to minimize the deviation of the predicted temperature history from the experimentally measured one.

The predicted temperatures, mechanical strains and stresses during welding are plotted in Figures 7.27, 7.28, 7.29. For ease of comparison with experimental data the same locations (0.5, 1.0, 1.5, 2.0 and 3.0 inches from the weld line) are selected.

During stress relieving at 500^{o}F the assumed temperature history is shown in Figure 7.30 and the predicted variations in stress and mechanical strain are plotted, versus time, in Figures 7.31 and 7.32. A comparison of the predicted residual stress distribution after welding and after stress relieving are given in Figure 7.33. The assumed temperature history and the respective predictions for stress relieving at 1100^{o}F can be found in Figures 7.34 to 7.37. It should, however, be noted that creep was taken into account only in the latter case (1100°F) where creep properties were available (Appendix A).

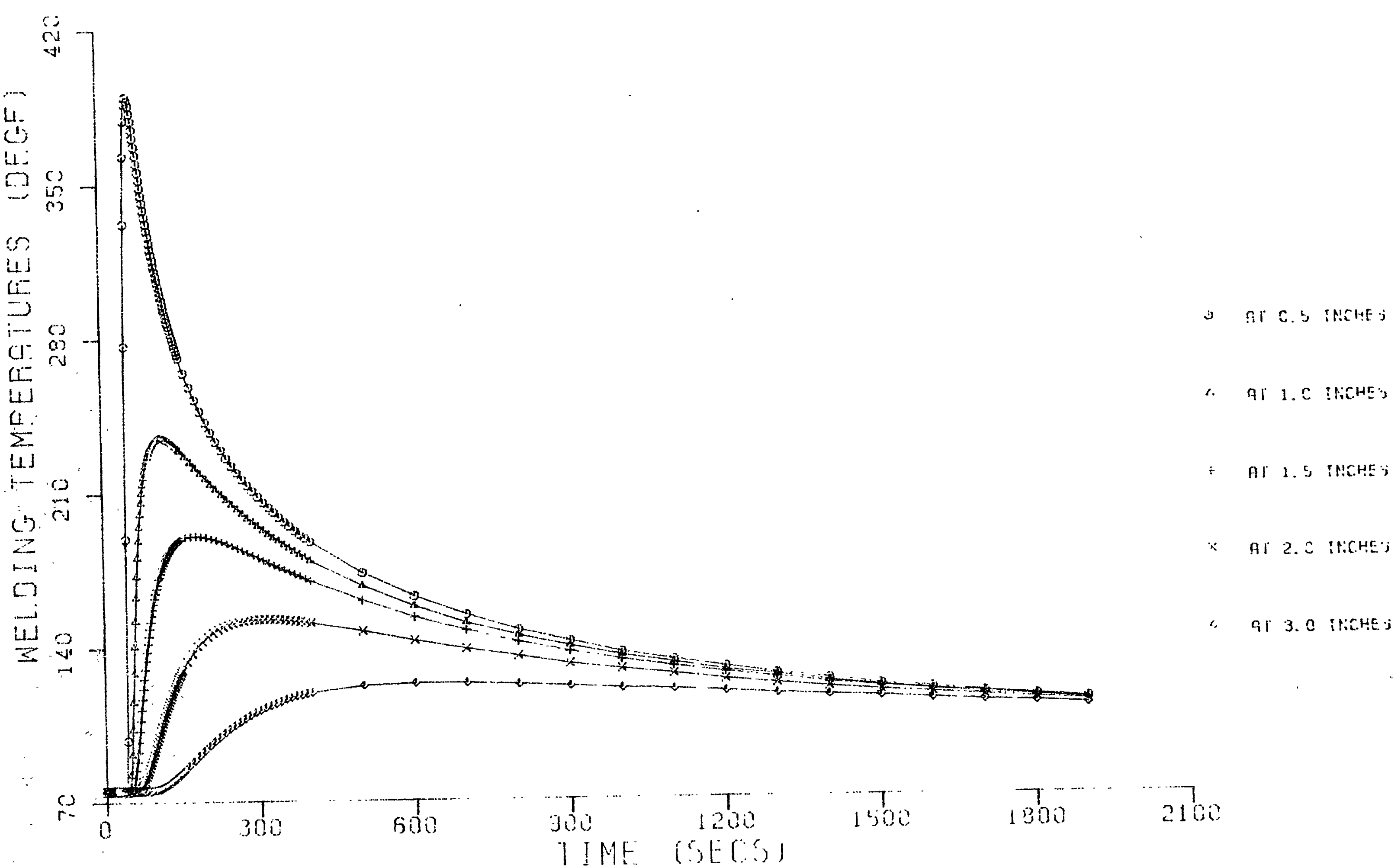

Figure 7.27 : Temperatures during edge welding, as predicted by the one-dimensional program

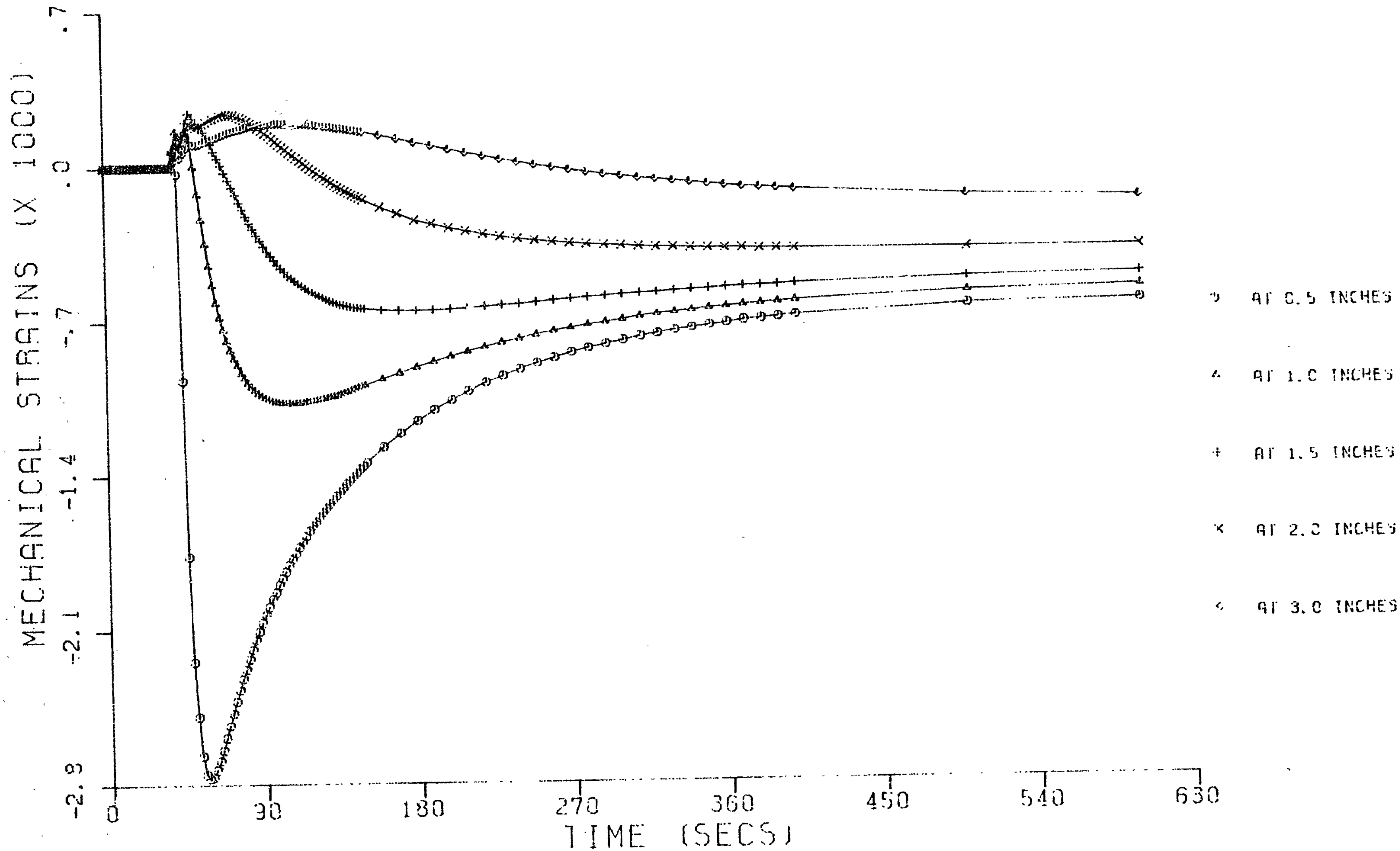

Figure 7.28 : Mechanical strains during edge welding as predicted by the one-dimensional program

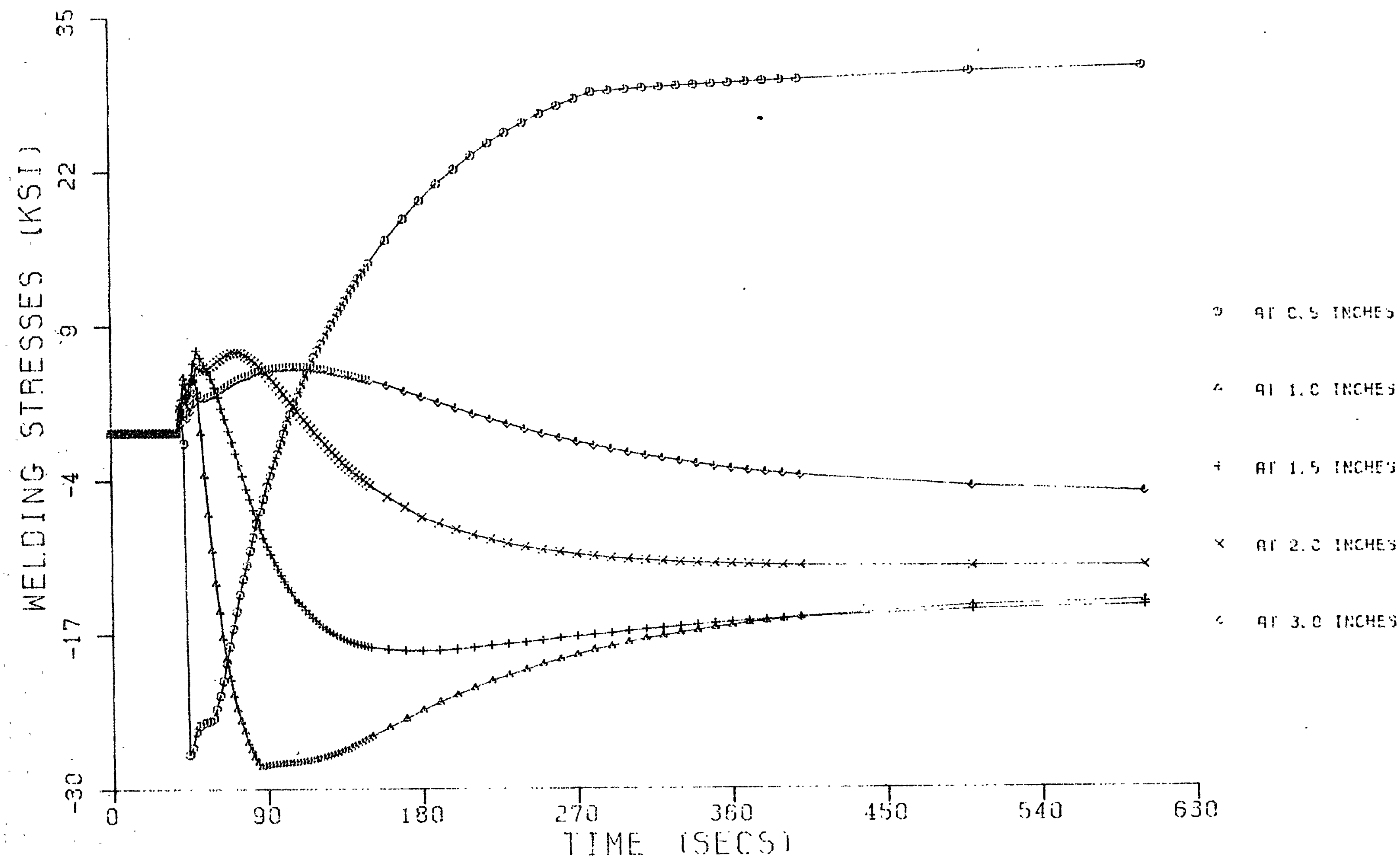

Figure 7.29 : Stresses during edge welding as predicted by the one-dimensional program

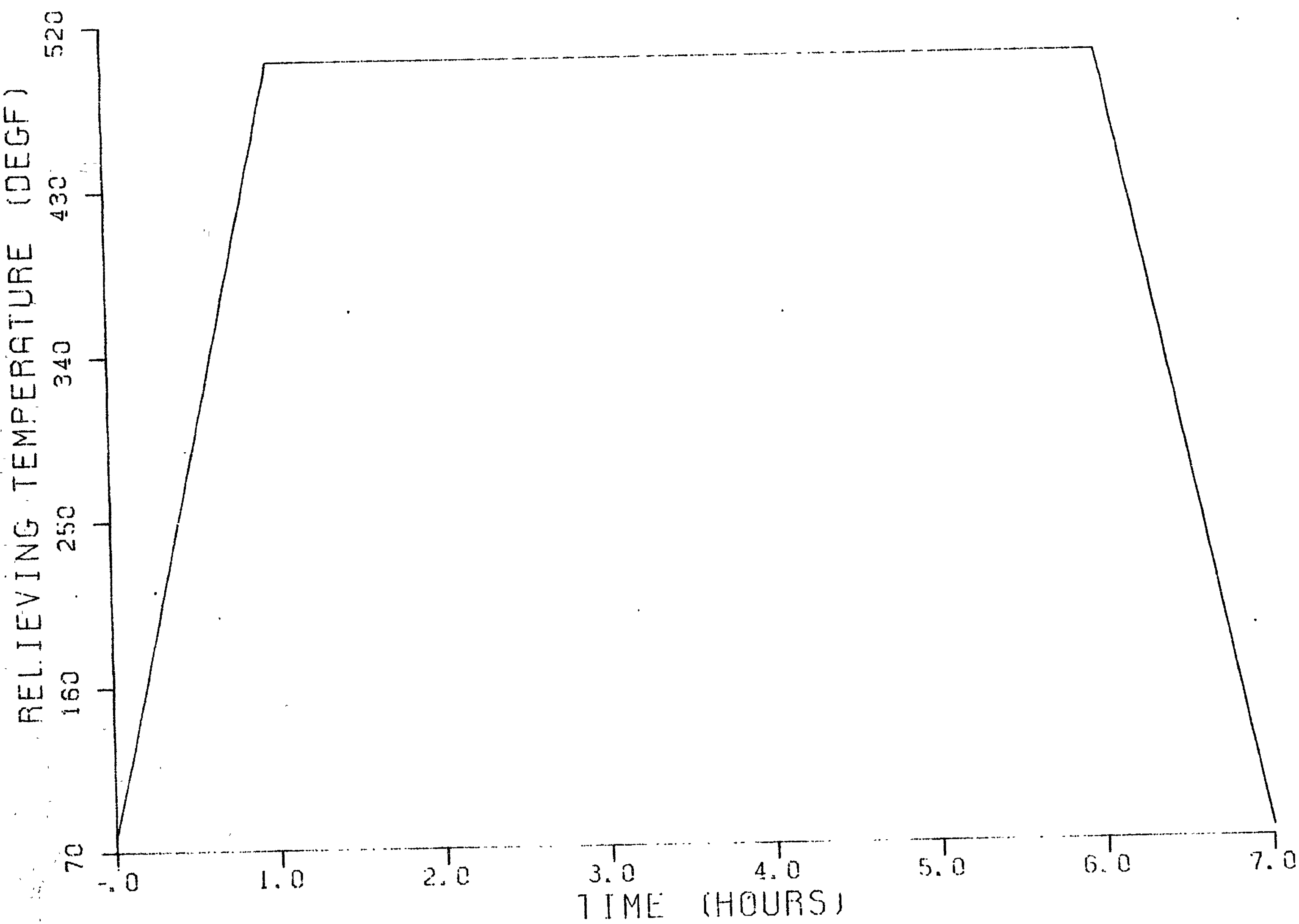

Figure 7.30 : Temperatures during stress-relieving at 500^{o}F

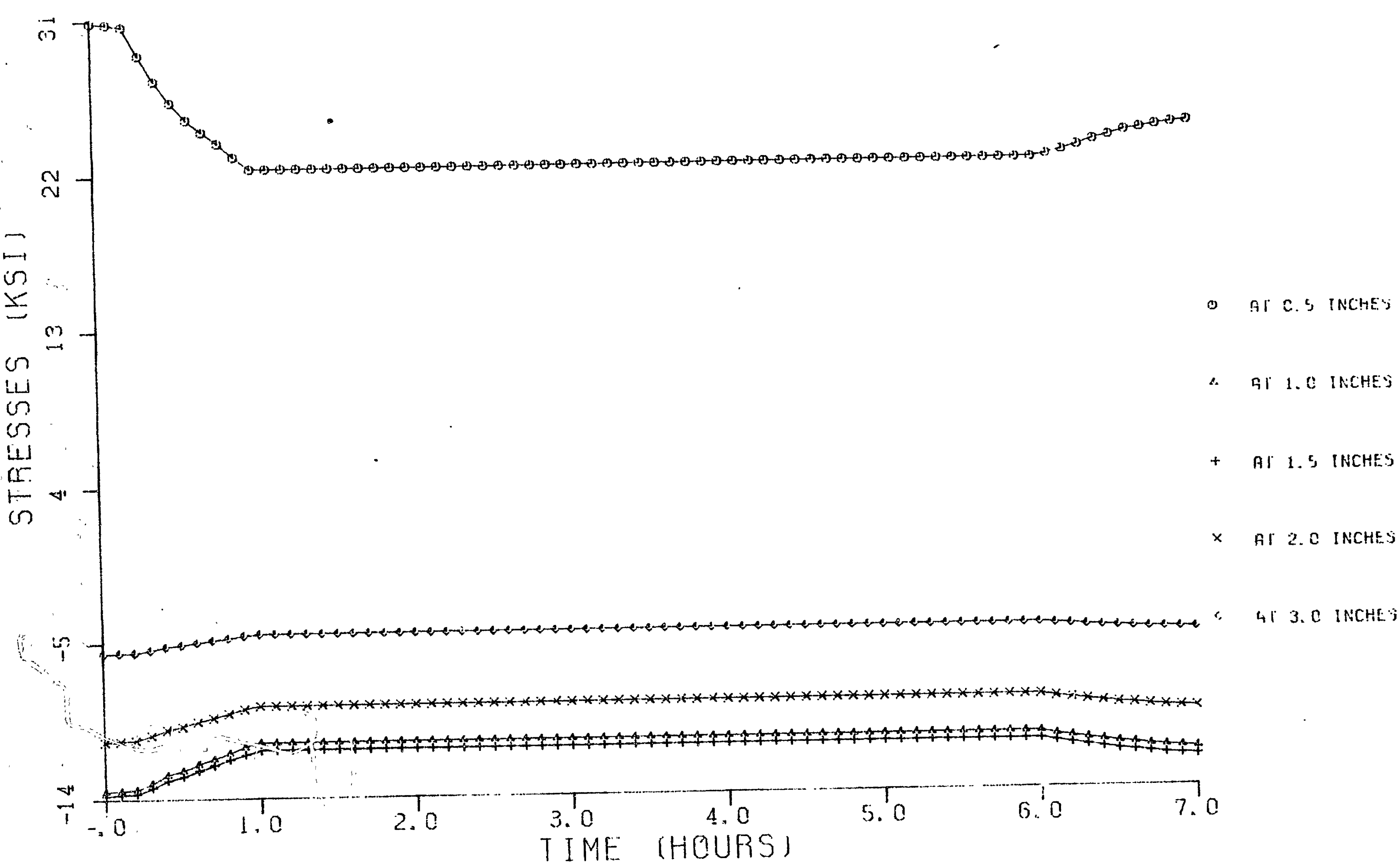

Figure 7.31 : Stresses during stress relieving at 500^{O}F, as predicted by the one-dimensional program

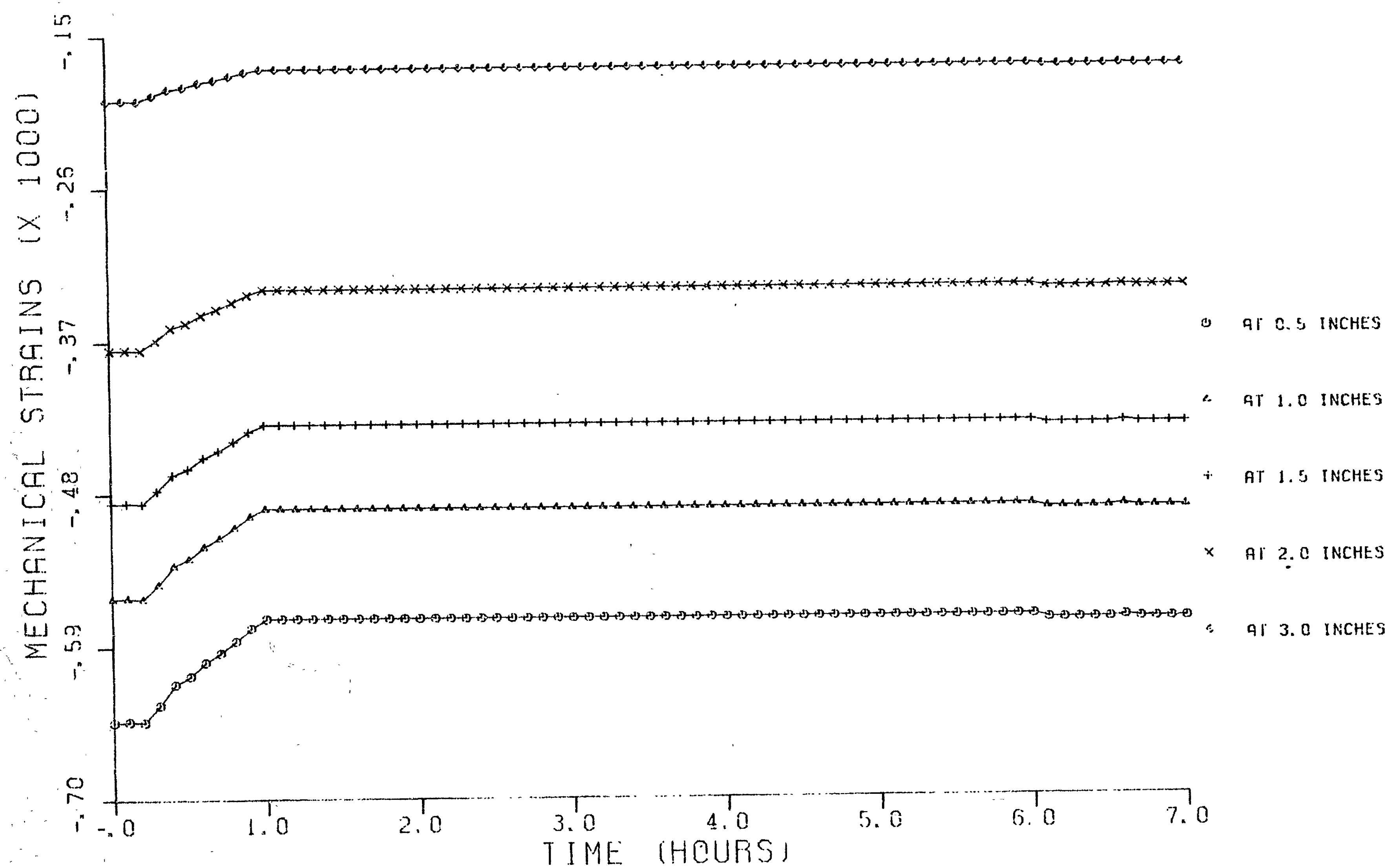

Figure 7.32 : Mechanical strains during stress relieving at 500°F, as predicted by the one-dimensional program

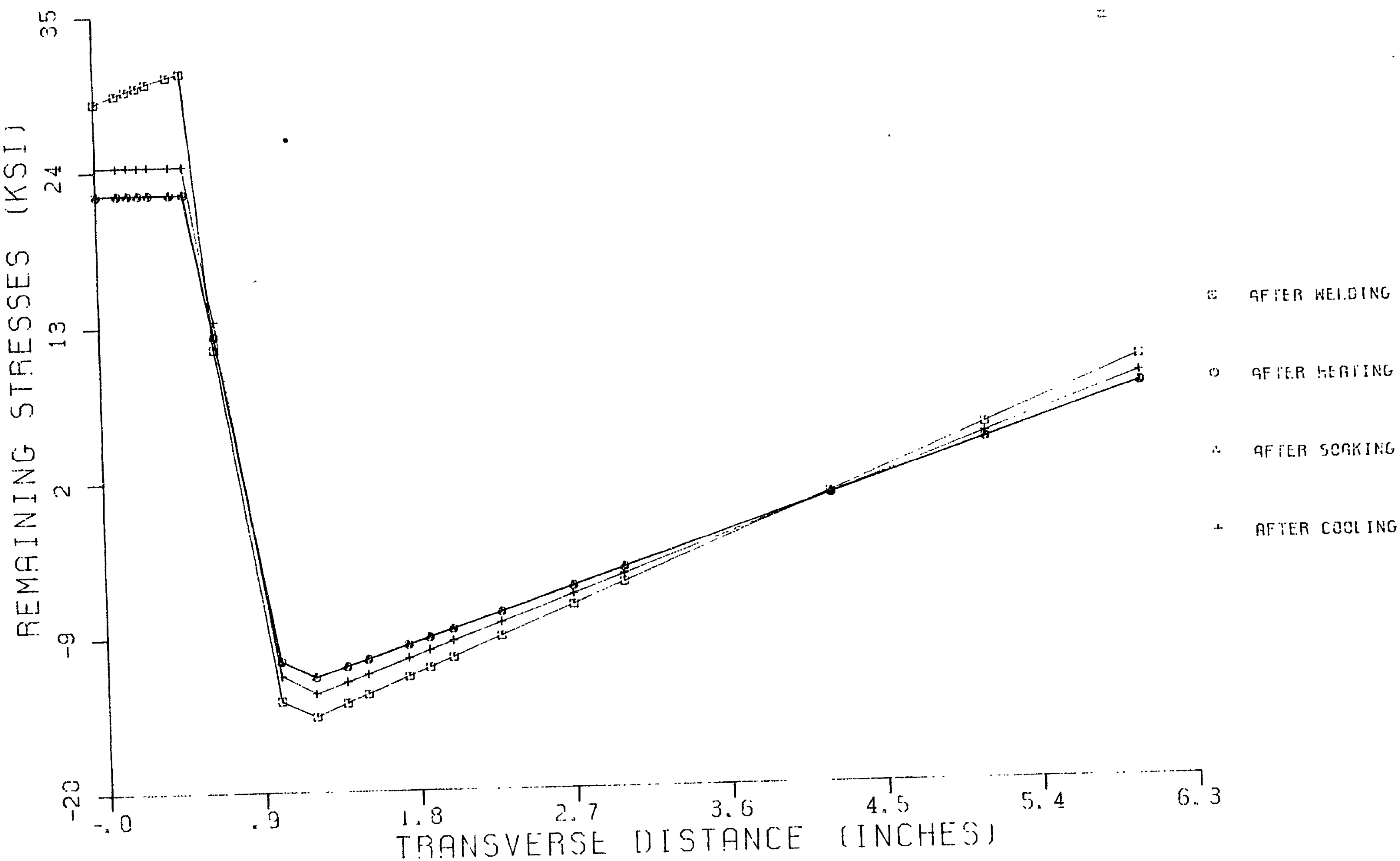

Figure 7.33 : Comparison of residual stresses before, during and after stress relieving at 500°F, as predicted by the one-dimensional program

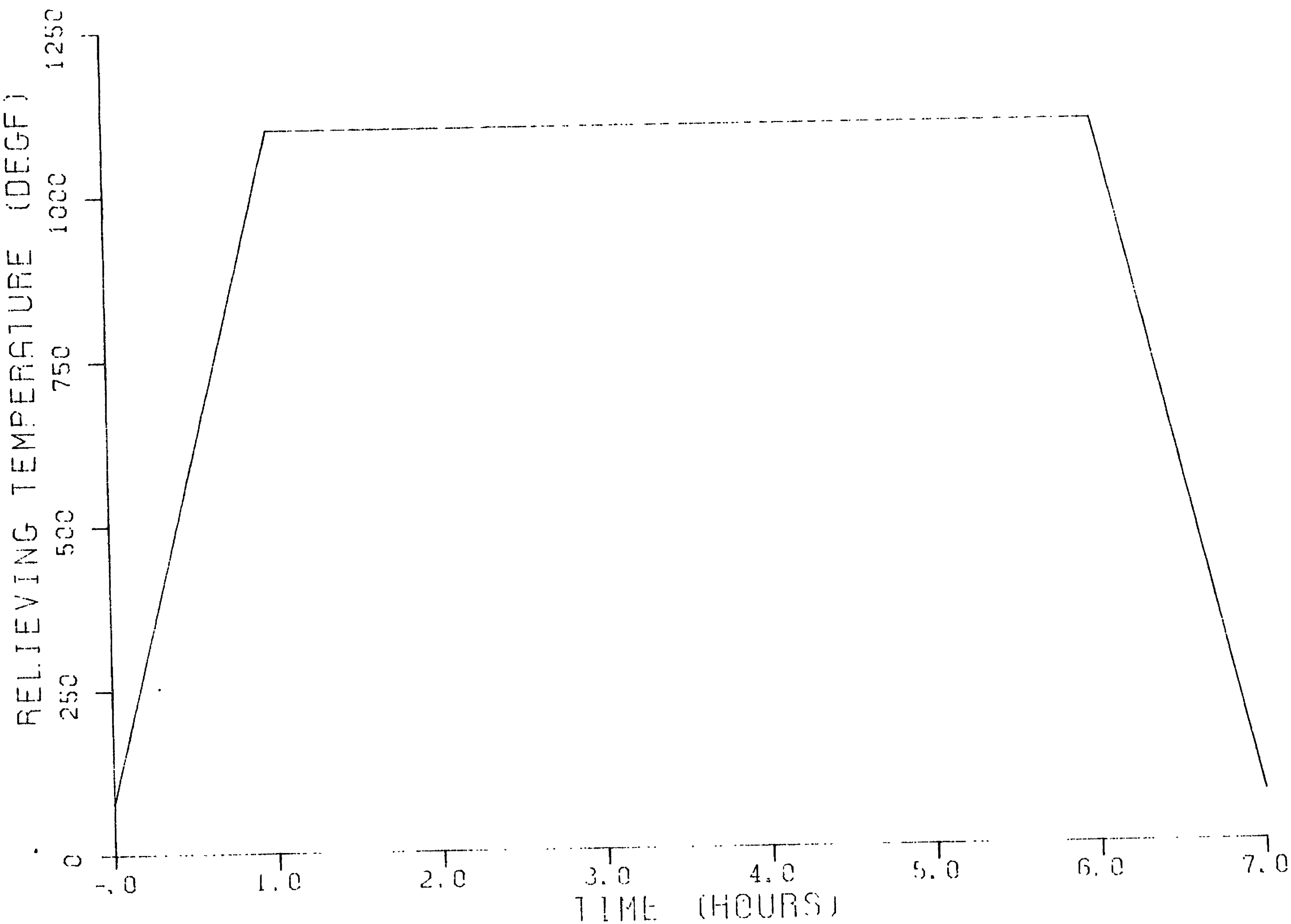

Figure 7.34 : Temperatures during stress relieving at 1100^{O}F

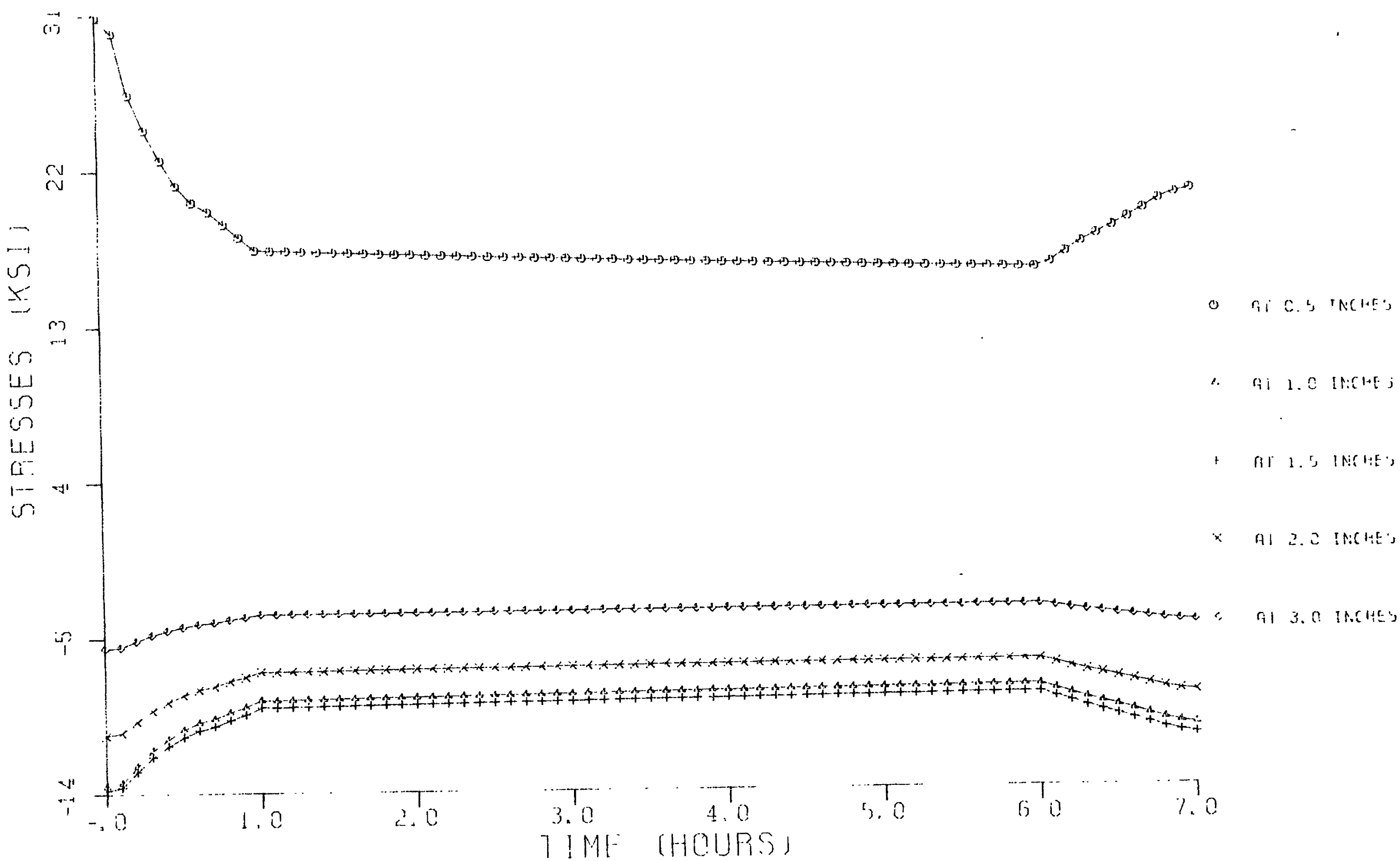

Figure 7.35 : Stresses during stress relieving at 1100^{o}F, as predicted by the one dimensional program

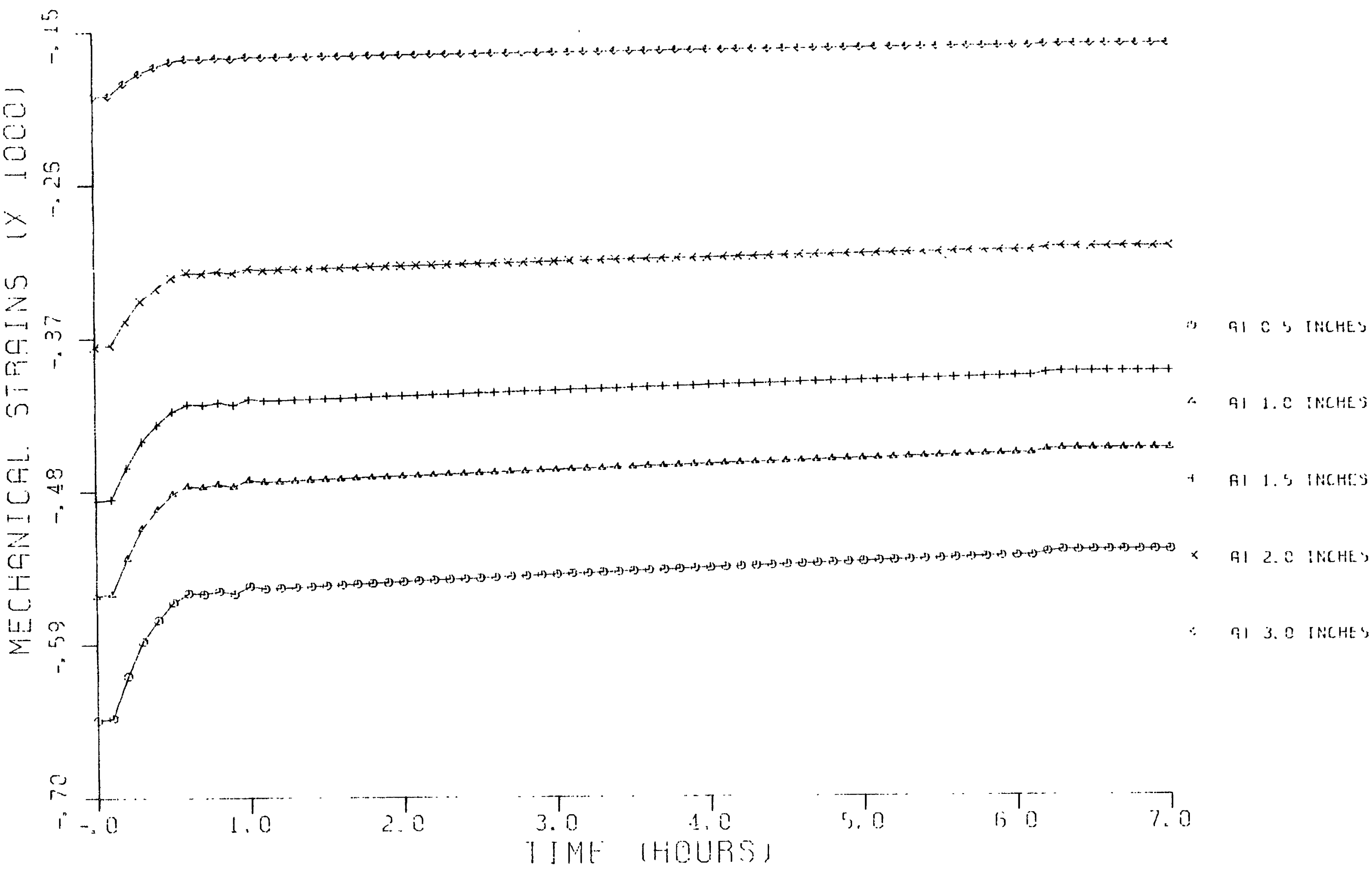

Figure 7.36 : Mechanical strains during stress relieving at 1100^{o}F, as predicted by the one-dimensional program

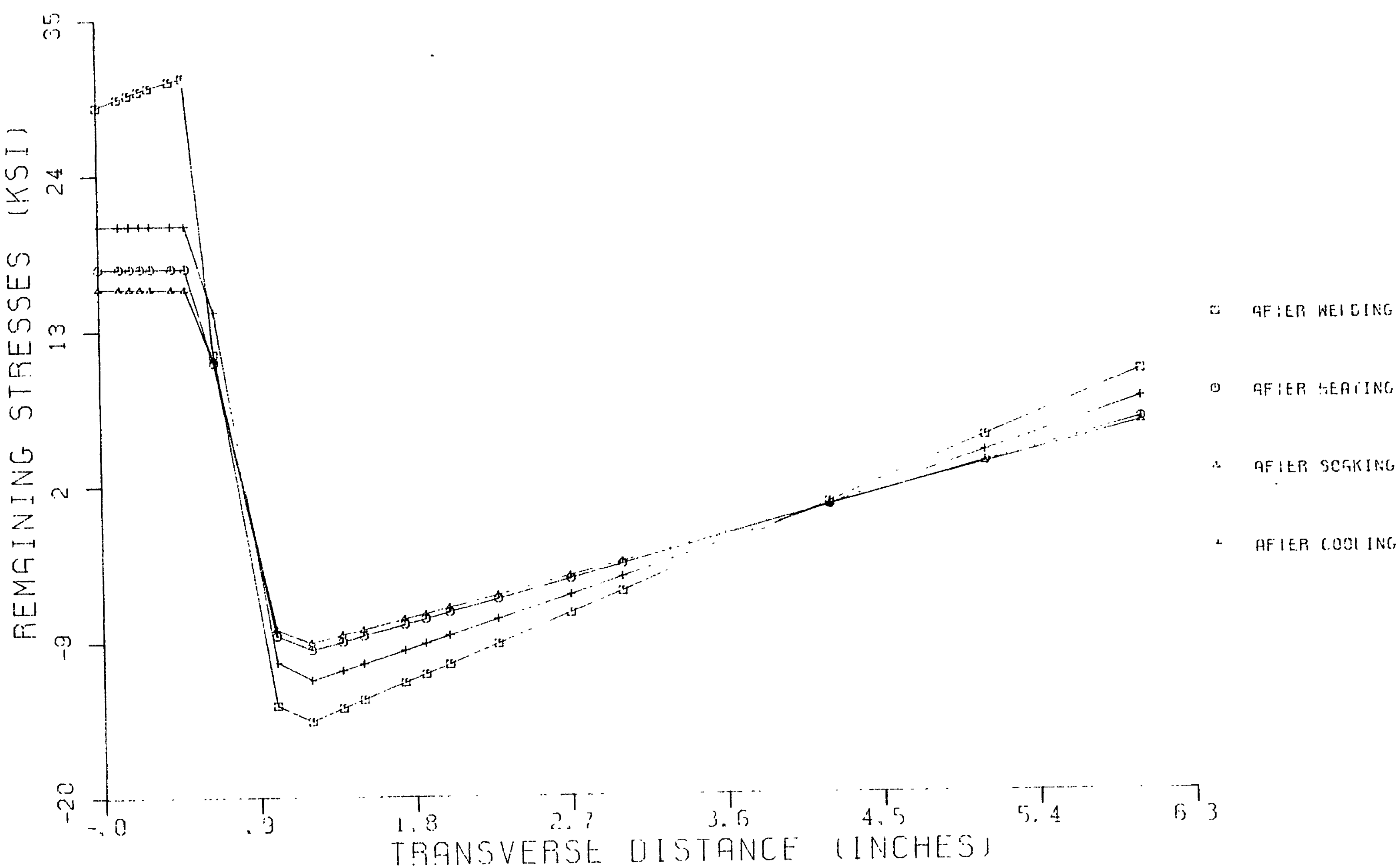

Figure 7.37 : Comparison of residual stresses before, during and after stress relieving at 1100°F as predicted by the one-dimensional program

7.3 Conclusions and Recommendations for Future Research

As evidenced in the previous sections, the correlation between the experimental results and the predictions of the one-dimensional model for temperatures strains and stresses during welding and subsequent stress relieving is quite good. However there exist a number of possibilities for further improvements, extensions and modifications:

(a) Further sensitivity analysis should be performed to investigate the effect of parameter variation on the model performance. Specifically, for example, it was noticed that small changes of the surface heat loss coefficient drastically affect the cooling rates. Furthermore the arc efficiency which is strongly dependend on the type of welding process, directly determines the heat input to the weld and thus the maximum temperatures attained.

(b) It is rather a straight forward procedure to modify the computer code so as it can accept any temperature history (as long as the temperature distribution is uniform over the specimen at any given time instant). However, it should be slightly more difficult to analyze the stress relaxation during localized heat treatments. Heat flow analysis - similar to the welding case - should be performed in the case of flame heating for example. As soon as the temperature distribution and history is known, however, the general stress analysis presented in chapter V is directly applicable.

(c) If the assumptions, on which the development of the one-dimensional model was based, are not any longer satisfied two - or three - dimensional heat flow and stress analyses should be performed. A finite element model should then most possibly be appropriate. This would be the case for the localized heating of a thick plate or a pipe for example.

(d) Direct application of the developed model to the case of high strength steels, and HY-130 in particular, was prevented due to the lack of comprehensive creep data for these materials. The available information is summarised in Appendix A.

Stress relieving experiments on HY-130 (both uniform and flame heating) are, however, currently performed at M.I.T. and will be described in [128].

(e) The underlying objective of this part of the study was to analyze the effectiveness of the various stress relieving heat treatments and to identify possible improvements. However, it is also hoped that it is one step towards the development of a rational procedure for the selection of optimal stress relieving treatments that would give maximum residual stress relaxation with minimal effects on the integrity of the welded structure.

PART IV

ECONOMIC ANALYSIS

CHAPTER VIII

ECONOMIC ASPECTS OF WELDING

8.1 Introduction

In a construction industry ,such as shipbuilding,welding operations can account for 10 to 20% of the total fabrication time and welding departments usually employ more than 10% of the total labor force. These relatively high percentages can only dictate efforts towards cost reductions and/or productivity increases in the welding sector.

The introduction of high deposition rate processes ,such as submerged arc or electroslag welding , together with special procedures ,such as one sided welding or narrow gap welding were some initial steps towards increased productivity and efficiency. These developments should certainly be viewed as coupled to the major advancements in production technology that occured during the past few decades ,such as rationalization of facilities and layout ,prefabrication of large units ,introduction of numerical control etc..

Nevertheless , the construction industry ,and especially shipbuilding was very slow to adopt,in large scale production, the recent advances in high energy processes (Electron Beam and Laser Welding) ,automation and robotics ,that would certainly boost productivity.This reluctance should be attributed to the low technology nature of the construction industry , the large investments necessary and the bad market conditions of 1970's , as well as to the technical difficulties of implementation.

When assessing the advantages of a new welding process or procedure,however, it is necessary to be able to estimate comparative costs savings and productivity increases.Further, the welding costs must be accurately determined since they represent a part of the total product or job costs, and as such are necessary in price setting and bidding.

The next sections of this chapter deal with the determination of welding costs and the factors that affect them.

8.2 The Elements of Welding Cost

The costing of welds and weldments should be done according to generally accepted accounting principles and must fit into the cost accounting practices of a particular company or activity.In general, however, the cost of welding, and any other industrial process as well, includes the cost of direct materials and direct labor and a fair share of the indirect production costs (overhead costs).

The direct material costs include the costs of filler metals, shielding gas, fluxes and other miscellaneous materials (e.g. guide tubes in consumable guide electroslag welding or ferrules and studs in arc stud welding) directly consumed in the welding process. The basis for the determination of material costs is usually the ammount of weld metal that must be deposited to produce the welded joint. In autogenous welding, where no filler metal is deposited the total weld length is used for the same purpose.

The direct labor costs are the ones that can be directly traced or related to welding operations. The basis for labor costing is time (time per weld, or time per unit length or time to weld a part). When a time-rate wage system is used the time directly translates to labor costs. When another wage system is employed, as payment by results for example, again labor costs can be related to time per part or to parts welded per unit of time. In the determination of time the most relevant parameters are the rate of depositing weld metal and welding speed.

Overhead costs include all the indirect production costs such as indirect labor (supervisors janitors, inspectors, toolroom personel, timekeepers),indirect material costs and such services as heating, lighting, power, maintenance, depreciation, taxes and insurance related to assets used in the fabrication process. Additionally distirbution costs (marketing and selling) and general and administrative costs also are included in the full cost of a welded product. The basis for allocating these overhead costs varies depending on the practices of the company and the nature of the cost. Usually these costs are prorated according to the direct labor involved in fabricating the part, using a predetermined overhead rate. Extensive discussion of this subject can be found in the varions cost accounting texts, [129],[130].

At this point, it should be emphasized that the cost of a specific weld is not necessarily the only cost that must be determined to establish the cost of a weldment.The latter includes the cost of the weld and also the material required for the weldment, the preparation of the parts prior to welding, and the postweld treatment that might be required. Joint preparation varies according to the material thickness and to joint design. Also some processes, such as electroslag and electrogas welding,require less accurate fit up and preparation than others. Postweld treatment includes final machining grinding and polishing, heat treating, shot blasting and possibly straightening.Some processes and some materials require more (or less) postweld treatment which influences the total cost of the weld and the weldment.

Although detailed analysis of the elements of welding cost and the factors influencing them, will be presented in the next few sections, some general comments are due here. Specifically it should be noted that field welding costs more than shop welding and welding in the horizontal,vertical, or overhead positions cost more than welding in the flat positions.Further, the local working conditions, availability of equipment, experience and skill of the welders, local power rates, special code requirements, weather and temperature conditions and industrial regulations might drastically affect the costs as well.

8.3 Material Costs

8.3.1 Weld Metal Requirements

For processes where filler metal is deposited, the basis for the calculation of the material cost is the amount of weld metal deposited in the joint. The latter can be estimated if the cross sectional area of the deposit, the length of the weld and the density of the weld metal are known.

Specifically:

$$(W.D.)=(C.S.A).(S.W.).(R.F.).a \qquad (8-1)$$

WELD	DESIGN	FORMULA FOR CROSS SECTION AREA
SINGLE V	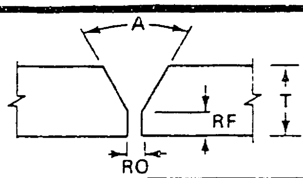	$CSA = (T - RF)^2 \tan\left(\frac{A}{2}\right) + RO \times T$
DOUBLE V	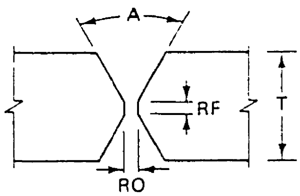	$CSA = 1/2(T - RF)^2 \tan\left(\frac{A}{2}\right) + RO \times T$
SINGLE BEVEL	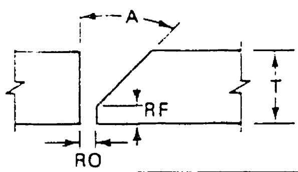	$CSA = 1/2(T - RF)^2 \tan A + RO \times T$
DOUBLE BEVEL	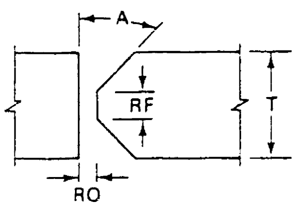	$CSA = 1/4(T - RF)^2 \tan A + RO \times T$
SINGLE U	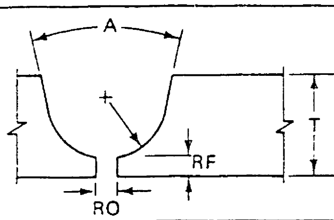	$CSA = (T - R - RF)^2 \tan\left(\frac{A}{2}\right) + 2R(T - R - RF) + 1/2\pi R^2 + RO \times T$
DOUBLE U	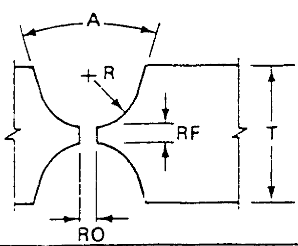	$CSA = 1/2(T - 2R - RF)^2 \tan\left(\frac{A}{2}\right) + 2R(T - 2R - RF) + \pi R^2 + RO \times T$
SINGLE J	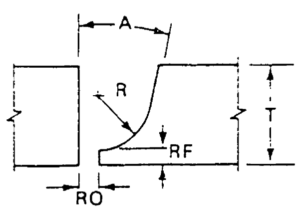	$CSA = 1/2(T - R - RF)^2 \tan(A + R)(T - R - RF) + 1/4\pi R^2 + RO \times T$
DOUBLE J	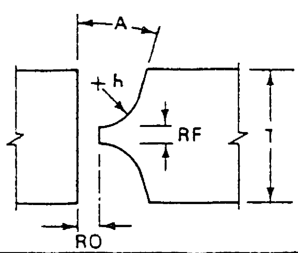	$CSA = 1/4(T - 2R - RF)^2 \tan(A + R)(T - 2R - RF) + 1/2\pi R^2 + RO \times T$

Figure 8.1 : Cross sectional areas for various designs

where: W.D. = Weight of deposit per unit length (lb/ft)

C.S.A.= Cross-sectional area (in^2)

S.W. = Specific weight of weld metal (lb/in^2)

R.F. = Reinforcement factor

a = Constant (12 for the units used)

The cross-sectional area can be calculated using straight forward geometric formulas if the exact joint preparation is known. Some cases are shown in figure 8.1 but more detailed tables can be found in the bibliography, [131].

The reinforcement factor has to be added to account for the fact that the weld surface will not be flush. A value of reinforcement of 10% is usually added to single groove welds and of 20% to double groove ones.10% reinforcement is also added to fillet welds.

The equation (8-1) can be readily applied in the comparison of the material costs of various weld designs. However for more accurate calculations, test welds must be performed.

8.3.2 Filler Metal

The weight of the filler metal required is greater than the weight of the weld metal deposit. This is due to a loss of filler metal through spatter and slag formation and due to the unused electrode stub.The ammount of this loss is accounted for by the deposition efficiency factor which is also called filler metal yield or recovery rate, and is the ratio of the weight of the deposited weld metal devided by the gross weight of the filler metal used.

Specifically the filler metal cost per unit length of weld seam deposited, C_{FM} , is

$$C_{(FM)} = \frac{(W.D)}{(Y_{FM}\%)} P_{FM} \text{ (in \$/ft)} \quad (8\text{-}2)$$

where:

$W.D$ = Weight of deposit per unit seam length (lb/ft)

$Y_{FM}\%$ = Filler metal yield (%)

P_{FM} = Price of filler metal per unit of weight ($/lb)

Filler metal yield varies with the process as can be seen in Table 8.1. The covered electrodes have the lowest yield of 55% to 75% due to a 7% to 15% end stub loss, 10% to 50% coating or slag loss and a 5% to 10% spatter loss. End losses are minimized when using continuous electrode wire where the scrap end weight is usually negligible compared to the total weight of the coil. Further the spatter loss is eliminated in submerged arc welding resulting in a 100% yield. In flux cored electrodes the deposition efficiency decrease to 75% or 85% due to the flux which is consumed and lost as slag.

An alternative way of calculating the cost of filler metal per unit length, C_{EL}, using short electrodes is based on the number of electrodes needed to produce a unit of weight of weld deposit, B (electrodes/lb), and the price per electrode, P_{EL} ($/electrode).

$$C_{EL} = (W.D) \cdot B \cdot P_{EL} \quad \text{(in \$/ft)} \quad (8\text{-}3)$$

For the case of continuous wire processes another approach can also be followed. Specifically the weight of filler metal required per hour is given by :

Electrode Type and Process	Yield %
Covered Electrode for:	
SMAW 14" manual	55 to 65%
SMAW 18" manual	60 to 70%
SMAW 28" automatic	65 to 75%
Solid Bare electrode for:	
Submerged arc	95 to 100%
Electroslag	95 to 100%
Gas metal arc welding	90 to 95%
Tubular-flux cored electrode for:	
Flux cored arc welding	80 to 85%

Table 8.1 Filler metal yield-various types of electrodes

$$w_{FM} = \frac{V_{WF} \cdot a}{L_W} \quad \text{(in lb/hr)} \tag{8-4}$$

where: V_{WF} = the wire feed speed (in/min)

L_W = the length of wire per unit of weight (in/lb)

a = constant (60 for the units used)

The wire feed speed can be determined from charts, supplied by the wire feeder manufacturer, that relate the welding current to wire feed speed, depending on the size and composition of the electrode wire, the welding process and the molten metal transfer mode such a chart is shown in figure 8-2, adapted from [116].The length per unit of wire weight is a physical property of the material and given in table 8-2 as a function of the were diameter and type.

The weight of filler metal required per unit length of seam welded, W_{FM} ,can now be calculated:

$$W_{FM} = \frac{w_{FM}}{V_{WT} \cdot a} \quad \text{(in lb/ft)} \tag{8-5}$$

where: V_{WT} = the weld travel speed (in/min)

a = constant (60 for the units used)

8.3.3 Flux Requirements

The cost of flux in submerged arc,electroslag or oxy-fuel gas welding can be related to the weight of weld metal deposited and may be calculated as:

$$C_{FLX} = P_{FLX} \cdot (W.D.) \cdot R_{FLX} \tag{8-6}$$

where : C_{FLX} = The cost of flux per unit weld seam deposited ($/ft)

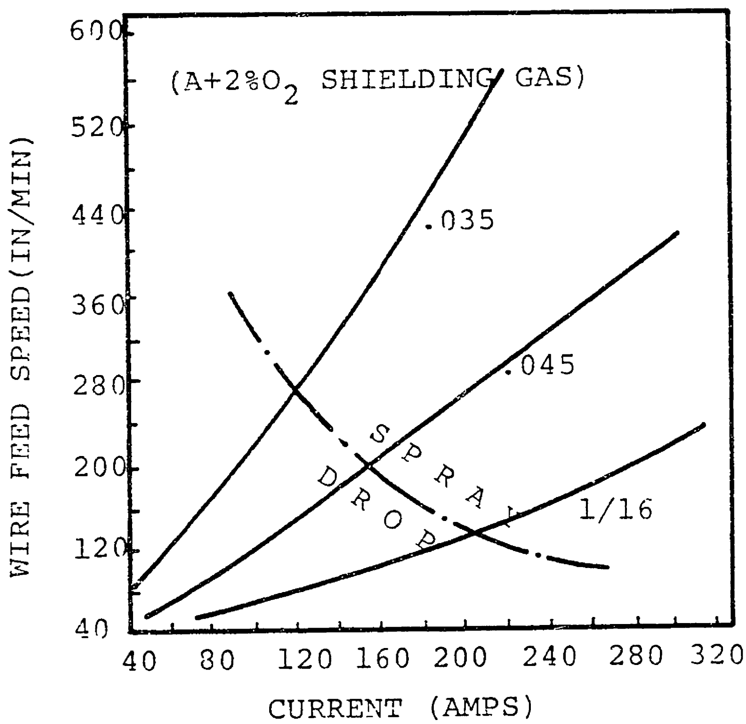

Figure 8-2: Wire feed speed vs current for stainless steel wires [116]

WIRE DIAMETER		MATERIAL								
Decimal Inches	Fraction Inches	Aluminum	Alum.10% Bronze	Silicon Bronze	Copper (deox)	Copper Nickel	Magnesium	Nickel	Steel, Mild	Steel, Stainless
0.020		32400	11600	10300	9800	9950	50500	9900	11100	10950
0.025		22300	7960	7100	6750	6820	34700	6820	7680	7550
0.030		14420	5150	4600	4360	4430	22400	4400	4960	4880
0.035		10600	3780	3380	3200	3260	16500	3240	3650	3590
0.040		8120	2900	2580	2450	2490	12600	2480	2790	2750
0.045	3/64	6410	2290	2040	1940	1970	9990	1960	2210	2170
0.062	1/16	3382	1120	1070	1020	1040	5270	1030	1160	1140
0.078	5/64	2120	756	675	640	650	3300	647	730	718
0.093	3/32	1510	538	510	455	462	2350	460	519	510
0.125	1/8	825	295	263	249	253	1280	252	284	279
0.156	5/32	530	189	169	160	163	825	162	182	179
0.187	3/16	377	134	120	114	116	584	115	130	127
0.250	1/4	206	74	66	62	64	320	63	71	70

Table 8-2 : Length vs weight (inches per pound) of bare electrode wire of type and size shown.

P_{FLX} = The price of flux per unit weight ($/lb)

R_{FLX} = The flux-to-steel weight ratio

The flux ratio varies with the process and the flux used, being approximately 1.0 for submerged arc welding and 0.05 to 0.1 for electroslag or oxy-fuel gas welding processes.

8.3.4 Shielding Gas Requirements

The cost of shielding gas is directly related to the time required to make the weld and the specified flow rate ,$V_{S.G.}$ Specifically:

$$C_{SG} = \frac{P_{SG} \cdot V_{SG}}{V_{WT} \cdot 5} \tag{8-7}$$

where : C_{SG} = The cost of gas per unit length of weld ($/ft)

P_{SG} = The price of gas ($/ft^3)

V_{WT} = The weld travel speed (in/min)

V_{SG} = The gas flow rate (ft^3/hr)

Slightly different formulas should be employed when using CO_2 gas which is marketed in liquid form and sold per unit weight, or when calculating the total cost of shielding gas per weld.

8.4 Labor Costs

Welding, and particularly manual welding is a highly labor intensive manufacturing process. The cost of labor is probably the single greatest conponent in the total welding cost. The basis for the determination of labor costs is generally the time required to make a weld or a weldment.

Various wage systems are employed in production processes today but we can in general distinguish between the flat hourly wage and the productivity, or incentives related, wage systems.

Table 8-3 : Suitable wage systems for welding

Sector	Nature of work	Supervision	Wage system
Shipbuilding, steel construction	Long or numerous welds of the normal type	Foremen, inspectors	Piecework by length
Construction of machines and apparatus	Series of small workpieces always with equal welds	Foremen, inspectors	Piecework by no of pieces or bonus per piece
Container construction	Pressure tanks	Welding engineer, NDT inspection, X-ray tests	Flat rate with wage allowance
Car and vehicle construction	Series, car frames	Foremen, inspectors	Piecework by no of pieces
Construction of apparatus for the chemical industry	Corrosion-resistant joints	Welding engineer, all kinds of tests, ultrasonics, X-ray, crack and halogen tests	Flat rate with wage allowance
Pressure tanks, bridge building	Highly refractory steel, fine-grain steel, preheating of butt welds	Welding engineer, X-ray and crack tests	Productivity wage, flat rate with wage allowance
All sectors	Straightening	Foreman	Flat rate with wage allowance
All sectors	Tacking, one-off production	Foreman	As for assembly line workers, flat rate with wage allowance
All sectors	Tacking, series	Foreman	Piecework by no of pieces or workpiece bonus

Detailed discussion on these systems can be found in [132] and [133] Table 8-3 lists suitable wage systems for various sectors of the fabrication industry together with some information on the nature of the work.

Only the time rate systems will be examined in this section however. Specifically for a single-pass weld or for Gas Tungsten Arc or Plasma Arc welding processes where weld metal is not deposited the labor costs per unit length of seam welded arc (in $/ft).

$$C_L = \frac{P_W}{V_{WT} \cdot (OF) \cdot a} \qquad (8\text{-}8)$$

where: P_W = The welder pay rate (in $/hr)

V_{WT} = The weld travel speed (in in./min)

OF = The operator factor (%)

a = Constant (5 for the units used)

The welder pay rate may, or may not, include fringe benefits (as cost of insurance,holidays, vacations etc) and should be determined according to the accounting practices of the company or activity.

The weld travel speed is known from the welding procedure schedule . Finally the operator factor , or arcing factor, is the same as duty cycle, that is the percentage of arc time against the total allowed or paid time . Specifically

$$OF = \frac{t_{arc}}{t_{arc} + t_{idle} + t_{electrode\ change} + t_{movement}} \qquad (8\text{-}9)$$

As can be seen from figure 8-3 operator factors vary considerably depending on the nature of the process, arrangement of the work use of fixtures and positioners, and also on the location (field or shop).

When the welding procedure schedule is not available or when welding involves more than one pass the following equation should be used for the labor cost per unit length of weld deposited (in \$/ft).

$$C_L = \frac{P_W \cdot (W.D.)}{(D.R.) \cdot (O.F.)} \qquad (8\text{-}10)$$

where : P_W = The welder pay rate (\$/hr)

W.D.= The weight of weld metal deposited per unit length (lb/ft)

D.R.= The deposition rate (lb/hr)

The deposition rate expresses the weight of filler metal deposited in a unit of time and can be calculated as:

$$D.R. = \frac{V_{WF} \cdot a}{L_W \cdot Y_{FM}} \quad (lb/hr) \qquad (8\text{-}11)$$

where : V_{WF} = The wire feed rate or melt off rate (in./min)

L_W = The length of electrode per unit weight (in./lb) (table 8-2)

Y_{FM} = The filler metal yield (%)

a = Constant (60 for the units used)

Deposition rates for various processes are given in figure 8.4, plotted versus weld current. Accurate calculation however requires some test welds to be performed.

8.5 Power and Overhead Costs

Electric power cost is usually considered as a part of

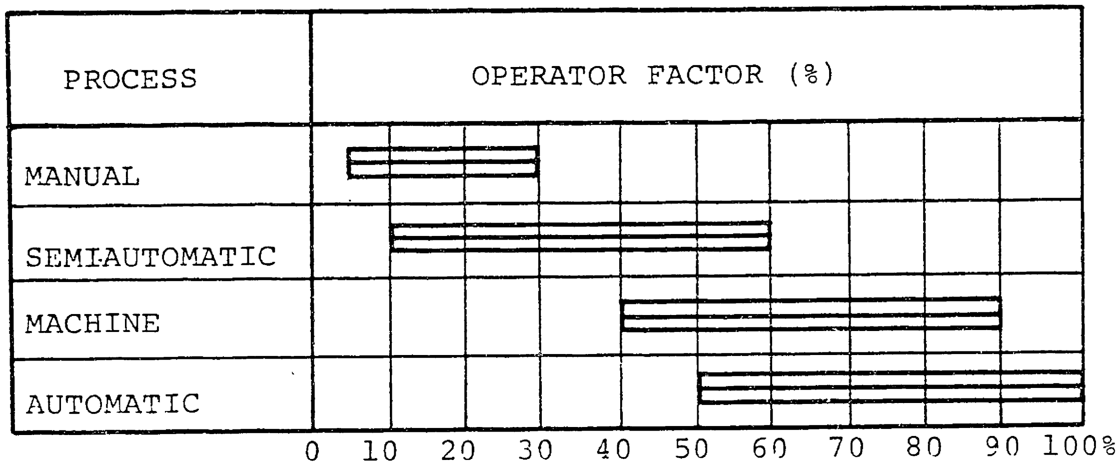

Figure 8-3 : Operator factor for various processes

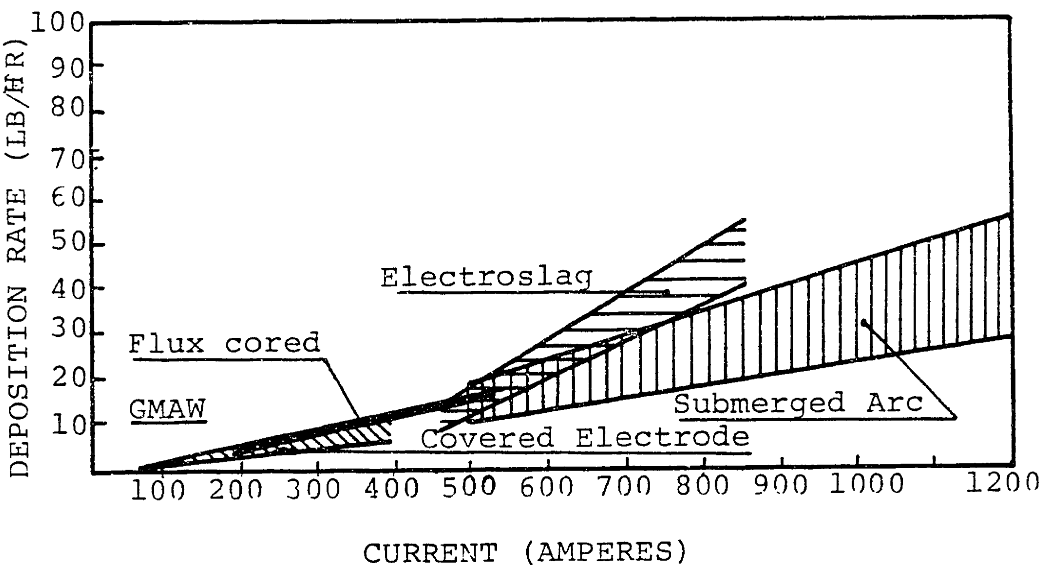

Figure 8-4 : Deposition rate vs current for various processes overhead expense. Specifically for welding, however, it is sometimes considered a direct cost and is charged against the particular job. In such a case the following equation should be used for the cost of electric power per unit length of seam welded: (in $/ft).

$$C_{EP} = \frac{P_{EP} \cdot V \cdot I \cdot (W.D.)}{(D.R.) \cdot (O.F.) \cdot n_{PS} \cdot a} \qquad (8\text{-}12)$$

where : P_{EP} = The local power rate ($/kwh)

V, I = The welding voltage and current

(W.D.) = The weight of weld metal deposited per unit length (lb/ft)

(D.R.) = The deposition rate (lb/hr)

(O.F.) = The operator factor (%)

n_{PS} = The power source efficiency (%)

a = Constant (1000 for the units used)

The power source efficiency varies with the equipment size and quality and is approximately as follows: [134]

d.c. welding generators	45-60%
a.c. welding generators	65-70%
welding rectifier	65-75%
welding transformers	75-85%

Overhead costs include as was already mentioned all the costs that cannot be directly charged to the individual job or weldment. These costs are allocated pro rata among all work going through the plant. If the overhead rate is known (in $/hr) then the total overhead cost per unit length of weld seam can be calculated from equation (8-8),for single pass welding, or equation (8-10),for multipass welding, with the overhead rate substituted for the welder pay rate.

8.6 Conclusions

The previous sections of this chapter focused on the calculation of the various elements of welding costs. The methods described should be used in order to compare different welding processes or procedures in terms of cost or efficiency. However, it should be noted that, as in all the cases of alternate choice decisions, only the costs that are actually different in the two alternatives should be taken into account. This is particularly true for the components of overhead costs, which do not always vary proportionally with direct labor costs, as the use of a standard overhead rate might superficially suggest.

Cost evaluation of the weld joint designs and the welding procedures should always be made, since weld metal is usually the most expensive metal involved in steel fabrication. The various possibilities for cost reductions are briefly highlighted in the next chapter.

CHAPTER IX

COST REDUCTIONS REALIZABLE THROUGH WELD METAL STRENGTH UNDERMATCHING

9.1 Introduction - Possibilities for Cost Reductions

As was mentioned in the previous chapter welding is a sector of the construction industry, where a small percentage of cost reduction or productivity improvement represents a significant overall cost saving. This is mainly due to the fact that welding is a highly labor intensive process.

Cost reductions can be realized in various ways. Some general guidelines that could be followed are:

(a) Eliminate welded joints whenever possible substituting them with rolled sections, formed plates, or small castings.

(b) Limit field welding by prefabricating larger units in the shop.

(c) Reduce the cross sectional area of welds, utilizing smaller root openings, smaller groove angles and double-instead of single-groove preparations.

(d) Utilize fillet welds with causion, since doubling their size and strength results in quadrapling their weight.

(e) Use positioners and fixtures to limit the extent of overhead or vertical welding that must be performed.

(f) Modify the design to permit easy accessibility to all welds.

(g) Reduce labor costs by utilizing, whenever applicable semi- or fully-automated welding processes and or welding robots.

(h) Limit the number of electrodes that should be used in the fabrication of a part.

(i) Avoid complex preparations or post welding treatments selecting proper weld and base metal combinations.

Particularirly for high strength steels, however, the existing specifications require preheat and interpass temperature controls, electrode controls and post weld magnetic particle testing that unavoidably result in increased fabrication costs. Most of these requirements are results of the well established philosophy of weld metal strength overmatching. However, as was shown by various investigators, whose work was presented in chapter II , some of these requirements can be relaxed, or eliminated, when a lower yield strength filler metal is used in conjuction with a lower hydrogen process.

A more detailed analysis of the possibilities for cost reductions in the fabrication of HY-80 steel, through weld metal strength undermatching, will be presented in the next few sections of this chapter.

9.2 Preheating and Preheat Control

9.2.1 Existing Preheating Requirements for HY-80 steels

The reason for preheating in HY-steels systems is to reduce cracking. It is generally believed that preheating results in slower cooling rates and thus permits greater quantities of hydrogen to diffuse from the weld zone. Additionally, the more uniform cooling results in lower thermal stresses and thus reduces the likelihood of cracking.

The existing preheat requirements when welding HY-80 steels are summarized in table 9-1. Lower preheating temperatures are accepted for thinner sections since the diffusion path is

THICKNESS	PREHEAT/INTERPASS MINIMUM			PREHEAT/INTERPASS MAXIMUM
	MIL-11018	MIL-9018 Gas Metal Arc Sub arc	Austenitic Electrodes(1)	All Electrodes
1 1/8" and over	200°F	150°F	125°F	300°F
From 1 1/8" to 1/2"	125°F	150°F	125°F	300°F
1/2" and less	60°F	60°F	60°F	300°F

(1) Post weld NDT is not required when using austenitic electrodes

Table 9-1: HY-80 Preheat requirements

reduced and the level of restraint is lowered. Also lower levels of preheat are permitted when welding with lower yield strength electrodes (MIL-9018) and lower hydrogen processes (G.M.A. and submerged arc welding). As was mentioned in earlier chapters, lower yield strength electrodes would result in lower residual stresses. Therefore, since hydrogen cracking is directly related to the level of imposed or residual stresses, the use of lower yield-strength filler metal should effectively reduce cracking.Therefore a corresponding reduction in preheat should be tolerated. Further it should then be possible even to eliminate preheat for certain combinations of material thicknesses and joint designs. This is where substantial savings would result, as will be analyzed in the next section.

9.2.2 Cost Reductions Realizable Through the Elimination of Preheat

The cost of preheating is the single most significant factor contributing to the higher cost of fabricating HY-80 steel structures . Thus the elimination of preheating, even in some cases only, would substantially reduce fabrication costs. The simple reduction of the level of preheat would marginally reduce costs, however, since it would only lower the power consumption but would not affect other more significant cost elements.

Specifically the main elements of the preheating cost are the following:

(a) Capital cost of the necessary facilities, such as the central power station and switch gear.

(b) Cost of electric power for preheating, which largerly exceeds the power costs of the welding operations.

(c) Capital and replacement costs of the preheating devices, which have relatively short lifespan. The cost of the necessary temperature control devices would also be included here.

(d) The direct labor costs of applying and supervising the heating operation.

Additionally the preheating operation increases the fabrication costs through:

(a) Reduced productivity due to the high temperature environment in which the welders would have to work. Temperatures between 200^{o}F and 300^{o}F are usually specified making it practicaly impossible to weld in a tight spot or an enclosed area.

(b) Scheduling problems due to the trades disruption caused by preheating. The areas being preheated are not accessible to other trades, when in high temperature.

(c) Delays in the outfitting phase caused when welding attachments to the basic HY-80 structures an operation which also requires preheating.

It should be emphasized again, at this point, that the simple reduction of the level of preheating in thick plate butt welds, possible when using lower strength electrodes, has only a minimal effect on the total cost. These welds are usually performed in open unrestricted areas, most often during prefabribation. Furthermore they only represent a small percentage of the total welding that must be performed.

There are, however, numerous attachments, brackets, stiffeners or foundations, usually made of a lower yield strength steel, which have to be welded on the basic HY-80 structures. It is believed that use of lower yield strength electrodes would permit the total elimination of preheating in these welds. Such an improvement would have a drastic effect on the total cost.

9.3 Electrode Selection and Moisture Controls

The existing specifications for electrode storage and handling require that electrodes should be baked after they are received from the manufacturer, and kept in special dry conditioners in order to ensure that their initial moisture level is minimal. Furthermore once issued they can only be exposed to the atmosphere for five hours and should then be rebaked.This results in issuing electrodes at least twice during the normal eight hour shift, a practice which certainly disrupts the work and reduces productivity.

Lower yield strength metals used in electrodes with special moisture resistant coatings were shown to permit exposure periods over the eight hour shift. This would certainly improve scheduling and productivity.

Additionally lower strength filler metal can permit the use of a single electrode (e.g. E 9018) for joining to HY-80 other steels of lower yield strength (35 to 55 ksi). This would alleviate the problem of having to identify the various materials during fabrication and to use a different electrode for each combination and therefore would certainly reduce the fabrication costs drastically.

The single electrode would undermatch HY-80, but would overmatch the lower yield strength attachments. This would cause no problem, however, since these steels do not have a microstructure sensitive to hydrogen cracking.

REFERENCES

1. K. Masubuchi, "Analysis of Welded Structures - Residual Stress and Distortion and their Consequences", Pergamon Press, Oxford/New York, 1980.

2. K. Masubuchi, "Materials for Ocean Engineering", M.I.T. Press, 1970.

3. W.S. Pellini, "Principles of Structural Integrity Technology", Office of Naval Research, Arlington, VA., 1976

4. K.J. Bathe, "A D I N A - A Finite Element Program for Automatic Dynamic Incremental Nonlinear Analysis", AVL Report No 82448-1, Mechanical Engineering Dept, M.I.T., Sept. 1975, (Revised December 1978).

5. K. Masubuchi, R.E. Monroe, and D.C. Martin, "Interpretive Report on Weld-Metal Toughness", Welding Research Council Bulletin No. 111, 1966.

6. P.M. Palermo , "A Designers View of Welding Requirements for Advanced Ship Structures", The Welding Journal, 55(12), 1039-1051, 1976.

7. O.A. Bakshi, and R.Z. Shron, "The Static Tensile Strength of Welded Joints with a Soft Interlayer", Svar. Proiz, (5), 6-10, 1962.

8. O.A. Bakshi, and R.Z. Shron, "The Problem of Gauging the Strength of Welded Joints in which there is a Soft Interlayer" Svar Proiz, (9), 11-14, 1962.

9. A.S. Gelman, and Kudrayavtzev, "The Effect of Mechanical non-uniformity on the Fatigue Strength of Welds", Svar Proiz, No. 11, 1964.

10. W. Soete, and R. Denys, "Strain Criteria for Butt Welds", Document No. X-774-75, Commission X of the International Institute of Welding, 1975.

11. "Study on Mechanical Behavior and Strength of Undermatched Weld Joints", Final Report of the Soft Joint Committee, Japan Welding Engineering Society, 1975 (in Japanese).

12. K. Satoh, and A. Nagai, "Fatigue Strength of Welded Bars Having a Hard or Soft Interlayer", Document No. XIII-530-69, Commission XIII, International Institute of Welding, 1969.

13. K. Satoh, and M. Toyoda, "Static Tensile Properties of Welded Joints Including Soft Interlayer", Trans. Japan Welding Society, Vol. 1 No. 1, 10-17, 1970.

14. K. Satoh, and M. Toyoda, "Static Strength of Welded Plates Including Soft Interlayer under Tension across a Weld Line", Trans. Japan Welding Society, Vol. 1, No. 2, 10-17, 1970.

15. K. Satoh, and M. Toyoda, "Mechanical Behaviors of Welded Plates Including a Soft Interlayer under Tension Parallel to the Weld Line", Trans. Japan Welding Society, Vol. 2, No. 1, 52-59, 1971.

16. J. Agapakis, K. Masubuchi, "Strength of Weldments in High Strength Steels, Input to the Committee on Effective Use of Weld Metal Yield Strength, National Materials Advisory Board, National Academy of Sciences, July 1980.

17. M. Yoshinaga and A. Nakamura,"Welding Technique", No. 2, 1964, pp.18-26.

18. N. Hasamitsu et. al. Summary of lecture, Journal of Japan Welding Society, 5, 1970.

19. K. Satoh, and M. Toyoda, "Effect of Mechanical Heterogeneity on the Static Tensile Strength of Welded Joints", Journal of Japan Welding Society, Vol. 40, No. 9, 885-900, 1971. (in Japanese).

20. K. Satoh, M. Toyoda, E. Fujii, "Tensile Behaviors and Strength of Soft Welded Joints", J. Society of Nav. Arch., Japan , 132, 381-393, 1972. (in Japanese).

21. K. Satoh, M. Toyoda, K. Ukita, T. Matsura, "Undermatching Electrode Applied to HT80 Heavy Plates for Penstock", The Welding Journal, 58(2), Research Supplement 25s-33s, 1979.

22. K. Satoh, M. Toyoda, K. Sakano, M. Toyosada, "Effect of Plastic Constraint on Brittle Fracture Initiation of Soft Welded Joints", Journal Soc. Nav. Arch. Japan, 132, 371-379, 1972 (in Japanese).

23. K. Satoh, and M. Toyoda, "Static Tensile and Brittle Fracture Strengths of Soft Welded Joints, Trans. of Journal of Welding Research Institute of Osaka University, Vol. 2, No. 1, 73-80, 1973.

24. K. Satoh, M. Toyoda, K. Arimochi, "Effect of Michanical Heterogeneity on Brittle Fracture Behaviors, J. Soc. Naval Arch. Japan, 134, 425-433, 1977 (in Japanese).

25. K. Masubuchi, "Thermal Stresses and Metal Movement during Welding Structural Materials, especially High Strength Steels", International Conference on Residual Stresses in Welded Construction and their Effects, London, November 15-17, 1977.

26. N. Yurioka, "Rational Approach to the Establishment of Acceptance levels of Heavy Weldments",M.S. Thesis at M.I.T. May 1972.

27. J.S. Hwang, "Residual Stresses in Weldments in High Strength Steels", M.S. Thesis at M.I.T., January 1976.

28. K. Satoh, and M. Toyoda, "Joint Strength of Heavy Plates with Lower Strength Weld Metal", The Welding Journal, 54(9), Research Supplement, 311-s to 319-s, 1975.

29. K. Satoh, M. Toyoda, K. Ukita, A. Nakamura, and T. Matsura, "Applicability of Undermatching Electrode to Circumferential Welded Joint of HT80 Penstock", Journal of Japan Welding Society, Vol. 47, No. 5, 283-288, 1978 (in Japanese).

30. K. Satoh, M. Toyoda, K. Ukita, A. Nakamura, and T. Matsura, "Prevention of Weld Crack in HT80 Heavy Plates with Undermatching Electrodes and its Application to Fabricating Penstock", Trans. Japan Welding Society, Vol. 9, No. 1, 1-5, April 1978.

31. N.N. Davidenkov, and N.I. Spiridonova, "Analysis of the State of Stress in the Neck of a Tension Specimen", Proc. A.S.T.M., 46, 1147-1158, 1946.

32. Bridgman, "Study of large plastic flow and fracture of solids",McGraw Hill.

33. K.J. Bathe, "Theory and Practice of Continuum Mechanics", Class Notes, Course 2.094, M.I.T., Spring 1980.

34. E. Macherauch, and H. Wohlfahrt, "Different Sources of Residual Stresses as a Result of Welding", Int'l Conf. on Residual Stresses in Welded Construction and their Effects, The Welding Institute, London, 1977, pp.267-282.

35. K. Masubuchi, and J. Agapakis, "Analysis and Control of Residual Stresses, Distortion and Their Consequences in Welded Structures", Trends in Welding Research in U.S., A.S.M. Conference, New Orleans, November 16-18, 1981.

36. V.J. Papazoglou, and K. Masubuchi, "Study of Residual Stresses and Distortion in Structural Weldments in High-Strength Steels", First Second and Third Technical Progress Reports under Contract No. N00014-75-0469 (M.I.T. OSP #82558) to the Office of Naval Research from M.I.T., 1979, 1980, and 1981.

37. V.J. Papazoglou, "Analytical Techniques for Determining Temperatures, Thermal Strains, and Residual Stresses during Welding", Ph.D. Thesis, M.I.T., 1981.

38. Society of Manufacturing Engineers, "Tool & Manufacturing Engineers Handbook", Third Edition, McGraw Hill Book Co, N.Y., 1976.

39. American Society for Metals "Metals Handbook", Volume 4, "Heat Freating, Ninth Edition, A.S.M., 1981.

40. F.M. Burdekin, "Heat Treatment of Welded Structures", Second Edition, The Welding Institute, 1969.

41. American Welding Society, "Local Heat Treatment of Welds in Piping and tubing",A.W.S. d10.10-75,A.W.S.,1975.

42. H.H.Muller,"Induction Heat Treating of Welds in Pipeline, Tank and Reactor Construction",International Institute of Welding Document X-863-77.

43. D.J. Cottrell, "An Examination of Postweld Heat Treatments", International Conference on Residual Stresses in Welded Construction and their Effects, London, 15-17 November 1977, pp. 195-208.

44. B. Cotterell, "Stress Relief of Butt Welds in Rectangular Plates by Local Heating", British Welding Journal, Vol. 9, May 1962, pp. 326-329.

45. F.M. Burdekin, "Local Stress Relief of Circumferential Butt welds in Cylinders", British Welding Journal, Vol. 10, September 1963, pp. 483-490.

46. E.G. Shifrin and M.I. Rich, "Effect of Heat Source Width in Local Heat Treatment of Piping", Welding Journal, Vol. 52, December 1973, pp. 792-799.

47. B. Cotterell, "Local Heat Treatment of Shperical Vessels", British Welding Journal, Vol. 10, March 1963, pp. 92-97.

48. S. Nicholson and J.C. Brook, "Review of Codes with Reference to Heat Treatment", Conference on the "Heat Treating Aspects of Metal Joining Processes", Iron and Steel Institute, London, December 1972, (IIW , Doc. X 680-72).

49. Working Group on Thermal Stress Relief, "Stress Relief Heat Treatments and Their Effect on Mechanical Properties of Welded Joints", Commission X, International Institute of Welding, Doc. X 707-73, March 1973.

50. Working Group on Thermal Stress Relief "Progress Report", IIW Doc. X 785-75.

51. Working Group in Thermal Stress Relief, "Final Report Desirability of Postweld Heat Treatments in Welded Construction", Commission X, IIW, Doc. X 913-78, February1979.

52. C.F. Meitzner, "Stress Relief Cracking in Steel Weldments", An Interpretive Report, Welding Research Council, Bulletin 211.

53. K. Kussmaul, D. Blind and J. Ewald, "Investigation Methods for the Detection and Study of Stress Relief Cracking", International Journal of Pressure Vessels and Piping ,No.(5) 1977, pp.159-180.

54. A. Dhooge, et al., "A Review of Work Related to Reheat Cracking in Nuclear Reactor Pressure Vessel Steels", International Journal of Pressure Vessels and Piping, No.(6) 1978, pp.329-409.

55. R.W. Nichols "Reheat Cracking in Welded Structures", Kyoto 1969, Joint Meeting of IIW Commissions IX and X, Doc. IX-665-69 and X-547-69.

56. A. Vinckier, "Progress Report of Working Group on Reheat Craching", University of Ghent, Belgium, 1971, IIW Doc. X-638-71.

57. A. Vinckier and A. Dhooge, "Susceptibility to Reheat Cracking of Nuclear Pressure Vessel Steels", Working Group on Reheat Cracking, Commission X, Tel-Aviv, July 1975, IIW Coc. X-791-75.

58. J. Kameda, H. Takahashi and M. Suzuki, "Residual Stress Relief and Local Embrittlement of Weld Heat Affected Zone in a Reactor Pressure Vessel Steel", Tohoku University, Japan, 1976, Doc. IX-1002-76 and X-800-76.

59. J.L. Ruge and W. Rabe, "Study on the Susceptibility to Stress. Relief Cracking of Low Alloy Steel Weldments by Means of Slow Tensile Tests and Creep Tests", Technische Universitaet Braunschweig, 1976, IIW Doc. X-803-76.

60. M. Velikonja, "The investigation of High Strength Structural Steel in Reference with Susceptibility to the Stress-Relief Embrittlement", IIW Annual Assembly, Bratislava 1979, IIW Doc. X-933-79.

61. H. Nakamura, T. Naiki, H. Okabayashi, "Stress Relief Cracking in Heat Affected Zone", Trans. Japan Welding Society, 1970, No. 2, p. 60-71 (Doc. IIW IX-648-69).

62. Y. Ito, and M. Nakanishi, "Study on Stress Relief Cracking in Welded low alloy steels", Doc. IIW X-668-72.

63. A.W. Dense,E.J. Galda and G.T. Powell, "Stress Relief Cracking in Pressure Vessel Steels", Welding Journal, August 1971, pp.374 s -378 s .

64. N.S.R.D.C. reports on "Stress Relief Embrittlement of AX-140 and E-11018 Weld Metals", and "Stress Relief Characteristics of a 5% Ni Weld Metal", obtained after private communication October 1981.

65. A.H. Rosenstein, "Phenomenological Investigations of Stress Relief Embrittlement, Welding Journal, March 1970, pp.122s-131s.

66. M.R. Cross and W.H. Asche, "Effect of Tempering on the Strength, Hardness and Notch Toughness of HY-130/150, 5Ni-Cr-Mo-V Steel",DDC. No. AD-630-464,March 1966.

67. G.G. Saunders, "V.S.R. a Current State-of-the-Art Apraisal", International Conference on Residual Stresses in Welded Construction and their effects, London, 15-17 November 1977.

68. R. Dawson and D.G. Moffat, "Vibratory Stress Relief. A Fundamental Study of its Effectiveness", Journal of Engineering Materials and Technology, April 1980, Vol.102, pp.169-176.

69. T. Brogden, "The Relieving of Stress by Vibration-a Critical Review of the Literature", Machine Tool Research, April 1969, pp.27-35.

70. R.T. McGoldrick and H.E. Saunders, "Some Experiments in Stress Relieving Castings and Welded Structures by Vibration" J.A.S.N.E., Vol. 55, 1943, No. 4, pp.589-609.

71. J.H.Buhler and H. Pfalzgraf, "Investigations Into the Reduction of Residual Welding Stresses by Alternating Stress Tests or Mechanical Vibration", Inst. of Machine Tools and Shaping Technology of the University, Hanover, Schweisse und Schreiden, Vol. 16, 1964, No. 5.

72. O.I. Zubehenko and A.A. Gruzd, "Vibrating Loads Used for Relieving the Residual Stresses in Welded Frames", Automatic Welding, 1974, No. 9, pp.64-66.

73. G.P. Wozney and G.R. Crawmer, "An Investigation of Vibrational Stress Relief in Steel", Welding Journal, September 1968, pp.411s-419s.

74. S. Weiss, G.S. Baker and R.D. Das Gupta, "Vibrational Residual Stress Relief in a Plain Carbon Steel Weldment", Welding Journal, February 1976, pp.47s-51s.

75. A.A. Kazimirov, et al, "The Mechanism of Reduction of Residual Stresses in the Pulsed Treatment of Welded Joints", Automatic Welding, 1974, No. 7, pp.39-43.

76. V.I. Makhnenko and N.I. Pivtorak, "Redistribution of

Residual Stresses in Welded Beams by Vibratory Treatment", Automatic Welding, 1978, No. 9, pp.28-31.

77. J. Mryka, "Static and Vibrational Stress Relief", International Institute of Welding Document X-858-77.

78. V.M. Sagalevich, et al., "Elininating Strains in Welded Beam Structures by Means of Vibrations", Welding Production, 1979, No. 9, pp.9-11.

79. D.L. Cheever and E.W. Rowlands, "Vibrational Stress Relief: The Answer to Dimensional Control?", Conference on Control of Distortion and Residual Stress in Weldments, A.S.M., November 1976.

80. Makhnenko, et al., "Calculation of the Efficiency of the Reduction in Residual Stresses in Annular Seams of Pipelines During Explosive Treatment", Automatic Welding, December 1975, pp.5-7

81. J.M. Fox, "An Overview of Intergranular Stress Corrosion Cracking in BWR's", Proceedings: Seminar on Countermeasures for Pipe Cracking in BWR's, EPRI WS-79-174, Vol. 1, May 1980.

82. R.M. Chrenko, "Thermal Modifications of Welding Residual Stresses", 28th Sagamore Army Material Research Conference, Lake Placid New York, 13-17 July 1981.

83. J.C. Lochhead, "Fabrication techniques to eliminate Postweld Heat Treatment", International Conference on Residual Stresses in Welded Construction and their effects, London, 15-17 November 1977.

84. J. Tanaka and T. Obata, "A Study on Stress Relief Heat Treatment (Reports 1 through 5)", Journal of Japan Welding Society, 36, 2, 1967, pp. 140-145, 36, 3, 1967, pp. 222-228, 36, 7, 1967, pp. 720-727, 39, 1, 1970, pp. 49-54, 39, 2, 1970, pp. 147-152.

85. J. Tanaka, "Decrease of Residual Stresses Change in Mechanical Properties and Cracking due to Stress Relieving Heat Treatment of HT-80 Steel", Welding in the World, 10, No. 1/2, 1972, pp. 54-67.

86. H. Ueda, and K. Fukuda, "Analysis of Welding Stress Relieving by Annealing Based on Finite Element Method", Trans. of Japan Weld. Res. Inst., 4 (1), 1975, pp. 39-45.

87. H. Ueda, and K. Fukuda, "Application of Finite Element Method for Analysis on Process of Stress Relief Annealing", Trans. of Japan Welding Society, 8, No. 1, April 1977, pp. 19-25.

88. Y. Fujita, T. Nomoto, A. Aoyagi, "A Study on Stress Relaxation due to Heat Treatment", Dept. of Naval Architecture, University of Tokyo, May 1973, IIW Doc. X-697-73.

89. I.G. Cameron, and C.S. Pemberton, "A Theoretical Study at Thermal Stress Relief in Thin Shells of Revolution", Intern. Journal of Numerical Methods in Engineering Vol. 11, 1977, pp. 1423-1437.

90. V.J. Papazoglou, "Computer Programs for the One-dimensional Analysis of Thermal Stresses and Metal Movement during Welding", M.I.T., January 1977.

91. D. Rosenthal, "Mathematical Theory of Heat Distribution During Welding and Cutting", Welding Journal, 20, (5), 1941, pp. 220s-234s.

92. A. Mendellson, "Plasticity : Theory and Applications", McMillan Publ. Co., New York, 1968.

93. L. Tall, "The Strength of Welded Built-Up Columns", Lehigh University, Ph.D. Dissertation, 1961.

94. L. Tall, "Residual Stresses in Welded Plates, A Theoretical Study", Welding Journal, 43, (1), 1964, pp. 10s-23s.

95. K. Masubuchi, F.B. Simmons and R.E. Monroe, "Analysis of Thermal Stresses and Metal Movement During Welding", RSIC-820, Redstone Scientific Information Center, Redstone Arsenal, Alabama, July, 1968.

96. C.E. Puch, et al., "Currently Recommended Constitutive Equations for Inelastic Design of FFTF Components", Oak Ridge National Laboratory Report ORNL-TM-3602, Sept. 1972.

97. J.M. Corum, et al., "Interim Guidelines for Detailed Inelastic Analysis of High-Temperature Reactor System Components", Oak Ridge National Laboratory Report ORNL-5014, Dec. 1974.

98. F.K.G. Odqvist, "Mathematical Theory of Creep and Creep Rupture, Oxford, 1966.

99. H. Crauss, "Creep Analysis", Willey-Interscience, N.Y., 1980.

100. W.F. Domis, "Creep and Creep Rupture Properties of HY-80 and HY-130 (T) Steels", U.S. Steel Applied Research Laboratory, Report No 39.012-006 (1), July 15, 1968.

101. Aerospace Structural Metals Handbook AFML-TR-68-115, Mechanical Properties Data Center, Bulfour Stulen, Inc., Michigan, 1975.

102. J.A. Clinard, et al., "Verification By Comparison of Independent Computer Program Solutions", Pressure Vessels and Piping Computer Program Evaluation and Qualification, Energy Technology Conference, Houston, Texas, September 1977, A.S.M.E., pp. 27-49.

103. J.F. Garofalo, C. Ritchmont, C. Domis, F. Von Gemmingen, "Strain-Time, Rate-Stress and Rate-Temperature Relations During Large Deformations in Creep", Joint International Conference on Creep, Book (I), Paper 30, p. 31, 1963.

104. M. Newman, Z. Zaphir and S. Bodner, "Finite Element Analysis for Time Dependent Inelastic Material Behavior", Scientific Report No 5, E.O.A.R., U.S.A.F., Grant AFOSR-74-2607B.

105. The Welding Institute, "The Metalurgy and Welding of QT 35 and HY-80 Steels", Welding Institute, Abington, England, Report Series 1974.

106. D.N. Shackleton, "Welding of HY-100 and HY-130 Steels: A Literature Review", The Welding Institute, Abington, England, Report Series September, 1973.

107. R.W. Flax, R.E. Keith, and M.D. Randal, "Welding the HY-Steels", ASTM Technical Publication 494, 1971.

108. American Society for Metals, "<u>Metals Handbook</u>", Vol. <u>1</u>, Ninth Edition, A.S.M., 19.

109. American Society for Metals, "<u>Source Book on Industrial Alloy and Engineering Data</u>", A.S.M., 1978.

110. D. Peckner, and I. Bernstein, "<u>Handbook of Stainless Steels</u>" Mc Graw Hill, N.Y., 1977.

111. J.M. Corum, "Appendix, Material Property Data for Elastic-Plastic-Creep Analysis of Benchmark Problems", Pressure Vessess and Piping Computer Program Evaluation and Qualification, Energy Technology Conference, Houston, Texas, September 1977, A.S.M.E., pp. 99-109.

112. American Society of Mechanical Engineers, "Symposium on Elevated Temperature Properties of Austenitic Stainless Steels", A.S.M.E. Pressure Vessels and Piping Conference, Miami Beach, Florida, June 24-28, 1974.

113. W.F. Simmons and J.A. Van Echo, "Report on the Elevated-Temperature Properties of Stainless Steels", American Society for Testing and Materials, Data Series Publication DS 5-S1, ASTM, 1965.

114. Iron and Steel Institute, Committe of Stainless Steels Producers, "High-Temperature Characteristics of Stainless

Steels:, A Designers' Handbook Series, Washington D.C., April 1979.

115. K. Isoda and Y. Ono, "Numerical Calculation Handbook in FORTRAN", Oomu-sha, Tokyo, Japan, 1979 (in Japanese).

116. Airco, "Welding Wire Guide", 1981.

117. N. Koreisha, "Investigation of Gas Metal Arc Welding Utilizing Dip Transfer at High Weld Speeds", Term Paper, Cource 13.17, Welding Engineering, Ocean Engineering Dept., M.I.T., December 1981.

118. J. Agapakis, "Computer Aided Data Acquisition for Welding Experiments", Special Research Report, Dept. of Ocean Engineering, M.I.T., due September 1982.

119. A. Osborne, "An Introduction to Microcomputers", Volume 1, Basic Concepts, 2nd Edition, Osborne/Mc Graw Hill, Berkeley, CA. 1980.

120. R.J. Tocci, L.P. Laskowski, "Microprocessors and Microcomputers, Hardware and Software", 2nd Edition, Prentice Hall, Englewood Cliffs, NJ, 1982.

121. B.A. Artwick, "Microcomputer Interfacing" Prentice Hall, Englewood Cliffs, NJ, 1980.

122. G.J. Lipovski, "Microcomputer Interfacing, Principle and Practices", Lexington Books, Lexington, MA, 1980.

123. Digital Equipment Corporation, "Microcomputer Interfaces Handbook" D.E.C., Maynard, MA, 1981.

124. Daytronic Corporation, "9000 Modular Instrument System, Instruction Manuals" Miamisburg, OH, 1981, 1982.

125. Digital Equipment Corporation, "Microcomputers and Memories", D.E.C., Maynard, MA, 1981.

126. J.W. Dally and W.F. Riley, "Experimental Stress Analysis", 2nd Edition, Mc Graw Hill, New York, 1978.

127. Micro-Measurements, "Temperature-Induced Apparent Strain and Gage Factor Variation in Strain Gages", M-M Tech Note, TN-504, Measurements Group, Raleigh, N.C., 1976.

128. K.P. Carpentier, "Thermal Stress Relief of HY-130 Weldments", S.M. Thesis, Ocean Engineering Dept., M.I.T., May 1982.

129. R. Antony and J. Reece, "Accounting Text and Cases", 6th Edition, R.D. Irwin, Honewood, Ill, 1979.

130. J.J.W. Neuer and E.B. Deadkin, "Cost Accounting: Principles and Practice", 9th Edition, Homewood, Ill, 1977.

131. H.B. Cary, "Modern Welding Technology", Prentice Hall, Englewood Cliffs, 1979.

132. A. Stroll and D. Newman, "Wage Systems Used in Industrial Production and More Particularly in Welding Engineering", Economic Aspects of Welding Conference, Welding Institute, 1971.

133. S. Roweden, "Wages and Insentives", ibid.

134. B.P. Mc Mahon, "The Price of MIG Welding", ibid.

135. C.L. Tsai, "Parametric Study on Cooling Phenomena in Underwater Welding", Ph.D. Thesis, M.I.T., Sept. 1977.

A P P E N D I C E S

APPENDIX A

MATERIAL PROPERTIES

A.1 HY-80 Steel

HY-80 is a low alloy Ni-Cr-Mo steel of a minimum yield strength of 80 Ksi (552 MPa) and excellent toughness. It is the primary U.S. Navy hull construction material and achieves its strength and toughness through a quenching and tempering heat treatment.

Table A.1 summarizes the compositional ranges for the steel. Mechanical properties specifications are, according to MIL-S-16216G,outlined in Table A.2.

TABLE A.1 Compositional Ranges of HY-80, HY-130 and 304 Stainless Steel (weight, %)

Element	HY-80[106]	HY-130[106]	304 Stainless[108]
C	0.18 max	0.08-0.12	0.08 max
Mn	0.10-0.40	0.60-0.90	2.00 max
Si	0.15-0.35	0.20-0.35	1.00 max
Ni	2.00-3.25	4.75-5.25	8.00-10.50(or 11.0)
Cr	1.00-1.80	0.40-0.70	18.00-20.00
Mo	0.20-0.60	0.30-0.65	0.50 max
V	0.03 max	0.05-0.10	-
S	0.025 max	0.010 max	0.030 max
P	0.025 max	0.010 max	0.045 max
S+P	0.045 max	-	-
Ti	0.02 max	0.02 max	-
Cu	0.25 max	0.25 max	-

Table A.2 : Specification Limits of HY-80 Mechanical Properties [2]

PROPERTY	PLATE THICKNESS	
	Less than 5/8 in.(16mm)	5/8 in.(16mm) and over
Ultimate Strength	For information	For information
Yield Strength at 0.2% Offset	80 to 100 Ksi (552 to 690 MPa)	80 to 95 Ksi (552 to 655 MPa)
Min. Elongation in 2 in. (50mm)	19%	20%
Reduction in area		
Longitudinal	--	55%
Transverse	--	50%

Charpy V-Notch Energy Requirements

Plate Thickness	Specimen Size	Absorbed Energy Minimum	Test Temperature
1/4 in.(6mm) to 1/2 in.(13mm) Excl.	10 x 5 mm (0.4x0.2 in.)	For information	-120^{o} F (-84^{o}C)
1/2 in.(13mm) to 2 in.(50mm) Incl.	10 x 10 mm (0.4x0.4 in.)	50 ft-lb (72.8 J)	-120^{o} F (-84^{o}C)
Over 2 in. (50mm)	10 x 10 mm (0.4x0.4 in.)	30 (43.7 J)	-120^{o} F (-84^{o}C)

A.2 HY-130 Steel

HY-130 steel is a Naval hull-construction steel with a minimum yield strength between 130 and 150 Ksi (895 MPa to 1030 MPa), also refered to, in different stages of development, as 5 Ni-Cr-Mo-V, HY-150, HY-140, HY-130/150 and HY-130(T). The steel is to be used in a quenched and tempered condition, in which the microstructure is primarily tempered martensite, as in the case of HY-80 steel.

The compositional ranges of this steel are given in Table A.1. Some as-received mechanical properties are shown in Table A.3 and Temperatures for thermal treatments in Table A.4.

Mechanical and physical properties of HY-130 at room and elevated temperatures are plotted in Figures A.1 and A.2.

Finally, the minimum observed creep rate for various temperatures and various applied stresses appears in Figures A.3 (a) and (b) adapted from [100] and [101].

TABLE A.3 : General Properties of HY-130 Type Steel [107]

Yield Strength	min 130 Ksi (895 MPa) at center of 4in(101.6mm) plate
Elongation	15-20% in 2in.(50mm)
Reduction of Area	50-64% transversely 70% through thickness
Charpy-V-Notch Impact Energy Absorbsion (ductile fracture region)	60ft-lb(87.3J) at $0^{o}F(-17.8^{o}C)$

TABLE A.4 : Thermal Treatment Related Properties for HY-130

A_{c1} Temperature	1210^{o} F (654^{o} C)
A_{c3} Temperature	1415^{o} F (768^{o} C)
M_s Temperature	715^{o} F (379^{o} C)
Recommended final austenitizing temperature	1500^{o} F (815^{o} C)
Recommended Quenching Medium	Water
Microstructure(as quenched, midthickness)	
0.5in (12.2mm) plate	100% martensite
4.0in (101mm) plate	60-75% martensite, remainder bainite
Recommended tempering temperature range	$1000-1150^{o}$ F ($538-621^{o}$C)

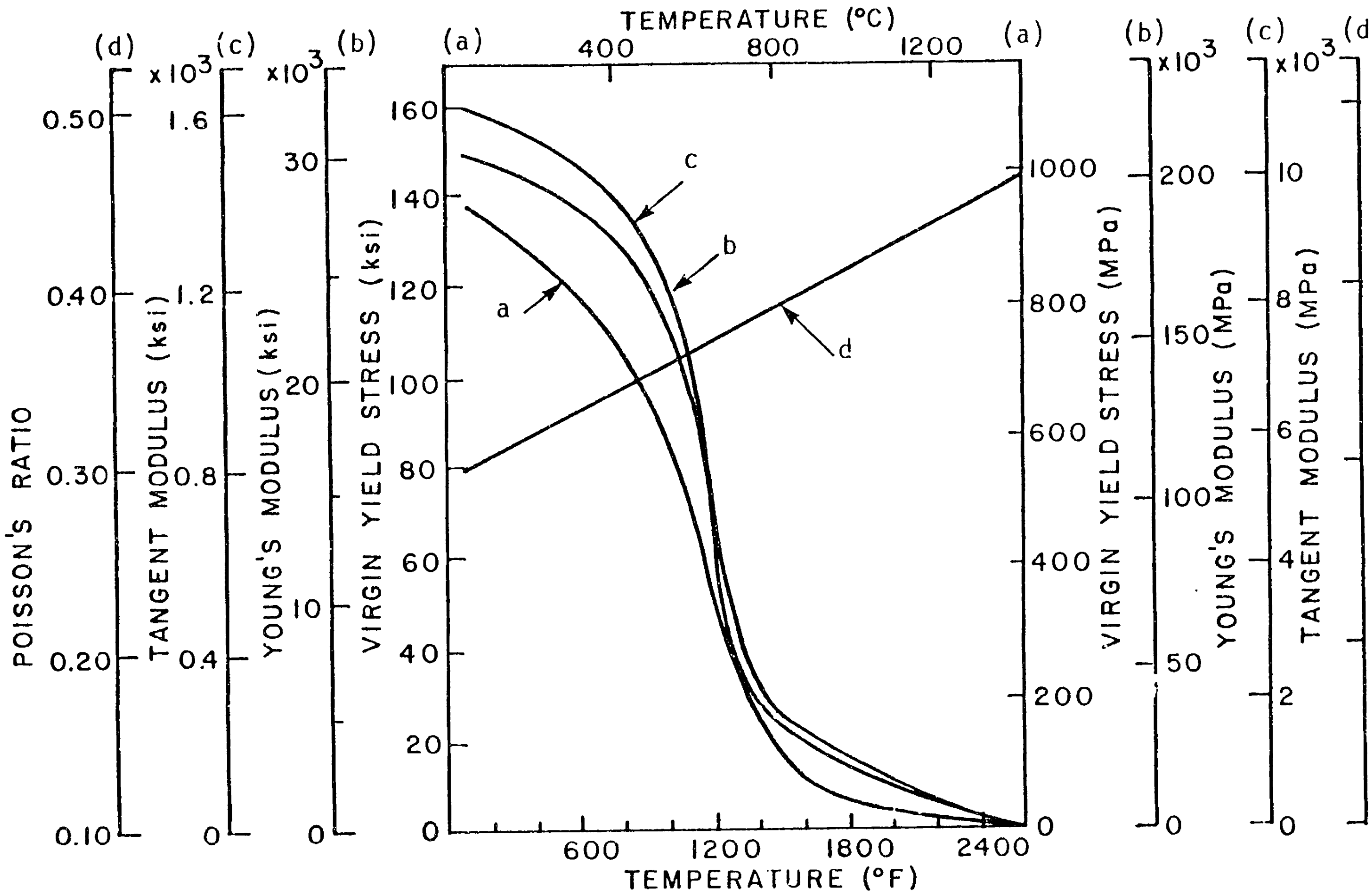

Figure A.1 (a) Variation of virgin yield stress with temperature for HY-130
(b) Variation of Young's modulus with temperature for HY-130
(c) Variation of tangent modulus with temperature for HY-130
(d) Variation of Poisson's ratio with temperature for HY-130

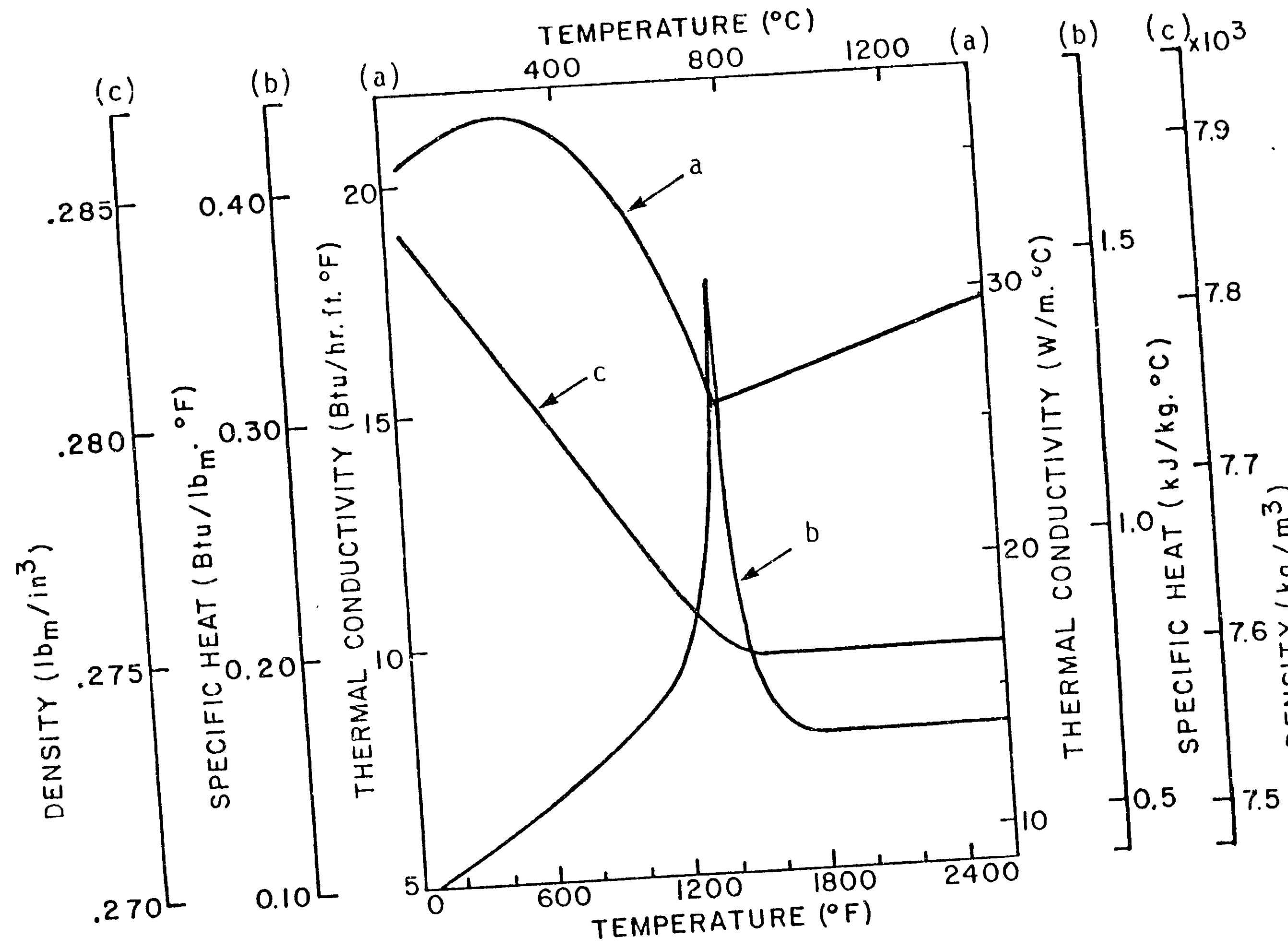

Figure A.2 (a) Variation of thermal conductivity with temperature for HY-130
(b) Variation of specific heat with temperature for HY-130
(c) Variation of density with temperature for HY-130

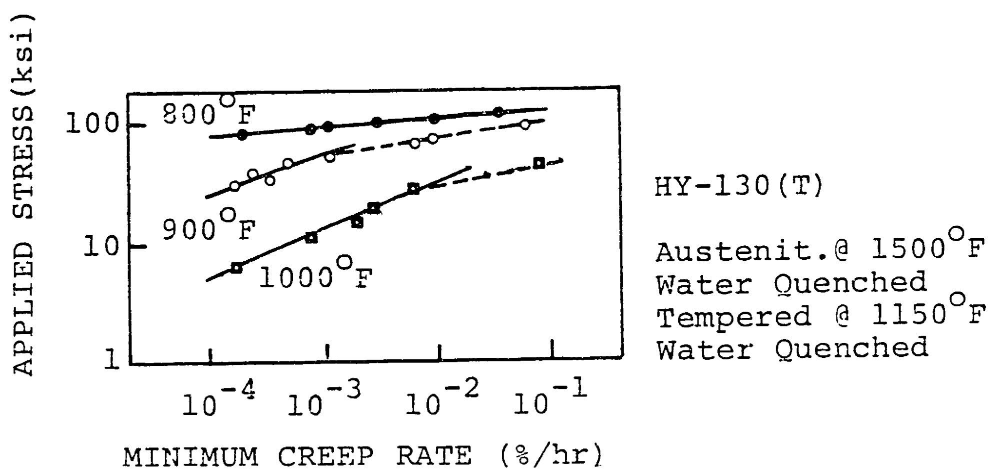

Figure A.3(a) : Minimum creep rate at various temperatures and levels of applied stress, for HY-130(T) standard 0.25 in. dia. specimens.[101]

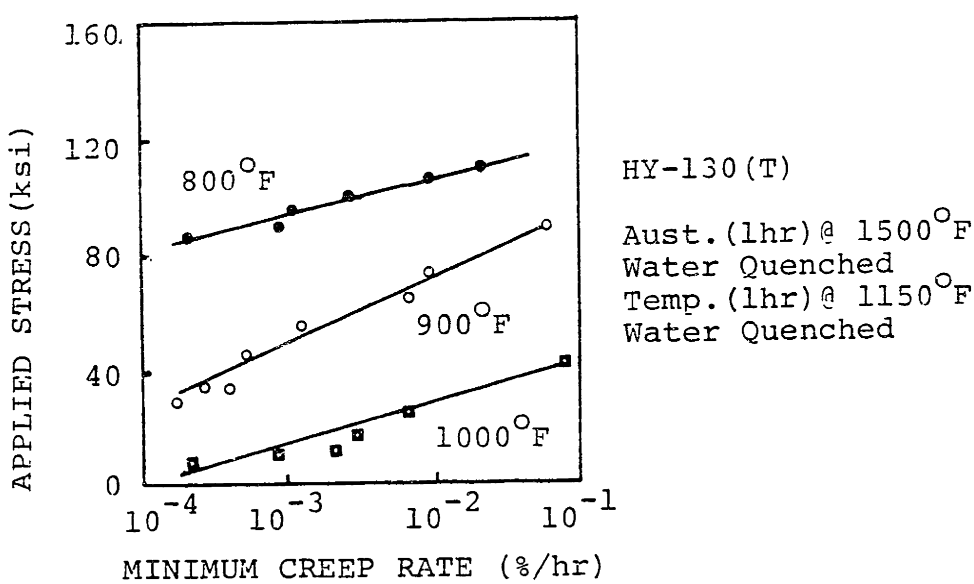

Figure A.3(b) : Minimum creep rate at various temperatures and levels of applied stress , for HY-130(T) 1 in. thick plates.[100],[101]

Table A.5 : Typical Mechanical Properties of Annealed 304 Stainless Steel at Room Temperature [109]

	U.T.S.		Yield Strength		Elongation	Hardness
Form	Ksi	MPa	Ksi	MPa	%	
Bar	85	586	35	241	60	Bhn 149
Plate	82	565	35	241	60	Bhn 149
Sheets	84	579	42	290	55	Rb 80
Strips	84	579	42	290	55	Rb 80
Tubing	85	586	35	241	50	Rb 80
Wire	90	621	35	241	60	Rb 83

Table A.6 : Thermal Treatment Temperatures for 304 St.Steel [108],[109].

Initial Forging Temperature	2100-2300 $^{\circ}$F (1149-1260 $^{\circ}$C)
Annealing Temperature	1850-2050 $^{\circ}$F (1010-1121 $^{\circ}$C)
Stress Relief Ann. Temperature	400-750 $^{\circ}$F (204-399 $^{\circ}$C)
Melting Range	2550-2650 $^{\circ}$F (1399-1454 $^{\circ}$C)
Carbide Precipitation range	800-1600 $^{\circ}$F (427-871 $^{\circ}$C)

A.3 304 - Stainless Steel

304 Stainless Steel is a low-carbon (max 0.08% C), unstabilized austenitic stainless steel specially developed for better corrosion resistance and for restriction of carbide precipitation during welding.

Chemical composition ranges are shown in Table A.1. Mechanical properties of annealed material at room temperature are given in Table A.5, and physical properties in Table A.7. Thermal treatment temperatures are shown in Table A.6. Physical and mechanical properties at both ambient and elevated temperatures are plotted in Figure A.4 to A.10 adapted from [108] through [113]. It should be noted, however, that in many instances data from different sources were not in complete agreement, reflecting the normal variations from heat-to-heat of the alloy and differences between the experimental procedures of different laboratories. In such cases either all the different data were presented, with their sources cited, or judgment was used, in order to obtain a single compromise curve for use in the computer modelling.

Creep data adapted from [100], [101], and [114] appear in Figures A.11 and A.12.

No data were found in the literature for the temperature dependence of density. Figure A.13 gives the assumed variation of density, calculated from the thermal expansion data of Figure A.9 and the known density at room temperature (Table A.7).

Table A.7 : Typical Physical Properties of 304 Stainless Steel, [108],[109],[110]

Density (ρ)	0.29 lb/in^3 (8000 Kg/m^3)
Elastic Modulus (E)	28.0x10^3 Ksi (1.93x10^5 MPa)
Tangent Modulus (E_T)	0.73x10^3 Ksi (5x10^3 MPa)
Average Thermal	[32^{o}F to 212^{o}F (0^{o}C to 100^{o}C)]
Expansion Coefficient (α)	9.6μ in/in^{o}F (17.2 μm/m^{o}C)
Thermal Conductivity at 212^{o}F (100^{o}C) (λ)	9.4 Btu/hr ft^{o}F (16.2 W/m^{o}K)
Specific Heat (c_p) [32 to 212^{o}F (0 to 100^{o}C)]	0.12 Btu/lb^{o}F (0.5 KJ/Kg^{o}K)

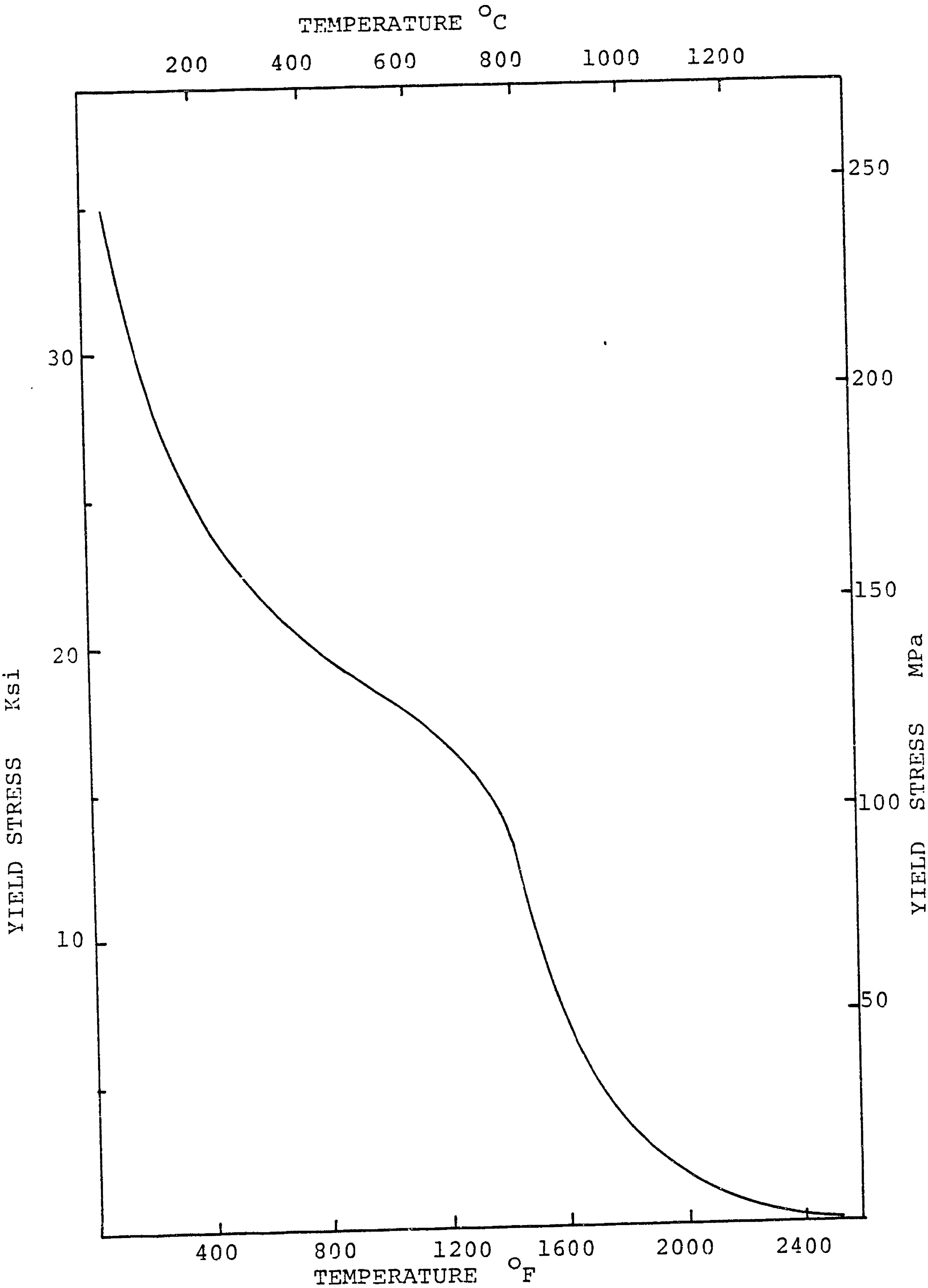

Figure A.4 : Variation of virgin yield stress with temperature for 304 stainless steel. [110], [112], [113]

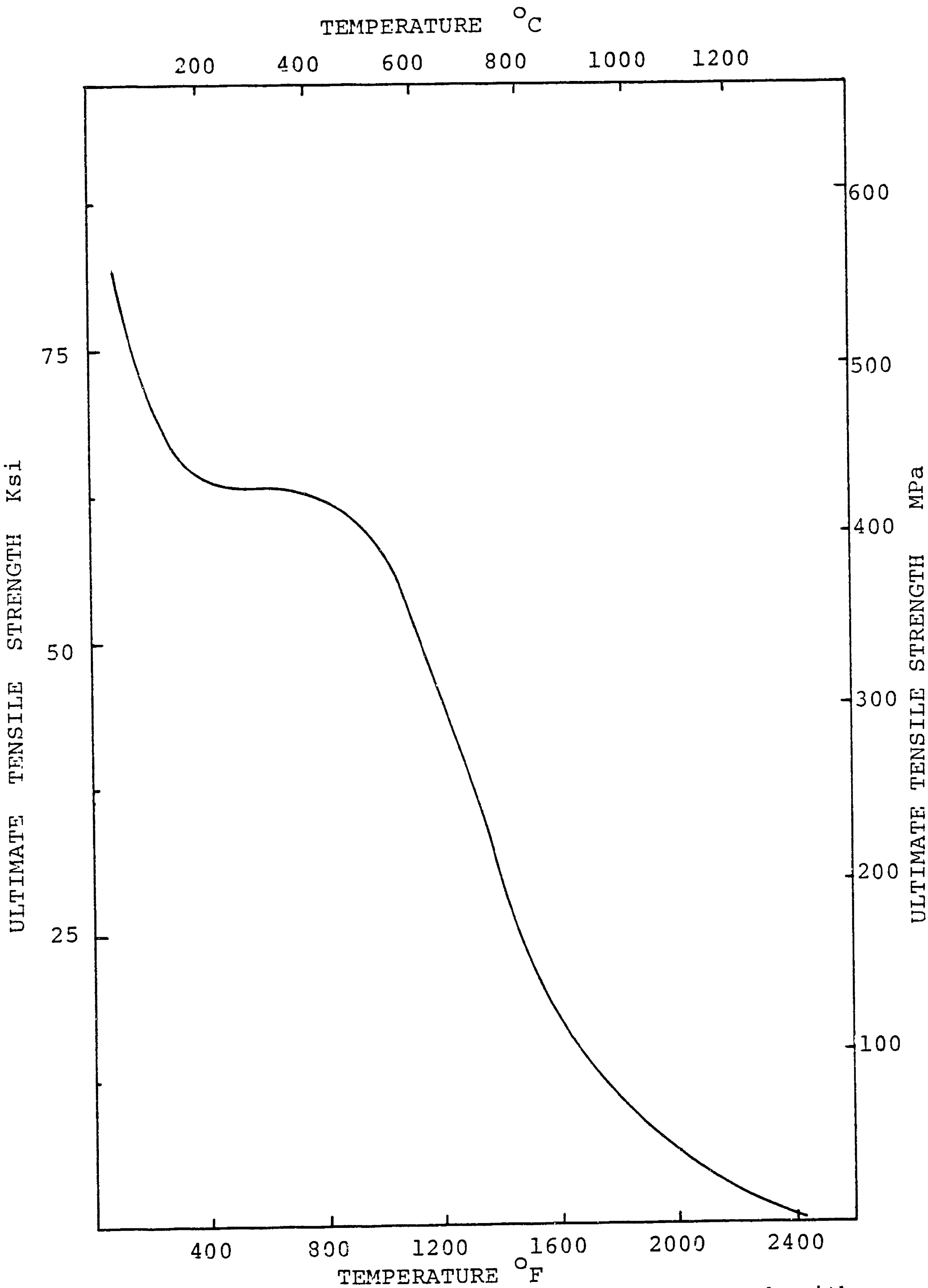

Figure A.5 : Variation of ultimate tensile strength with temperature for 304 stainless steel. [110],[112]

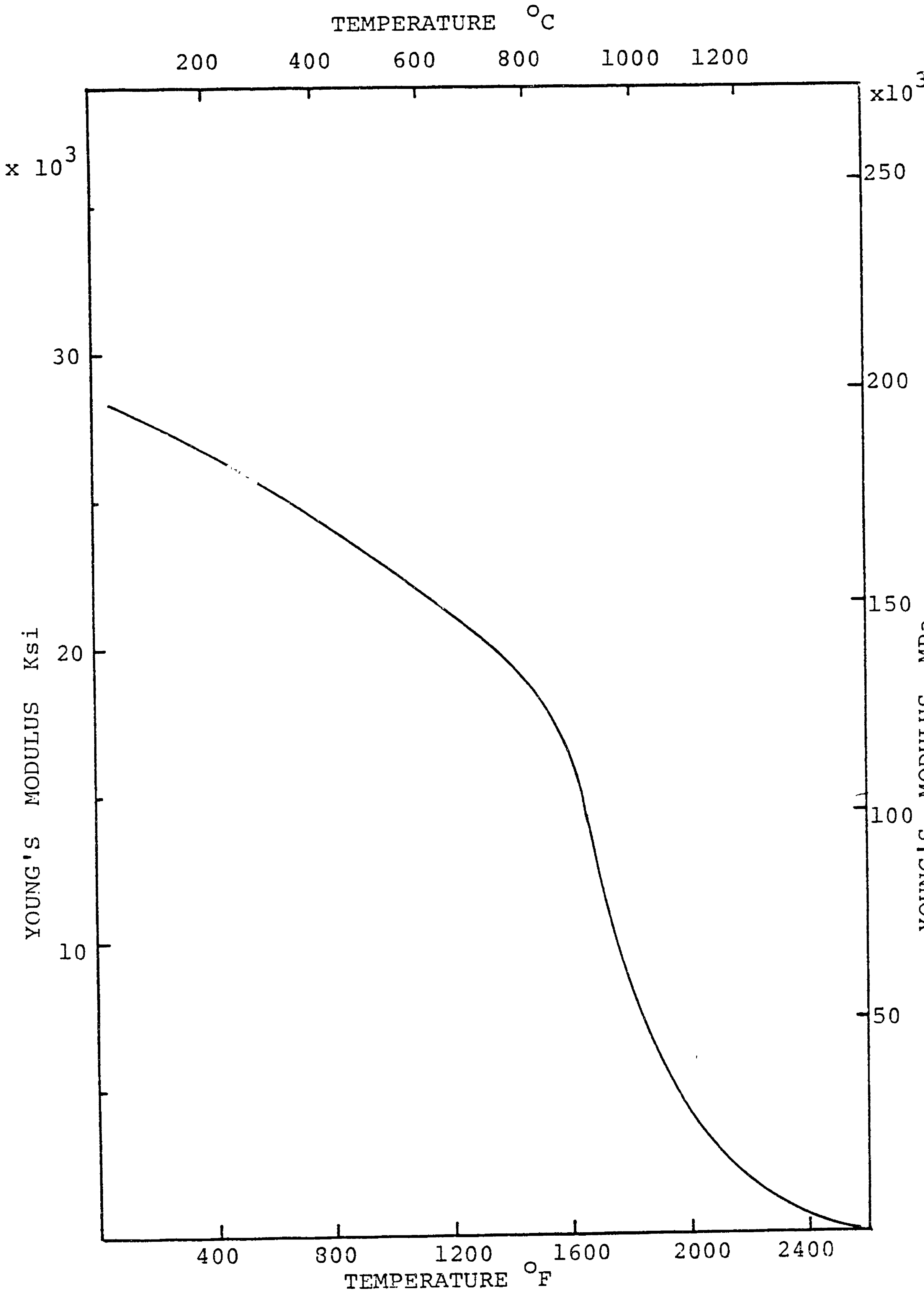

Figure A.6 : Variation of Young's modulus with temperature for 304 stainless steel. [108],[112]

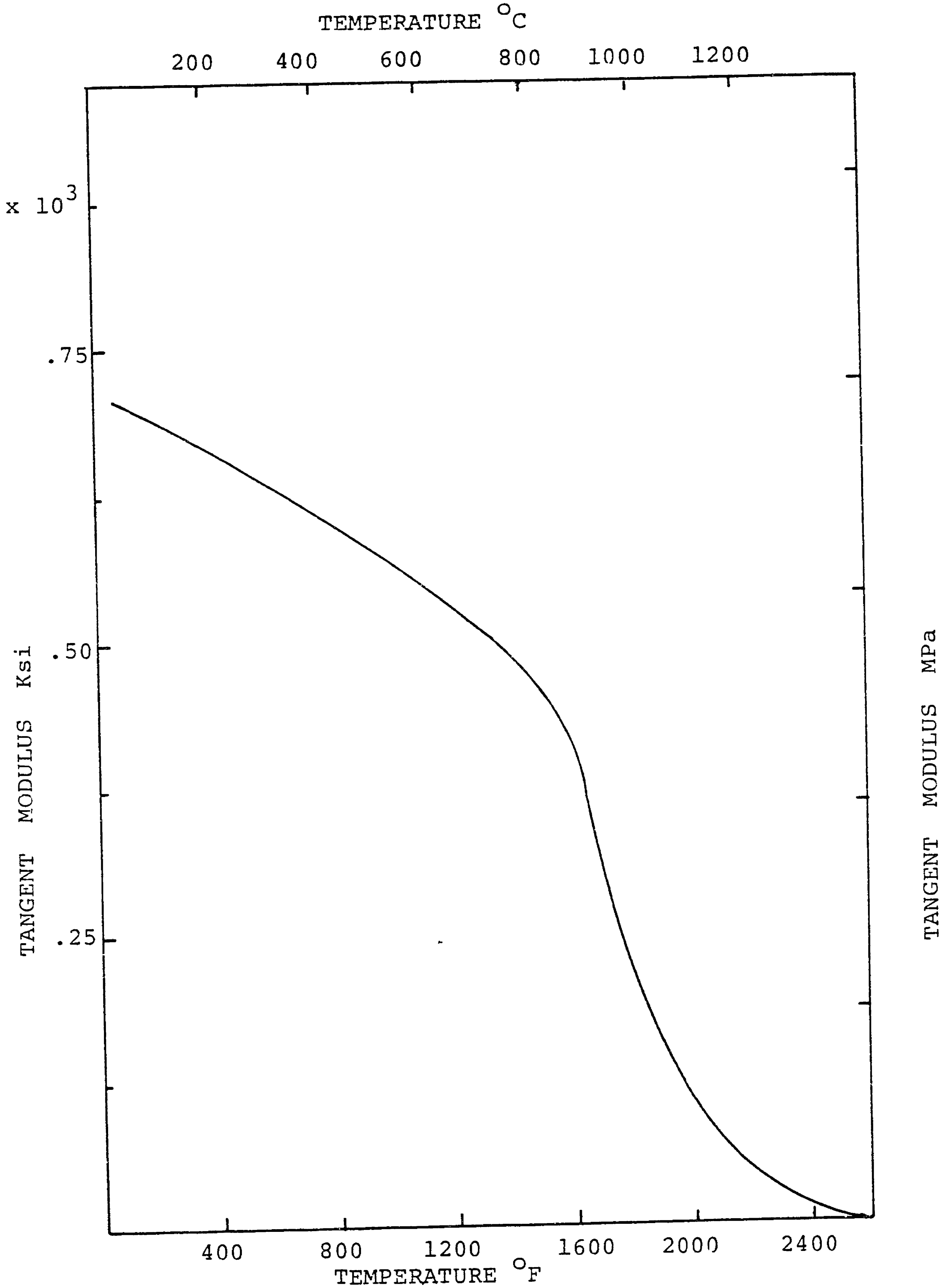

Figure A.7 : Variation of tangent modulus with temperature for 304 stainless steel. [111]

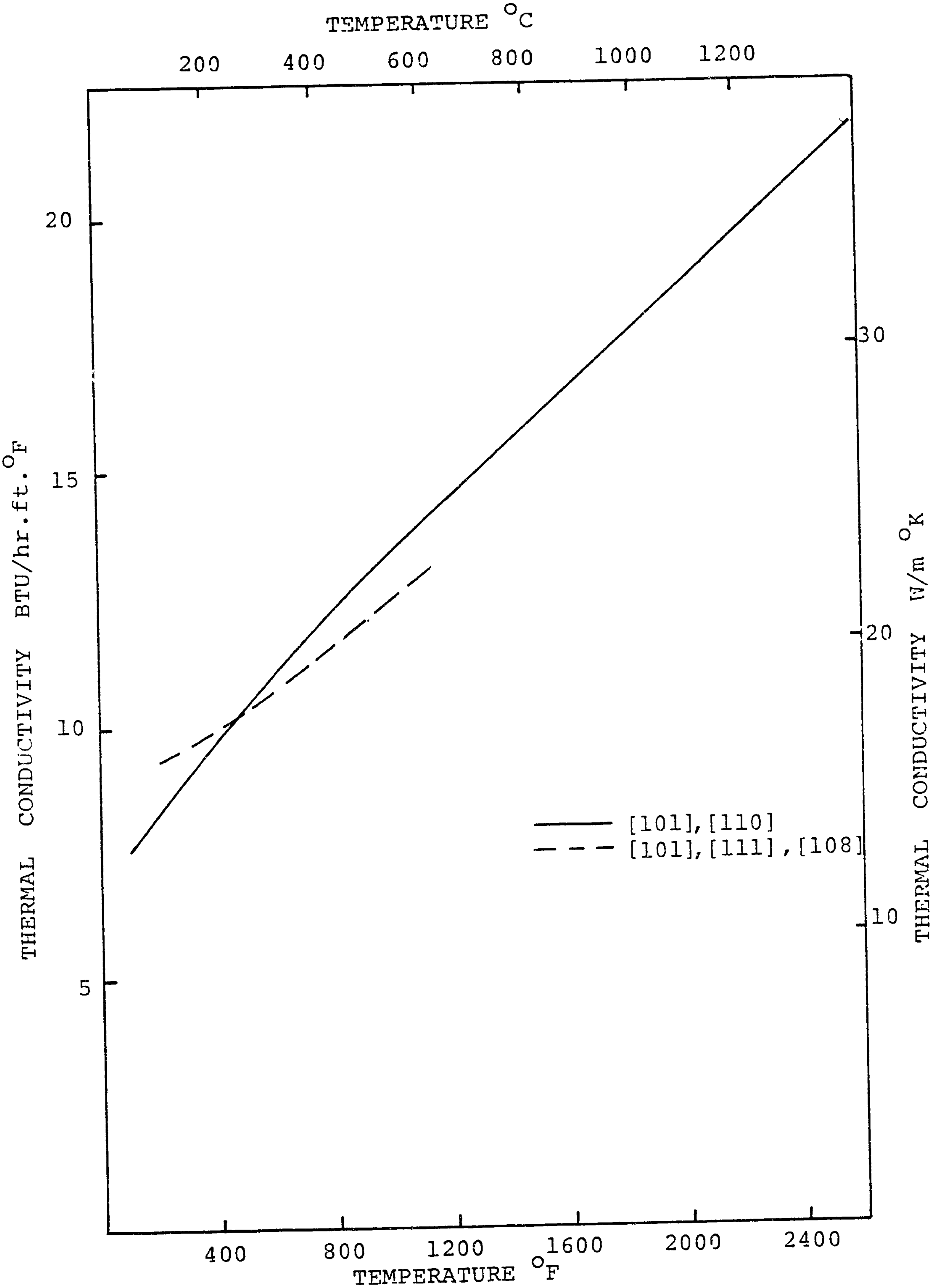

Figure A.8 : Variation of thermal conductivity with temperature for 304 stainless steel.

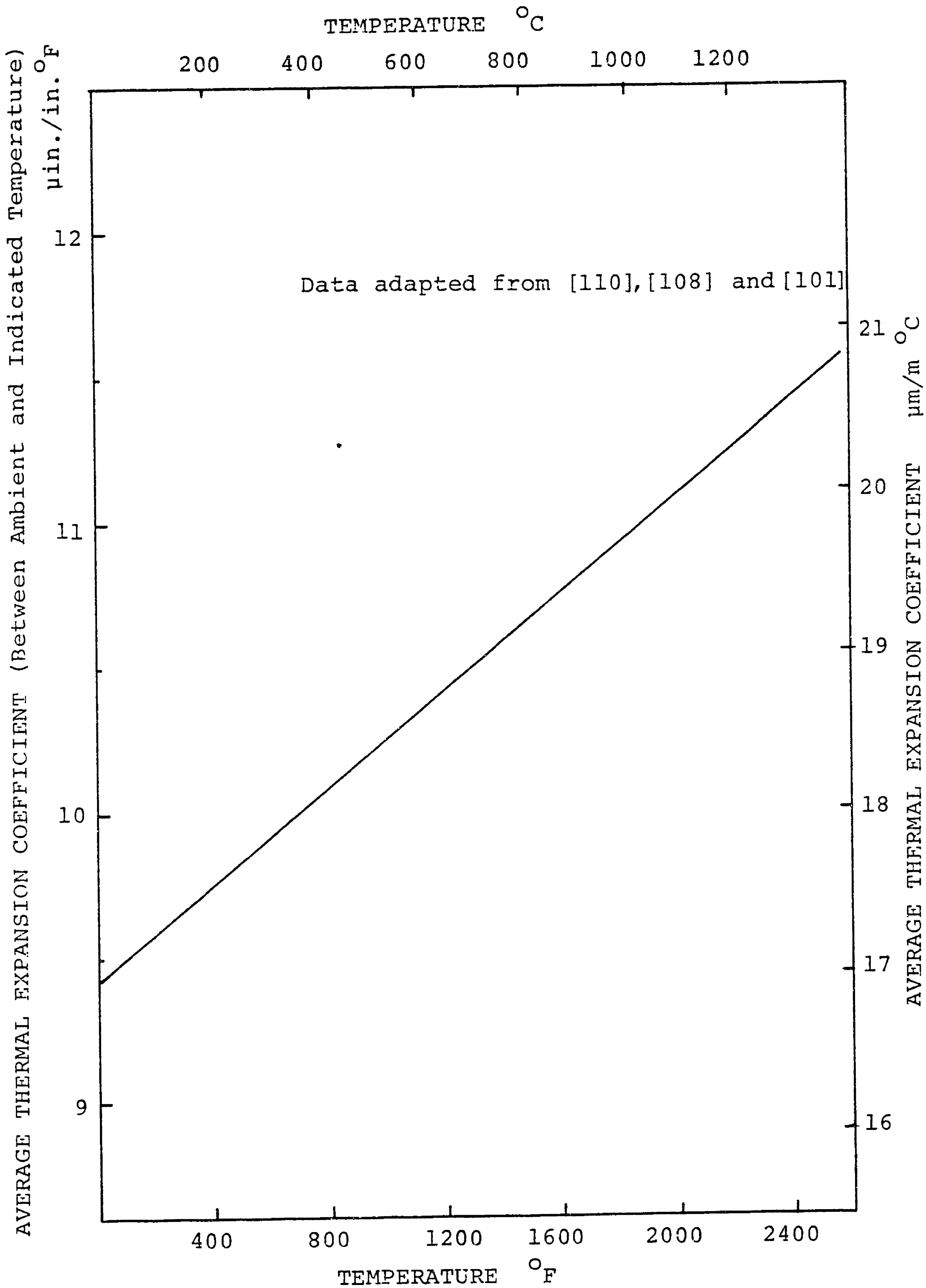

Figure A.9 : Average thermal expansion coefficient for 304 SS

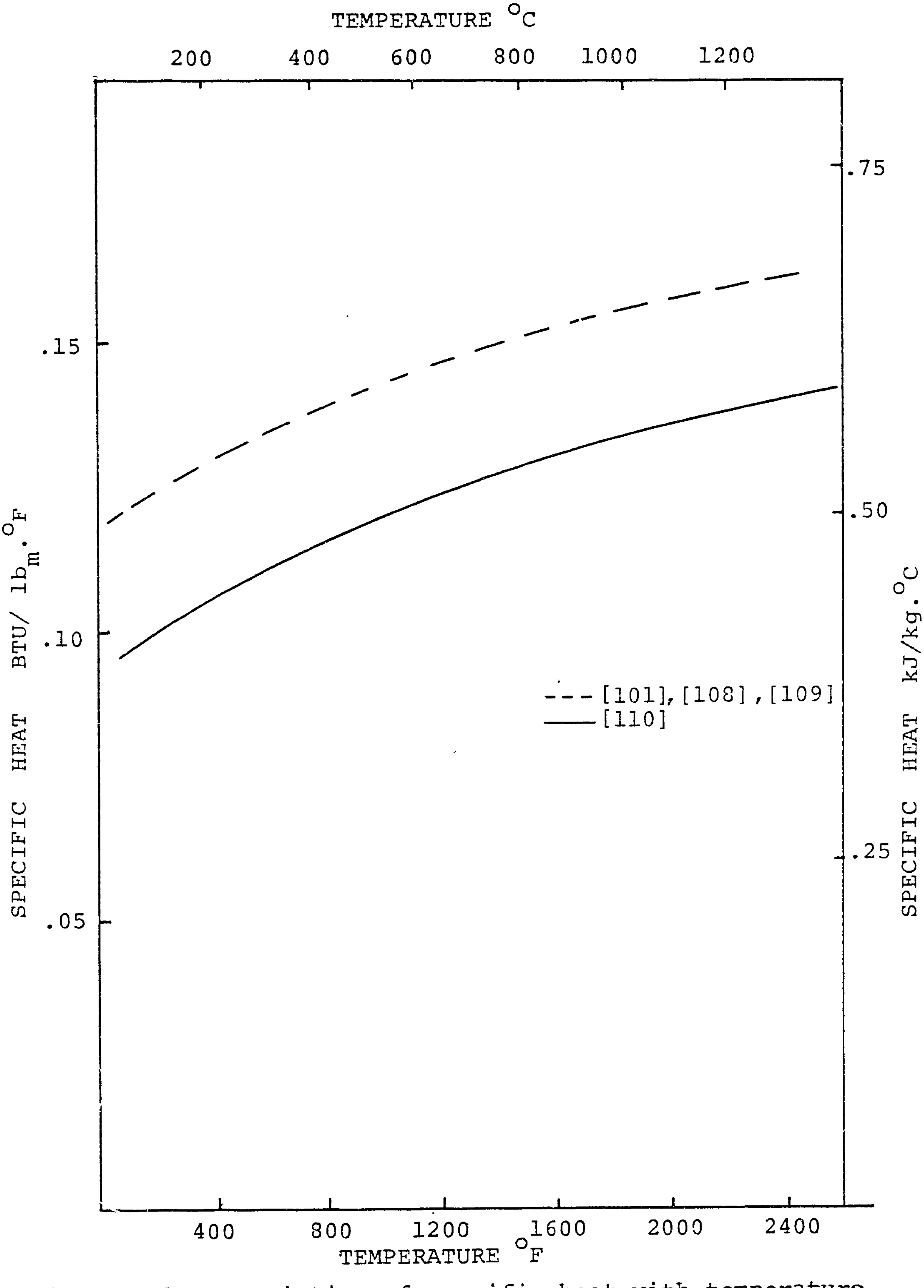

Figure A.10 : Variation of specific heat with temperature for 304 stainless steel .

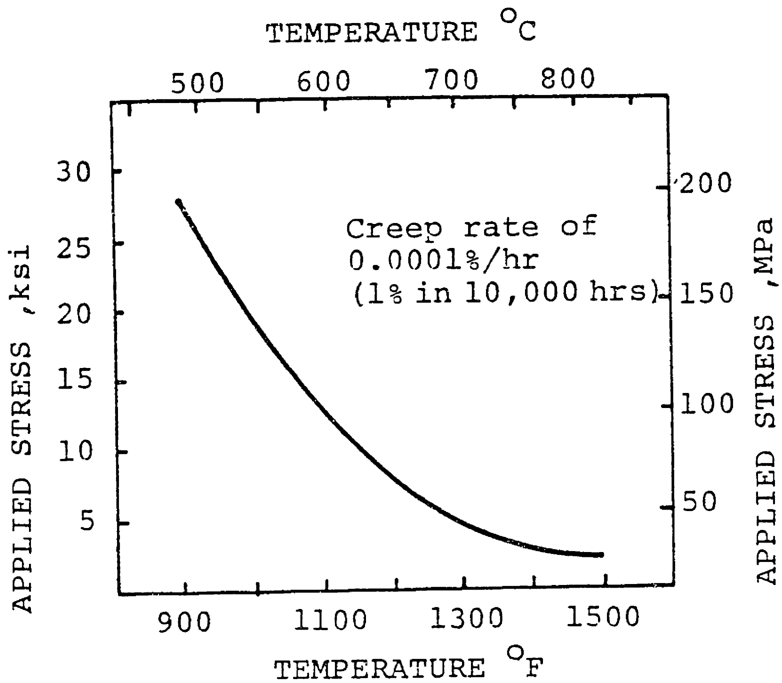

Figure A.11 : Creep rate curve for 304 stainless steel
Adapted from [114].

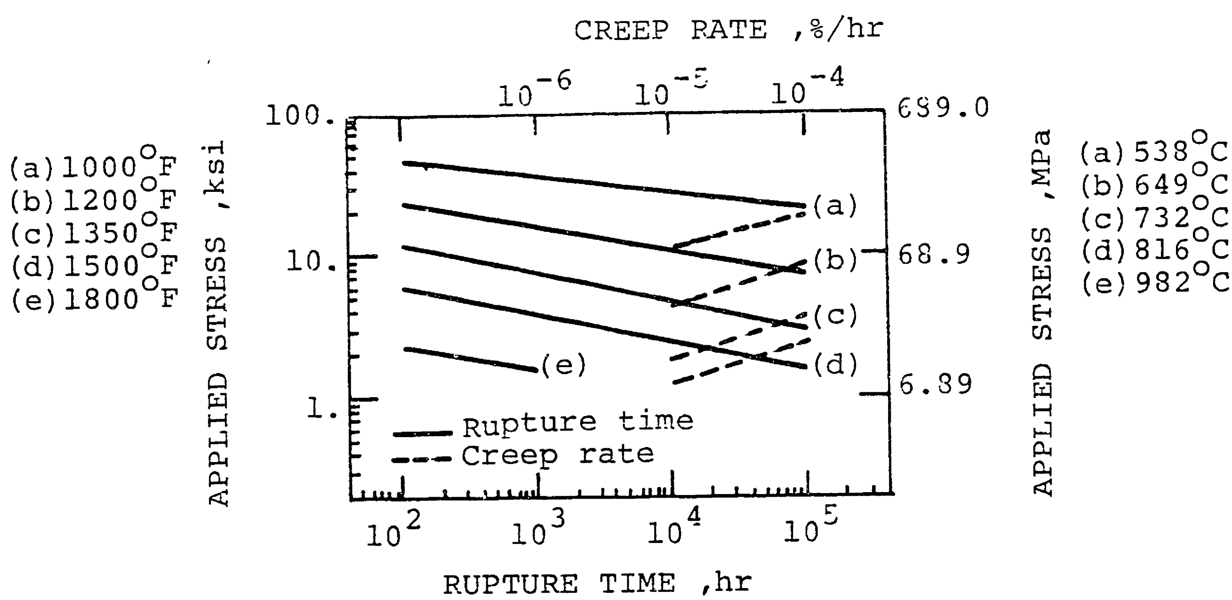

Figure A.12 : Stress vs. rupture-time and creep-rate curves for annealed type 304 stainless steel .[114]

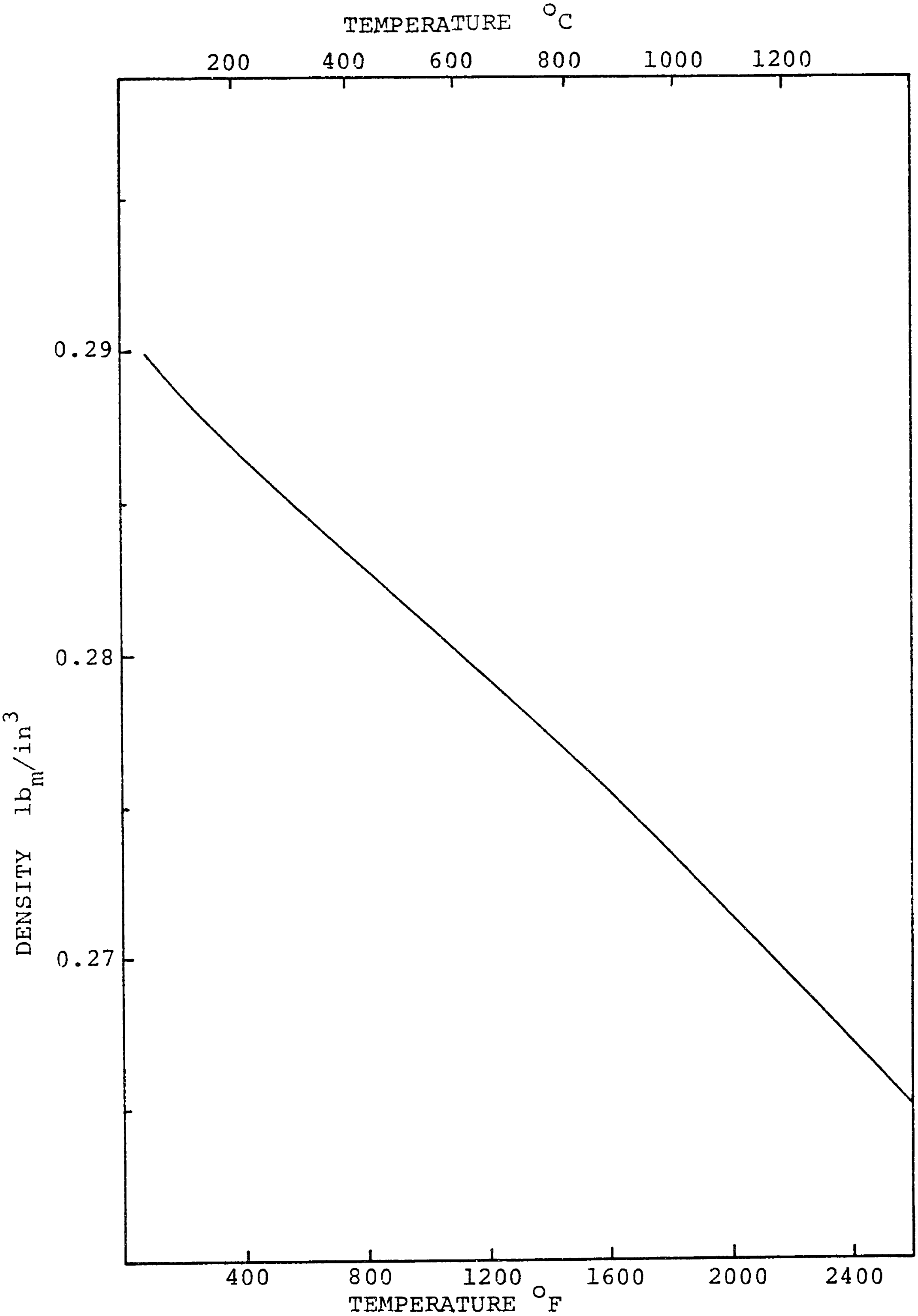

Figure A.13 : Variation of density with temperature for 304 stainless steel (based on thermal expansion)

APPENDIX B

NUMERICAL INTEGRATION

In the program the various integrations are performed numerically for twenty one integration points, unequally spaced along the breadth of the plate. The numerical integration scheme used was based on Newton-Cotes closed integration formulas and was adapted by Imakita from Isoda [115].

In general, if the integral

$$I = \int_{x_1}^{x_N} f(x)\, dx \qquad \text{(B-1)}$$

is to be evaluated given the set of data $[x_i, f(x_i)]$, $i=1,2,..,N$ the following cases are distinguished, in the numerical integration scheme used: (I) If N=2, the trapezoidal rule is used (assuming a first order approximation to f(x))

$$I = \frac{h}{2}\,[f(x_1) + f(x_2)] \qquad \text{(B-2)}$$

where

$$h = x_2 - x_1 \qquad \text{(B-3)}$$

(i) If $N \geq 3$ and odd then two subcases have to be considered

(iia) If all integration points are equally spaced then the integral can be calculated using Simpsons first rule for every three consecutive integration points (assuming a second order approximation to f(x)):

$$I = \frac{h}{3}\,[f(x_1) + 4f(x_2) + f(x_3)] \qquad \text{(B-4)}$$

where

$$h = x_2 - x_1 = x_3 - x_2 \qquad \text{(B-5)}$$

(iib) If the integration points are unequally spaced then a modified version of equation (B-4) is used for every three consecutive points. Specifically, assuming again a second order approximation to f(x), the respective Lagrange interpolation polynomial will be:

$$p(x) = \frac{(x-x_2)(x-x_3)}{(x_1-x_2)(x_1-x_3)} f(x_1) + \frac{(x-x_1)(x-x_3)}{(x_2-x_1)(x_2-x_3)} f(x_2) +$$

$$+ \frac{(x-x_1)(x-x_2)}{(x_3-x_1)(x_3-x_2)} f(x_3) \qquad \text{(B-6)}$$

where $x_1 \leqq x_2 \leqq x_3$

If as in Figure B.1(a), α is the midpoint between x_1 and x_3 then

$$\alpha = (x_1+x_3)/2 \qquad \text{(B-7)}$$

and substituting in (B-6) we get

$$p(\alpha) = \frac{d}{2(h+d)} f(x_1) + \frac{h^2}{(h+d)(h-d)} f(x_2) - \frac{d}{2(h-d)} f(x_3) \qquad \text{(B-8)}$$

where h and d such as

$$\begin{aligned} x_3 - x_1 &= 2h \\ x_2 - x_1 &= h + d \\ x_3 - x_2 &= h - d \end{aligned} \qquad \text{(B-9)}$$

For the equally spaced points now (x_1, α, x_3) integral I can be calculated as in (B-4), that is

$$I = \frac{h}{3}\left[f(x_1) + 4p(\alpha) + f(x_3)\right]$$

$$= \frac{h}{3}\left[f(x_1)+(\frac{d}{2(h+d)}f(x_1)+\frac{h^2}{(h+d)(h-d)}f(x_2)-\frac{d}{2(h-d)}f(x_3))+f(x_3)\right]$$

$$= \frac{h}{3}\ ((1+\frac{2d}{h+d})f(x_1)+2(\frac{h}{h+d}+\frac{h}{h-d})f(x_2)+(1-\frac{2d}{h-d})f(x_3)) \quad \text{(B-10)}$$

(iii) If N ≥ 4 and even the following subcases have to be considered.

(iiia) If all integration points are equally spaced then I is calculated using (B-4) for all the points, taken three at a time, except the last four, where the Simpson's second rule is used (assuming a third order approximation to f(x)):

$$I = \frac{3h}{8}\left[f(x_1) + 3f(x_2) + 3f(x_3) + f(x_4)\right] \quad \text{(B-11)}$$

(iiib) If the integration points are unequally spaced then the same method is employed as in (iiia), but now we use (B-10) instead of (B-4), and a modified version of (B-11) for unequal intervals. Specifically, refering to Figure B-1(b), we finally have (assuming a third order Lagrange interpolation polynomial):

$$I = \frac{h}{3}\ ((1 + \frac{2d_1d_2}{(h+d_1)(h+d_2)})\ f(x_1) + \frac{4h^2}{d_2-d_1}(\frac{d_2}{h^2-d_1^2}\ f(x_2) -$$

$$\frac{d_1}{h^2-d_2^2}\ f(x_3)) + (1 + \frac{2d_1d_2}{(h-d_1)(h-d_2)}\ )\ f(x_4)) \quad \text{(B-12)}$$

where $h = (x_4-x_1)/2$

$$d_1 = x_2-x_1-h \quad \text{(B-13)}$$

$$d_2 = x_3 - x_1 - h$$

The integration subroutine QUDR, used in the one - dimensional program was adapted from Isoda, [115].

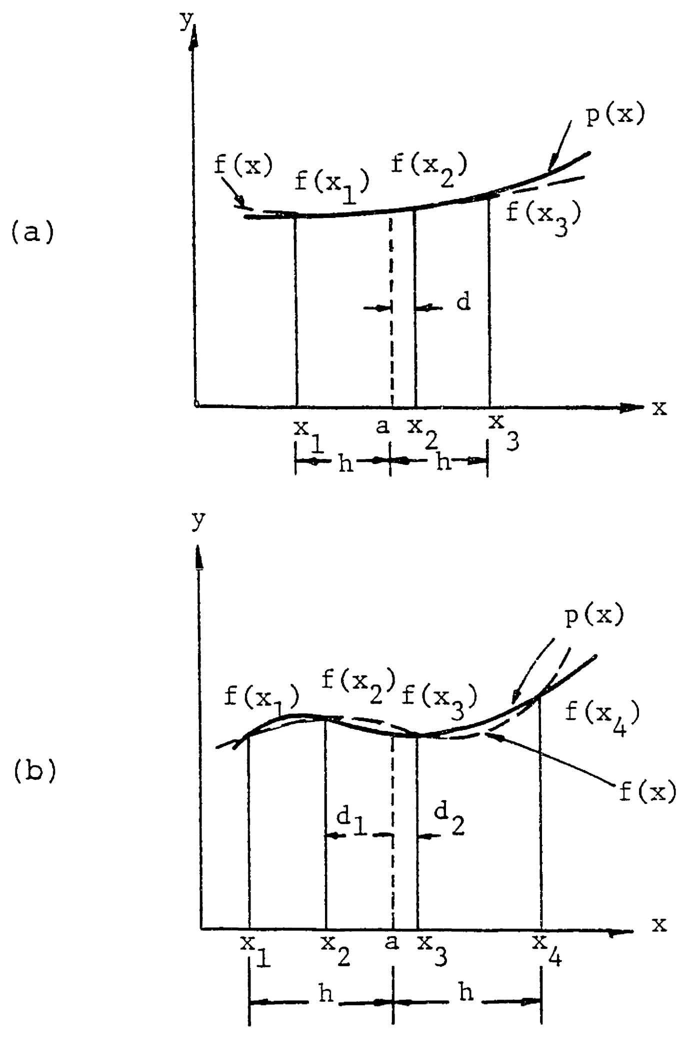

Figure B.1 : Second and third order approximations to function f(x) used in numerical integration

APPENDIX C

FORTRAN LISTING OF THE MODIFIED ONE-DIMENSIONAL PROGRAM

A listing of the one-dimensional program, as modified by the author for the prediction of temperatures, strains and stresses, during welding and subsequent stress relieving, is presented in this Appendix.

Although the input and output format is somewhat different from the original version of the program the inclusion of comment statements and the existence of - READ and WRITE - FORMAT statements makes it unnecessary to repeat the input specifications here.

The program is general enough to handle, with minor only modifications,any type of stress relieving temperature history and profile. Only one creep model, for 304 stainless steel, was included. If for any other material, however, the uniaxial creep law is known, subroutine CREPLO has to be changed accordingly.

```
C*****************************************************************
C
C     ONE DIMENSIONAL PROGRAM AS MODIFIED BY J A  FOR STRESS RELIEVING
C
C
C*****************************************************************
C
C
      DIMENSION  EXR(21),STRSK(21),EMR(21),EPNR(21),STRESR(21),STRPL(21)
      DIMENSION STRHT(21),ST1(200),EM1(200),TY1(200)
      DIMENSION ST7(200),EM7(200),TY7(200)
      DIMENSION ST9(200),EM9(200),TY9(200)
      DIMENSION ST11(200),EM11(200),TY11(200)
      DIMENSION ST15(200),EM15(200),TY15(200)
      DIMENSION ST18(200),EM18(200),TY18(200)
      DIMENSION TPL(300),TME(300),SSS1(300),EMM1(300)
      DIMENSION SSS7(300), SSS9(300),SSS11(300),SSS15(300),SSS18(300)
      DIMENSION EMM7(300), EMM9(300),EMM11(300),EMM15(300),EMM18(300)
      COMMON /TEM/TY(21),TEMP(10),CAP(10),RHO(10),COND(10),TREFN(10,21)
      COMMON /E/E(10),YP(10),ALPH(10),SLOP(10)
      COMMON /ST/RAT(20),T(2000),EX(21),EM(21),EPN(21),STRES(21),EL(21)
      COMMON /YW/Y(21),YD(21)
      COMMON  /YP/YPN(10),YTHN(10,21)
      COMMON /PP/P,V,YS,YEP,YOUT,THICK
      COMMON /SC/NEDGE,HCOT(10)
      COMMON  /RS/EPO(21)
      COMMON /P/YDIS,TMAX,TIX,TREF
      COMMON /T/T1,TI1,T2,TI2,T3,TI3,TST
      COMMON /IO/KI,KO
      COMMON /CRP/ECREEP(21)
      COMMON /SREV/NUP,TIUP,NSOAK,TISK,NDN,TIDN,TSREV
C
C  ****  READ INPUT DATA  ****
C
  888 READ(KI,100)VOLT,AMP,EFF,THICK,V
      IF(VOLT EQ.0.0) GO TO 999
  100 FORMAT(5F10 4)
      READ(KI,110)(RAT(K),K=1,20)
  110 FORMAT(20A4)
      READ(KI,101)(TEMP(I),I=1,10)
     .READ(KI,101)(COND(I),I=1,10)
      READ(KI,101)(CAP (I),I=1,10)
      READ(KI,101)(RHO (I),I=1,10)
      READ(KI,101)(E   (I),I=1,10)
      READ(KI,101)(YP  (I),I=1,10)
      READ(KI,101)(ALPH(I),I=1,10)
      READ(KI,101)(SLOP(I),I=1,10)
  101 FORMAT(10F8.3)
      READ(KI,101)  (HCOT(I),I=1,10)
      READ(KI,104) NEDGE
C
C  ** NEDGE = 1 EDGE WELD ,0 BUTT WELD ,-1 BEAD ON PLATE **
C
```

```
0040                READ(KI,104) NPAS
0041          104   FORMAT(I2)
0042                READ(KI,101) (YPN(I),I=1,NPAS)
0043                READ(KI,105) ((YTHN(NP,I),I=1,11),NP=1,NPAS)
0044          105   FORMAT(11F7.4)
0045                DO 301 NP=1,NPAS
0046                DO 301 I=12,21
0047          301   YTHN(NP,I)=THICK
0048                READ(KI,102)YDIS,TMAX,TIX,TREF
0049          102   FORMAT(4F10.4)
0050                READ(KI,103)T1,TI1,T2,TI2,T3,TI3,TST
0051          103   FORMAT(7F10 2)
0052                READ(KI,103) TLAST
0053                READ(KI,109) NPC,N1,N2,N3
0054          109   FORMAT(4I5)
              C
              C     NPC = O TO PRINT AND PLOT,1 PRINT ONLY,2 PLOT ONLY
              C     PLOT THE FIRST N1,N2,N3 POINTS ONLY
              C     FOR TEMPERATURES,STRESSES,STRAINS RESPECTIVELY
              C
0055                READ (KI,191) ISREV
0056          191   FORMAT (I2)
              C
              C     ISREV = 1 FOR STRESS RELIEVING ,O FOR WELDING
              C
0057                IF(ISREV.EQ.O) GO TO 192
0058                READ (KI,171) ICREP,NUP,NSOAK,NDN,TIUP,TISK,TIDN,ISREV
0059          171   FORMAT(4I5,4F10 2)
              C
              C  ****  PRINT INPUT DATA  *****
              C
0060          192   WRITE(KO,223)(RAT(K),K=1,20)
0061          223   FORMAT(/18X,20A4/)
0062                WRITE(KO,266)
0063          266   FORMAT(////49X,'WELDING CONDITIONS'/)
0064                WRITE(KO,221)VOLT,AMP,EFF,V
0065          221   FORMAT(/24X,'VOLTS=',F6.2,'  AMPS=',F6.2,'  ARC EFF.=',F4.2,
                   1'  WELD SPEED =',F7.5,' (INCHES/SEC)')
0066                WRITE(KO,179) NEDGE
0067          179   FORMAT(/31X,'NEDGE =',I2,3X,'(1 FOR EDGE ,O FOR BUTT,-1 FOR BEAD O
                   1N PLATE)')
0068                WRITE(KO,224)
0069          224   FORMAT(/40X,35HMATERIAL PROPERTIES VS  TEMPERATURE/)
0070                WRITE(KO,250)(TEMP(I),I=1,10)
0071          250   FORMAT(/3X,11HTEMPERATURE,4X,10(F7.2,1X),5X,'(DEGREES F)')
0072                WRITE(KO,251)(COND(I),I=1,10)
0073          251   FORMAT(/3X,12HCONDUCTIVITY,3X,10F8.3,5X,'(WATTS/INCH/DEG F)')
0074                WRITE(KO,252)(CAP(I),I=1,10)
0075          252   FORMAT(/3X,'SPECIFIC HEAT',2X,10F8.3,5X,'(WATTS*SEC/POUND/DEG F)')
0076                WRITE(KO,253)(RHO(K),K=1,10)
0077          253   FORMAT(/5X,7HDENSITY,6X,10F8.4,5X,'(POUNDS/CUBIC INCH)')
0078                WRITE(KO,254)(E(I),I=1,10)
0079          254   FORMAT(/1X,15HYOUNG S MODULUS,2X,10F8.3,5X,'(KSI*10**3)')
```

```
FORTRAN IV G1  RELEASE 2 0             MAIN              DATE = 82126          14/42/06              PAGE 0003

0080              WRITE(KO,255)(YP(I),I=1,10)                                        JOHO1070
0081        255   FORMAT(/2X,'INITIAL YIELD',3X,10F8.3,5X,'(KSI)'/6X,'STRESS')       JOHO1080
0082              WRITE(KO,256)(ALPH(I),I=1,10)                                      JOHO1090
0083        256   FORMAT(/2X,'COEFFICIENT OF',2X,10F8.3,5X,                          JOHO1100
                 1'(MICRO INCHES/INCH/DEG F)'/4X,'EXPANSION')                        JOHO1110
0084              WRITE(KO,257) (SLOP(I),I=1,10)                                     JOHO1120
0085        257   FORMAT(/' TANGENT MODULUS ',1X,10F8 3,5X,'(KSI*10**3)')            JOHO1130
0086              WRITE(KO,280) (HCOT(I),I=1,10)                                     JOHO1140
0087        280   FORMAT(/1X,'SURFACE HEAT LOSS',10F8.3,5X,'(WATTS/INCH/DEG F)'/4X,  JOHO1150
                 1'COEFFICIENT')                                                     JOHO1160
0088              WRITE (KO,175) TMAX                                                JOHO1170
0089        175   FORMAT(/1X,'MELTING TEMPERATURE (DEG F) = ',F8.2)                  JOHO1180
0090              WRITE (KO,176) TREF                                                JOHO1190
0091        176   FORMAT(/1X,'REFERENCE TEMPERATURE (DEG F) = ',F8.2)                JOHO1200
0092              WRITE (KO,177)                                                     JOHO1210
0093              WRITE (KO,178) THICK,YDIS                                          JOHO1220
0094        177   FORMAT(//49X,'PLATE GEOMETRY'/)                                    JOHO1230
0095        178   FORMAT(/40X,'PLATE THICKNESS (INCHES) =',F6.3/                     JOHO1240
                 140X,'PLATE WIDTH  (INCHES) =',F7.2)                                JOHO1250
0096              WRITE(KO,271) NPAS                                                 JOHO1260
0097        271   FORMAT(1H1//2X,'NUMBER OF WELDING PASSES = ',I2)                   JOHO1270
0098              WRITE(KO,272) (YPN(I),I=1,NPAS)                                    JOHO1280
0099        272   FORMAT(1HO, 10X,'POSITION OF WELDING ARC FROM CENTER (INCHES)',//  JOHO1290
                 * 11X,'PASS NO     1        2        3        4        5        6   JOHO1300
                 *7        8        9',/19X,9F8.3,/)                                 JOHO1310
0100               WRITE(KO,273) (NP,(YTHN(NP,I),I=1,11),NP=1,NPAS)                  JOHO1320
0101        273   FORMAT(1HO,10X,'CHANGE OF JOINT SHAPE BY EFFECT OF MULTIPASS ',/   JOHO1330
                 */( 4X,'PASS=',I2,11F8.3/) )                                        JOHO1340
0102              YD(1)=0.0                                                          JOHO1350
0103              DO 1 J=2,21                                                        JOHO1360
0104          1   YD(J)=Y(J)+YDIS                                                    JOHO1370
0105              WRITE(KO,274)  (YD(J),J=1,11),(YD(J),J=13,21,2)                    JOHO1380
0106        274   FORMAT(//3X,'LOCATION',5X,16F7.3)                                  JOHO1390
            C                                                                        JOHO1400
            C     WELDING HEAT INPUT CALCULATION                                     JOHO1410
            C                                                                        JOHO1420
0107              P=EFF*VOLT*AMP/THICK                                               JOHO1430
0108              IF(NEDGE.GE  1)  P=2.0*P                                           JOHO1440
            C                                                                        JOHO1450
            C     TIME STEPS CALCULATION                                             JOHO1460
            C                                                                        JOHO1470
0109              TI=TI1                                                             JOHO1480
0110              N=1                                                                JOHO1490
0111              T(1)=TST                                                           JOHO1500
0112         40   IF(T(N).GE T1) TI=TI2                                              JOHO1510
0113              IF(T(N) GE.T2) TI=TI3                                              JOHO1520
0114              IF(T(N) GE.T3) GO TO 41                                            JOHO1530
0115              T(N+1)=T(N)+TI                                                     JOHO1540
0116              N=N+1                                                              JOHO1550
0117              GO TO 40                                                           JOHO1560
0118         41   CONTINUE                                                           JOHO1570
0119              N=N+1                                                              JOHO1580
0120              T(N)=TLAST                                                         JOHO1590
```

```
FORTRAN IV G1  RELEASE 2.0              MAIN              DATE = 82126          14/42/06              PAGE 0004

0121        55     WRITE(KO,181)                                                              JOHO1600
0122       181     FORMAT(1H1/49X,'TIME STEP INFORMATION')                                    JOHO1610
0123               WRITE(KO,259)T1,TI1,T2,TI2,T3,TI3,TST                                      JOHO1620
0124       259     FORMAT(/5X,'T1=',F7 1,'  TI1= ',F7.1,'  T2=',F7.1,'  TI2=',F7.1,          JOHO1630
                  *'  T3=',F7.1,'  TI3=',F7.1,'  TST=',F7.1)                                   JOHO1640
                                                                                              JOHO1650
0125               WRITE(KO,211) TIX                                                          JOHO1660
0126       211     FORMAT(//1X,'ARC PASSES FROM OBSERVATION SECTION AT T=',F8 2,               JOHO1670
                  1' SECS')                                                                   JOHO1680
0127               WRITE(6,1226) (T(IJK),IJK=1,N)                                             JOHO1690
0128      1226     FORMAT(1H ,'T(I)=',15(/1X,10F10 2))                                        JOHO1700
0129               WRITE(KO,182)                                                              JOHO1710
0130       182     FORMAT(1H1//49X,'***** WELDING *****'//)                                   JOHO1720
0131               WRITE(KO,210)(YD(J),J=1,11),(YD(J),J=13,21,2)                              JOHO1730
0132       210     FORMAT(37X,46HTRANSVERSE DISTANCE FROM CENTER LINE IN INCHES//             JOHO1740
                  1    16X,16F7.3)                                                            JOHO1750
0133               TMAX=TEMP(10)                                                              JOHO1760
           C                                                                                  JOHO1770
           C       CHANGE UNITS TO PSI AND INCH/INCH                                          JOHO1780
           C                                                                                  JOHO1790
0134               DO 50 I=1,10                                                               JOHO1800
0135               E(I)=E(I)*1000000.                                                         JOHO1810
0136               YP(I)=YP(I)*1000.                                                          JOHO1820
0137        50     ALPH(I)=ALPH(I)/1000000.                                                   JOHO1830
0138               YEP=YP(1)/E(1)                                                             JOHO1840
0139               YOUT=YEP*1000.0                                                            JOHO1850
0140               DO  668 J=1,21                                                             JOHO1860
0141               TREFN(1,J)=TREF                                                            JOHO1870
0142       668     CONTINUE                                                                   JOHO1880
0143               DO 51 J=1,21                                                               JOHO1890
0144               ECREEP(J)=0.0                                                              JOHO1900
0145        51     EPO(J)=0.0                                                                 JOHO1910
           C                                                                                  JOHO1920
           C       LOOP FOR ALL WELD PASSES                                                   JOHO1930
           C                                                                                  JOHO1940
0146               DO  666  K=1,NPAS                                                          JOHO1950
           C                                                                                  JOHO1960
           C       LOOP FOR ALL TIME STEPS                                                    JOHO1970
           C                                                                                  JOHO1980
0147               DO 777 I=1,N                                                               JOHO1990
0148               XT=(TIX-T(I))*V                                                            JOHO2000
           C                                                                                  JOHO2010
           C       CALCULATE TEMPERATURE HISTORY DURING WELDING                               JOHO2020
           C                                                                                  JOHO2030
0149               CALL   TEMP1(XT,K)                                                         JOHO2040
           C                                                                                  JOHO2050
           C       CALCULATE STRESSES DURING WELDING                                          JOHO2060
           C                                                                                  JOHO2070
0150               CALL   STRESS(K,I)                                                         JOHO2080
           C                                                                                  JOHO2090
           C       STORE TEMPERATURES STRAINS AND STRESSES FOR PLOTTING                       JOHO2100
           C                                                                                  JOHO2110
0151               TY1(I)=TY(1)                                                               JOHO2120
0152               TY7(I)=TY(7)
```

```
      TY9(I)=TY(9)
      TY11(I)=TY(11)
      TY15(I)=TY(15)
      TY18(I)=TY(18)
      ST1(I)=STRES(1)
      ST7(I)=STRES(7)
      ST9(I)=STRES(9)
      ST11(I)=STRES(11)
      ST15(I)=STRES(15)
      ST18(I)=STRES(18)
      EM1(I)=EM(1)
      EM7(I)=EM(7)
      EM9(I)=EM(9)
      EM11(I)=EM(11)
      EM15(I)=EM(15)
      EM18(I)=EM(18)
C
C     PRINT TEMPERATURES   IN DEGREES F
C           STRAINS        IN INCHES/INCH *10**-3
C           STRESSES       IN KSI
C
      IF(NPC.EQ.2) GO TO 777
      I5=(I/5)*5
      IF(I.NE.I5) GO TO 711
      WRITE(KO,274)  (YD(J),J=1,11),(YD(J),J=13,21,2)
  711 CONTINUE
      WRITE(KO,277) T(I)
  277 FORMAT( //1X,5HTIME=,F8.2,5X,'SECS')
      WRITE(KO,299)  K
 299  FORMAT(1H+,35X,'PASS NO ',I2)
  555 WRITE(KO,200)(TY(J),J=1,11),(TY(J),J=13,21,2)
      WRITE(KO,234)(EL(J),J=1,11),(EL(J),J=13,21,2)
  200 FORMAT(/16H TEMPERATURE     ,16F7.2)
      WRITE(KO,235)(EPN(J),J=1,11),(EPN(J),J=13,21,2)
      WRITE(KO,189)(ECREEP(J),J=1,11),(ECREEP(J),J=13,21,2)
      WRITE(KO,239) (EM(J),J=1,11),(EM(J),J=13,21,2)
      WRITE(KO,236) (EX(J),J=1,11),(EX(J),J=13,21,2)
      WRITE(KO,233)(STRES(J),J=1,11),(STRES(J),J=13,21,2)
  234 FORMAT( 16H ELASTIC STRAIN ,16F7.3)
 189  FORMAT( 16H CREEP STRAIN   ,16F7 3)
  235 FORMAT( 16H PLASTIC STRAIN ,16F7.3)
  239 FORMAT( 13H MECH. STRAIN,3X,16F7.3)
  236 FORMAT( 13H TOTAL STRAIN,3X,16F7.3)
  233 FORMAT( 7H STRESS,9X,16F7.2)
 777  CONTINUE
      DO 667  J=1,21
 667  TREFN(K+1,J)=TY(J)
  666 CONTINUE
      DO 987  IPL =1,21
 987  STRPL(IPL)= STRES(IPL)
      TPL(1)=TY(1)
      TME(1)=0.0
      SSS1(1)=STRES(1)
```

```
FORTRAN IV G1  RELEASE 2.0            MAIN            DATE = 82126        14/42/06            PAGE 0006

0201              SSS7(1)=STRES(7)                                                     J0H02660
0202              SSS9(1)=STRES(9)                                                     J0H02670
0203              SSS11(1)=STRES(11)                                                   J0H02680
0204              SSS15(1)=STRES(15)                                                   J0H02690
0205              SSS18(1)=STRES(18)                                                   J0H02700
0206              EMM1(1)=EM(1)                                                        J0H02710
0207              EMM7(1)=EM(7)                                                        J0H02720
0208              EMM9(1)=EM(9)                                                        J0H02730
0209              EMM11(1)=EM(11)                                                      J0H02740
0210              EMM15(1)=EM(15)                                                      J0H02750
0211              EMM18(1)=EM(18)                                                      J0H02760
            C                                                                          J0H02770
            C  ****  STRESS RELIEVING BY UNIFORM HEATING  ****                         J0H02780
            C                                                                          J0H02790
0212              IF(ISREV EQ.O) GO TO 9090                                            J0H02800
0213              NSREV=NUP+NSOAK+NDN                                                  J0H02810
0214              WRITE(KO,172)                                                        J0H02820
0215        172   FORMAT(1H1//49X,'****** STRESS RELIEVING ******'//)                  J0H02830
0216              WRITE (KO,183) ICREP                                                 J0H02840
0217        183   FORMAT(//37X,'ICREP=',I5,' (O IF CREEP IS IGNORED,1 IF INCLUDED)')J0H02850
0218              WRITE(KO,184) TSREV                                                  J0H02860
0219        184   FORMAT (/37X,'STRESS RELIEVING TEMPERATURE (DEG F) =',F10.2)         J0H02870
0220              WRITE (KO,185) NUP,TIUP,NSOAK,TISK,NDN,TIDN                          J0H02880
0221        185   FORMAT(/37X,'TEMPERATURE HISTORY PARAMETERS '/37X,                   J0H02890
                 18X,'NUMBER OF STEPS',3X,'STEP SIZE IN SECONDS'/37X,                  J0H02900
                 2'HEATING',5X,I5,13X,F10.2/37X,'HOLDING',5X,I5,13X,                   J0H02910
                 3F10.2/37X,'COOLING',5X,I5,13X,F10.2/)                                J0H02920
0222              WRITE(KO,210)(YD(J),J=1,11),(YD(J),J=13,21,2)                        J0H02930
0223              DO 331 I=1,NSREV                                                     J0H02940
0224              IS=I+N                                                               J0H02950
0225              IF(I.GT.NUP) GO TO 3331                                              J0H02960
0226              DO 3019 J=1,21                                                       J0H02970
0227        3019   TY(J)=(TSREV-TREF)*FLOAT(I)/FLOAT(NUP)+TREF                         J0H02980
0228              T(IS)=T(N)+TIUP*FLOAT(I)                                             J0H02990
0229              CALL STRESS(1,IS)                                                    J0H03000
0230              DO 3099 J=1,21                                                       J0H03010
0231        3099  STRHT(J)=STRES(J)                                                    J0H03020
0232              GO TO 330                                                            J0H03030
0233        3331  IF(I.GT.(NUP+NSOAK)) GO TO 3332                                      J0H03040
0234              DO 302 J=1,21                                                        J0H03050
0235        302   TY(J)=TSREV                                                          J0H03060
0236              T(IS)=T(N)+TIUP*FLOAT(NUP)+TISK*FLOAT(I-NUP)                         J0H03070
0237              IF(ICREP.EQ.1) GO TO 3021                                            J0H03080
0238              CALL STRESS(1,IS)                                                    J0H03090
0239              GO TO 3301                                                           J0H03100
0240        3021  CALL STCRP(IS)                                                       J0H03110
0241        3301  DO 3302 J=1,21                                                       J0H03120
0242        3302  STRSK(J)=STRES(J)                                                    J0H03130
0243              GO TO 330                                                            J0H03140
0244        3332  DO 303 J=1,21                                                        J0H03150
0245        303   TY(J)=(TSREV-TREF)*FLOAT(NSREV-I)/FLOAT(NDN)+TREF                    J0H03160
0246              INU=I-NUP-NSOAK                                                      J0H03170
0247              T(IS)=T(N)+TIUP*FLOAT(NUP)+TISK*FLOAT(NSOAK)+TIDN*FLOAT(INU)         J0H03180
```

```
            CALL STRESS(1,IS)                                                  J0H03190
      C                                                                        J0H03200
      C ***  PRINT TEMPERATURES (DEG F), STRAINS (*1000), STRESSES (KSI)    ***J0H03210
      C                                                                        J0H03220
      330   IF(NPC.EQ 2) GO TO 194                                             J0H03230
            I5=(I/5)*5                                                         J0H03240
            IF (I.NE I5) GO TO 332                                             J0H03250
            WRITE (KO,274)(YD(J),J=1,11),(YD(J),J=13,21,2)                     J0H03260
      332   CONTINUE                                                           J0H03270
            WRITE(KO,277) T(IS)                                                J0H03280
            WRITE (KO,200)(TY(J),J=1,11),(TY(J),J=13,21,2)                     J0H03290
            WRITE (KO,234)(EL(J),J=1,11),(EL(J),J=13,21,2)                     J0H03300
            WRITE(KO,235)(EPN(J),J=1,11),(EPN(J),J=13,21,2)                    J0H03310
            WRITE (KO,189)(ECREEP(J),J=1,11),(ECREEP(J),J=13,21,2)             J0H03320
            WRITE (KO,239)(EM(J),J=1,11),(EM(J),J=13,21,2)                     J0H03330
            WRITE (KO,236)(EX(J),J=1,11),(EX(J),J=13,21,2)                     J0H03340
            WRITE(KO,233)(STRES(J),J=1,11),(STRES(J),J=13,21,2)                J0H03350
      194   TPL(I+1)=TY(1)                                                     J0H03360
            TME(I+1)=(T(IS)-T(N))/3600.                                        J0H03370
            SSS1(I+1)=STRES(1)                                                 J0H03380
            SSS7(I+1)=STRES(7)                                                 J0H03390
            SSS9(I+1)=STRES(9)                                                 J0H03400
            SSS11(I+1)=STRES(11)                                               J0H03410
            SSS15(I+1)=STRES(15)                                               J0H03420
            SSS18(I+1)=STRES(18)                                               J0H03430
            EMM1(I+1)=EM(1)                                                    J0H03440
            EMM7(I+1)=EM(7)                                                    J0H03450
            EMM9(I+1)=EM(9)                                                    J0H03460
            EMM11(I+1)=EM(11)                                                  J0H03470
            EMM15(I+1)=EM(15)                                                  J0H03480
            EMM18(I+1)=EM(18)                                                  J0H03490
      331   CONTINUE                                                           J0H03500
            NSREV1=NSREV+1                                                     J0H03510
      C                                                                        J0H03520
      C                        PLOTTING PHASE                                  J0H03530
      C                                                                        J0H03540
      C     USE CALCOMP PLOTTER SUBROUTINES ON IBM VM/370                      J0H03550
      C                                                                        J0H03560
      9090  IF(NPC.EQ.1) GO TO 9991                                            J0H03570
            CALL PLOTS (120,IDUM,25)                                           J0H03590
      C                                                                        J0H03600
      C     WELDING PART                                                       J0H03610
      C     PLOT THE FIRST N1,N2,N3 TIME STEPS                                 J0H03620
      C     FOR TEMPERATURES,STRESSES AND STRAINS RESPECTIVELY                 J0H03630
      C                                                                        J0H03640
            CALL PLOT(3.0,0.0,3)                                               J0H03650
            CALL SYMBOL(7 15,3.05, 05,1,0 0,-1)                                J0H03660
            CALL SYMBOL(7 4,3.0,.07,'AT 0 5 INCHES',0 0,13)                    J0H03670
            CALL SYMBOL(7.15,2 55,.05,2,0.0,-1)                                J0H03680
            CALL SYMBOL(7 4,2.5,.07,'AT 1.0 INCHES',0 0,13)                    J0H03690
            CALL SYMBOL(7.15,2 05,.05,3,0 0,-1)                                J0H03700
            CALL SYMBOL(7.4,2.0,.07,'AT 1 5 INCHES',0 0,13)                    J0H03710
            CALL SYMBOL(7.15,1 55,.05,4,0 0,-1)                                J0H03720
```

```
                                                                                JOHO3730
0288          CALL SYMBOL(7 4,1 5, 07,'AT 2.0 INCHES',0 0,13)                   JOHO3740
0289          CALL SYMBOL(7 15,1.05, 05,5,0.0,-1)                               JOHO3750
0290          CALL SYMBOL(7 4,1.0, 07,'AT 3 O INCHES',0 0,13)                   JOHO3760
0291          CALL PLOT(3.0,0.0,3)                                              JOHO3770
0292          CALL PICTUR(7.0,5 0,'TIME (SECS)',11,                             JOHO3780
             1'WELDING TEMPERATURES (DEGF)',27,T,TY7,N1,.05,1,T,TY9,N1, 05,2,   JOHO3790
             2T,TY11,N1,.05,3,T,TY15,N1, 05,4,T,TY18,N1, 05,5)                  JOHO3800
0293          CALL PLOT(3.0,0 0,3)                                              JOHO3810
0294          CALL SYMBOL(7.15,3.05,.05,1,0 0,-1)                               JOHO3820
0295          CALL SYMBOL(7 4,3.0,.07,'AT 0.5 INCHES',0 0,13)                   JOHO3830
0296          CALL SYMBOL(7 15,2.55,.05,2,0 0,-1)                               JOHO3840
0297          CALL SYMBOL(7.4,2 5,.07,'AT 1.0 INCHES',0 0,13)                   JOHO3850
0298          CALL SYMBOL(7 15,2.05, 05,3,0.0,-1)                               JOHO3860
0299          CALL SYMBOL(7 4,2.0,.07,'AT 1 5 INCHES',0 0,13)                   JOHO3870
0300          CALL SYMBOL(7 15,1.55,.05,4,0 0,-1)                               JOHO3880
0301          CALL SYMBOL(7.4,1.5,.07,'AT 2.0 INCHES',0 0,13)                   JOHO3890
0302          CALL SYMBOL(7.15,1.05,.05,5,0 0,-1)                               JOHO3900
0303          CALL SYMBOL(7.4,1.0,.07,'AT 3 O INCHES',0 0,13)                   JOHO3910
0304          CALL PLOT(3.0,0.0,3)                                              JOHO3920
0305          CALL PICTUR(7.0,5.0,'TIME (SECS)',11,                             JOHO3930
             1'WELDING STRESSES (KSI)',22,T,ST7,N2,.05,1,T,ST9,N2,.05,2,        JOHO3940
             2T,ST11,N2,.05,3,T,ST15,N2, 05,4,T,ST18,N2, 05,5)                  JOHO3950
0306          CALL PLOT(3.0,0.0,3)                                              JOHO3960
0307          CALL SYMBOL(7.15,3.05,.05,1,0.0, 1)                               JOHO3970
0308          CALL SYMBOL(7 4,3.0,.07,'AT 0.5 INCHES',0 0,13)                   JOHO3980
0309          CALL SYMBOL(7.15,2.55, 05,2,0.0,-1)                               JOHO3990
0310          CALL SYMBOL(7 4,2.5,.07,'AT 1.0 INCHES',0 0,13)                   JOHO4000
0311          CALL SYMBOL(7 15,2.05,.05,3,0 0,-1)                               JOHO4010
0312          CALL SYMBOL(7.4,2 0,.07,'AT 1.5 INCHES',0 0,13)                   JOHO4020
0313          CALL SYMBOL(7.15,1.55,.05,4,0.0,-1)                               JOHO4030
0314          CALL SYMBOL(7.4,1.5, 07,'AT 2.0 INCHES',0 0,13)                   JOHO4040
0315          CALL SYMBOL(7.15,1.05,.05,5,0 0,-1)                               JOHO4050
0316          CALL SYMBOL(7.4,1.0, 07,'AT 3 O INCHES',0.0,13)                   JOHO4060
0317          CALL PLOT(3.0,0 0,3)                                              JOHO4070
0318          CALL PICTUR(7.0,5.0,'TIME (SECS)',11,                             JOHO4080
             1'MECHANICAL STRAINS (X 1000)',27,T,EM7,N3, 05,1,T,EM9,N3,.05,2,   JOHO4090
             2T,EM11,N3,.05,3,T,EM15,N3,0 05,4,T,EM18,N3,.05,5)                 JOHO4100
0319          IF (ISREV.EQ.0) GO TO 9091                                        JOHO4110
        C                                                                       JOHO4120
        C     STRESS RELIEVING PART                                             JOHO4130
        C                                                                       JOHO4140
0320          CALL PLOT(3.0,0 0,3)                                              JOHO4150
0321          CALL PICTUR(7.0,5 0,'TIME (HOURS)',12,                            JOHO4160
             1'RELIEVING TEMPERATURE (DEGF)',28,TME,TPL,NSREV1,0 0,0)           JOHO4170
0322          CALL PLOT(3.0,0 0,3)                                              JOHO4180
0323          CALL SYMBOL(7 15,3.05,.05,1,0 0,-1)                               JOHO4190
0324          CALL SYMBOL(7.4,3.0,.07,'AT 0.5 INCHES',0 0,13)                   JOHO4200
0325          CALL SYMBOL(7 15,2.55,.05,2,0.0,-1)                               JOHO4210
0326          CALL SYMBOL(7.4,2.5,.07,'AT 1.0 INCHES',0.0,13)                   JOHO4220
0327          CALL SYMBOL(7.15,2.05,.05,3,0.0,-1)                               JOHO4230
0328          CALL SYMBOL(7 4,2.0, 07,'AT 1.5 INCHES',0 0,13)                   JOHO4240
0329          CALL SYMBOL(7.15,1.55,.05,4,0.0,-1)                               JOHO4250
0330          CALL SYMBOL(7 4,1.5, 07,'AT 2.0 INCHES',0 0,13)
```

```
FORTRAN IV G1  RELEASE 2.0           MAIN            DA'E = 82126         14/42/06              PAGE 0009
0331                CALL SYMBOL(7.15,1.05,.05,5,0.0,-1)                                      J0H04260
0332                CALL SYMBOL(7.4,1.0,.07,'AT 3.0 INCHES',0.0,13)                          J0H04270
0333                CALL PLOT(3.0,0 0,3)                                                     J0H04280
0334                CALL PICTUR(7.0,5 0,'TIME (HOURS)',12,                                   J0H04290
                   1' STRESSES (KSI)',15,TME,SSS7,NSREV1,0 05,1,TME,SSS9,NSREV1, 05,2,J0H04300
                   2TME,SSS11,NSREV1,0 05,3,TME,SSS15,NSREV1,.05,4,TME,SSS18,NSREV1,  J0H04310
                   3.05,5)                                                            J0H04320
0335                CALL PLOT(3.0,0.0,3)                                                     J0H04330
0336                CALL SYMBOL(7.15,3.05,.05,1,0.0,-1)                                      J0H04340
0337                CALL SYMBOL(7 4,3.0,.07,'AT 0 5 INCHES',0.0,13)                          J0H04350
0338                CALL SYMBOL(7 15,2.55,.05,2,0.0,-1)                                      J0H04360
0339                CALL SYMBOL(7.4,2.5,.07,'AT 1.0 INCHES',0.0,13)                          J0H04370
0340                CALL SYMBOL(7.15,2 05,.05,3,0.0,-1)                                      J0H04380
0341                CALL SYMBOL(7.4,2.0,.07,'AT 1.5 INCHES',0 0,13)                          J0H04390
0342                CALL SYMBOL(7 15,1 55,.05,4,0.0,-1)                                      J0H04400
0343                CALL SYMBOL(7.4,1.5,.07,'AT 2.0 INCHES',0.0,13)                          J0H04410
0344                CALL SYMBOL(7.15,1.05,.05,5,0.0,-1)                                      J0H04420
0345                CALL SYMBOL(7.4,1.0,.07,'AT 3 0 INCHES',0.0,13)                          J0H04430
0346                CALL PLOT(3.0,0.0,3)                                                     J0H04440
0347                CALL PICTUR(7.0,5.0,'TIME (HOURS)',12,                                   J0H04450
                   1' MECHANICAL STRAINS (X 1000)',28,TME,EMM7,NSREV1,.05,1,            J0H04460
                   2TME,EMM9,NSREV1,.05,2,TME,EMM11,NSREV1,.05,3,TME,EMM15,NSREV1,.05,J0H04470
                   34,TME,EMM18,NSREV1,.05,5)                                         J0H04480
0348                CALL PLOT(3.0,0.0,3)                                                     J0H04490
0349                CALL SYMBOL(7.15,3.05,.05,0,0.0,-1)                                      J0H04500
0350                CALL SYMBOL(7.4,3.0,.07,'AFTER WELDING',0.0,13)                          J0H04510
0351                CALL SYMBOL(7.15,2.55,.05,1,0.0,-1)                                      J0H04520
0352                CALL SYMBOL(7.4,2.5,.07,'AFTER HEATING',0.0,13)                          J0H04530
0353                CALL SYMBOL(7.15,2.05, 05,2,0 0,-1)                                      J0H04540
0354                CALL SYMBOL(7.4,2.0,.07,'AFTER SOAKING',0.0,13)                          J0H04550
0355                CALL SYMBOL(7.15,1.55,.05,3,0.0,-1)                                      J0H04560
0356                CALL SYMBOL(7.4,1.5, 07,'AFTER COOLING',0.0,13)                          J0H04570
0357                CALL PLOT(3.0,0.0,3)                                                     J0H04580
0358                CALL PICTUR(7.0,5.0,'TRANSVERSE DISTANCE (INCHES)',28,                   J0H04590
                   1'REMAINING STRESSES (KSI)',24,YD,STRPL,21, 05,0,YD,STRHT,21, 05,1,J0H04600
                   2YD,STRSK,21,.05,2,YD,STRES,21,.05,3)                              J0H04610
0359         9091   CALL ENDPLT (11.0,0.0,999)                                               J0H04620
0360         9991   GO TO 888                                                                J0H04630
0361         999    CONTINUE                                                                 J0H04640
0362                STOP                                                                     J0H04650
0363                END                                                                      J0H04660
```

```
FORTRAN IV G1  RELEASE 2 0            TEMP1             DATE = 82126          14/42/06              PAGE 0001
                                                                                          J0H04670
0001                SUBROUTINE  TEMP1(XT,K)                                               J0H04680
              C                                                                           J0H04690
              C  ****  TEMPERATURE DISTRIBUTION DURING WELDING  ****                      J0H04700
              C                                                                           J0H04710
0002                DIMENSION  YB(8)                                                      J0H04720
0003                COMMON /TEM/TY(21),TEMP(10),CAP(10),RHO(10),COND(10),TREFN(10,21)     J0H04730
0004                COMMON /E/E(10),YP(10),ALPH(10),SLOP(10)                              J0H04740
0005                COMMON /ST/RAT(20),T(2000),EX(21),EM(21),EPN(21),STRES(21),EL(21)     J0H04750
0006                COMMON /YW/Y(21),YD(21)                                               J0H04760
0007                COMMON  /YP/YPN(10),YTHN(10,21)                                       J0H04770
0008                COMMON /PP/P,V,YS,YEP,YOUT,THICK                                      J0H04780
0009                COMMON /SC/NEDGE,HCOT(10)                                             J0H04790
0010                COMMON /P/YDIS,TMAX,TIX,TREF                                          J0H04800
0011                COMMON /T/T1,TI1,T2,TI2,T3,TI3,TST                                    J0H04810
0012                COMMON /IO/KI,KO                                                      J0H04820
0013                YS=YPN(K)                                                             J0H04830
0014                DO 70 J=1,21                                                          J0H04840
0015                YT=YD(J)                                                              J0H04850
0016                YT=YT+YS                                                              J0H04860
0017                DO 20 NN=1,4                                                          J0H04870
0018                NP=2*(NN-1)                                                           J0H04880
0019                NM=-2*NN                                                              J0H04890
0020                YB(NN)=YT+FLOAT(NP)*(YDIS-YS)                                         J0H04900
0021                NN1=NN+4                                                              J0H04910
0022                YB(NN1)=YT+FLOAT(NM)*(YDIS+YS)                                        J0H04920
0023             20 CONTINUE                                                              J0H04930
0024                R=SQRT(XT*XT+YT*YT)                                                   J0H04940
0025                IF(R-0.001)  410,410,411                                              J0H04950
0026           410  TN=TMAX                                                               J0H04960
0027                GO TO 11                                                              J0H04970
0028           411  CON=COND(4)                                                           J0H04980
0029                CA=CAP(4)                                                             J0H04990
0030                RH=RHO(4)                                                             J0H05000
0031                HCON=HCOT(4)                                                          J0H05010
0032                TO=TREFN(K,J)                                                         J0H05020
0033                IT=0                                                                  J0H05030
0034            10  CONTINUE                                                              J0H05040
0035                IT=IT+1                                                               J0H05050
0036                CON=CON+YTHN(K,J)/THICK                                               J0H05060
0037                RH =RH +YTHN(K,J)/THICK                                               J0H05070
0038                C1=V*CA*RH/2.0/CON                                                    J0H05080
0039                C2=P/6.28318/CON                                                      J0H05090
0040                RV2=C1*C1+HCON/CON/THICK                                              J0H05100
0041                RV=SQRT(RV2)                                                          J0H05110
0042                EK=0.0                                                                J0H05120
0043                DO  45    JJ=1,8                                                      J0H05130
0044                YT=YB(JJ)                                                             J0H05140
0045                R=SQRT(XT*XT+YT*YT)                                                   J0H05150
0046                ZZ=RV*R                                                               J0H05160
0047                Z=-1.0*C1*XT                                                          J0H05170
0048                CALL  RBES(ZZ,Z,EKR,B)                                                J0H05180
0049                EK=EK+EKR                                                             J0[illegible]5190
0050            45  CONTINUE
```

```
FORTRAN IV G1  RELEASE 2.0          TEMP1          DATE = U2126          14/42/06          PAGE 0002

                                                                                   JOH05200
           TN=C2*EK                                                                JOH05210
      44   TN=TN+TREFN(K,J)                                                        JOH05220
           IF(TN.GT.TMAX) TN=TMAX                                                  JOH05230
           AB=ABS(TN-TO)                                                           JOH05240
           IF(AB-0.5)11,11,12                                                      JOH05250
      12   TM=(TO+TN)/2.0                                                          JOH05260
           IF(IT.GT.90) GO TO 998                                                  JOH05270
           TO=TN                                                                   JOH05280
           CON=FILLIN(TM,TEMP,COND,10)                                             JOH05290
           HCON=FILLIN(TM,TEMP,HCOT,10)                                            JOH05300
           CA =FILLIN(TM,TEMP,CAP  ,10)                                            JOH05310
           RH =FILLIN(TM,TEMP,RHO  ,10)                                            JOH05320
           GO TO 10                                                                JOH05330
      11   TY(J)=TN                                                                JOH05340
           GO TO 888                                                               JOH05350
     998   WRITE(KO,298)     J,TM,TO,TN                                            JOH05360
     298   FORMAT(/1X,22HTEMP DOES NOT CONVERGE ,'  J=',I2,'  TM,TO,TN= ',         JOH05370
          *3F10.2,'****** USED TM ******')                                         JOH05380
           TY(J)=TM                                                                JOH05390
     888   CONTINUE                                                                JOH05400
      70   CONTINUE                                                                JOH05410
           RETURN                                                                  JOH05420
           END
```

```
FORTRAN IV G1  RELEASE 2.0            RBES              DATE = 82126          14/42/06            PAGE 0001

                                                                                        J0H05430
0001                SUBROUTINE  RBES(ZZ,Z,EK,B)                                         J0H05440
0002                IF(ZZ-155.0) 42,42,43                                               J0H05450
0003          43    Q=2./ZZ                                                             J0H05460
0004                QQ=Q*Q                                                              J0H05470
0005                QQQ=QQ*Q                                                            J0H05480
0006                IF((Z-ZZ).LT.-170 0) GO TO 45                                       J0H05490
0007                EK=EXP(Z-ZZ)*(1.253314  -.0783235 *Q+.0218956 *QQ-.0106244 *QQQ+.0J0H05500
                   105878  *QQ*QQ-.0025154*QQQ*QQ+.0005320 *QQQ*QQQ)/SQRT(ZZ)           J0H05510
0008                B=0.0                                                               J0H05520
0009                RETURN                                                              J0H05530
0010          42    CALL BES(ZZ,B)                                                      J0H05540
0011                IF(Z.LE.-15.0) Z=-15.0                                              J0H05550
0012                EK=B*EXP(Z)                                                         J0H05560
0013                RETURN                                                              J0H05570
0014          45    EK=0.0                                                              J0H05580
0015                RETURN                                                              J0H05590
0016                END
```

```
FORTRAN IV G1  RELEASE 2.0              STRESS             DATE = 82126          14/42/06              PAGE 0001
                                                                                                 J0H05600
0001              SUBROUTINE  STRESS(K,I)                                                        J0H05610
            C                                                                                    J0H05620
            C  ****  STRESS ANALYSIS (WELDING ,HEATING ,COOLING)  ****                           J0H05630
            C                                                                                    J0H05640
0002              DIMENSION H2(21),CAT(20),H1(21)                                                J0H05650
0003              DIMENSION  EYN(21),HE(21),H(21),HTE(21),HTEY(21),A(21)                         J0H05660
0004              DIMENSION  SY(21),SPS(21),TAU(21),EPLA(21),ECR(21)                             J0H05670
0005              COMMON /TEM/TY(21),TEMP(10),CAP(10),RHO(10),COND(10),TREFN(10,21)              J0H05680
0006              COMMON /E/E(10),YP(10),ALPH(10),SLOP(10)                                       J0H05690
0007              COMMON /ST/RAT(20),T(2000),EX(21),EM(21),EPN(21),STRES(21),EL(21)              J0H05700
0008              COMMON /YW/Y(21),YD(21)                                                        J0H05710
0009              COMMON  /YP/YPN(10),YTHN(10,21)                                                J0H05720
0010              COMMON /PP/P,V,YS,YEP,YOUT,THICK                                               J0H05730
0011              COMMON /SC/NEDGE,HCOT(10)                                                      J0H05740
0012              COMMON  /RS/EPO(21)                                                            J0H05750
0013              COMMON /P/YDIS,TMAX,TIX,TREF                                                   J0H05760
0014              COMMON /T/T1,TI1,T2,TI2,T3,TI3,TST                                             J0H05770
0015              COMMON /IO/KI,KO                                                               J0H05780
0016              COMMON /CRP/ECREEP(21)                                                         J0H05790
0017              TAUEO=TREF*FILLIN(TREF,TEMP,ALPH,10)/YEP                                       J0H05800
0018              DO 70 J=1,21                                                                   J0H05810
0019              HE(J)=FILLIN(TY(J),TEMP,E,10)                                                  J0H05820
0020              H(J)=HE(J)/E(1)                                                                J0H05830
0021              A(J)=H(J)                                                                      J0H05840
0022              H(J)=A(J)*YTHN(K,J)/THICK                                                      J0H05850
0023              SY(J)=FILLIN(TY(J),TEMP,YP,10)/YP(1)                                           J0H05860
0024              SPS(J)=FILLIN(TY(J),TEMP,SLOP,10)                                              J0H05870
0025              TAU(J)=TY(J)*FILLIN(TY(J),TEMP,ALPH,10)/YEP                                    J0H05880
0026              TAU(J)=TAU(J)-TAUEO                                                            J0H05890
0027              ECR(J)=ECREEP(J)/YOUT                                                          J0H05900
0028          70  CONTINUE                                                                       J0H05910
0029              IF(NEDGE.GE. 1)  GO TO  630                                                    J0H05920
0030              IF(NEDGE.LE.-1)  GO TO  633                                                    J0H05930
0031              IF(K.NE 1)  GO TO 633                                                          J0H05940
0032              IF(T(I).LE.TIX) GO TO 630                                                      J0H05950
0033         633  CONTINUE                                                                       J0H05960
0034              IF(TY(1) GE.TMAX) GO TO 630                                                    J0H05970
0035              CALL QUDR(Y,O O,H,21,AI1,IERROR)                                               J0H05980
0036              A1=1.0/AI1                                                                     J0H05990
0037              GO TO 632                                                                      J0H06000
0038         630  DO 631 J=1,21                                                                  J0H06010
0039              H2(J)=H(J)*Y(J)                                                                J0H06020
0040         631  H1(J)=H(J)*Y(J)*Y(J)                                                           J0H06030
0041              CALL QUDR(Y,O O,H,21,AI3,IERROR)                                               J0H06040
0042              CALL QUDR(Y,O.O,H2,21,AI2,IERROR)                                              J0H06050
0043              CALL QUDR(Y,O.O,H1,21,AI1,IERROR)                                              J0H06060
0044              DEN=AI1*AI3-AI2*AI2                                                            J0H06070
0045              A1=AI1/DEN                                                                     J0H06080
0046              A2=AI2/DEN                                                                     J0H06090
0047              A3=AI3/DEN                                                                     J0H06100
0048         632  DO 61 J=1,21                                                                   J0H06110
0049              IF(A(J)) 48,48,49                                                              J0H06120
0050          48  EYN(J)=O.O
```

```
          SPS(J)=0
          HE(J)=1
          GO TO 61
   49     EYN(J)=SY(J)/A(J)
   61     EPLA(J)=0 0
          NC=0
  666     CONTINUE
          NC=NC+1
          IF(NC GT.20) GO TO 989
          DO 63 J=1,21
          HTE(J)=H(J)*(TAU(J)+EPLA(J)+ECR(J))
   63     HTEY(J)=HTE(J)*Y(J)
          CALL QUDR(Y,O.O,HTEY,21,TEYH,IERROR)
          CALL QUDR(Y,O.O,HTE,21,TEH,IERROR)
          DO 65 J=1,21
          IF(NEDGE GE. 1)  GO  TO  650
          IF(K.NE.1)  GO  TO  652
          IF(TY(1).GE.TMAX) GO TO 650
          IF(T(I) LE.TIX) GO TO 650
  652     CONTINUE
          EX(J)=A1*TEH
          GO TO 651
  650     EX(J)=(A1-Y(J)*A2)*TEH-(A2-Y(J)*A3)*TEYH
  651     EM(J)=EX(J)-TAU(J)
          IF(EPO(J)) 80,81,81
   81     IF(EM(J)) 82,83,83
   80     IF(EM(J)) 84,85,85
   84     EYN(J)=-1 O*EYN(J)
   83     IF(ABS(EM(J)).GT ABS(EYN(J)))
         *       EPN(J)=(1 O-SPS(J)/HE(J))*(EM(J)-EYN(J))
          IF(ABS(EM(J)) LE.ABS(EYN(J))) EPN(J)=0.0
          IF(ABS(EPN(J)).LT ABS(EPO(J))) GO TO 831
          GO TO 65
  831     IF(ABS(EM(J))+ABS(EYN(J))-ABS(EPO(J))) 833,832,832
  832     EPN(J)=EPO(J)
          GO TO 65
  833     EPN(J)=EM(J)+EYN(J)+SPS(J)/HE(J)*(EPO(J) EM(J)-EYN(J))
          GO TO 65
   82     EYN(J)=-1 O*EYN(J)
   85     IF(ABS(EM(J))-ABS(EYN(J)+EPO(J))) 822,822,823
  822      EPN(J)=EPO(J)
          GO TO 65
  823     IF(EM(J) GE.O.O)
         *        EPN(J)=EM(J)-EYN(J)-SPS(J)/HE(J)*(EM(J)-EYN(J)-EPO(J))
          IF(EM(J) LT.O )
         *        EPN(J)=EM(J)-EYN(J)+SPS(J)/HE(J)*(EM(J)-EYN(J)-EPO(J))
   65     EYN(J)=ABS(EYN(J))
          DO 88 J=1,21
          IF(ABS(EPN(J)-EPLA(J))-O O1*ABS(EPLA(J))) 88,88,86
   88     CONTINUE
          GO TO 89
   86     DO 87 J=1,21
   87     EPLA(J)=EPN(J)
```

```
FORTRAN IV G1  RELEASE 2.0          STRESS          DATE = 82126          14/42/06          PAGE 0003

             GO TO 666                                                    J0H06660
      89     CONTINUE                                                     J0H06670
             DO 33 J=1,21                                                 J0H06680
             EPO(J)=EPN(J)                                                J0H06690
             STRES(J)=YP(1)*A(J)*(EM(J)-EPN(J)-ECR(J))/1000.0             J0H06700
             EX(J)=EX(J)*YOUT                                             J0H06710
             EL(J)=(EM(J)-EPN(J)-ECR(J))*YOUT                             J0H06720
             EM(J)=(EM(J))*YOUT                                           J0H06730
      33     EPN(J)=EPN(J)*YOUT                                           J0H06740
             GO TO 888                                                    J0H06750
     989     WRITE(KO,238)                                                J0H06760
     238     FORMAT(/1X,24HSTRAIN DOES NOT CONVERGE)                      J0H06770
     888     CONTINUE                                                     J0H06780
     999     CONTINUE                                                     J0H06790
             RETURN                                                       J0H06800
             END                                                          J0H06810
```

```
FORTRAN IV G1  RELEASE 2 0          STCRP          DATE = 82126          14/42/06          PAGE 0001
0001              SUBROUTINE STCRP(IS)                                                     J0H06820
            C                                                                              J0H06830
            C  ****  STRESS ANALYSIS DURING SOAKING  ****                                  J0H06840
            C                                                                              J0H06850
            C  ****  CREEP INCLUDED  ****                                                  J0H06860
            C                                                                              J0H06870
0002              DIMENSION TAU(21),EINTY(21),EINTOT(21),DECRPN(21),HE(21)                J0H06880
0003              DIMENSION H(21),H2(21),H3(21),ECR(21),DECRP(21),H1(21)                  J0H06890
0004              COMMON /TEM/TY(21),TEMP(10),CAP(10),RHO(10),COND(10),TREFN(10,21)       J0H06900
0005              COMMON /E/E(10),YP(10),ALPH(10),SLOP(10)                                J0H06910
0006              COMMON /ST/RAT(20),T(2000),EX(21),EM(21),EPN(2'` STRES(21),EL(21)       J0H06920
0007              COMMON /YW/Y(21),YD(21)                                                 J0H06930
0008              COMMON  /YP/YPN(10),YTHN(10,21)                                         J0H06940
0009              COMMON /PP/P,V,YS,YEP,YOUT,THICK                                        J0H06950
0010              COMMON /SC/NEDGE,HCOT(10)                                               J0H06960
0011              COMMON  /RS/EPO(21)                                                     J0H06970
0012              COMMON /P/YDIS,TMAX,TIX,TREF                                            J0H06980
0013              COMMON /T/T1,TI1,T2,TI2,T3,TI3,TST                                      J0H06990
0014              COMMON /IO/KI,KO                                                        J0H07000
0015              COMMON /CRP/ECREEP(21)                                                  J0H07010
0016              COMMON /SREV/NUP,TIUP,NSOAK,TISK,NDN,TIDN,TSREV                         J0H07020
0017              TAUO=TREF+FILLIN(TREF,TEMP,ALPH,10)/YEP                                 J0H07030
0018              DO 70 J=1,21                                                            J0H07040
0019              HE(J)=FILLIN(TY(J),TEMP,E,10)                                           J0H07050
0020              TAU(J)=TY(J)+FILLIN(TY(J),TEMP,ALPH,10)/YEP                             J0H07060
0021              TAU(J)=TAU(J)-TAUO                                                      J0H07070
0022              H(J)=HE(J)/E(1)                                                         J0H07080
0023              ECR(J)=ECREEP(J)/YOUT                                                   J0H07090
0024              EPN(J)=EPN(J)/YOUT                                                      J0H07100
0025        70    CONTINUE                                                                J0H07110
0026              IF(NEDGE.GE.1) GO TO 630                                                J0H07120
0027              CALL QUDR (Y,0.0,H,21,AI1,IER)                                          J0H07130
0028              A1=1./AI1                                                               J0H07140
0029              GO TO 632                                                               J0H07150
0030        630   DO 631 J=1,21                                                           J0H07160
0031              H2(J)=H(J)*Y(J)                                                         J0H07170
0032        631   H1(J)=H(J)*Y(J)*Y(J)                                                    J0H07180
0033              CALL QUDR(Y,0.0,H,21,AI3,IER)                                           J0H07190
0034              CALL QUDR(Y,0.0,H2,21,AI2,IER)                                          J0H07200
0035              CALL QUDR(Y,0 0,H1,21,AI1,IER)                                          J0H07210
0036              DEN=AI1*AI3-AI2*AI2                                                     J0H07220
0037              A1=AI1/DEN                                                              J0H07230
0038              A2=AI2/DEN                                                              J0H07240
0039              A3=AI3/DEN                                                              J0H07250
0040        632   TI=T(IS)-T(N)-TIUP*FLOAT(NUP)                                           J0H07260
0041              TI=TI/3600.                                                             J0H07270
0042              TO=TI+(TISK/3600.)                                                      J0H07280
0043              DO 71 J=1,21                                                            J0H07290
0044        71    DECRP(J)=0.0                                                            J0H07300
0045              NC=0                                                                    J0H07310
0046        666   CONTINUE                                                                J0H07320
0047              NC=NC+1                                                                 J0H07330
0048              IF (NC.GT 20) GO TO 989                                                 J0H07340
```

```
FORTRAN IV G1  RELEASE 2 0          STCRP          DATE = 82126          14/42/06          PAGE 0002

           DO 72 J=1,21                                                  J0H07350
           EINTOT(J)=H(J)*(TAU(J)+ECR(J)+DECRP(J)+EPN(J))                J0H07360
      72   EINTY(J)=EINTOT(J)*Y(J)                                       J0H07370
           CALL QUDR(Y,0.0,EINTOT,21,EIN,IER)                            J0H07380
           CALL QUDR(Y,0.0,EINTY,21,EINY,IER)                            J0H07390
           DO 65 J=1,21                                                  J0H07400
           IF(NEDGE.GE.1) GO TO 650                                      J0H07410
           EX(J)=A1*EIN                                                  J0H07420
           GO TO 651                                                     J0H07430
     650   EX(J)=(A1-Y(J)*A2)*EIN-(A2-Y(J)*A3)*EINY                      J0H07440
     651   EM(J)=EX(J)-TAU(J)                                            J0H07450
           EL(J)=EM(J)-EPN(J)-ECR(J)                                     J0H07460
           STRES(J)=H(J)*YP(1)*EL(J)/1000                                J0H07470
           SS=STRES(J)                                                   J0H07480
           CALL CREPLO(SS,TI,TO,DE)                                      J0H07490
           DECRPN(J)=DE/YEP                                              J0H07500
      65   CONTINUE                                                      J0H07510
           DO 88 J=1,21                                                  J0H07520
           IF(ABS(DECRP(J)-DECRPN(J))-0 01*ABS(DECRP(J))) 88,88,86       J0H07530
      88   CONTINUE                                                      J0H07540
           GO TO 89                                                      J0H07550
      86   DO 87 J=1,21                                                  J0H07560
      87   DECRP(J)=DECRPN(J)                                            J0H07570
           GO TO 666                                                     J0H07580
      89   DO 33 J=1,21                                                  J0H07590
           ECR(J)=ECR(J)+DECRP(J)                                        J0H07600
           ECREEP(J)=ECR(J)*YOUT                                         J0H07610
           EM(J)=EM(J)*YOUT                                              J0H07620
           EL(J)=EL(J)*YOUT                                              J0H07630
           EX(J)=EX(J)*YOUT                                              J0H07640
      33   EPN(J)=EPN(J)*YOUT                                            J0H07650
           GO TO 888                                                     J0H07660
     989   WRITE(KO,238)                                                 J0H07670
     238   FORMAT(/1X,'-*-*-*- CREEP STRAIN DOES NOT CONVERGE -*-*-*-')  J0H07680
     888   CONTINUE                                                      J0H07690
           RETURN                                                        J0H07700
           END                                                           J0H07710
```

```
FORTRAN IV G1  RELEASE 2.0            CREPLO           DATE = 82126          14/42/06              PAGE 0001
0001              SUBROUTINE CREPLO(S,TI,TO,DE)                                           J0H07720
            C                                                                             J0H07730
            C **** UNIAXIAL CREEP LAW FOR 304 S S  AT 1100 DEG F ****                     J0H07740
            C                                                                             J0H07750
0002              F=5.436E-05*(ABS(S))**1.843                                             J0H07760
0003              R=5.929E-05*EXP(0 2029*ABS(S))                                          J0H07770
0004              G=6.73E-09*(SINH(0.1479*ABS(S)))**3 0                                   J0H07780
0005              DE=F*(EXP(-R*TI)-EXP(-R*TO))+G*(TO-TI)                                  J0H07790
0006              IF (S.GE 0.0) GO TO 1                                                   J0H07800
0007              DE=-DE                                                                  J0H07810
0008        1     RETURN                                                                  J0H07820
0009              END                                                                     J0H07830
```

FORTRAN IV G1 RELEASE 2.0 FILLIN DATE = 82126 14/42/06 PAGE 0001

```
      FUNCTION FILLIN(X,AB,OR,NO)
C
C       PARABOLIC INTERPOLATION
C
      DIMENSION AB(NO),OR(NO)
      ANTRA(X1,X2,X3,X,Y1,Y2,Y3)=Y1*(X-X2)*(X-X3)/((X1-X2)*(X1-X3))+
     1 Y2*(X-X1)*(X-X3)/((X2-X1)*(X2-X3))+Y3*(X-X1)*(X-X2)/((X3-X1)*
     2 (X3-X2))
      IF(X-AB(1)) 1,3,2
    3 Y=OR(1)
      GO TO 99
    1 Y=ANTRA(AB(1),AB(2),AB(3),X,OR(1),OR(2),OR(3))
      GO TO 99
    2 IF(X-AB(2))1,6,5
    6 Y=OR(2)
      GO TO 99
    5 DO 7 I=3,NO
      M=I
      IF(X-AB(I))8,9,7
    9 Y=OR(I)
      GO TO 99
    7 CONTINUE
    8 Y=ANTRA(AB(M-2),AB(M-1),AB(M),X,OR(M-2),OR(M-1),OR(M))
   99 FILLIN=Y
      RETURN
      END
```

FORTRAN IV G1 RELEASE 2 0 BES DATE = 82126 14/42/06 PAGE 0001

```
      SUBROUTINE BES(X,B)
      DIMENSION C(6),CI(6),CK(6)
      DATA C/- 0025154, 0058787,- 0106244, 0218956,-.0783235,1.253314/
      DATA CI/ 0360768,.2659732,1.206749,3.089942,3.515622,1 /
      DATA CK/ 0001075, 0026269, 0348859, 2306975,.4227842,-.5772156/
      IF (X) 11,10,20
   10 B=999
      RETURN
   11 X=-X
   20 IF (X-2.) 30,50,50
   30 XL=ALOG( 5*X)
      XSK=X**2/4
      XSI=X**2/14 0625
      SI= 0045813
      SK=.00000740
      DO 35 L=1,6
      SI=SI*XSI+CI(L)
   35 SK=SK*XSK+CK(L)
      B=SK-SI*XL
      RETURN
   50 XRE=SQRT(X)*EXP(X)
      XS=2 /X
      SK=.00053208
      DO 55 L=1,6
   55 SK=SK*XS+C(L)
      B=SK/XRE
      RETURN
      END
```

FORTRAN IV G1 RELEASE 2 0 QUDR DATE = 82126 14/42/06 PAGE 0001

```
      SUBROUTINE QUDR(ARG,H,VAL,N,Q,IER)
      DIMENSION ARG(21),VAL(21)
      IER=0
      Q=0
      IF(N-2) 10,20,50
   10 IER=1
      RETURN
   20 IF(ARG(1) NE ARG(N)) GO TO 40
   30 IER=2
      RETURN
   40 Q=(ARG(N)-ARG(1))*(VAL(1)+VAL(N))/2.
      RETURN
   50 IF(H.NE.O ) GO TO 100
      J=2
   60 IF(ARG(J) NE.ARG(J-1)) GO TO 80
      IER=2
      N=N-1
      IF(J.GT.N) GO TO 90
      DO 70 K=J,N
      ARG(K)=ARG(K+1)
   70 VAL(K)=VAL(K+1)
   80 J=J+1
      IF(J LE N) GO TO 60
   90 IF(N-2) 10,20,100
  100 I=-1
  110 I=I+2
      IF((N-I).LE 3) GO TO 150
C
C     ADD THE AREA BETWEEN ARG(I) AND ARG(I+2)
C
  120 IF(H.NE.O.) GO TO 140
      H1=(ARG(I+2)-ARG(I))/2
      D=ARG(I+1)-ARG(I)-H1
  130 Q=Q+H1/3 *((1 +2.*D/(H1+D))*VAL(I)+2 *(H1/(H1+D)+H1/(H1-D))*VAL(I+
     1 1)+(1.-2 *D/(H1-D))*VAL(I+2))
      IF(I.LT (N-2)) GO TO 110
      RETURN
C
C     EQUAL INTERVAL
C
  140 D=O.
      H1=H
      GO TO 130
  150 IF((N-1) EQ 2) GO TO 120
C
C     ADD THE LAST THREE AREAS
C
      H1=(ARG(N)-ARG(N-3))/2
      D1=ARG(N-2)-ARG(N-3)-H1
      D2=ARG(N-1)-ARG(N-3)-H1
      Q=Q+H1/3 *((1 +2.*D1+D2/(H1+D1)*(H1+D2))*VAL(N-3)+4 *H1*H1/(D2-D1)
     1 *(D2/(H1+H1-D1+D1)*VAL(N-2)-D1/(H1+H1-D2+D2)*VAL(N-1))+(1.+2.*D1
     1 *D2/(H1-D1)*(H1-D2))*VAL(N))
```

```
FORTRAN IV G1  RELEASE 2 0          QUDR          DATE - 82126          14/42/06          PAGE 0002

 0042                 RETURN                                                   JOH08910
 0043                 END                                                      JOH08920
```

```
FORTRAN IV G1  RELEASE 2.0          BLK DATA          DATE = 82126          14/42/06          PAGE 0001
                                                                                    J0H08930
0001              BLOCK DATA                                                        J0H08940
0002              COMMON /YW/Y(21),YD(21)                                           J0H08950
0003              COMMON /IO/KI,KO                                                  J0H08960
0004              DATA  KI/5/,KO/6/                                                 J0H08970
            C                                                                       J0H08980
            C     NON DIMENSIONAL INTEGRATION POINTS                                J0H08990
            C                                                                       J0H09000
0005              DATA Y/0 0,0.02,0.03,0.04,0.05,0.07,0 0833,0.11,0.1666,0 2,       J0H09010
                 1 0.23,0 250,0.29,0 31,0.333,0 38,0.45,0.50,0.7,0.85,1.0/          J0H09020
0006              END
```

```
FILE  BUT1100  DATA     A                VM/SP CONVERSATIONAL MONITOR SYSTEM                    PAGE 001

23 0       90.00      0 650      0 375      266
BUTT WELDING OF 304 PLATE  AND STRESS RELIEVING AT 1100 DEG F
75       200      400      800.     1000     1200.    1400     1600.    1800.    2600
0 183    0 197    0 233    0.296    0.324    0.351    0.374    0 401    0 427    0 531
100.23   105.506  110 781  121.331  127.662  131.882  133.992  137 157  140 850  149 818
0 29     0 288    0 286    0 283    0.281    0 279    0.277    0 275    0 273    0 265
28 3     27 9     26 6     24 1     22 5     21 1     19 4     16.1     8.3      0 0
35       29 05    24 15    19 6     18 2     16 45    13.65    7 0      3.5      0.0
9 48     9 59     9 75     10 11    10 25    10 40    10 60    10.75    10 93    11.59
0 730    0.720    0 686    0 622    0 580    0 544    0.500    0.415    0.214    0 00
0 003    0 003    0 003    0 003    0 003    0 003    0.003    0.003    0 003    0.003
 0
 1
0 0
0 375  0 375  0 375  0 375  0 375  0 375  0 375  0 375  0.375  0 375  0.375
6 0      2600       40.       75 0
150      2          400 0     10 0      2000.      100.      0 0
10000
   0  116  103  103
 1
   1   10   50   10     360.     360      360.    1100.
```

```
FILE  EG1100   DATA     A                VM/SP CONVERSATIONAL MONITOR SYSTEM                    PAGE 001

23 0      90 00      0 50      0.375      266
EDGE WEIDING OF 304 PLATE  AND STRESS RELIEVING AT 1100 DEG F
75.      200      400      800.      1000      1200.      1400.      1600.      1800.      2600.
0 183    0 197    0 233    0 296     0.324     0 351      0.374      0 401      0.427      0.531
100 23   105.506  110.781  121 331   127.662   131.882    133.992    137 157    140.850    149.818
0 29     0.288    0.286    0.283     0.281     0.279      0.277      0 275      0.273      0.265
28 3     27.9     26 6     24.1      22.5      21.1       19.4       16.1       8.3        0.0
35       29.05    24 15    19.6      18.2      16 45      13.65      7.0        3.5        0.0
9 48     9 59     9 75     10.11     10 25     10.40      10.60      10.75      10.93      11.59
0 730    0 720    0.686    0.622     0.580     0.544      0.500      0 415      0.214      0.00
0 003    0 003    0 003    0.003     0 003     0.003      0 003      0 003      0.003      0.003
 1
 1
0 0
0 375   0 375   0 375   0 375   0 375   0 375   0 375   0.375   0 375   0 375   0 375
6.0       2600       40.        75 0
150.      2          400 0      10.0       2000.      100.       0 0
10000.
    0   116   103   103
 1
    1    10    50    10       360       360.       360       1100.
```

```
23.0        90.00       0.50        0 375       .266
EDGE WELDING OF 304 PLATE  AND STRESS RELIEVING AT 500 DEG F
75.     200.    400.    800.    1000.   1200.   1400.   1600    1800.   2600.
0.183   0.197   0 233   0.296   0.324   0.351   0 374   0.401   0.427   0 531
100.23  105.506 110.781 121.331 127.662 131.882 133.992 137.157 140.850 149.818
0.29    0.288   0 286   0.283   0.281   0.279   0.277   0.275   0.273   0.265
28.3    27.9    26 6    24.1    22.5    21.1    19.4    16.1    8.3     0.0
35.     29.05   24.15   19.6    18 2    16.45   13 65   7.0     3.5     0 0
9.48    9.59    9 75    10.11   10.25   10.40   10.60   10.75   10 93   11.59
0.730   0.720   0 686   0.622   0.580   0 544   0 500   0.415   0.214   0 00
0.003   0 003   0.003   0.003   0.003   0.003   0 003   0 003   0 003   0.003
 1
 1
0.0
0.375  0.375  0.375  0.375  0.375  0.375  0 375  0.375  0 375  0 375  0.375
6.0      2600.    40.      75.0
150.     2.       400.0    10 0     2000.     100.      0.0
10000.
    0  116  103  103
 1
    0   10   50   10      360.      360.      360.     500
```

APPENDIX D

LISTINGS OF DATA ACQUISITION AND REDUCTION PROGRAMS

```
C*****************************************************************
C       PROGRAM     SMPL5.FOR                                    *
C                                                                *
C       PROGRAM TO TRANSFER ASCII DATA SERIALY BETWEEN           *
C                                                                *
C       MINC-23 AND DAYTRONIC 9635 COMPUTER INTERFACE MODULE     *
C                                                                *
C           NOW SET TO SAMPLE ONLY 10 CHANNELS :                 *
C           #05 TO 09 FOR STRAIN GAGES                           *
C           #10 TO 14 FOR T/C's                                  *
C                                                                *
C       CHANGE IX VALUES ACCORDING TO WHAT YOU SAMPLE            *
C                                                                *
C                                                                *
C       (BUFFER SIZE IN CIN SET TO 20 CHARACTERS)                *
C                                                                *
C*****************************************************************
C
C
        LOGICAL*1 BUF1(4),FNAME(16),BUF(20),BUF3(4)
        LOGICAL*1 BUF2(6),IX(2,10),BOUT(90)
        LOGICAL*1 BOT(9,10),VAL(9,10)
        DIMENSION T(3000)
        EQUIVALENCE (BOUT(1),VAL(1,1))
        INTEGER*4 ITM1,ITMO
        DATA BUF1/'L','O','C',"15/
        DATA BUF2/'C','H','N','I','X',"15/
        DATA BUF3/'U','N','L',"15/
        DATA IX/'0','5','0','6','0','7','0','8','0','9',
       2'1','0','1','1','1','2','1','3','1','4'/
        NCHR1=4
        NCHR2=6
        NCHR3=4
        IFLAG1=0
        IFLAG2=0
        IFLAG3=0
C
C       OUTPUT FILE INITIALIZATION
C
        TYPE *, 'WHAT IS THE NAME OF THE OUTPUT FILE'
        ACCEPT 701,(FNAME(I),I=1,14)
  701   FORMAT(14A1)
        FNAME(15)=0
        OPEN(UNIT=15,NAME=FNAME,TYPE='NEW',ACCESS='SEQUENTIAL',
       1FORM='FORMATTED')
C
C       TIME STEPS DEFINITION
C
  100   TYPE *,'     ENTER TIME LIMITS FOR EVERY INTERVAL'
        TYPE *,'          ( ENTER T1,T2,T3 IN SECONDS )'
        ACCEPT *,T1,T2,T3
        TYPE *,'   ENTER TIME STEP SIZE FOR EVERY INTERVAL '
        TYPE *,'          (TI1,TI2,TI3 IN SECONDS)'
        TYPE *,'NOTE THAT TIME STEPS MUST BE GREATER THAN 4.5 SECS !!! '
```

```
FORTRAN IV      V02.5                                              PAGE 002

              TYPE *,'    (FOR 5 STRAIN GAGES AND 5 THERMOCOUPLES)    '
              ACCEPT *,TI1,TI2,TI3
              N=1
              TI=TI1
              T(1)=0.0
        40    IF(T(N).GE.T1) TI=TI2
              IF(T(N).GE.T2) TI=TI3
              IF(T(N).GE.T3) GO TO 41
              T(N+1)=T(N)+TI
              N=N+1
              GO TO 40
        41    CONTINUE
              TYPE 702 ,(T(IJK),IJK=1,N)
       702    FORMAT(1H ,15(/1X,8F10.2))
              TYPE *,'**** ARE TIME STEPS OK ?? (YES=1,NO=0) ****'
              ACCEPT *,IYE
              IF (IYE.EQ.0) GO TQ 100
      C
      C       SAMPLING PHASE
      C
              PAUSE ' TYPE A CARRIAGE RETURN TO START SAMPLING !!'
              TYPE *,'TYPE A SECOND CARRIAGE RETURN TO STOP !!'
      C
      C       GET INITIAL TIME
      C
              CALL GTIM(ITMO)
              CALL CVTTIM(ITMO,IHO,IMO,ISO,ITO)
      C
      C       LOOP FOR ALL TIME STEPS
      C
              DO 121 JJ=1,N
         1    CALL GTIM(ITM1)
              CALL CVTTIM(ITM1,IH1,IM1,IS1,IT1)
              TIM=(IH1-IHO)*3600.+(IM1-IMO)*60.+(IS1-ISO)+(IT1-ITO)/60.
              IF(TIM.LT.T(JJ)) GO TO 1
              CALL GTIM(ITM1)
              CALL CVTTIM(ITM1,IH1,IM1,IS1,IT1)
              TIM=(IH1-IHO)*3600.+(IM1-IMO)*60.+(IS1-ISO)+(IT1-ITO)/60.
      C
      C       SEND  'LOC'  (9635 MEMORY FREEZE)  COMMAND
      C
       901    CALL COUT (BUF1,NCHR1,IFLAG1)
              IF (IFLAG1.EQ.1) GO TO 901
              JJ1=JJ-1
              TYPE 718,JJ1,TIM
       718    FORMAT(3X,I5,F10.3)
      C
      C       LOOP FOR ALL CHANNELS
      C
              DO 103 JL=1,10
              CALL CINRST
              DO 104 J=1,20
       104    BUF(J)=' '
              BUF2(4)=IX(1,JL)
```

```
      BUF2(5)=IX(2,JL)
C
C     SEND  "CHN X"  (CHANNEL SAMPLING) COMMAND
C
902   CALL COUT (BUF2,NCHR2,IFLAG2)
      IF (IFLAG2.EQ.1) GO TO 902
      IFL=0
      NCNT=0
C
C     INPUT SERIAL DATA FROM 9635
C
900   CALL CIN(BUF,IFL,NCNT)
      IF (IFL.EQ.0) GO TO 900
C
C     GET RID OF LF,CR OR UREADABLE CHARACTERS
C
      DO 11 I=4,12
      JLI=(JL-1)*9+I-3
      IF (BUF(I).NE."15) GO TO 112
      BUF(I)=' '
112   IF (BUF(I).NE."0) GO TO 11
      BUF(I)=' '
11    BOUT(JLI)=BUF(I)
103   CONTINUE
C
C     SEND  "UNL" (9635 MEMORY UNFREEZE) COMMAND
C
903   CALL COUT(BUF3,NCHR3,IFLAG3)
      IF (IFLAG3.EQ.1) GO TO 903
C
C     SET DATA TO PROPER FORMAT
C
      DO 93 I=1,10
      J9=9
      DO 92 IL=1,9
      IL1=9-IL+1
      IF(VAL(IL1,I).EQ.' ') GO TO 92
      BOT(J9,I)=VAL(IL1,I)
      J9=J9-1
92    CONTINUE
      DO 94 J1=1,J9
94    BOT(J1,I)=' '
93    CONTINUE
C
C     WRITE THE DATA TO THE DISC AND DISPLAY SOME IN THE TERMINAL
C
      WRITE (15,703)TIM,((BOT(IL,I),IL=1,9),I=1,10)
703   FORMAT(1X,F10.3,4X,10(1X,9A1))
      TYPE 704,((BOT(IL,I),IL=1,9),I=1,3),((BOT(ML,M),ML=1,9),M=6,8)
704   FORMAT (15X,6(1X,9A1))
C
C     CHECK IF A CARRIAGE RETURN HAS BEEN TYPED TO STOP SAMPLING
C
      IY=ITTINR()
```

```
FORTRAN IV      V02.5                                                   PAGE 004

0112            IF(IY.GE.0) GO TO 122
0114      121   CONTINUE
          C
          C     END OF TIME STEPS LOOP
          C
0115            GO TO 125
0116      122   TYPE *,'DO YOU WANT TO CONTINUE SAMPLING IN THE SAME FILE ??'
0117            TYPE *,'(YES=1,NO=0)'
0118            ACCEPT *,IYST
0119            IF (IYST.NE.0) GO TO 121
0121      125   CLOSE (UNIT=15)
0122            STOP
0123            END
```

```
FORTRAN IV      V02.5                                        PAGE 001

      C***********************************************************
      C                                                          *
      C     SEND.FOR                                             *
      C                                                          *
      C     PROGRAM TO SEND CONTROL COMMANDS                     *
      C     TO THE 9635 DAYTRONIC MODULE                         *
      C                                                          *
      C     EXAMPLE: LOC   (FOR MEMORY FREEZE)                   *
      C              UNL   (FOR MEMORY UNFREEZE)                 *
      C              RST X (TO RESET CHNNL X TO MILLIVOLTS)      *
      C              ZRO X (TO SET CHNNL X TO ZERO)              *
      C                                                          *
      C     COMMAND TEXT CAN BE UP TO 9 CHARACTERS               *
      C     (CARRIAGE RETURN IS ADDED BY THE PROGRAM)            *
      C                                                          *
      C***********************************************************
      C
      C
            LOGICAL*1 BUF1(10)
            DATA BUF1(10)/"15/
      1     TYPE *,'WHAT DO YOU WANT TO BE SENT ?'
            ACCEPT 11,(BUF1(I),I=1,9)
      11    FORMAT(9A1)
            N1=10
            I1=0
      2     CALL COUT(BUF1,N1,I1)
            IF(I1.EQ.1) GO TO 2
            TYPE *,'DO YOU WANT TO SEND MORE ? (YES=1,NO=0)'
            ACCEPT 12,IY
      12    FORMAT(I1)
            IF(IY.EQ.1) GO TO 1
            STOP
            END
```

```
C*************************************************************
C                                                            *
C       REDUCE.FOR                                           *
C                                                            *
C       PROGRAM TO COMPENSATE FOR TEMPERATURE INDUCED        *
C       APPARENT STRAIN AND GAGE FACTOR VARIATION            *
C               OR TO SCREEN SOME MEASUREMENTS               *
C       FOR THE CASE OF VERY LARGE INPUT FILES               *
C                                                            *
C       READINGS ARE INPUT FROM FILE "FLIN"                  *
C       IN INTEGER FORMAT (FORMATS 702 OR 703)               *
C                                                            *
C       CORRECTED STRAINS ARE OUTPUT TO FILE "FLOUT"         *
C       IN REAL FORMAT (FORMATS 704 OR 705)                  *
C                                                            *
C*************************************************************
C
C
      LOGICAL*1 FLIN(16),FLOUT(16)
      DIMENSION IVSG(10),IVTC(10),STR(10),TEMP(10),STRAIN(10)
C
C     I/O FILES INITIALIZATION AND DATA INPUT
C
      TYPE *,'WHAT IS THE NAME OF THE INPUT DATA FILE ?'
      ACCEPT 701,(FLIN(I),I=1,14)
701   FORMAT (14A1)
      FLIN(15)=0
      OPEN (UNIT=15,NAME=FLIN,TYPE='OLD',ACCESS='SEQUENTIAL',
     1FORM='FORMATTED')
      TYPE *,'WHAT IS THE NAME OF THE OUTPUT DATA FILE ?'
      ACCEPT 701,(FLOUT(I),I=1,14)
      FLOUT(15)=0
      OPEN (UNIT=16,NAME=FLOUT,TYPE='NEW',ACCESS='SEQUENTIAL',
     1FORM='FORMATTED')
      TYPE *,'ENTER NUMBER OF STRAIN GAGE CHANELS  (MAX=10)'
      ACCEPT *,NSG
      TYPE *,'ENTER NUMBER OF THERMOCOUPLE CHANELS  (MAX=10)'
      ACCEPT *,NTC
      NCH=NSG+NTC
C
C     IF NSG IS GREATER THAN NTC THE PROGRAM WILL ASSUME THAT
C     THE LAST (NSG-NTC) STRAIN GAGES ARE AT THE SAME TEMPERATURES
C     AS THE FIRST NTC OF THEM
C
      TYPE *,'ENTER NUMBER OF RUNS '
      ACCEPT *,NR
      TYPE *,'EVERY HOW MANY POINTS DO YOU WANT TO READ AND WRITE ?'
      ACCEPT *,NJ
      NCOUNT=NJ
      TYPE *,'DO YOU WANT TO COMPENSATE FOR TEMPERATURE EFFECTS ?'
      TYPE *,'(YES=1,NO=0)'
      ACCEPT *,ITMP
C
C     IF NO COMPENSATION IS REQUIRED THE "SCREENED" DATA
```

```
C       WILL BE WRITTEN IN THE OUTPUT FILE
C       WITH THE SAME FORMAT AS IN THE INPUT FILE
C
        TYPE *,'DO YOU WANT TO CHANGE THE SIGN OF THE STRAIN READINGS ?'
        TYPE *,'(YES=1,NO=0)'
        ACCEPT *,ISGN
C
C       DEPENDING ON THE CONNECTIONS OF THE BRIDGE COMPLETION CIRCUITS
C       IN THE STRAIN GAGE CONDITIONER SIGN CHANGE OF S.G. READINGS
C       MIGHT BE NEEDED
C
        DO 100 I=1,NR
        IF(NSG.GT.5)GO TO 2
        READ (15,702) TIM,(IVSG(J),J=1,NSG),(IVTC(J),J=1,NTC)
702     FORMAT (1X,F10.3,4X,10(1X,I9))
        GO TO 3
2       READ (15,703) TIM,(IVSG(J),J=1,NSG),(IVTC(J),J=1,NTC)
703     FORMAT (1X,F10.3,4X,10(1X,I9)/15X,10(1X,I9))
3       IF (ISGN.NE.1)GO TO 300
        DO 30 J=1,NSG
30      IVSG(J)=-IVSG(J)
300     NCOUNT=NCOUNT-1
        IF (NCOUNT.NE.0) GO TO 100
        DO 101 I1=1,NSG
        STR(I1)=IVSG(I1)
        IF (I1.GT.NTC) GO TO 102
        TEMP(I1)=IVTC(I1)
        GO TO 103
102     TEMP(I1)=IVTC(I1-NTC)
103     IF (ITMP.NE.1) GO TO 101
        CALL COMP(TEMP(I1),STR(I1),STRAIN(I1))
101     CONTINUE
        IF (ITMP.NE.1)GO TO 104
        IF(NSG.GT.5)GO TO 21
        WRITE (16,704) TIM,(STRAIN(J),J=1,NSG),(TEMP(J),J=1,NTC)
704     FORMAT (1X,F10.3,4X,10(1X,F9.2))
        GO TO 31
21      WRITE (16,705) TIM,(STRAIN(J),J=1,NSG),(TEMP(J),J=1,NTC)
705     FORMAT (1X,F10.3,4X,10(1X,F9.2)/15X,10(1X,F9.2))
        GO TO 31
104     IF(NSG.GT.5)GO TO 22
        WRITE (16,702) TIM,(IVSG(J),J=1,NSG),(IVTC(J),J=1,NTC)
        GO TO 31
22      WRITE (16,703) TIM,(IVSG(J),J=1,NSG),(IVTC(J),J=1,NTC)
31      NCOUNT=NJ
100     CONTINUE
        CLOSE (UNIT=15)
        CLOSE (UNIT=16)
        STOP
        END
```

```
FORTRAN IV      V02.5                                                   PAGE 001

      C*****************************************************************
      C                                                                *
      C      COMP.FOR                                                  *
      C                                                                *
      C      SUBROUTINE TO CORRECT ERRORS IN                           *
      C      STRAIN MEASUREMENTS DUE TO TEMPERATURE-INDUCED            *
      C      APPARENT STRAIN AND GAGE FACTOR VARIATION                 *
      C                                                                *
      C      NOTE THAT THE FORMULAS USED FOR APPARENT STRAIN           *
      C      OR GAGE FACTOR VARIATION VERSUS TEMPERATURE               *
      C      APPLY ONLY TO THE STRAIN GAGES USED                       *
      C      (M-M WK-09-062AP-350  LOT#K14FE01)                        *
      C      BONDED ON 304 STAINLESS STEEL                             *
      C                                                                *
      C      STRAIN IN MICROSTRAIN AND TEMPERATURE IN DEGREES F        *
      C                                                                *
      C*****************************************************************
      C
      C
0001         SUBROUTINE COMP(T,SIN,SOUT)
      C
      C      CHECK IF TEMPERATURE IN ACCEPTABLE LIMITS
      C
0002         IF ((T.LT.0.).OR.(T.GT.550.)) GO TO 100
      C
      C      APPARENT STRAIN CALCULATION (-360 DEG F< TEMP < 500 DEG F)
      C
0004         EAPP=-81.4+1.39*T-4.63E-3*T**2+8.57E-6*T**3-9.33E-9*T**4
      C
      C      PERCENT VARIATION OF GAGE FACTOR (0 DEG F< TEMP < 500 DEG F)
      C
0005         SGROOM=2.01
0006         SGCLBR=2.0
0007         IF(T.GT.200.) GO TO 1
0009         DSG=0.17-0.69*T/200.
0010         GO TO 3
0011  1      IF(T.GT.400.) GO TO 2
0013         DSG=-0.52-1.18*(T-200.)/200.
0014         GO TO 3
0015  2      DSG=-1.70-1.03*(T-400.)/100.
0016  3      SG=SGROOM*(1.+DSG/100.)
      C
      C      STRAIN CORRECTION
      C
0017         SOUT=(SIN-EAPP)*SGCLBR/SG
0018         RETURN
0019  100    SOUT=SIN
0020         RETURN
0021         END
```

```
FORTRAN IV      V02.5                                         PAGE 001

      C*****************************************************************
      C                                                                *
      C     PLO.FOR                                                    *
      C                                                                *
      C     PROGRAM TO PLOT STRAIN GAGE AND T/C READINGS               *
      C                                                                *
      C     ASSUME READINGS ARE IN FILE "FNAME"                        *
      C                                                                *
      C*****************************************************************
      C
            LOGICAL*1 FNAME(16),OUNAM(16)
            DIMENSION VAL(300,15),TIM(300),PLO(300)
            DIMENSION IVSG(10),IVTC(10),VSG(10),VTC(10)
            TYPE *,'WHAT IS THE NAME OF THE INPUT DATA FILE ?'
            ACCEPT 701,(FNAME(I),I=1,14)
      701   FORMAT(14A1)
            OPEN(UNIT=15,NAME=FNAME,TYPE='OLD',ACCESS='SEQUENTIAL',
           1FORM='FORMATTED')
            TYPE *,'          ARE DATA IN INTEGER FORMAT ? (YES=1,NO=0)'
            TYPE *,'NOTE : ORIGINAL READINGS ARE IN INTEGER FORMAT BUT'
            TYPE *,'          AFTER COMPENSATION ARE STORED IN REAL FORMAT'
            ACCEPT *,IINT
            TYPE *,'ENTER NUMBER OF STRAIN GAGE CHANNELS (MAX=10)'
            ACCEPT *,NSG
            TYPE *,'ENTER NUMBER OF THERMOCOUPLE CHANNELS (MAX=5)'
            ACCEPT *,NTC
            NCH=NSG+NTC
            TYPE *,' ENTER NUMBER OF RUNS (MAX=300)'
            ACCEPT *,NR
      C
      C     READ INPUT DATA FILE
      C
            DO 100 J=1,NR
            IF (IINT.NE.1) GO TO 1
            IF (NSG.GT.5) GO TO 2
            READ (15,702)TIM(J),(IVSG(I),I=1,NSG),(IVTC(I),I=1,NTC)
            GO TO 3
      2     READ (15,703)TIM(J),(IVSG(I),I=1,NSG),(IVTC(I),I=1,NTC)
      3     DO 301 IS=1,NSG
      301   VAL(J,IS)=IVSG(IS)
            DO 302 IT=1,NTC
      302   VAL(J,IT+NSG)=IVTC(IT)
            GO TO 100
      1     IF (NSG.GT.5) GO TO 21
            READ (15,704)TIM(J),(VSG(I),I=1,NSG),(VTC(I),I=1,NTC)
            GO TO 31
      21    READ (15,705)TIM(J),(VSG(I),I=1,NSG),(VTC(I),I=1,NTC)
      31    DO 311 IS=1,NSG
      311   VAL(J,IS)=VSG(IS)
            DO 312 IT=1,NTC
      312   VAL(J,IT+NSG)=VTC(IT)
      100   CONTINUE
      C
      C     PLOTING PHASE (USE OF PLTSVK PLOTING PACKAGE)
```

```
FORTRAN IV      V02.5                                              PAGE 002

      C
              DO 110 I=1,NCH
              DO 11 J=1,NR
      11      PLO(J)=VAL(J,I)
              TYPE *,'ENTER OPTION (2 FOR SAME PARAMETERS AS PREVIOUS GRAPH)'
              ACCEPT *,IOPT
              CALL GRAPHS(TIM,PLO,NR,IOPT)
      110     CONTINUE
      702     FORMAT(1X,F10.3,4X,10(1X,I9))
      703     FORMAT(1X,F10.3,4X,10(1X,I9)/15X,10(1X,I9))
      704     FORMAT(1X,F10.3,4X,10(1X,F9.2))
      705     FORMAT(1X,F10.3,4X,10(1X,F9.2)/15X,10(1X,F9.2))
              CLOSE (UNIT=15)
              STOP
              END
```